NASA Tech Briefs

National
Aeronautics and
Space
Administration

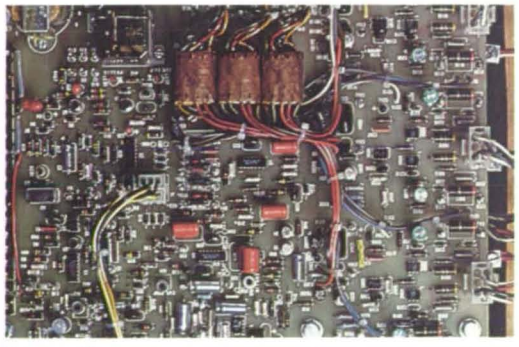

Up to 40 percent energy savings were realized when NASA's ac motor power-factor controller (PFC) was added to the escalators in a Maryland department store. Shown above is one commercial implementation of the PFC. [*See the bottom of page A1.*]

Vol. 7, No. 2

Winter 1982

About the NASA Technology Utilization Program

The National Aeronautics and Space Act of 1958, which established NASA and the United States civilian space program, requires that "The Administration shall provide for the widest practicable and appropriate dissemination of information concerning its activities and the results thereof."

To help carry out this objective, NASA's Technology Utilization (TU) Program was established in 1962. Now, as an element of NASA's Technology Utilization and Industry Affairs Division, this program offers a variety of valuable services to help transfer aerospace technology to nonaerospace applications, thus assuring American taxpayers maximum return on their investment in space research; thousands of spinoffs of NASA research have already occurred in virtually every area of our economy.

The TU program has worked for engineers, scientists, technicians, and businessmen; and it can work for you.

NASA Tech Briefs

Tech Briefs is published quarterly and is free to engineers in U.S. industry and to other domestic technology transfer agents. It is both a current-awareness medium and a problem-solving tool. Potential products . . . industrial processes . .. basic and applied research . . . shop and lab techniques . . . computer software . . . new sources of technical data . . . concepts . . . can be found here. The short section on New Product Ideas highlights a few of the potential new products contained in this issue. The remainder of the volume is organized by technical category to help you quickly review new developments in your areas of interest. Finally, a subject index makes each issue a convenient reference file.

Further Information on Innovations

Although some new technology announcements are complete in themselves, most are backed up by Technical Support Packages (TSP's). TSP's are available without charge and may be ordered by simply completing a TSP Request Card found at the back of this volume. Further information on some innovations is available for a nominal fee from other sources, as indicated. In addition, Technology Utilization Officers at NASA Field Centers will often be able to lend necessary guidance and assistance.

Patent Licenses

Patents have been issued to NASA on some of the inventions described, and patent applications have been submitted on others. Each announcement indicates patent status and availability of patent licenses if applicable.

Other Technology Utilization Services

To assist engineers, industrial researchers, business executives, Government officials, and other potential users in applying space technology to their problems, NASA sponsors Industrial Applications Centers. Their services are described on page A7. In addition, an extensive library of computer programs is available through COSMIC, the Technology Utilization Program's outlet for NASA-developed software.

Applications Program

NASA conducts applications engineering projects to help solve public-sector problems in such areas as safety, health, transportation, and environmental protection. Two applications teams, staffed by professionals from a variety of disciplines, assist in this effort by working with Federal agencies and health organizations to identify critical problems amenable to solution by the application of existing NASA technology.

Reader Feedback

We hope you find the information in *NASA Tech Briefs* useful. A reader-feedback card has been included because we want your comments and suggestions on how we can further help you apply NASA innovations and technology to your needs. Please use it; or if you need more space, write to the Manager, Technology Transfer Division, P.O. Box 8757, Baltimore/ Washington International Airport, Maryland 21240.

NASA Tech Briefs

National Aeronautics and Space Administration

Winter 1982
Volume 7, Number 2

COVERS: The photographs on the front and back covers illustrate developments by NASA and its contractors that have resulted in commercial and nonaerospace spinoffs. You can use the TSP Request Card at the back of this issue to learn more about the Power-Factor Controller [Circle 66] and High-Intensity Xenon Lamps [Circle 67]

About This NASA Publication

NASA Tech Briefs, a quarterly publication, is distributed free to qualified U.S. citizens to encourage commercial application of U.S. space technology. For information on publications and services available through the NASA Technology Utilization Program, write to the Manager, Technology Transfer Division, P.O. Box 8757, Baltimore/Washington International Airport, Maryland 21240.

"The Administrator of National Aeronautics and Space Administration has determined that the publication of this periodical is necessary in the transaction of the public business required by law of this Agency. Use of funds for printing this periodical has been approved by the Director of the Office of Management and Budget."

Change of Address

If you wish to have NASA Tech Briefs forwarded to your new address, use the Subscription Card enclosed at the back of this volume of NASA Tech Briefs. Be sure to check the appropriate box indicating change of address, and also fill in your identification number (T number) in the space indicated.

Communications Concerning Editorial Matter

For editorial comments or general communications about NASA Tech Briefs, you may use the Feedback card in the back of NASA Tech Briefs, or write to: The Publications Manager, Technology Utilization Office (LGT-1), NASA Headquarters, Washington, DC 20546. Technical questions concerning specific articles should be directed to the Technology Utilization Officer of the sponsoring NASA Center (addresses listed on page A4).

Acknowledgements

NASA Tech Briefs is published quarterly by the National Aeronautics and Space Administration, Technology Transfer Division, Washington, DC: Administrator: **James M. Beggs;** Director, Technology Utilization and Industry Affairs Division: **Ronald J. Philips;** Publications Manager: **Leonard A. Ault.** Prepared for the National Aeronautics and Space Administration by **Logical Technical Services Corp.:** Editor-in-Chief: **Jay Kirschenbaum;** Art Director: **Ernest Gillespie;** Managing Editor: **Jerome Rosen;** Chief Copy Editor: **Oden Browne;** Staff Editors: **Donald Blattner, Larry Grunberger, Jordan Randjelovich, Ted Selinsky, George Watson, Fred Wetzler;** Graphics: **Luis Martinez, Janet McCrie, Huburn Profitt;** Editorial & Production: **Richard Johnson, Leslie Iwaskow, Frank Ponce, Elizabeth Texeira, Vincent Susinno, Ernestine Walker.**

NASA TU SERVICES

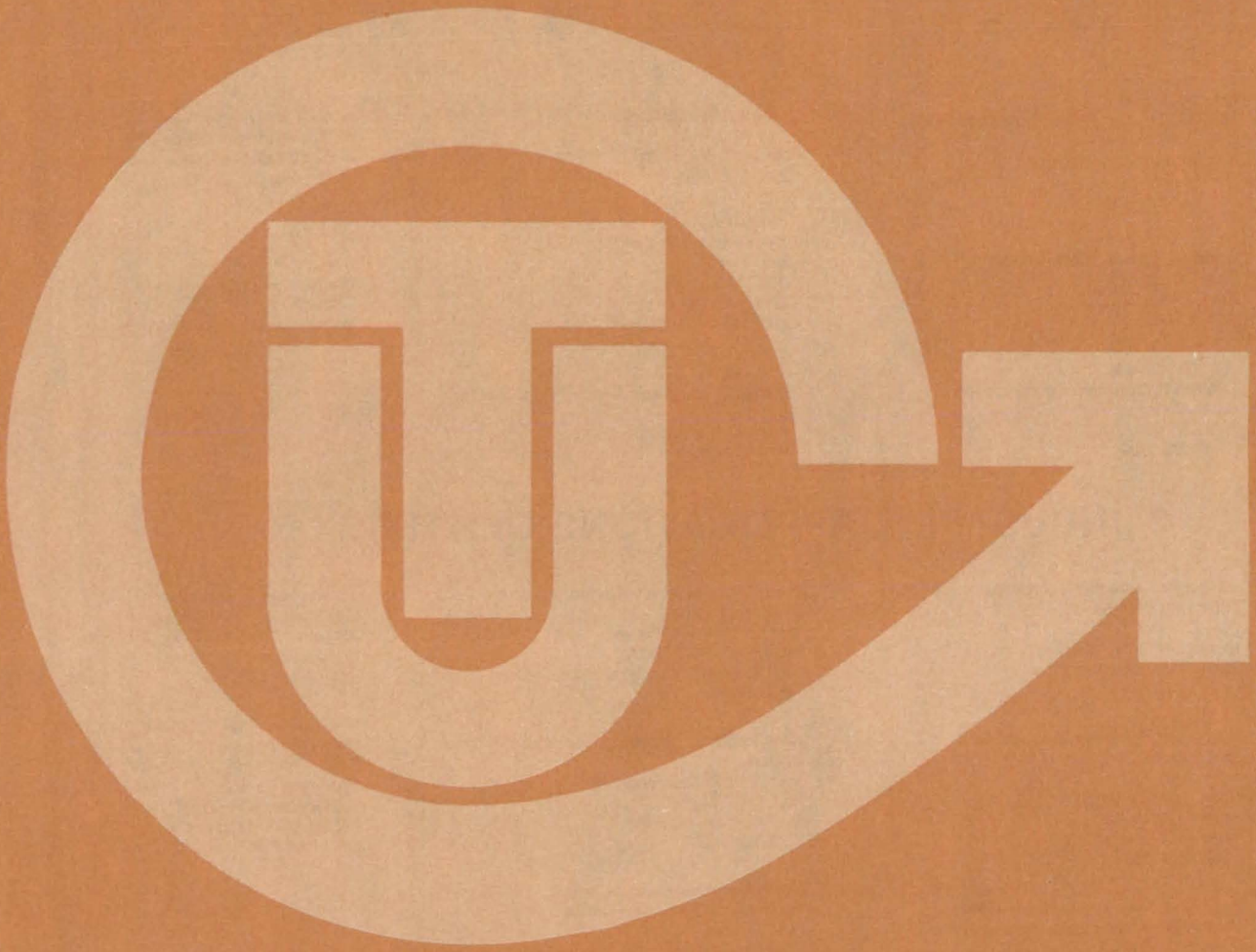

NASA TECHNOLOGY UTILIZATION NETWORK

★ TECHNOLOGY UTILIZATION OFFICERS

Stanley A. Miller
Ames Research Center
Code 240-10
Moffett Field, CA 94035
(415) 965-6471

Stanley A. Miller
Hugh L. Dryden Flight Research Center
Code 240-10
Moffett Field, CA 94035
(415) 965-6471

Donald S. Friedman
Goddard Space Flight Center
Code 702.1
Greenbelt, MD 20771
(301) 344-6242

John T. Wheeler
Lyndon B. Johnson Space Center
Code AT-3
Houston, TX 77058
(713) 483-3809

U. Reed Barnett
John F. Kennedy Space Center
Code PT-SPD
Kennedy Space Center, FL 32899
(305) 867-3017

John Samos
Langley Research Center
Mail Stop 139A
Hampton, VA 23665
(804) 865-3281

Harrison Allen, Jr.
Lewis Research Center
Mail Code 7-3
21000 Brookpark Road
Cleveland, OH 44135
(216) 433-4000, Ext. 6422

Ismail Akbay
George C. Marshall Space Flight Center
Code AT01
Marshall Space Flight Center, AL 35812
(205) 453-2224

Leonard A. Ault
NASA Headquarters
Code ETD-6
Washington, DC 20546
(202) 755-2244

Aubrey Smith
NASA Resident Office-JPL
4800 Oak Grove Drive
Pasadena, CA 91103
(213) 354-4849

Gilmore H. Trafford
Wallops Flight Center
Code OD
Wallops Island, VA 23337
(804) 824-3411, Ext. 201

● INDUSTRIAL APPLICATIONS CENTERS

Aerospace Research Applications Center
1201 East 38th Street
Post Office Box 647
Indianapolis, IN 46223
John M. Ulrich, director
(317) 264-4644

Computer Software Management and Information Center (COSMIC)
Suite 112, Barrow Hall
University of Georgia
Athens, GA 30602
John A. Gibson, director
(404) 542-3265

Kerr Industrial Applications Center
Southeastern Oklahoma State University
Durant, OK 74701
James Harmon, director
(405) 924-0121, Ext. 413

NASA Industrial Applications Center
710 LIS Building
University of Pittsburgh
Pittsburgh, PA 15260
Paul A. McWilliams, executive director
(412) 624-5211

New England Research Applications Center
Mansfield Professional Park
Storrs, CT 06268
Daniel Wilde, director
(203) 486-4533

North Carolina Science and Technology Research Center
Post Office Box 12235
Research Triangle Park, NC 27709
James E. Vann, director
(919) 549-0671

Technology Applications Center
University of New Mexico
Albuquerque, NM 87131
Stanley Morain, director
(505) 277-3622

NASA Industrial Applications Center
University of Southern California
Denny Research Building
University Park
Los Angeles, CA 90007
Robert Mixer, acting director
(213) 743-6132

■ STATE TECHNOLOGY APPLICATIONS CENTERS

NASA/University of Florida
State Technology Applications Center
500 Weil Hall
University of Florida
Gainesville, FL 32611
J. Ronald Thornton, director

Gainesville:	(904) 392-6760
Boca Raton:	(305) 395-5100, Ext. 2292
Fort Lauderdale:	(305) 776-6645
Jacksonville:	(904) 646-2478
Orlando:	(305) 275-2706
Pensacola:	(904) 476-9500, Ext. 426
Tampa:	(813) 974-2499

NASA/University of Kentucky
State Technology Applications Program
109 Kinkead Hall
University of Kentucky
Lexington, KY 40508
William R. Strong, manager
(606) 258-4632

◆ PATENT COUNSELS

Robert F. Kempf
Asst. Gen. Counsel for patent matters
NASA Headquarters
Code GP-4
400 Maryland Avenue, SW.
Washington, DC 20546
(202) 755-3954

Darrell G. Brekke
Ames Research Center
Mail Code: 200-11A
Moffett Field, CA 94035
(415) 965-5104

Darrell G. Brekke
Hugh L. Dryden Flight Research Center
Mail Code: 200-11A
Moffett Field, CA 94035
(415) 965-5104

John O. Tresansky
Goddard Space Flight Center
Mail Code: 204
Greenbelt, MD 20771
(301) 344-7351

Marvin F. Matthews
Lyndon B. Johnson Space Center
Mail Code: AL-3
Houston, TX 77058
(713) 483-4871

James O. Harrell
John F. Kennedy Space Center
Mail Code: SA-PAT
Kennedy Space Center, FL 32899
(305) 867-2544

Howard J. Osborn
Langley Research Center
Mail Code: 279
Hampton, VA 23665
(804) 827-3725

Norman T. Musial
Lewis Research Center
Mail Code: 500-311
21000 Brookpark Road
Cleveland, OH 44135
(216) 433-4000, Ext. 346

Leon D. Wofford, Jr.
George C. Marshall Space Flight Center
Mail Code: CC01
Marshall Space Flight Center, AL 35812
(205) 453-0020

Paul F. McCaul
NASA Resident Office-JPL
Mail Code: 180-601
4800 Oak Grove Drive
Pasadena, CA 91103
(213) 354-2700

▲ APPLICATION TEAMS

Doris Rouse, director
Research Triangle Institute
Post Office Box 12194
Research Triangle Park, NC 27709
(919) 541-6980

James P. Wilhelm, director
SRI International
333 Ravenswood Avenue
Menlo Park, CA 94026
(415) 326-6200, Ext. 3520

TECHNOLOGY UTILIZATION OFFICERS

Technology transfer experts can help you apply the innovations in NASA Tech Briefs.

The Technology Utilization Officer at each NASA Field Center is an applications engineer who can help you make use of new technology developed at his center. He brings you NASA Tech Briefs and other special publications, sponsors conferences, and arranges for expert assistance in solving technical problems.

Technical assistance, in the form of further information about NASA innovations and technology, is one of the services available from the TUO. Together with NASA scientists and engineers, he can often help you find and implement NASA technology to meet your specific needs.

Technical Support Packages (TSP's) are prepared by the center TUO's. They provide further technical details for articles in NASA Tech Briefs. This additional material can help you evaluate and use NASA technology. You may receive most TSP's free of charge by using the TSP Request Card found at the back of this issue.

Technical questions about articles *in NASA Tech Briefs are answered in the TSP's. When no TSP is available, or you have further questions, contact the Technology Utilization Officer at the center that sponsored the research* [*see page A4*].

NASA INVENTIONS AVAILABLE FOR LICENSING

Over 3,500 NASA inventions are available for licensing in the United States — both exclusive and nonexclusive.

Nonexclusive licenses for commercial use of NASA inventions are encouraged to promote competition and to achieve the widest use of inventions. They must be used by a netotiated target date.

Exclusive licenses may be granted to encourage early commercial development of NASA inventions, especially when considerable private investment is required. These are generally for 5 to 10 years and usually require royalties based on sales or use.

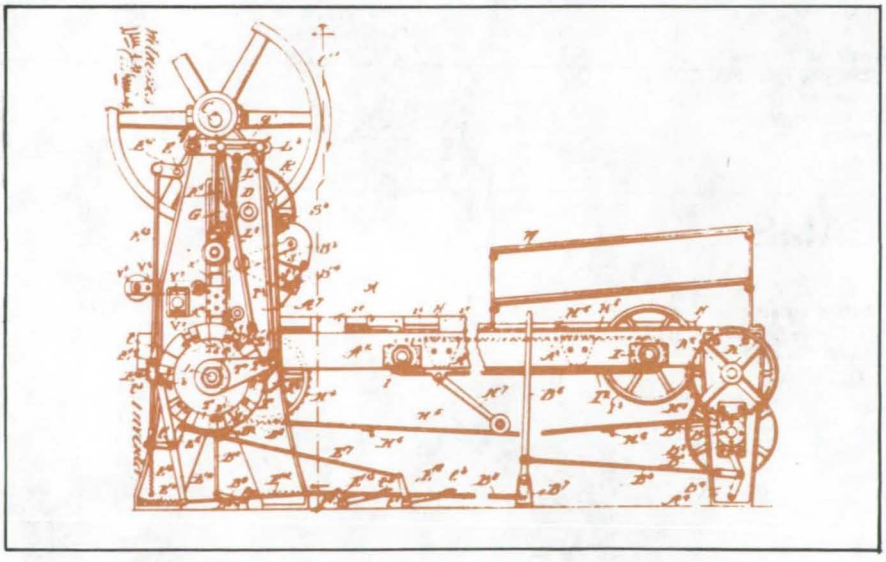

Additional licenses available include those of NASA-owned foreign patents. In addition to inventions described in NASA Tech Briefs, *"NASA Patent Abstract Bibliography"* (PAB), containing abstracts of all NASA inventions, can be purchased from National Technical Information Service, Springfield, VA 22161. The PAB is updated semiannually.

Patent licenses for Tech Briefs *are frequently available. Many of the inventions reported in NASA Tech Briefs are patented or are under consideration for a patent at the time they are published. The current patent status is described at the end of the article; otherwise, there is no statement about patents. If you want to know more about the patent program or are interested in licensing a particular invention, contact the Patent Counsel at the NASA Field Center that sponsored the research* [*see page A5*]. *Be sure to refer to the NASA reference number at the end of the Tech Brief.*

APPLICATION TEAMS

Technology-matching and problem-solving assistance to public-sector organizations

Application engineering projects are conducted by NASA to help solve public-sector problems in such areas as safety, health, transportation, and environmental protection. Some application teams specialize in biomedical disciplines; others, in engineering and scientific problems. Staffed by professionals from various disciplines, these teams work with other Federal agencies and health organizations to identify critical problems amenable to solution by the application of existing NASA technology.

Public-sector organization *representatives can learn more about application teams by contacting a nearby NASA Field Center Technology Utilization Office* [see page A4].

INDUSTRIAL APPLICATIONS CENTERS

Computerized access to over 10 million documents worldwide

Computerized information retrieval from one of the world's largest banks of technical data is available from NASA's network of industrial Applications Centers (IAC's). The IAC's give you access to 1,800,000 technical reports in the NASA data base and to more than 10 times that many reports and articles found in nearly 200 other computerized data bases.

The major sources include:

- *750,000 NASA Technical Reports*
- *Selected Water Resources Abstracts*
- *NASA Scientific and Technical Aerospace Reports*
- *Air Pollution Technical Information Center*
- *NASA International Aerospace Abstracts*
- *Chem Abstracts Condensates*
- *Engineering Index*
- *Energy Research Abstracts*
- *NASA Tech Briefs*
- *Government Reports Announcements*

and many other specialized files on food technology, textile technology, metallurgy, medicine, business, economics, social sciences, and physical science.

The IAC services range from tailored literature searches through expert technical assistance:

- *Retrospective Searches:* Published or unpublished literature is screened, and documents are identified according to your interest profile. IAC engineers tailor results to your specific needs and furnish abstracts considered the most pertinent. Complete reports are available upon request.
- *Current-Awareness Searches:* IAC engineers will help design a program to suit your needs. You will receive selected monthly or quarterly abstracts on new developments in your area of interest.
- *Technical Assistance:* IAC engineers will help you evaluate the results of your literature searches. They can help find answers to your technical problems and put you in touch with scientists and engineers at appropriate NASA Field Centers.

Prospective clients *can obtain more information about these services by contacting the nearest IAC* [see page A4]. *User fees are charged for IAC information services.*

STATE TECHNOLOGY APPLICATIONS CENTERS

Technical information services for industry and state and local government agencies

Government and private industry in Florida and Kentucky can utilize the services of NASA's State Technology Applications Centers (STAC's). The STAC's differ from the Industrial Applications Centers described on page A7, primarily in that they are integrated into existing state technical assistance programs and serve only the host state, whereas the IAC's serve multistate regions.

Many data bases, including the NASA base and several commercial bases, are available for automatic data retrieval through the STAC's. Other services such as document retrieval and special searches are also provided. (Like the IAC's, the STAC's normally charge a fee for their services.)

To obtain information *about the services offered, write or call the STAC in your state* [*see page A4*].

COSMIC®

An economical source of computer programs developed by NASA and other government agencies

A vast software library is maintained by COSMIC — the Computer Software Management and Information Center. COSMIC gives you access to approximately 1,600 computer programs developed for NASA and the Department of Defense and selected programs for other government agencies. Programs and documentation are available at reasonable cost.

Available programs range from management (PERT scheduling) to information science (retrieval systems) and computer operations (hardware and software). Hundreds of engineering programs perform such tasks as structural analysis, electronic circuit design, chemical analysis, and the design of fluid systems. Others determine building energy requirements and optimize mineral exploration.

COSMIC services go beyond the collection and storage of software packages. Programs are checked for completeness; special announcements and an indexed software catalog are prepared; and programs are reproduced for distribution. Customers are helped to identify their software needs; and COSMIC follows up to determine the successes and problems and to provide updates and error corrections. In some cases, NASA engineers can offer guidance to users in installing or running a program.

Information about programs *described in NASA Tech Briefs articles can be obtained by completing the COSMIC Request Card at the back of this issue. Just circle the letters that correspond to the programs in which you are interested.*

NEW PRODUCT IDEAS

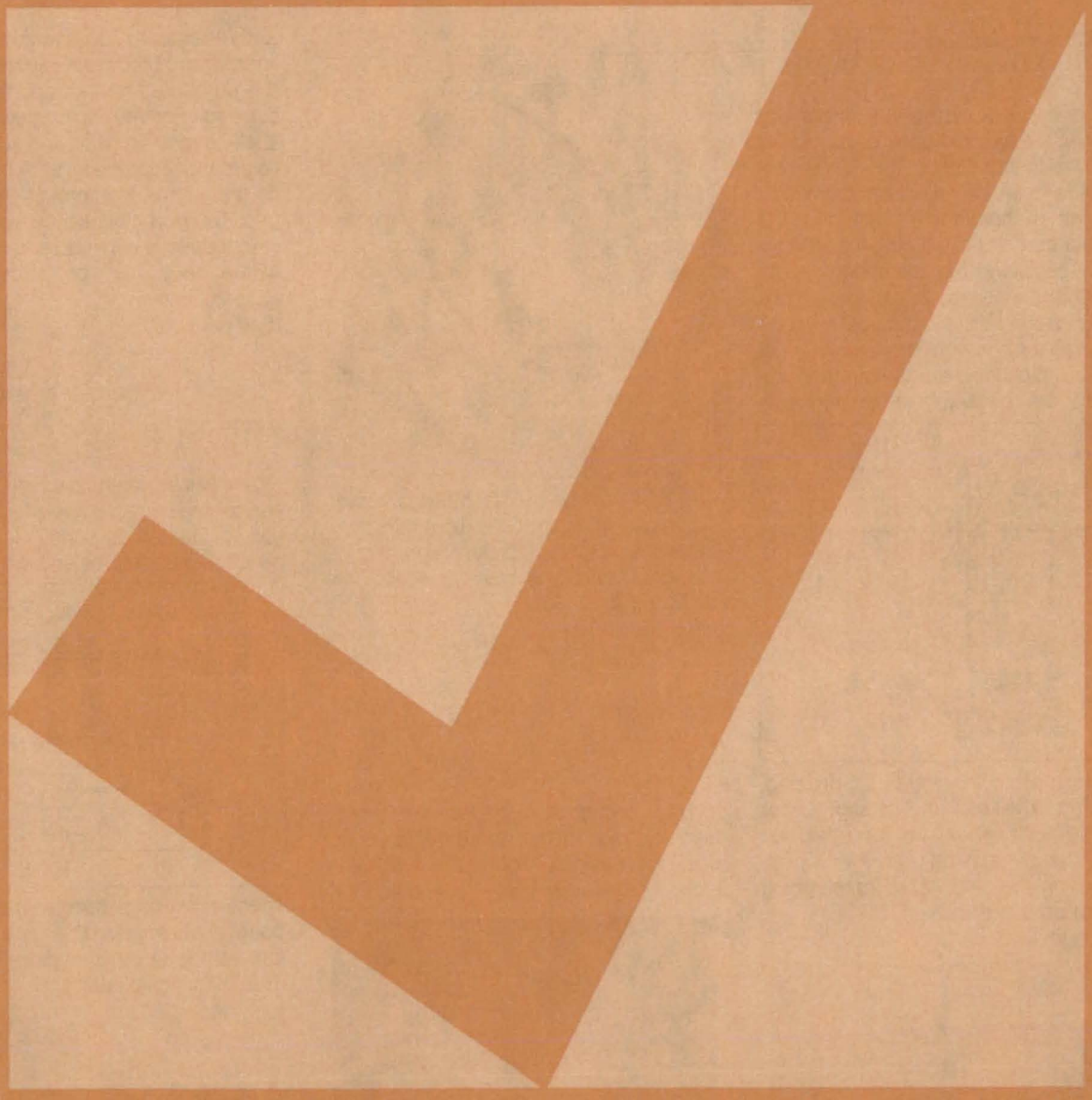

NEW PRODUCT IDEAS are just a few of the many innovations described in this issue of NASA Tech Briefs and having promising commercial applications. Each is discussed further on the referenced page in the appropriate section in this issue. If you are interested in developing a product from these or other NASA innovations, you can receive further technical information by requesting the TSP referenced at the end of the full-length article or by writing the Technology Utilization Office of the sponsoring NASA center (see page A4). NASA's patent-licensing program to encourage commercial development is described on page A6.

Quick-Disconnect Fastener

A proposed quick-disconnect fastener for two or more parts resists shear loads and torque. It would center the parts to be joined, clamp them, and then tighten them into a single unit. The fastener consists of a spring-loaded hexagonal actuating pin, six springy collet fingers, and a hexagonal-nut locking collar. An adjustable locking collar compensates for component assemblies of different thicknesses. Potential applications for the removable fastener include

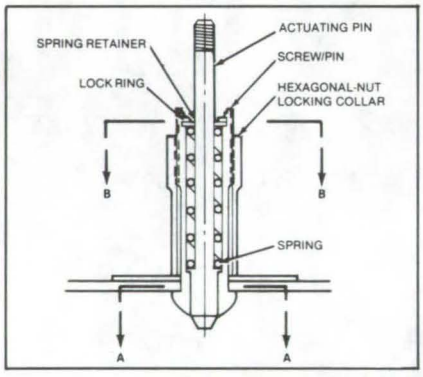

holding parts for welding, brazing, soldering, riveting, and gluing. Other possible uses would be for attaching removable panels and panels with poor access on one side and for plugging leaks in pressure vessels.
(See page 190.)

Ball Bearings Are Lubricated Automatically

Inserts on the ball-separator ring of ball bearings could provide a steady flow of lubricant to the ball surfaces. Developed for hard-to-lubricate turbopumps for cryogenic liquids, the self-lubricating bearings could be utilized on equipment for which maintenance is difficult and the lubrication interval is uncertain, such as household appliances, automobiles, and boat engines. The small inserts are made of a material rich in molybdenum disulfide and PTFE.

The material can be machined or molded. In operation, the balls rub against the inserts as they turn, picking up a film of lubricant, which is transferred to the bearing races.
(See page 196.)

Improved Gloves for Firefighters

New firefighter's gloves are more flexible and more comfortable than previous designs. There are two versions of the new glove, one made of

composite material and the other dip-coated. An aramid fabric was selected as the material for the outer shell of the composite glove because it is strong and resistant to flame and heat. For the liner, aramid felt was selected because it is puncture resistant and thermally insulating. For the dip-coated glove, the shell is coated with a yellow, flame-retardant neoprene layer. A friction layer on the palm side improves the wearer's grip. The new gloves may also find uses in foundries, steel mills, and other plants where they can be substituted for asbestos gloves.
(See page 211.)

Fiber-Optics Temperature Sensor

A new instrument uses an optical sensor to measure temperature. A small gap in the sensor widens as the temperature rises, increasing the number of

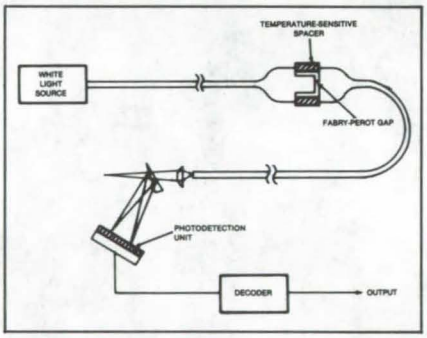

spectral bands passed to a receiver. A count of the received bands is translated into temperature changes. The instrument has digital output.
(See page 177.)

Acoustic Ground-Impedance Meter

A portable instrument uses a Helmholtz resonator to measure the acoustic impedance of the ground or other surfaces. The meter can be used in conjunction with other acoustic measurements in predicting the effects of aircraft noise. The sound pressure generated by a cam-driven piston in the chamber is measured near the ground surface by a microphone mounted flush

with the wall of the chamber. Using a five-lobed cam, sound vibrations up to 300 Hz are excited and measured. This

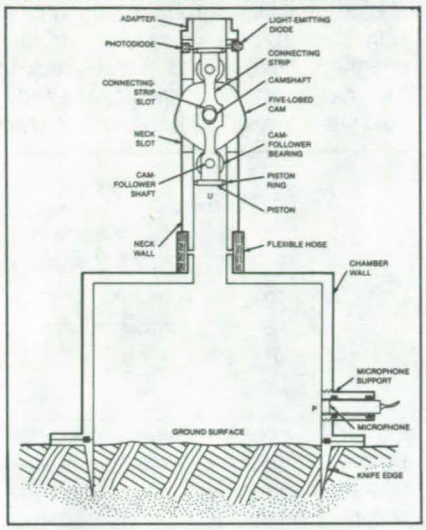

range is extended to nearly 1,000 Hz by a 15-lobed cam.
(See page 181.)

High-Performance PMR Polyimides

Highly-cross-linked PMR polyimides are formed at 600° F (315° C) from the in situ thermopolymerization of four monomer reactants. A variety of compositions are formed by adding 4 to 20 mole percent PN to the standard PMR-15 composition. These modified resins, intended for use in advanced composites, adhesives, and neat resin articles, show better processability and elevated-temperature stability than state-of-the-art PMR-15 polymers.
(See page 159.)

Metering Fluid Container

A hand-held container accepts, stores, and discharges a preset amount of fluid from a pressurized supply. The supply pressure drives a spring-loaded piston that stores enough mechanical

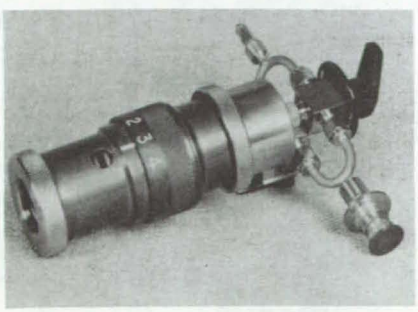

energy to discharge the measured liquid into another container. The container attaches to a fluid supply through a quick-disconnect fitting. The desired amount of fluid is selected by turning a collar that controls the length of the piston travel. Possible applications include the dispensing of toxic fluids or metering liquids for household, commercial, or laboratory uses.
(See page 189.)

Regulating Oxygen Pressure Safely

A pressure regulator for oxygen allows gas flow to be shut off on its low-pressure side rather than its high-pressure side. The initial rush of oxygen occurs in the second stage rather than in the first stage of pressure reduction. The regulator thus avoids the fire hazard associated with the rapid pressurization and consequent adiabatic heating of oxygen on the input side when the

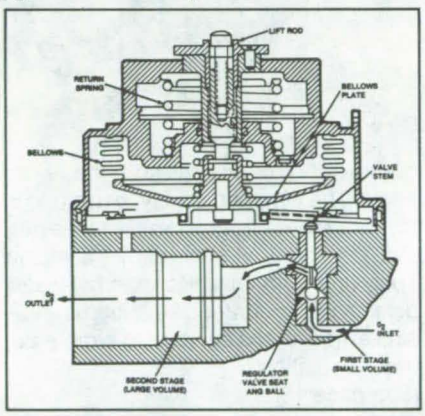

regulator is turned on. The new regulator can reduce the danger of fire in aircraft and in systems that supply oxygen for medical emergencies.
(See page 194.)

Fasteners for Solar Panels

A simple articulating linkage secures solar panels into a supporting framework. The five-element linkage collapses into a W-shape for easy placement into the framework, then expands to form a rectangle of the same dimensions as those of the panel. The result is a large retaining ring around the outer edges of the panel. Removal of the linkage is simply by the reverse of installation. The fastener could also be used on

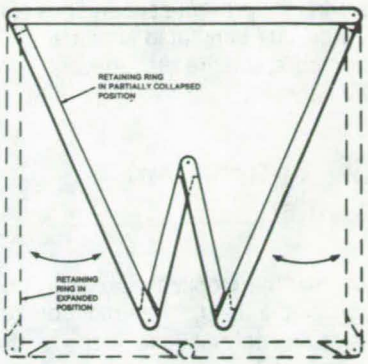

removable wall panels, photographs, and signs.
(See page 182.)

Microwaves Detect Icing on Aircraft Surfaces

A new instrument can be used in aircraft to warn pilots of the onset of dangerous ice buildup. It also has potential as a research tool in cloud studies and in investigations of icing phenomena. The instrument employs microwave waveguides implanted just below the surface to be monitored. A change in the resonant frequency of the waveguides, caused by ice buildup, is measured by a microprocessor and converted to a dc voltage that is proportional to the ice thickness. A microprocessor also computes the change in ice thickness with respect to time to obtain the ice-accretion rate. The ice thickness and accretion rates are displayed digitally.
(See page 178.)

Hydraulic Tubing Cutter

A hydraulically powered tool cuts tubing and cable in areas of limited accessibility. Mounted on one end of a flexible "gooseneck" extension, the cutter jaws are closed by a hydraulic piston when the operator squeezes the handle grip. The jaws are released by flipping an on/off lever. The hydraulic cutter was originally designed to deactivate aircraft ejection seats in rescue operations by

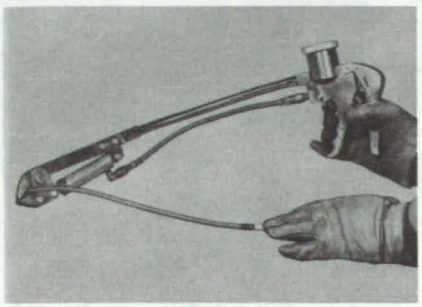

severing the pressure supply lines to the ejector. It can also be useful in automobile and fire rescue work.
(See page 199.)

Solvent-Resistant Polymer

A new thermoplastic polymer incorporates the best properties of polyimides and polysulfones. It can be used

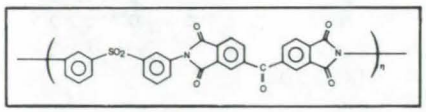

as a molding resin, as an adhesive, and as a matrix resin for fiber-reinforced composites. The new structure is obtained by incorporating an aromatic sulfone moiety in the backbone of an aromatic linear polyimide to yield an aromatic poly(imidesulfone) prepared in bis(2-methoxyethyl) ether solvent. This polymer system results in a thermoplastic with better processability than the base polyimide. The incorporation of an imide segment into the base polysulfone results in a polymer that is insoluble in common solvents.
(See page 159.)

Easy-Change Terminal Strip

A laminated copper and polyimide terminal strip makes it easy to modify a printed-circuit board, after the board has

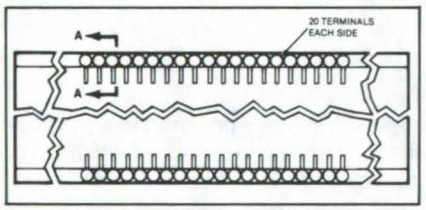

been fabricated. The "easy-change" strip is composed of two parallel rows of pins on an insulating base. It is epoxied over conductors or an insulating portion of the PC board. Copper conductors, attached to the pins, serve as bonding pads for integrated-circuit leads. The strip can be bonded to a board directly over existing conductor patterns, making it unnecessary to remove unused portions of the circuit pattern.
(See page 134.)

Portable Pipe Wrapper

A new tool applies fragile layered insulation to cryogenic tubing. It has been used routinely to apply two layers of fiberglass and one layer of aluminum foil on pipe used as the inner line in vacuum-jacketed cryogenic plumbing. The new pipe wrapper has three freely revolving drums that hold the wrapping material. It

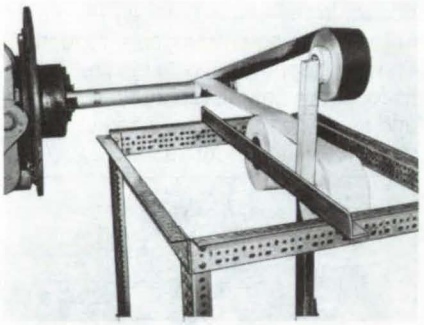

controls both tension and the wrap angle. The wrapper is easy to use and is made from inexpensive, readily available parts. It could prove useful in applying thermal insulation to hot-water pipes and refrigerant-distribution lines. A similar tool could be used to wrap electrical insulation.
(See page 198.)

Ferrofluid Would Seal a Linear-Motion Valve

A proposed valve would employ a ferrofluid to make a tight seal against vacuum and pressure. The seal would require no precisely machined parts, and hand lapping of valve seats would be unnecessary. The valve consists of a hollow shaft with magnetically soft sheaths that slide through a ring magnet with annular pole pieces. A ferrofluid (magnetic fluid) is held in place around the shaft by the ring magnet. The ferrofluid seals the space between the shaft

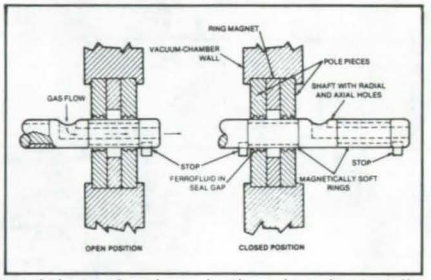

and the pole piece in the chamber wall. If more than one ferrofluid seal is used on a shaft, the valve could be used as a switching valve in a plumbing system.
(See page 197.)

Multipanel Trough Solar Concentrator

A cylindrical solar concentrator composed of many flat-plate mirrors is efficient even when pointing away from the Sun by as much as 5°. The concentrator is designed to backlight an array of photovoltaic cells. However, unlike ordinary backlit concentrators, the multiple-flat-plate reflector does not lose

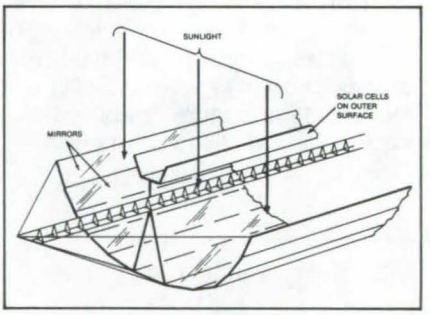

very much efficiency if it is slightly out of alinement with the Sun. The design is economical and easy to fabricate.
(See page 206.)

Electronic Components and Circuits

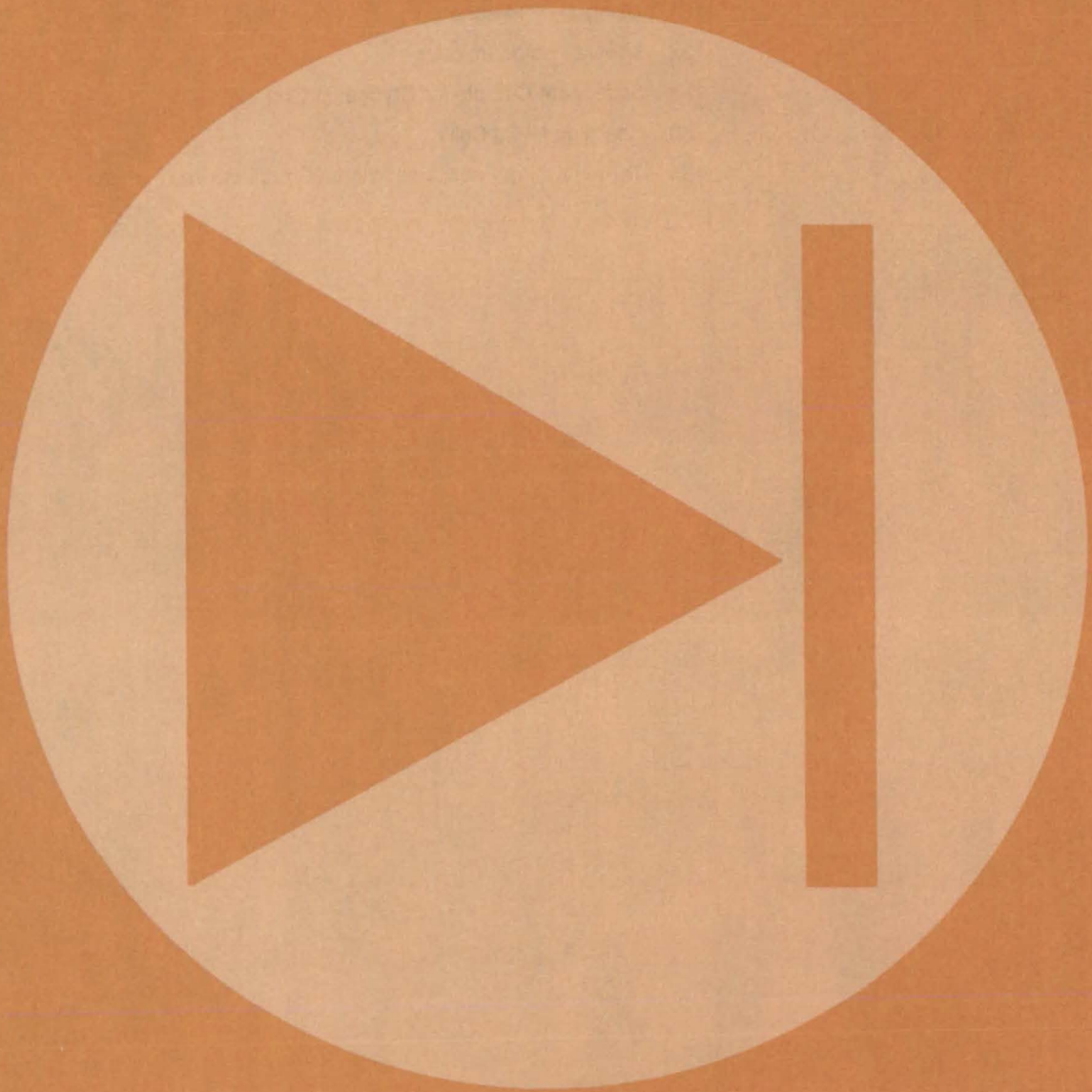

Hardware, Techniques, and Processes

Voltage Regulator for a dc-to-dc Converter

An extra transformer winding eliminates the need for isolation components.

NASA's Jet Propulsion Laboratory, Pasadena, California

A voltage regulator for a dc-to-dc converter momentarily short-circuits the secondary winding on its drive transformer. The short circuit temporarily turns off the drive to the output transistors. In effect, the short circuit changes the width of the drive pulses, thereby regulating the output voltage.

The new voltage regulator isolates signals from the power-switching converter without the use of complex circuitry or optical couplers. The only addition is an extra secondary winding on the existing interstage transformer. Error signals short-circuit the new winding and inhibit converter action. A resistor in series with the primary winding limits the short-circuit current to prevent damage to circuit components.

In the circuit (see figure), a signal representing the instantaneous voltage at the 12-volt regulated output is sampled and applied through a resistor network to the inverting input of an error amplifier. A nonvarying reference voltage established by a Zener diode is applied to the noninverting input of the error amplifier. The error amplifier operates in a closed loop with a fixed gain. When the sampled regulated output is at precisely 12 volts, the error amplifier dc output does not change. However, microvolt changes in the sampled voltage — either upward or downward — produce significant shifts in the error amplifier dc output level. This changed output is the error signal used for regulation.

The error signal is applied to the inverting input of a voltage comparator and a ramp voltage is applied to the noninverting input. The ramp-voltage input to the comparator is generated in the following way: A constant current is supplied to the capacitor C_R by the constant-current diode D_{CC}. The discharge of the capacitor is controlled by a positive-going spike applied to the base of transistor Q_1. A diode-bridge doubler provides the spike pulses at twice the frequency of the synchronizing pulses furnished by the clock circuit. Capacitor C_R charges — producing a linearly increasing voltage — until a spike discharges it, whereupon it starts to charge again until the next spike discharges it.

The voltage comparator modulates the ramp with the error signal, raising or lowering the ramp peak. The output of the comparator short-circuits the output of the interstage current-limiting transformer through diodes D_{10} and D_{11} of the center-tapped secondary winding L_{12} — the extra winding added to the interstage transformer. When the output of the comparator goes high, L_{12} is essentially open circuited. During the interval when the comparator output goes low, both diodes go to ground, short-circuiting the winding and therefore removing drive current from the switching transistors. The output pulses from the transistors are thus shortened by the amount of this interval, and the output voltage is proportionately reduced.

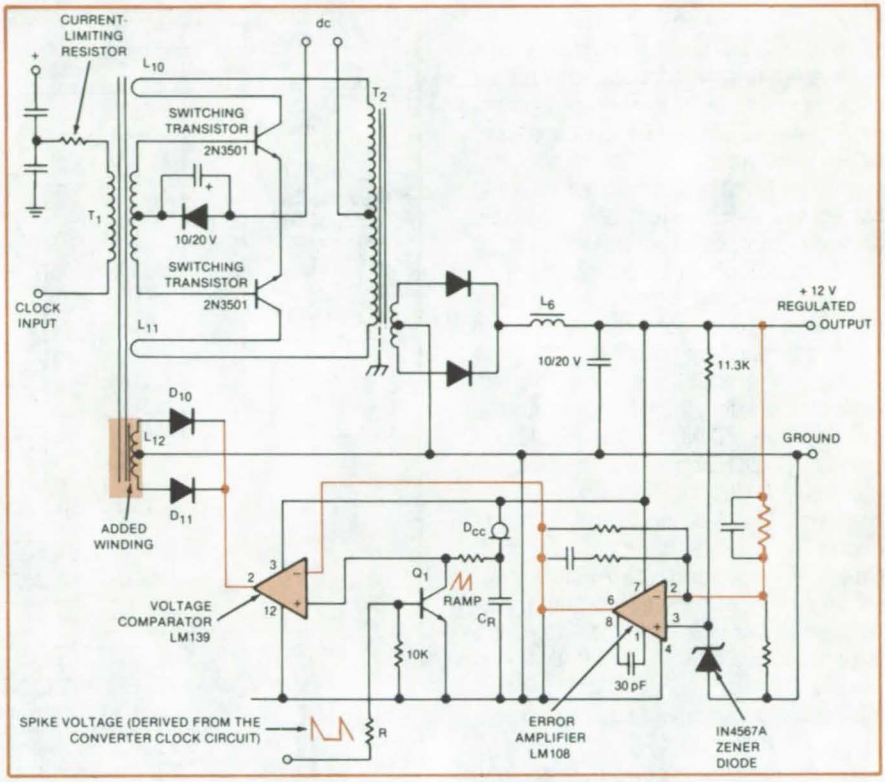

The **Feedback Path** applies a shorting signal to winding L_{12} if the output voltage strays from the 12-volt nominal level. There is virtually no interaction between the regulation voltages and the power-switching portions of the dc-to-dc converter.

This work was done by Colonel W. T. McLyman of Caltech for **NASA's Jet Propulsion Laboratory.** *For further information, Circle 1 on the TSP Request Card.*

NPO-15208

Microprogramed Sequencer for Tunable RF Oscillator

Standard IC chips and digitally tuned oscillator are combined.

Langley Research Center, Hampton, Virginia

A circuit originally designed to "dither" the transmitter frequency of a K-band radar at high rates may find application in such other areas as automated test equipment or computer-controlled receiver tuning. The circuit consists of a PROM-based microprogramed control sequencer, which drives a group of diode switches to select one of eight tuning capacitors in an L-C oscillator.

A synchronizing pulse is used to clock the various mode-control inputs and a "next address" into the 74LS377 latch shown in the circuit diagram. The outputs of the latch then become an address for the PROM, and the PROM outputs $DO_5 - DO_7$ form a 3-bit code to determine the desired frequency for the oscillator. The 3-bit code is further decoded in the 74S138 1-of-8 decoder. Only one output from the 74S138 is active at a time, and the active output provides a current sink for the PIN diode switch connected to it. All other diodes in the array are cut off, and only one tuning capacitor is active at a time, except for parasitic effects.

The control inputs perform the following functions:

- The WIDE/NARROW switch selects either a wideband sweep (i.e., large separation between frequencies) or a narrowband sweep (i.e., small deviations close to the undeviated carrier).
- The MANUAL/AUTO switch allows an operator to take control of the system and select any one of the eight frequencies using the thumbwheel switch.
- The DEFAULT/NORMAL input is provided to allow removal of the control switches and thumbwheel switch by disconnecting a connector. The connector provides a return to ground for the A_8 input to the PROM. When disconnected from the control switches, the circuit defaults to an automatic wideband sweep mode.

The contents of the TBP18S42 PROM are determined by the desired sequence of frequencies. Bits $DO_1 - DO_3$ form the memory address of the next desired frequency. Bits $DO_5 - DO_7$ are an encoded version of the current desired frequency. The sequence is arbitrary.

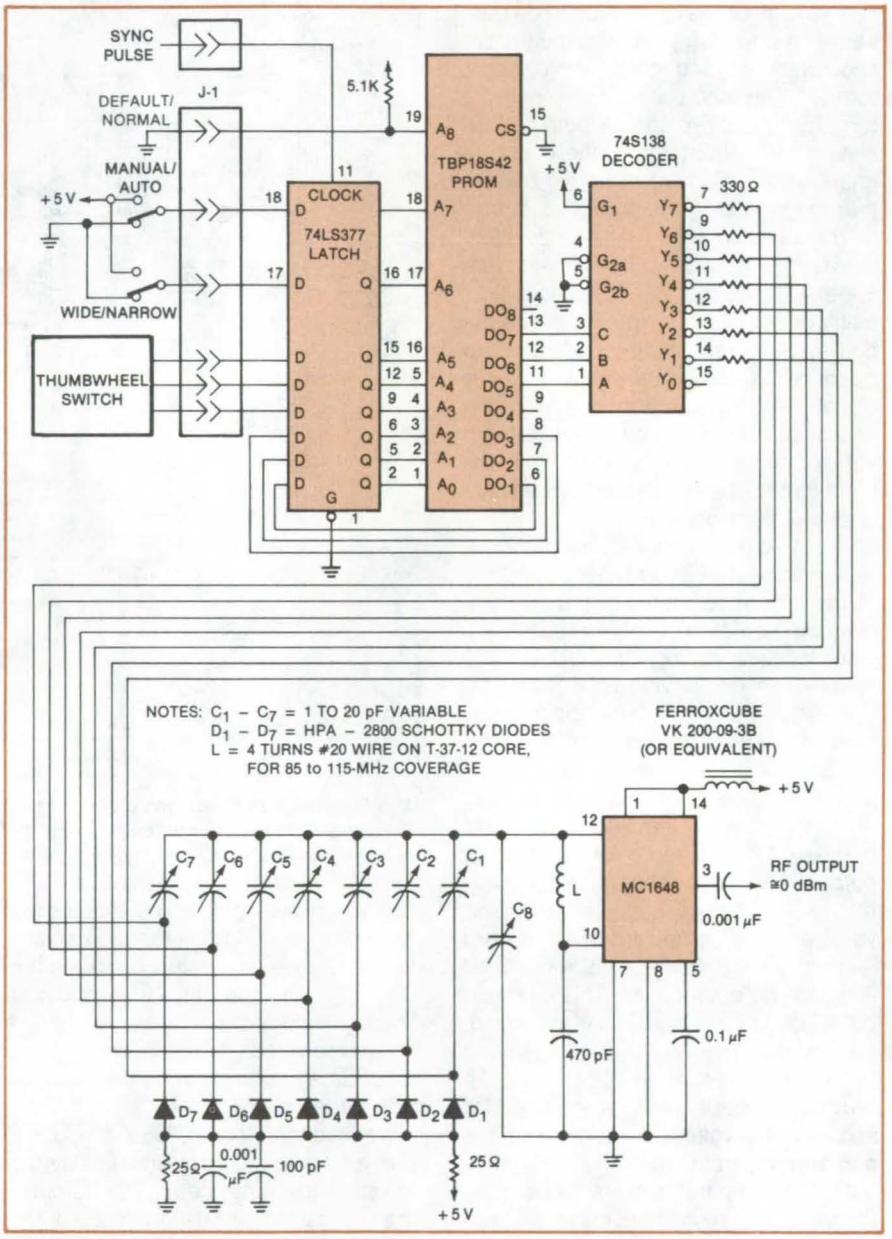

Standard IC Chips are combined with a digitally-tuned RF oscillator in the programable frequency source.

The oscillator is required to provide a near-sinusoidal signal, the frequency of which is controlled by the tuning capacitance and the amplitude of which is constant with changing frequency. This system utilizes an emitter-coupled-pair circuit in the form of an MC1648. The tuning system is actually a "delta" tune approach, in which the highest frequency is determined by the main tuning capacitor, C_8, and frequency deltas are produced by shunting appropriate trimmer capacitors to ground via a PIN diode. This approach, as opposed to using separate tuning capacitors, results in less interaction between tuning adjust-

ments, potentially better stability, and faster switching since a small capacitance is involved.

The procedure for setting the frequency is to start with the highest frequency and progress down to the lowest frequency. There is a slight interaction because of the residual shunt capacitance of the diodes in the "off" state, making it necessary to perform this procedure twice to achieve precise adjustments of all eight frequencies.

This work was done by Richard H. Couch, Chase P. Hearn, and James B. Williams of **Langley Research Center.** *No further documentation is available.*
LAR-12903

Tangleproof Rotary Electrical Coupling

Electrical cables are carefully dressed to permit 320° rotation.

Marshall Space Flight Center, Alabama

A new rotary coupling connects a large number of elecrical cables to a turntable without stressing the cables or tangling them. The device accommodates 246 cables containing a total of 758 conductors and allows the turntable to rotate through an arc of 320° (see figure). At the extremes of rotation (±160°), the cables are loose enough that they are not pulled taut and overstressed. At the halfway point (0°), the cables are not so loose that they become entangled.

The cables are held in a hollow shaft 5 inches (12.7 cm) in diameter and 18 inches (45.7 cm) long. At the rotating end of the shaft, the cables are distributed among five large circular holes around the periphery of a disk. At the ends of the shaft, the cables are bunched together and embedded in a resilient potting compound. The cables thus form a shape reminiscent of a truncated cone with the narrow portion at the fixed end of the coupling. The conical configuration prevents undue slackness or tension.

The rotary connector was developed to carry electrical signals to and from a telescope platform on a satellite without a complex and electrically noisy set of slip rings. The principle is also suitable to rotary actuators.

This work was done by Franz Keller of American Science & Engineering, Inc., for **Marshall Space Flight Center.** *No further documentation is available.*
MFS-25174

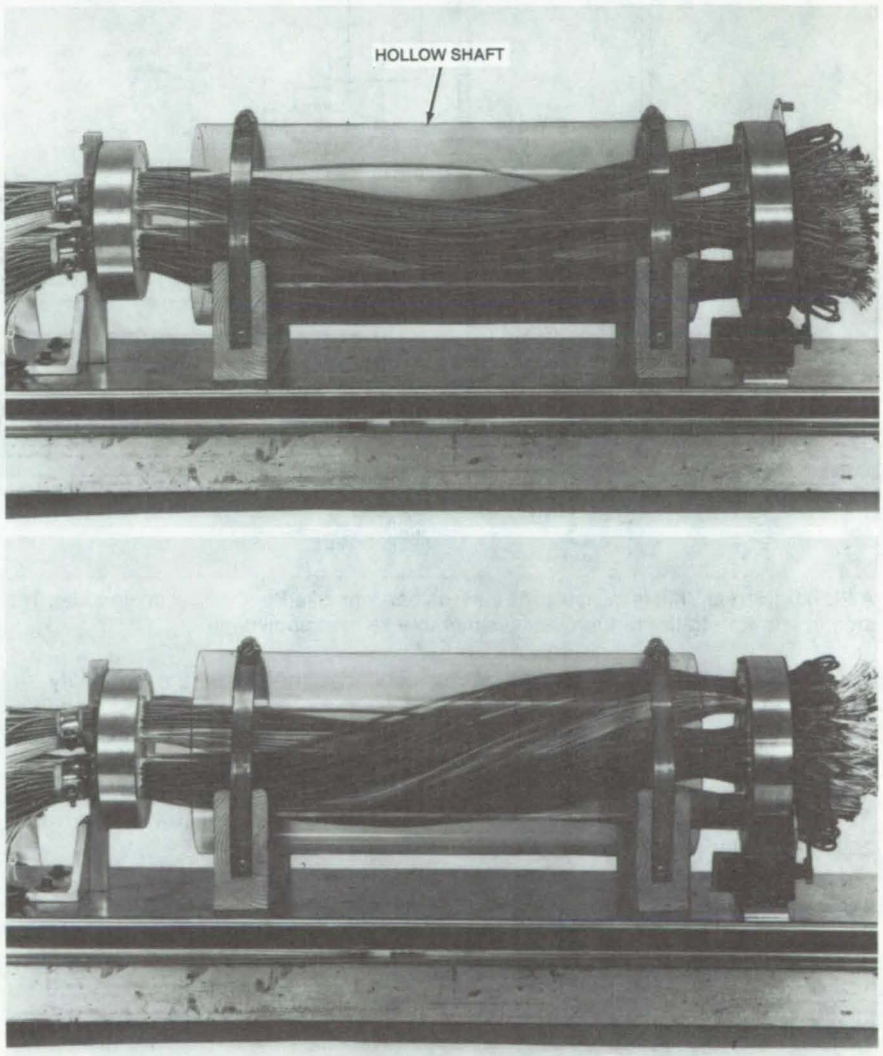

In Life-Cycle Tests, a rotary coupling was turned back and forth through an arc of ±160°. The top photograph shows the assembly at +40° rotation: The cables sag against the transparent containing tube but are not tangled. The lower photograph shows the cables at −140° rotation: They are not tight and will not become tight at −160°.

VLSI Reed-Solomon Encoder

Very-large-scale integrated chips are cascaded to yield the desired level of reliability.

NASA's Jet Propulsion Laboratory, Pasadena, California

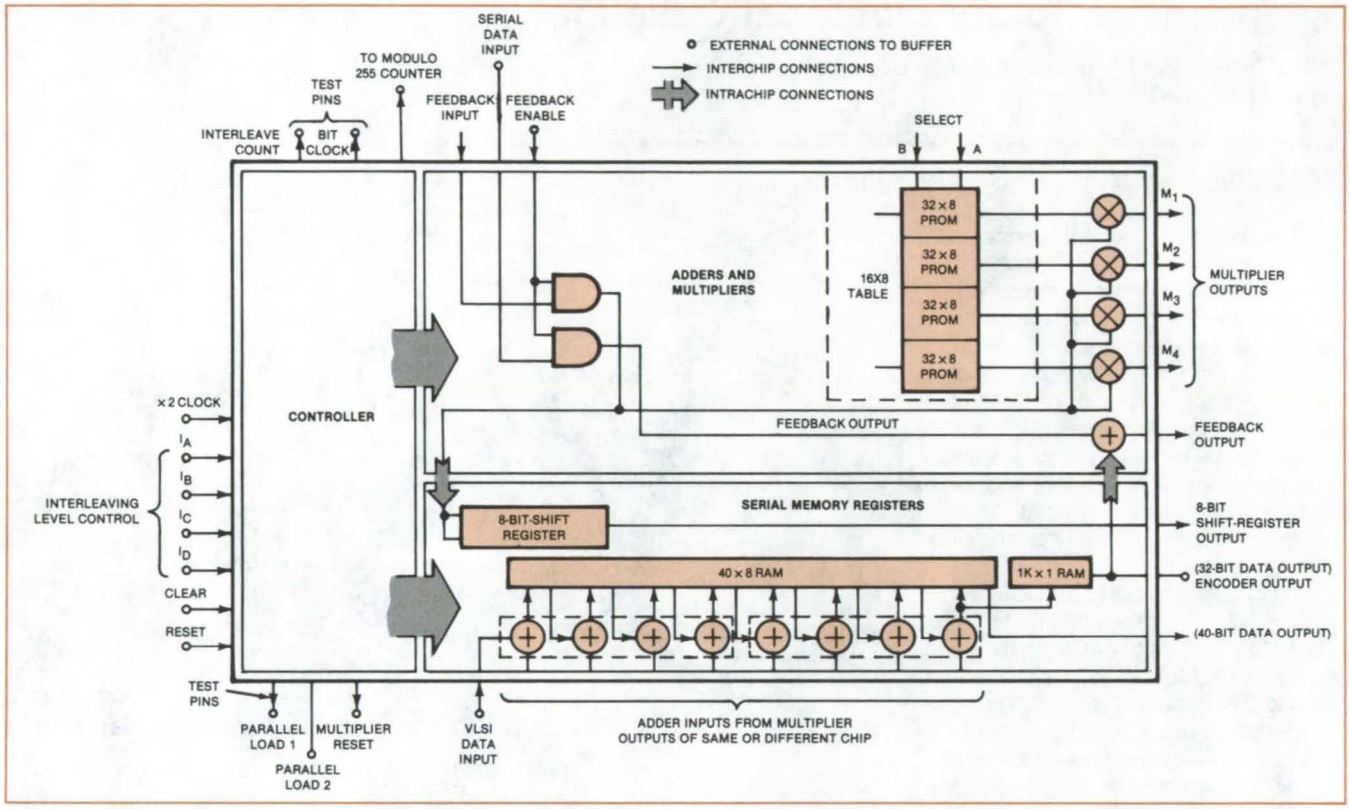

A **VLSI Universal Chip** is used for the various portions of a Reed-Solomon encoder. The chip has been designed in a shift-register version in addition to the random-access-memory version shown here.

A modular Reed-Solomon encoder uses identical custom VLSI chips called "symbol slices." By cascading and properly interconnecting a group of these chips, an encoder can be made for any desired error-correcting capability and interleaving level.

Two versions of the symbol-slice chip have been designed: One uses shift registers as the internal serial memory while the other uses a random-access memory (see figure). The multiplier configuration is the same in both.

Reed-Solomon codes are used to detect and correct random and burst errors in the transmission of binary signals. The coding may be simple or complex, depending on the reliability required for the application. Concatenated (interlinked) coding systems using Reed-Solomon codes have been suggested for space-communication channels requiring low error probabilities.

The new VLSI chips are utilized in an encoder in which the Reed-Solomon code is concatenated with a Viterbi convolutional code in five-level interleaving. (The Reed-Solomon code is the outer code.)

The chips use internal serial memory and a read-only memory (lookup table). Serial input and output circuits, together with a two-phase serial parallel finite-field multiplication circuit, and on-chip clock control circuits keep the number of input and output pins to a minimum. To minimize the number of multipliers required, a generator polynomial that yields symmetrical coefficients is used in a special interchip-connection technique. The resulting VLSI encoder requires only one-tenth the number of chips required by a conventional Reed-Solomon circuit implemented with discrete IC's.

This work was done by Kuang Y. Liu of Caltech for **NASA's Jet Propulsion Laboratory.** *For further information, Circle 2 on the TSP Request Card.*
NPO-15470

Using SAW Resonators in RF Oscillators

Two circuits illustrate the potential of surface-acoustic-wave resonators.

Ames Research Center, Moffett Field, California

Surface-acoustic-wave (SAW) resonators are used as the frequency-determining elements in radio-frequency oscillator circuits at NASA's Ames Research Center. The oscillators can be frequency-modulated, phase-modulated, or pulse-modulated. Two such circuits are described here.

The SAW resonators are especially applicable to low-power subminiature applications, such as biotelemetry and wind-tunnel instrumentation, where they can advantageously replace crystals. The resonators are smaller than crystals and very thin — an advantage where small package size is important. They are fabricated with integrated-circuit techniques, so their use in place of crystals gives promise of totally-integrated telemetry systems in the future. SAW oscillators can be directly modulated without the need for the multiplying stages often required with crystals, which simplifies the circuitry and further reduces size.

The transistor used as the amplifying element in the oscillator has three connections, and the two-port SAW resonator has four. Therefore numerous circuit configurations are possible. Figure 1 shows a single-pole two-port SAW resonator used as the frequency-controlling element in a Colpitts-type oscillator operating at 150 MHz. The SAW device uses an ST-cut quartz substrate to achieve a higher temperature stability than can be obtained with other substrates, such as lithium niobate or lithium tantalate. However, since the ST-cut quartz has a higher insertion loss than the other substrates, the voltage is fed back directly from the collector rather than from a capacitor tap as is usual with this type of oscillator. The variable capacitor is adjusted for resonance at the operating frequency. This version of the oscillator can be used with supplies ranging from 1 to 6 volts, and current drains as low as 0.4 mA can be achieved by increasing the values of the bias resistors.

(continued on next page)

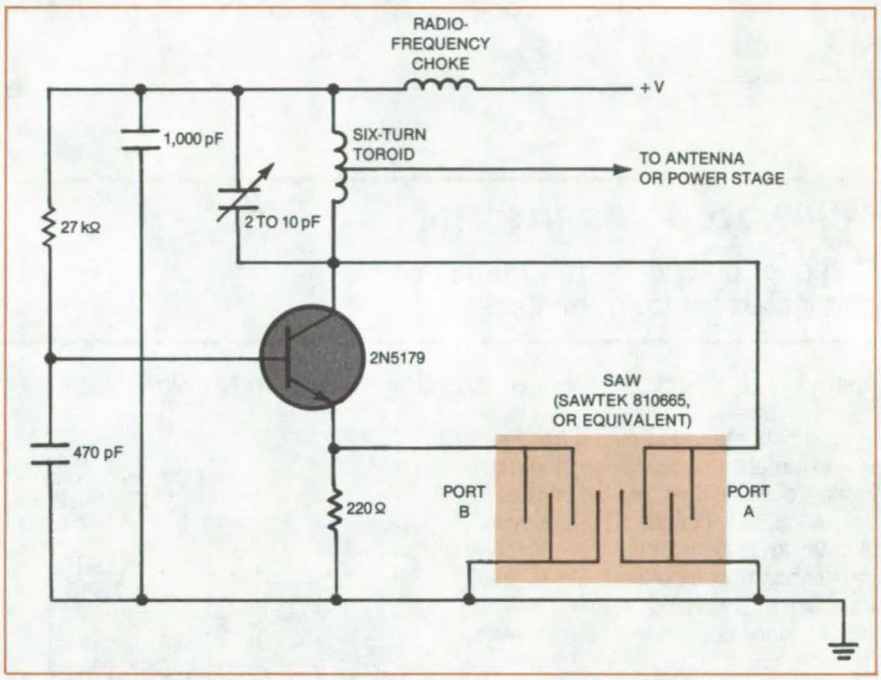

Figure 1. This **Integrated-Circuit Oscillator** operates at a frequency (150 MHz) determined by the surface-acoustic-wave resonator.

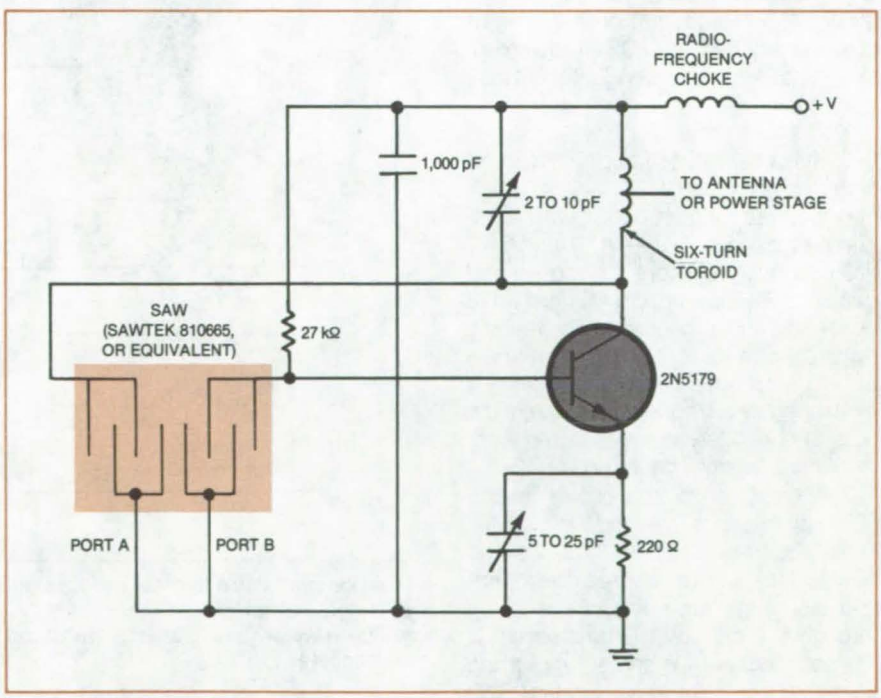

Figure 2. This **Base/Emitter-Tuned Circuit** isolates the frequency-control elements from the output circuit; but, unlike the circuit in Figure 1, a separate tuning is needed for the collector and base/emitter circuits.

Frequency trimming or modulation is accomplished with the mechanically variable or voltage-variable capacitor between the SAW resonator and the emitter of the transistor; deviations of up to 100 kHz are possible without the loss of frequency stability. For pulse modulation, the 27-kilohm bias resistor is connected to a control voltage source that swings from ground to the positive supply level.

A second circuit that uses the SAW device is shown in Figure 2. This circuit is base/emitter-tuned, with the voltage fed back from the collector. Again, frequency trimming is accomplished with a variable capacitor at the emitter of the transistor, while the collector capacitor can be used to peak the power output. Pulse modulation is accomplished in the same manner as in the circuit of Figure 1.

Of the two circuits, the first is easier to frequency-modulate and only requires a single adjustment for peaking output power. However, the second circuit isolates the frequency-control elements from the output circuit, providing better frequency stability when the output is loaded than does the first circuit.

This work was done by Richard M. Westbrook and Gordon J. Deboo of **Ames Research Center.** *No further documentation is available.*
ARC-11390

Milliwatt dc/dc Inverter

Compact unit shifts dc voltage level and isolates it from the input.

NASA's Jet Propulsion Laboratory, Pasadena, California

Only one integrated circuit and just a few external components are needed to make a dc-to-dc inverter with isolated input and output voltages. The required IC is a hex inverter, such as the 7404, and the outboard components are a small transformer, two diodes, and a few resistors and capacitors. The inverter gates function as the switching oscillator and the driver amplifier for the circuit. If the IC is a transistor-transistor-logic (TTL) module, the inverter delivers 100 to 150 milliwatts; if only microwatt power is required, a CMOS (complementary metal-oxide semiconductor) IC may be used.

The figure shows an inverter circuit that has been designed, built, and tested. It uses the CMOS 74C04, which contains six independent inverters. Three of the inverters — A, B, and C — are used with resistors R_1 and R_2 and capicitor C_1 to form a square-wave generator that produces the switching required for voltage inversion. Operation at 100 kHz is feasible. This relatively high operating frequency reduces the size of the filter capacitors required, resulting in a small packaged unit.

The oscillator output power is amplified by inverters D, E, and F in parallel. Their square-wave output allows the 10-Vdc local power source to charge and discharge capacitors C_2 and C_3 through the primary of transformer T. The secondary of T is center-tapped and connected to a full-wave rectifier (two 1N916 diodes) to charge a 0.1-microfarad capacitor to the new, isolated, output voltage level.

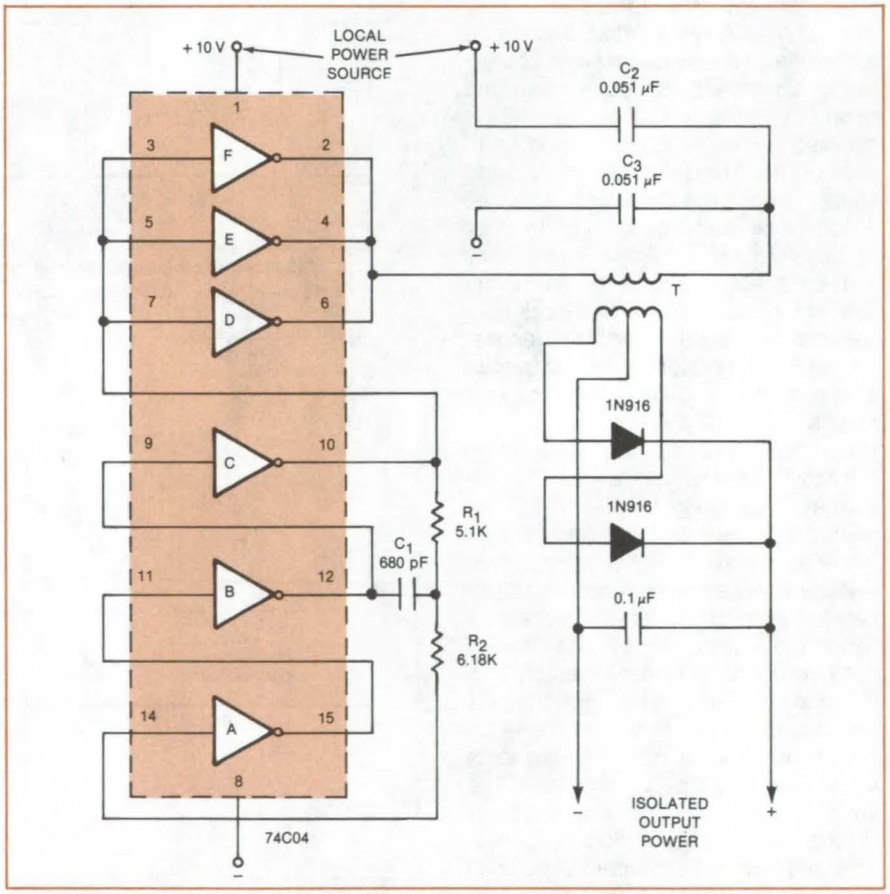

This Compact dc/dc Inverter uses a single integrated-circuit package containing six inverter gates that generate and amplify a 100-kHz square-wave switching signal. The square-wave switching inverts the 10-volt local power to an isolated voltage at another desired level.

This work was done by Colonel W. T. McLyman of Caltech for **NASA's Jet Propulsion Laboratory.** *For further information, Circle 3 on the TSP Request Card.*
NPO-15157

Solid-State Circuits for Cryogenic Operation

Selected commercially available components perform satisfactorily at 1.25 K.

NASA's Jet Propulsion Laboratory, Pasadena, California

Tests at NASA's Jet Propulsion Laboratory confirm the operation of five commercial semiconductor devices at cryogenic temperatures. The five devices — one tunnnel diode, one field-effect transistor, and three CMOS integrated circuits — all perform well in circuits immersed in a liquid-helium bath. For some of the tests, the bath temperature was reduced to 1.25 K by pumping.

While intrinsic semiconductors such as pure silicon and pure germanium turn into insulators at cryogenic temperatures, some extrinsic materials, such as InSb and GaAs, retain free charge carriers and are candidates for low-temperature semiconductor devices. In addition, devices that produce free carriers by field effect, rather than by thermal excitation, and devices dependent on carrier tunneling are also possibilities for cryogenic operation. Circuit properties vary from batch to batch, however, and each unit has to be tested to verify its performance in a cryogenic environment.

The transistor tested for the NASA work is a low-current 3N128 MOSFET. It was used in a buffer amplifier operating at supply voltages between 2.3 and 7 volts dc. Low-current, low-power operation is important for cryogenic operation since large power dissipation would rapidly boil off the liquid helium. Power consumption for the transistor was about 1 milliwatt.

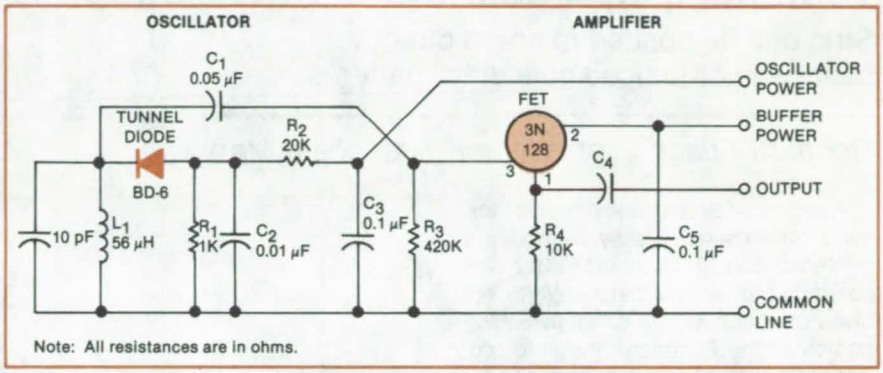

An **Oscillator/Buffer Amplifier** circuit that operates reliably at both normal and cryogenic temperatures, after repeated cycling between the two, uses a tunnel diode for the 4-MHz oscillator and a MOSFET source follower for the amplifier.

The figure shows the amplifier circuit and a tunnel-diode oscillator circuit, both of which performed well at temperatures below 4.2 K. The BD-6 tunnel diode has been used previously for low-temperature work; however, designers may be interested in the specific circuit configuration shown here. Metal-film resistors are used since the resistance of carbon increases substantially at low temperature.

A multiplexer circuit for signals from 133 liquid-level sensors was assembled using CD4051 CMOS multiplexers, a CD4028 BCD-to-decimal decoder, and a CD4049 buffer/level converter. Drivers for the circuit were located outside the cryostat, but the main circuit elements were operated in liquid helium. The liquid-level sensors were short lengths of constantan-alloy wire covered by a superconducting alloy with a transition temperature of 2.9 K.

This work was done by Dusan Petrac and Robert L. Spencer of Caltech for **NASA's Jet Propulsion Laboratory.** *For further information, Circle 4 on the TSP Request Card.*
NPO-15255

Charging Ni/Cd Cells

Procedure is faster, reduces heating, and yields a higher end-of-charge voltage.

Goddard Space Flight Center, Greenbelt, Maryland

A new procedure for recharging nickel/cadmium batteries is fast and eliminates overcharging. The method charges "dead" cells using current increments rather than continuous, constant current.

Formerly, Ni/Cd cells removed from storage were activated by a C/20 charging current (i.e., an amperage equal to one-twentieth of the ampere-hour capacity of the battery) maintained for 48 hours. This practice involved an overcharge of 100 percent, which evolved a great deal of heat. The end-of-charge voltage was relatively low because of the low charging rate and the elevated temperature.

The new procedure starts with a low charging rate (C/20) for 8 hours to remove some of the passive material that adds to the impedance of the electrochemical cell. Then the charging rate is maintained at C/10 for another 6 hours. Next, the cell is charged at C/5 until 1.435 volts per cell are reached. Charging is continued at this fixed voltage until

(continued on next page)

the current has tapered down to the C/10 to C/20 rate.

The time required for the procedure is approximately 18 hours, and the correspondingly reduced overcharging reduces the generation of heat. A further advantage is that the cells are more electrochemically active than after the 48 hours of charging by the old method.

This work was done by Gerald Halpert and C. Michael Tasevoli of **Goddard Space Flight Center.** *No further documentation is available.*
GSC-12779

Terminal Strip Facilitates Printed-Circuit Board Changes

Strip can be bonded to board directly over used or unused conductor patterns.

Goddard Space Flight Center, Greenbelt, Maryland

A laminated copper and polyimide terminal strip makes it easy to modify a printed-circuit (PC) board, after the board has been fabricated. When epoxied over conductors or an insulating portion of the PC board, the strip provides a series of solder-coated copper conductor pads to which integrated-circuit leads can be soldered for functional changes. The terminal strips can accommodate the leads on a dual, in-line IC package or as staggered single or multiple leads on planar mounted flat-packs.

The conductors are laminated to a polyimide base (see figure) with each conductor brazed to a copper pin. Wires soldered to the pins connect the integrated circuit to other components on the circuit board.

The terminal strip is bonded to a circuit board with an epoxy adhesive. It can be attached over any existing metalization. The strip-insulating base of polyimide makes it unnecessary to remove unwanted patterns on the board. It is usually unnecessary to disconnect unwanted patterns in other layers of a multilayer board by drilling out plated-through holes. However, plated-through holes can be used when needed to connect strip-soldered leads of integrated circuits on opposite sides of a board.

With the new terminal strip, changes can be made at any stage of circuit-board population, up until the installation of the board in the final product. Besides serving as a soldering pad for integrated-circuit leads, the terminal strip can perform the same function for the circuit-board connector inputs and outputs when their links with board components must be changed.

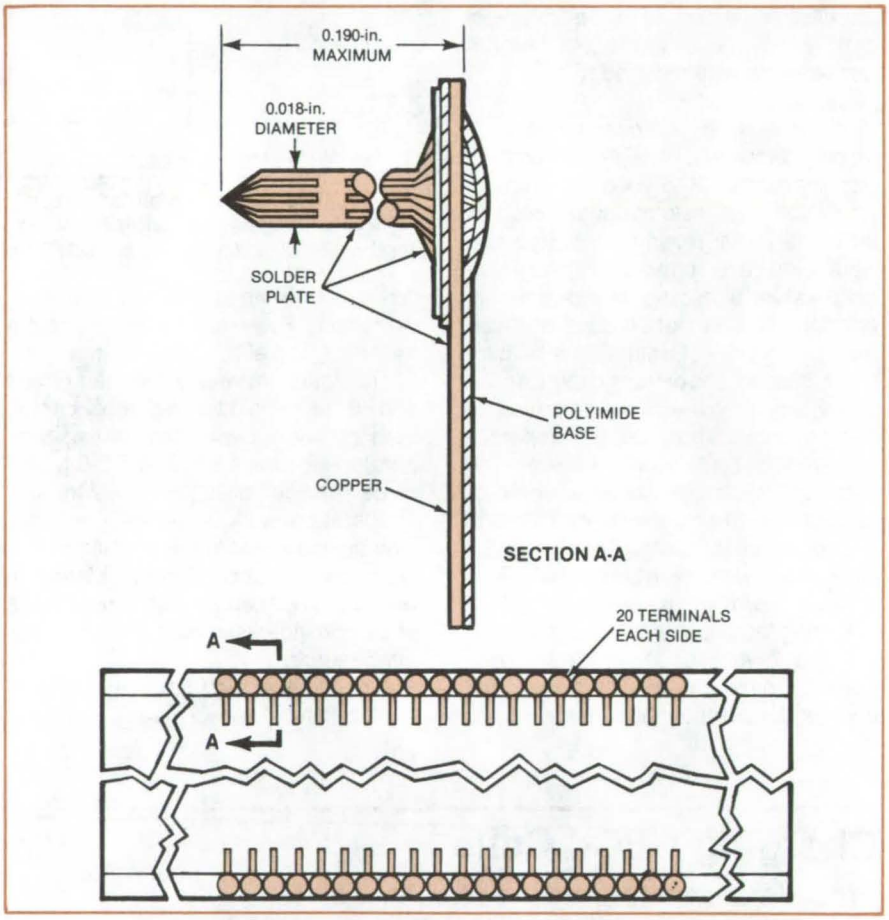

An **Easy-Change Terminal Strip** is composed of two parallel rows of pins on an insulating base. As the cross-sectional view shows, copper conductors are attached to the pins. The conductors are bonding pads for integrated-circuit leads. The length and width of the terminal strip can be chosen by the manufacturer; usually a strip contains 20 pairs of pins. The shape of the pins is optional; they can be rounded instead of pointed, for example.

This work was done by E. A. Pinto and C. E. McOsker of General Electric Co. for **Goddard Space Flight Center.** *For further information, Circle 5 on the TSP Request Card.*
GSC-12748

Electronic Systems

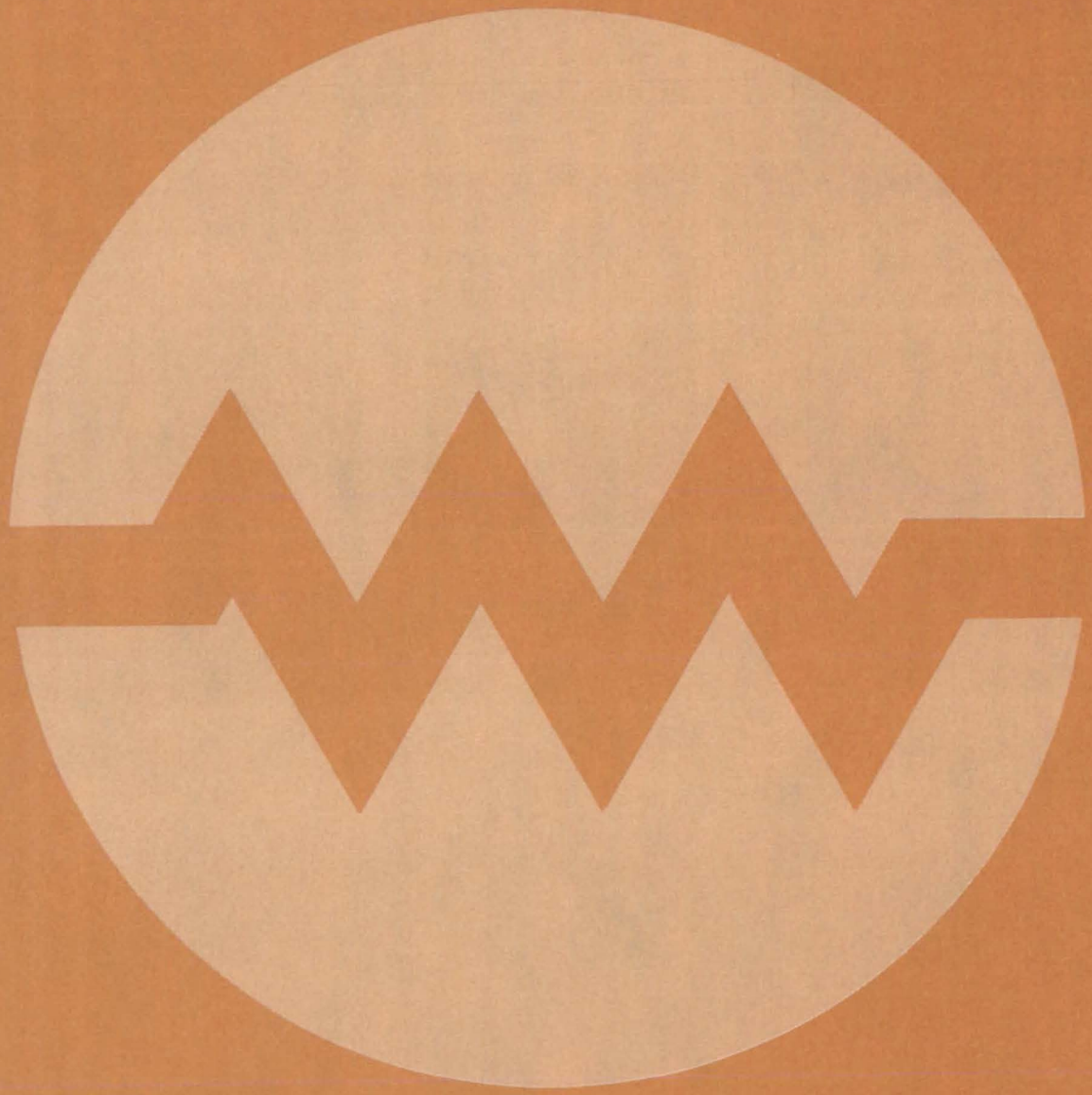

Video Target Tracking and Ranging System

A microcomputer-controlled two-camera TV system would track a moving object and determine its range and range rate.

Lyndon B. Johnson Space Center, Houston, Texas

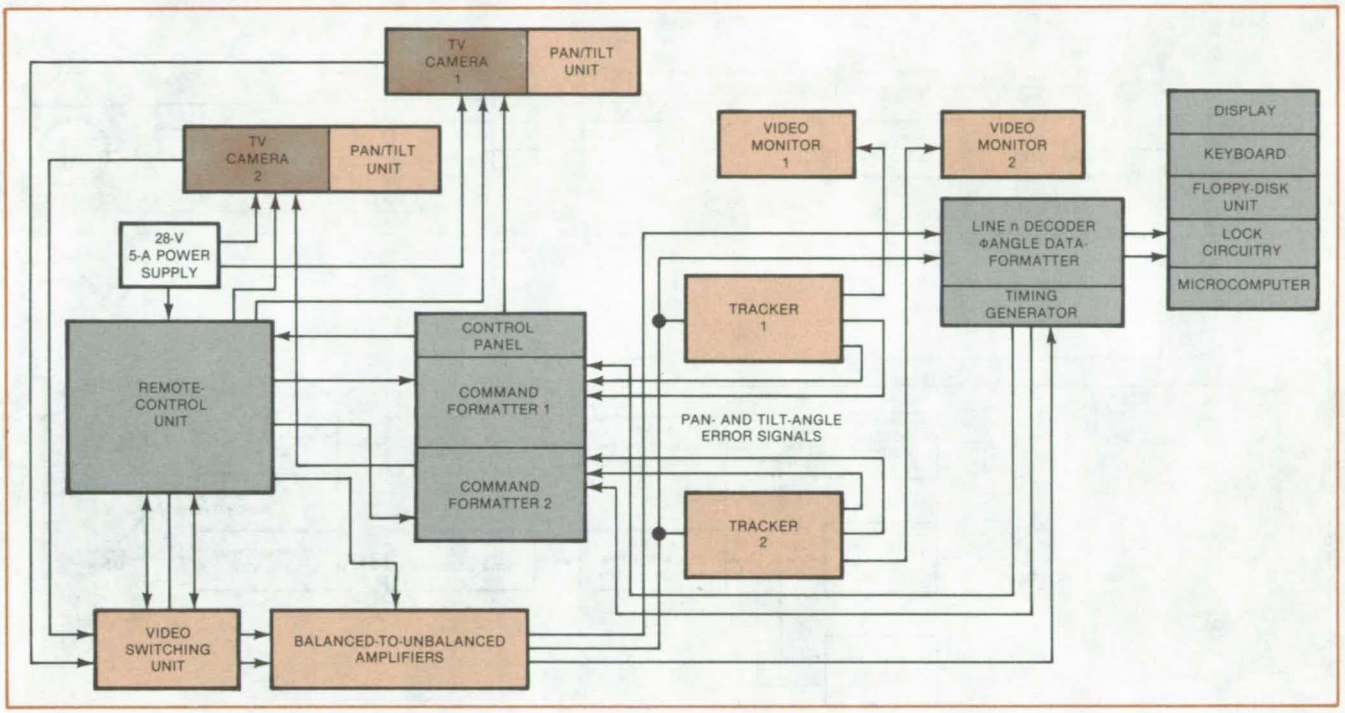

A proposed **Target Tracking and Ranging System** uses two automatic video target trackers to keep two TV cameras trained on the object being tracked. A microcomputer calculates range and range-rate information by triangulation. The input data for this calculation are the position coordinates of the two cameras and the pan and tilt aiming angles of the two cameras.

A proposed microcomputer-controlled system computes the range and range rate of a moving object being tracked by two TV cameras. The pan and tilt (azimuth and elevation) angles of each camera are controlled by correction signals derived from the camera video signals. The range and range rate of the object are computed by triangulation from pan- and tilt-angle data and known camera coordinates.

The system could be useful for target ranging at distances up to about 1,000 feet (300 m) in such applications as vehicle collison avoidance, traffic monitoring, and surveillance. It might also substitute for short-range radar in situations where the radar signal could not be tolerated.

The figure shows a block diagram of one proposed configuration. The two TV cameras are aimed at the object being tracked. They are mounted on pan and tilt units that are controlled by the remote-control unit. Camera aiming might be controlled manually in some applications; but in the configuration shown, a closed feedback loop that keeps the cameras aimed at the moving object. Each camera digitally encodes its current angle settings into one TV frame line.

The two TV signals are fed to TV monitors and to video target trackers by the video switching unit and the remote-control unit. The balanced-to-unbalanced amplifiers convert the video into the standard unbalanced format required by the trackers.

The trackers do two things: They insert cursors into the video signals to mark the camera aim points on the monitor screens, and they develop analog error-signal voltages that indicate the direction and magnitude of aiming errors in both the horizontal and vertical directions. The error signals go to zero when the target edge being tracked coincides with the cursor location. The command formatter converts the analog error signals into digital commands for the pan and tilt units to aim the cameras directly at the object.

The line n decoder retrieves the pan- and tilt-angle data from the TV signals and feeds them to the microcomputer system in which the triangulation calculations are performed. The range and range-rate results are displayed, either on the video monitors or else on separate readout units. The range data could also be used to control directly other automatic-response systems.

This work was done by Larry A. Freedman of RCA Corp. for **Johnson Space Center.** *For further information, Circle 6 on the TSP Request Card.*
MSC-20098

Transport Control for High-Density Digital Recorder

New servo feedback technique controls tape transport by monitoring deskew buffers.

Goddard Space Flight Center, Greenbelt, Maryland

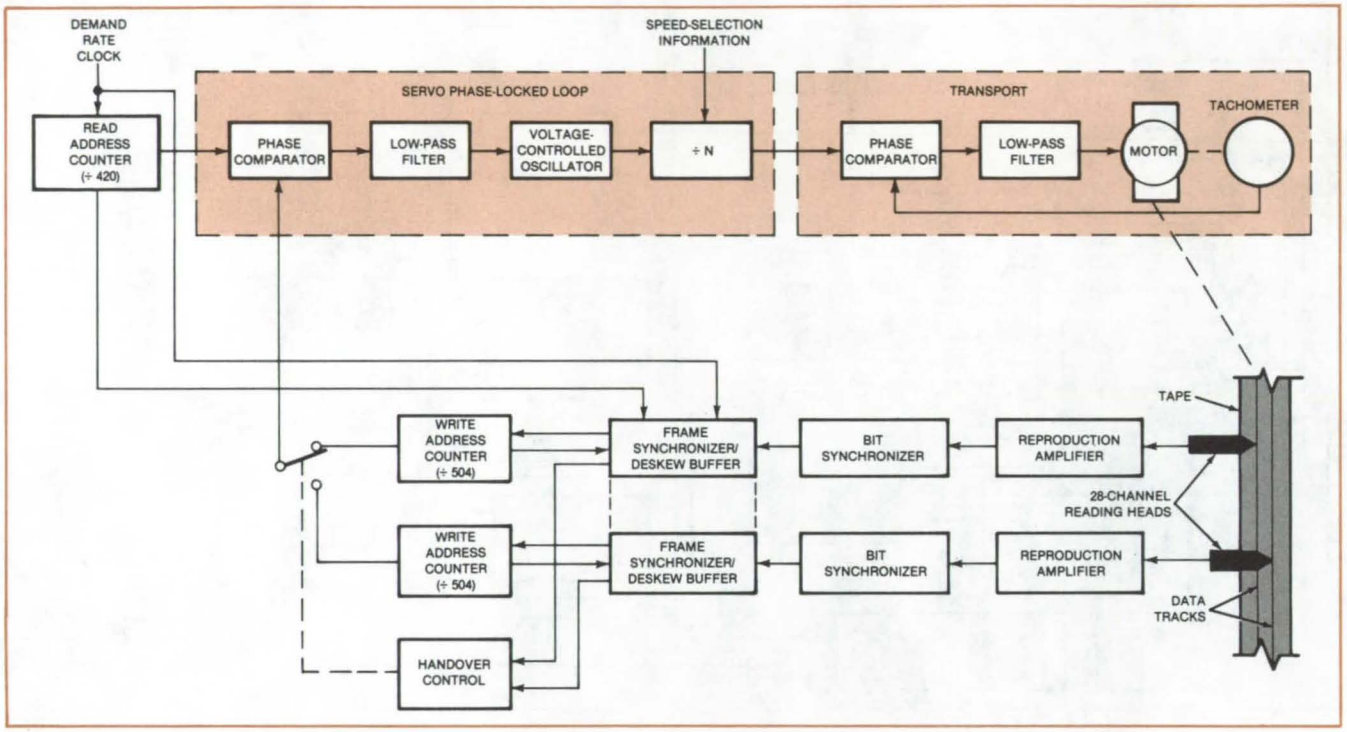

The **Tape Capstan Drive Motor** speed is controlled by a phase-locked loop to keep the data rate off of tape compatible with the the demand clock rate, thus preventing deskew-buffer overflow or underflow. Immunity to speed perturbations caused by data dropouts is obtained by switching to a different data-channel reference signal whenever a dropout is detected by the frame synchronizer in the channel currently in use. The desired tape speed is selected by changing the frequency of the demand rate clock and changing the divisor N in the programable divider.

At data densities above 33 kbit/in. (13 kbit/cm), conventional servocontrol techniques proved to be inadequate for controlling tape movement in a ground-support recorder for a NASA satellite. Tachometer feedback did not have the required resolution; conventional tape feedback lacked stability (particularly at low speeds) and was sensitive to tape dropouts. A new system has the necessary resolution and is less sensitive to dropouts than are other tape feedback systems. It is also stable at low speeds.

In the new system the servo feedback signal is derived from the data track signals, so that no separate servo track is required. The system can be adapted to any recorder that uses deskew buffers. It requires no overhead information beyond the synchronizing words already required for data deskewing.

At high bit densities a skew occurs between the data read from different tracks; that is corresponding data bits on different tracks arrive at slightly different times. To correct skew error, sync words are recorded periodically in each track. During reproduction, the data read from different tracks are resynchronized using the sync words for framing reference. Frame synchronization is achieved by storing the data bits from each track in a separate deskew buffer memory as they are read from the tape and then clocking out corresponding bits from all the deskew buffers simultaneously.

The figure shows the signal paths of the servo loop. A phase-locked-loop circuit compares the phase of a signal derived from the demand rate clock to that of a signal derived from one of the data tracks being written. The phase error between these two signals is directly proportional to the level of data in the deskew buffer. Depending on the sign and magnitude of the detected phase error, the reference frequency of the tape-transport servo is raised or lowered slightly to reduce the phase error toward zero, thus maintaining a constant net level of data in the buffer.

The tape transport is also phase-locked using a motor/tachometer feedback signal. This allows the transport to have constant gain (20 dB) out to about 700 Hz. Since the bit sync circuit also has constant gain (0 dB) to about 500 Hz, it is possible to control the entire system response with the servo phase-locked loop. By keeping the servo bandwidth very small (2 Hz at the lowest tape speed), total system stability is ensured.

In effect, the servo phase-locked loop monitors the level of data in one of the deskew buffers and adjusts the speed of the transport accordingly. By regulating the speed of the transport, it controls the rate at which data are written into the

buffer, thereby preventing buffer overflow and underflow. It also maintains the optimum level of fullness, which provides maximum deskew capability.

Dropouts in the data channel providing the feedback signal cause a phase error in that signal, which, if uncorrected, would cause bit errors. A dropout tends to reveal itself, however, by causing the following sync word to turn up at an incorrect separation. The frame synchronizer detects this and signals the handover control to switch to a second data channel that is still properly phased, before erroneous information gets to the phase detector. Thus, phase lock is maintained in spite of data dropouts. In applications where frequent data dropouts can be tolerated, this makes it possible to use cheaper tape.

This work was done by Mark D. Matlin and Arthur M. York of Martin Marietta Corp. for **Goddard Space Flight Center.** *For further information, Circle 7 on the TSP Request Card.*

This invention is owned by NASA, and a patent application has been filed. Inquiries concerning nonexclusive or exclusive license for its commercial development should be addressed to the Patent Counsel, Goddard Space Flight Center [see page A5]. Refer to GSC-12727.

Phase-Sensing Guidance for Wire-Following Vehicles

An array of coils senses phase changes that occur when the wire is crossed.

NASA's Jet Propulsion Laboratory, Pasadena, California

A guidance system for wire-following vehicles has been tested successfully at speeds exceeding 50 mi/h (80 km/h) on a difficult 1-mile (1.6-km) course. Unlike previous sensors that compare the amplitudes of signals picked up from the guide wire, the new system compares the signal phases.

In the new system, an array of coils, mounted in a line along the front bumper of the vehicle (see figure) monitors the electromagnetic signal radiating from the wire. The guide wire on the ground beneath the vehicle carries a 6- to 7-kHz alternating current.

The phase-sensing system is less sensitive to electromagnetic noise than was the amplitude-sensing system. In addition, the system "remembers" the last position of the wire and validates a new position only if it falls immediately on either side of the previous position. The remembered position is also used during brief periods of lost signal.

The signals picked up by the two coils mounted horizontally serve as a phase reference. The vertically mounted coils are sensitive only to the vertical component of the guide-wire magnetic field which changes sign from one side of the wire to the other. As the vehicle moves to one side with respect to the wire, one coil after another undergoes a phase reversal, indicating the change in the position of the vehicle.

The amplitude of the signal varies somewhat from coil to coil due to the differing distances from the wire and to the variation in angle between the coils and the magnetic field. Before the phase comparisons are done, the signals are amplified and clipped to constant amplitude. The phase state of each coil is stored in a flip-flop. Only a coil passing directly over the wire should undergo a phase reversal; any other reversal is considered spurious — indicating noise interference or other undesirable effects. Spurious reversals of each flip-flop are prevented by controlling the set and reset inputs with signals from the two adjacent flip-flops. If those two flip-flops have identical output polarity, change is inhibited. (The inhibition logic could be extended to as many adjacent flip-flops as desired.)

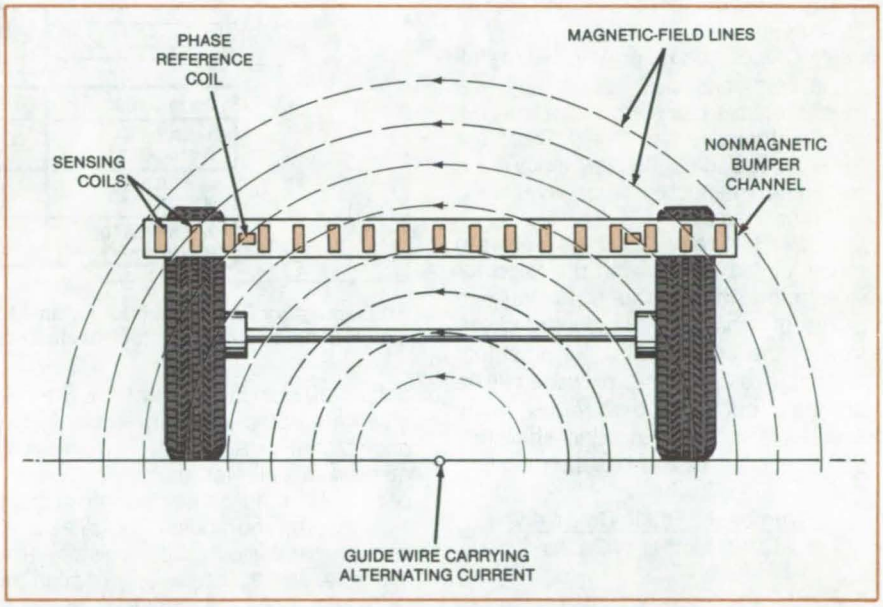

The Phase-Sensitive Guidance Sensor uses a series of vertical-axis coils and two horizontal-axis coils to detect an alternating-current signal from the guide wire. The arrows indicate the direction of the magnetic field at one moment. The signals from the horizontal coils serve as a phase reference for the electronics. Signals from the vertical coils to the left of the wire are 180° out of phase with the signals from the coils to the right of the wire. The phase-transition point indicates the position of the guide-wire.

The flip-flop outputs can encode numerical values of wire position for telemetry, data processing, and control. The deviation in position with respect to the wire can be expressed as a number proportional to the tracking error. This error signal can be used to control the vehicle-steering motors.

This work was done by George R. Hansen of Caltech for **NASA's Jet Propulsion Laboratory.** *For further information, Circle 8 on the TSP Request Card.*

NPO-15341

Hardware Fault Simulator for Microprocessors

A breadboarded circuit is faster and more thorough than a software simulator.

NASA's Jet Propulsion Laboratory, Pasadena, California

A fault simulator built in hardware for a commercially available microprocessor operates twice as fast as a comparable simulator implemented in software. According to tests at NASA's Jet Propulsion Laboratory, a microprocessor circuit can be tested for "stuck" faults more quickly and more efficiently by using the fault-simulator circuit. Designers of fault-test circuits should consider a hardware approach where speed is more important than cost of parts and where there are facilities available for breadboarding and testing the circuits.

In CMOS (complementary metal-oxide semiconductor) technology, the most probable faults are those where a gate is stuck at either 1 or 0. Therefore the stuck-fault detection efficiency is the parameter measured when evaluating test procedures.

A fault simulator may be a software model of the circuit, with provision for simulating malfunctions at various points; or it may be a breadboarded version of the circuit, with fault injectors added. In either case, proposed tests are tried out on a deliberately faulty simulator, and the detection efficiency of the test is measured as the ratio:

$$\frac{\text{Number of Faults Detected}}{\text{Total Number of Faults}}$$

The object is to detect 100 percent of possible malfunctions. An optimum set of tests should detect all malfunctions with a minimum number of tests.

To test the new hardware simulator concept, an 1802 microprocessor was first duplicated in breadboard form by about 200 standard commercially available integrated circuits, with all the nodes that are usually inaccessible made available for entry. The breadboard was then converted into a fault simulator by the addition of gates and serial-in/parallel-out shift registers (for example, see figure), which function as fault injectors. The injectors made it possible to select and simulate single or multiple stuck faults.

Experimental results showed that the hardware fault simulator for the microprocessor gave faster results than a software simulator, by two orders of magnitude, with one test being applied every 4 microseconds.

The testing of all large-scale and very-large-scale integrated-circuits for stuck-high and stuck-low faults can benefit from this type of hardware fault simulator. More recently, it was found that with proper initialization and sorting of the list of test vectors, stuck-open faults can also be identified.

This work was done by Lawrence M. Hess and Constantin C. Timoc of Caltech for **NASA's Jet Propulsion Laboratory.** *For further information, Circle 9 on the TSP Request Card.*
NPO-15080

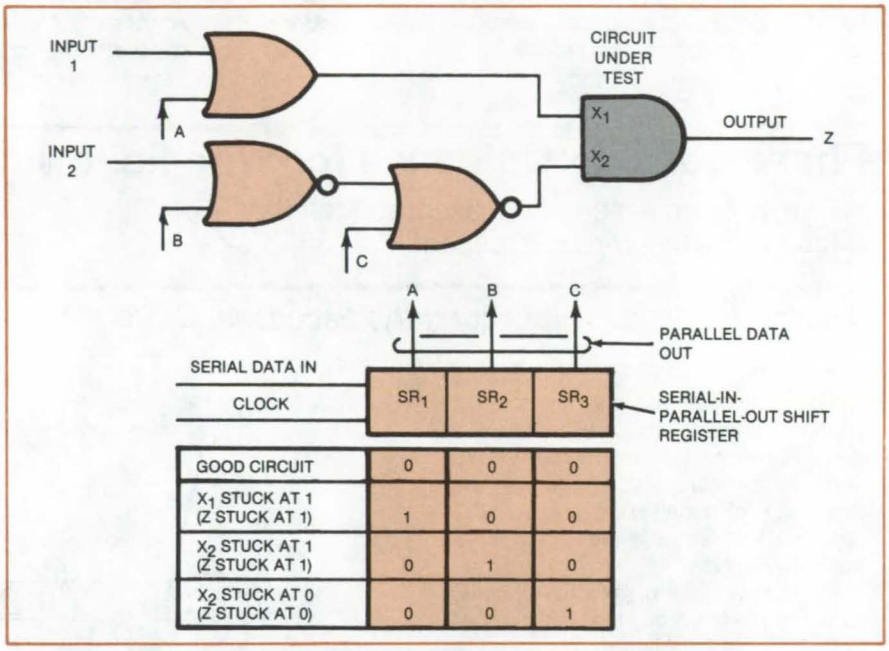

An Elementary Fault Simulator for an AND Gate uses three gates and a shift register to simulate stuck-at-one or stuck-at-zero conditions at the inputs and output.

Microprogramed Sequencer for Tunable RF Oscillator

A programable frequency synthesizer originally designed to test K-band radar transmitters is applicable to automated test equipment and computer-controlled receiver tuning. The circuit consists of a PROM-based control sequencer driving a group of diode switches, which select one of eight tuning capacitors in an L-C oscillator.
(See page 128.)

Tangleproof Rotary Electrical Coupling

A new rotary coupling connects up to 246 cables containing a total of 758 conductors to a turntable without overstressing or tangling the cables. The device permits turntable rotation through 320°. At the rotation extremes (± 160°), cables maintain enough slack to eliminate overstressing and enough stress to prevent cable entanglement at the midpoint (0°).
(See page 129.)

Using SAW Resonators in RF Oscillators

Surface-acoustic-wave (SAW) resonators are direct replacements for crystals as frequency-determining elements in RF oscillators. Because SAW's are fabricated using integrated-circuit technology, they are much smaller than crystals and are especially applicable in low-power, subminiature instrumentation, such as in biotelemetry devices.
(See page 131.)

Control System Damps Vibrations

An electromechanical control system compensates for the natural vibrational modes of a structure.

NASA's Jet Propulsion Laboratory, Pasadena, California

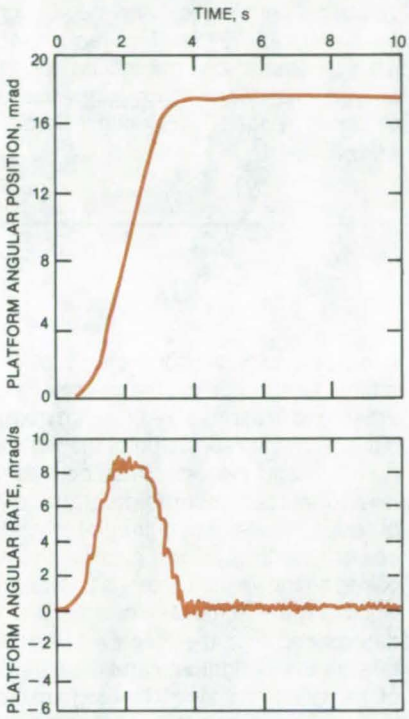

The Motion Of A Torque-Motor-Driven Camera platform is shown by position and rate curves. Structural vibrations excited by the motion are seen in the rate curve, but are effectively damped by the torque-command signals generated in the phase-locked-loop compensation system.

A new control system damps vibrations in rotating equipment with the help of phase-locked-loop techniques. Vibrational modes are controlled by applying suitable currents to the drive motor. The control signals are derived from sensors mounted on the equipment.

This system was developed for stabilizing the stator section of the Galileo spacecraft. The stator has four elastic modes below 10 Hz. One phase-locked loop (PLL) captures the resonance signal for each mode.

In a PLL, a local signal is generated with a variable-frequency oscillator. This signal is fed as a reference into a phase detector, where it is compared to the input to develop an error signal that is proportional to the phase angle between the input and reference signals. The error signal corrects the oscillator phase and frequency. This signal is then used to generate a compensating element of the torque-command signal. The PLL is easily implemented in either hardware or software: For Galileo it is all software, with oscillator signals generated by integrating rate equations.

In one example of compensation performance, the gyro moved a camera to take a series of 1-second exposures for a photo mosaic. The PLL compensated for a 5.5-Hz vibration. The angular position and rate of the camera platform are shown as functions of time in the figure. Structural vibrations at 5.5 Hz were excited by the motion. However, the vibrations are damped in less than 2 seconds.

This work was done by Edward H. Kopf, Jr., Thomas K. Brown, and Elbert L. Marsh of Caltech for **NASA's Jet Propulsion Laboratory.** *For further information, Circle 10 on the TSP Request Card.*
NPO-15002

Books and Reports

These reports, studies, and handbooks are available from NASA as Technical Support Packages (TSP's) when a Request Card number is cited; otherwise they are available from the National Technical Information Service.

Space-Platform Technology

Future needs and technology are projected.

A study has examined the possibility of using a few large platforms in space instead of many small satellites to provide communications and other services. The study was based in large measure on a user survey. A list of 31 potential services was presented to leading telecommunications firms (including carriers, programers, users, and manufacturers). Both favorable and antagonistic viewpoints were solicited. The result was a wealth of information on individual satellite system requirements of the future.

The study produced information on a variety of subjects, including:

- Best locations for geostationary platforms,
- Potential missions and their characteristics,
- Interface requirements between a geostationary platform and equipment for specific services,
- A compendium of payload characteristics, and
- Comparative antenna characteristics.

Platforms will be transported to low Earth orbit by Space Shuttle in one or more launches. Sections of the platform will be assembled and partially tested in low orbit. Upper-stage vehicles, such as the Centaur rocket, will carry the platform to geostationary orbit. The basic platform will provide electric power, telemetry, stationkeeping, coarse pointing, and heat control for the individual services, which may include voice and data telecommunications, television and

(continued on next page)

radio broadcasting, data collection, intersatellite links, navigation, maritime and aircraft communications, and many others.

One of the major conclusions of the study was that additional work is needed on multibeam antennas using wide scan angles. The shape of the individual beams from such antennas varies over the area to be covered (the shape is not a simple hexagon as is often assumed), and interference from side lobes can be considerable. However, the study found that if the area to be covered is broken into different parts (for example, if a country is divided into several regional markets covered by various independent reflectors), the scan angle can be reduced so that the beam pattern is more sharply defined and side-lobe levels are reduced.

A platform will be required to generate about 20 kilowatts of power and to dissipate about 16 kilowatts as heat. In many cases, it will have to maintain attitude within $\pm 0.1°$, with subplatforms providing additional pointing accuracy where required.

This work was done by the COMSAT Laboratories of Communications Satellite Corp. for **Marshall Space Flight Center.** *Further information may be found in NASA CR-161807, [N81-26164/NSP] and CR-161808 [N81-26165/NSP], "Final Report Geostationary Platforms Mission and Payload Requirements Study," Volume I [$10.50] and Volume II [$15]. Paper copies may be purchased [prepayment required] from the National Technical Information Service, Springfield, Virginia 22161. The reports are also available on microfiche at no charge. To obtain microfiche copies, Circle 11 on the TSP Request Card.*
MFS-25704

Computer Programs

These programs may be obtained at very reasonable cost from COSMIC, a facility sponsored by NASA to make new programs available to the public. For information on program price, size, and availability, circle the reference letter on the COSMIC Request Card in this issue.

Shuttle Communications Blackout Study

The RF power loss through a three-dimensional plasma sheath is computed.

The atmospheric reentry and landing of the Space Shuttle orbiter require precise targeting control from the deorbit point to ground touchdown. Radio communications with the orbiter during this time period are critical to provide accurate state vector updates for vehicle guidance programs. The Space Shuttle Orbiter Entry Communications Blackout Study computer program models, investigates, and predicts communication blackout envelopes based on mission entry trajectory and associated data from tracking stations. It should be of interest to those designing and using communications systems susceptible to blackout.

When the orbiter reenters the Earth's atmosphere during a typical deorbit-to-landing trajectory, it initially travels at hypersonic speeds. Shock-heated air envelops the entire orbiter in a layer of dissociated and ionized air molecules termed the "plasma sheath." This plasma sheath is electrically conducting, and electromagnetic interaction with the free electrons in the plasma can significantly impair radio-frequency transmissions. In addition to the signal attenuation due to propagation in the plasma, the reflections and refractions at the plasma interface can also represent a significant power loss to the overall communications link with the orbiter.

The Orbiter Entry Communications Blackout Study program determines the three-dimensional shock shape of the orbiter, used to define the plasma properties and plasma sheath aerodynamically, from the real shape of the vehicle flow field and the associated boundary-layer displacement. The program computes the electromagnetic-radiation power loss through the plasma sheath based on the vehicle antenna characteristics and the actual line-of-sight vector determined by the receiver station relative to the flightpath and the attitude of the vehicle in space. The program can be readily adapted to predict the entry communications blackout for any nonablative entry vehicle.

This program is written in FORTRAN IV for batch execution and has been implemented on a CDC 6000-series computer with a central memory requirement of approximately 163K (octal) of 60-bit words. The program was developed in 1980.

This program was written by Robert L. Haben and Robert J. Budica of Rockwell International Corp. for **Johnson Space Center.** *For further information, Circle M on the COSMIC Request Card.*
MSC-20141

Physical Sciences

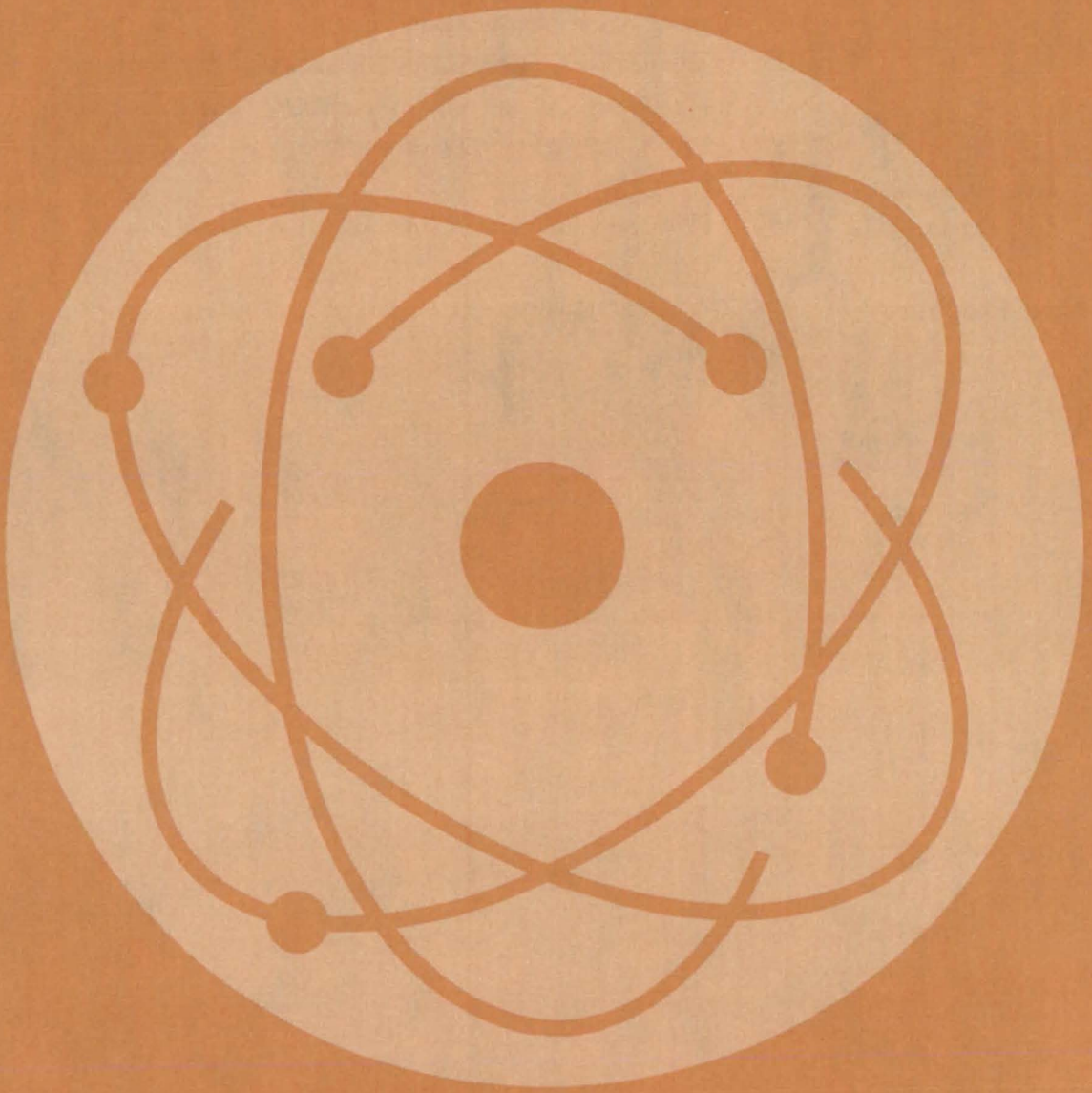

Curved-Surface Beam Splitter

Spherical entrance and exit surfaces minimize optical aberrations.

Goddard Space Flight Center, Greenbelt, Maryland

A beam splitter with curved entrance and exit surfaces introduces less chromatic aberration and Seidel aberrations in some optical systems than traditional plate or block beam splitters. The new design is used in pupil-concentric systems, such as the Schmidt-type mirror objective shown in the figure.

Many optical applications require one objective to form images at several focal planes. Examples include color-TV cameras with three vidicon tubes and cameras used to separate a color image into separate colors for color printing presses.

In pupil-concentric systems, all the optical elements are concentric about the aperture stop; the system has no preferred axis, and therefore there are no off-axis aberrations. Such systems exhibit only spherical and chromatic aberrations.

The introduction of a block beam splitter destroys the symmetry of pupil-concentric systems and introduces severe Seidel and chromatic aberrations. Compensating elements can be added but only at the expense of weight and compactness.

The proposed beam splitter — like the block beam splitter — has an optically-flat, partially-reflecting interior surface. Unlike the conventional design, however, the beam entrance and exit surfaces are spherical and concentric about the aperture stop. Thus the beam splitter surfaces generate only spherical and chromatic aberrations. While these aberrations may be larger than without the beam splitter, no new types of aberration are introduced.

The interior reflecting surface can be metallic for wavelength-independent beam splitting or dichroic (showing different color in different directions) to split the beam into different wavelength bands. Since the lens power and spherical aberration of the proposed beam splitter are quite low, systems with a very large wavelength range are possible without resorting to additional optical

(continued on next page)

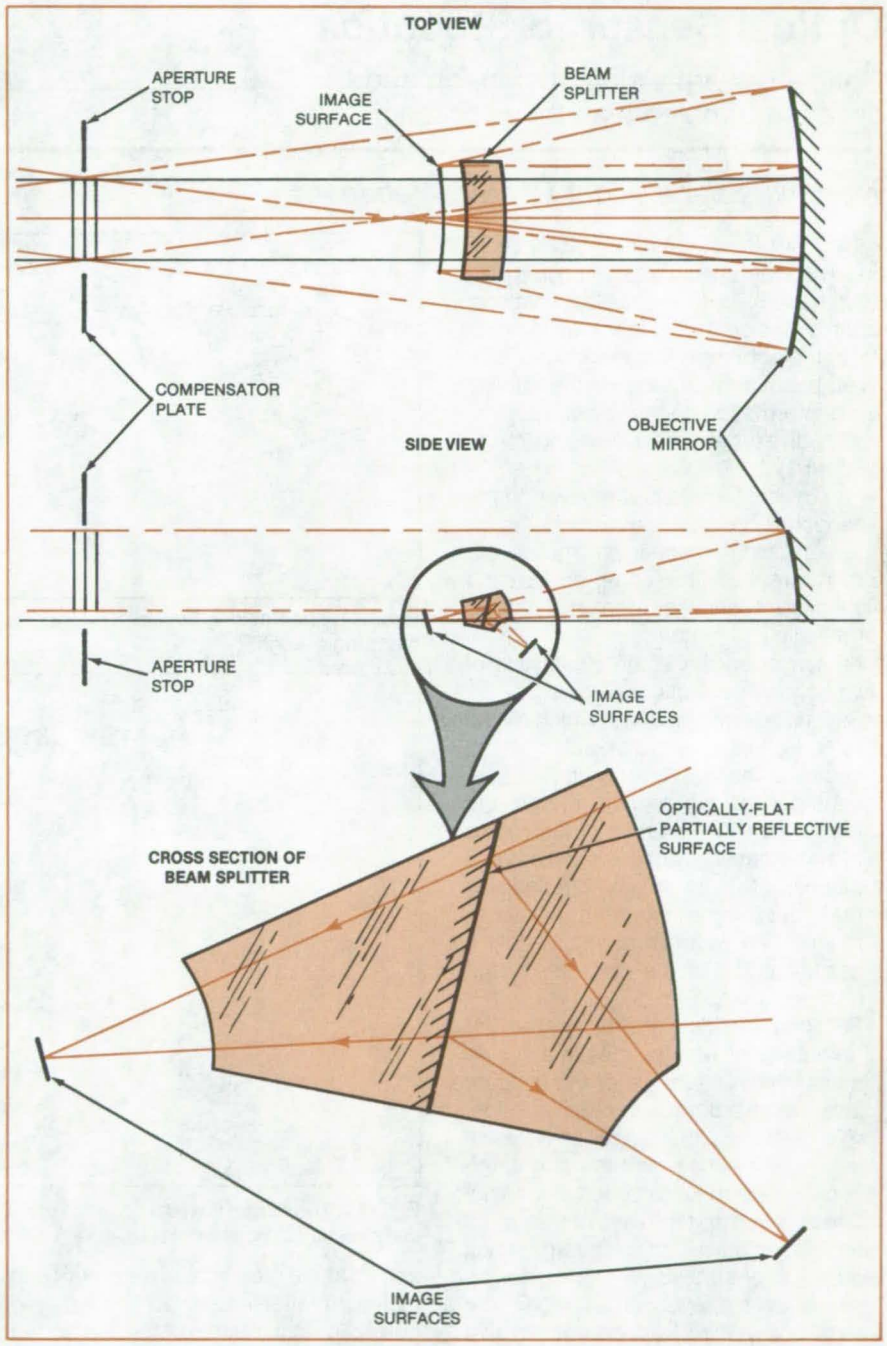

The **Spherical-Surface Beam Splitter** can be used in a Schmidt-type mirror objective to split the converging image-forming beam so that two images are formed. The small aberrations introduced can be corrected by a compensator plate located at or near the aperture stop.

components for the compensation of chromatic aberration.

The scheme can be extended to more than two images. The number of splits is limited only by energy absorption in the splitter and by available space.

This work was done by Peter O. Minott of **Goddard Space Flight Center.** *For further information, Circle 12 on the TSP Request Card.*

This invention is owned by NASA, and a patent application has been filed. Inquiries concerning nonexclusive or exclusive license for its commercial development should be addressed to the Patent Counsel, Goddard Space Flight Center [see page A5]. Refer to GSC-12683.

Optical Sensor for Robotics

Optical pattern yields orientation and distance of objects as they approach.

Marshall Space Flight Center, Alabama

An optical method for precisely docking a spacecraft and a satellite promises to be useful in terrestrial applications, such as the control of robot movements in manufacturing. The reflections of a laser beam from patterns on the satellite yield information on the radial misalinement, angle between axes, and range (Figure 1).

An optical transmitter/receiver on the spacecraft projects the laser beam on the satellite. A mechanism moves the beam direction in a cone, so that the light beam scans the target in a circular or an elliptical pattern.

A target on the satellite consists of two concentric sections (Figure 2):

- Section A is an annulus in which reflectivity decreases with distance from the center of the target. It consists of concentric rings, alternately of high and low reflectivity. The ratio of the widths of two adjacent zones is tapered as a function of radius to give a reflectivity that decreases exponentially with radius. The width of a ring is only a small fraction of the diameter of the moving light spot.
- Section B is a central circular area, the reflectivity of which varies in a known manner with the angle of the incident laser beam but not with radial position.

To determine the range, or distance between the sensor and the target, the optical system adjusts the scanning-cone angle so that the ratio of maximum to minimum power from the target rings equals a preset value. As a consequence of the exponential taper, the range is inversely proportional to this scanning-cone angle. (When there is angular misalinement, the range heading may be slightly in error on account of the consequent elliptical shape of the scan.)

The direction of the radial misalinement is derived from the beam-scan angles at the moments of maximum and minimum reflected power. The required correction is a rotation of the spacecraft in the plane defined by the scanning-beam positions at maximum and minimum reflection, toward the position of maximum reflection from section A. A sequence of such corrections will cause the center of the cone to approach the center of the target.

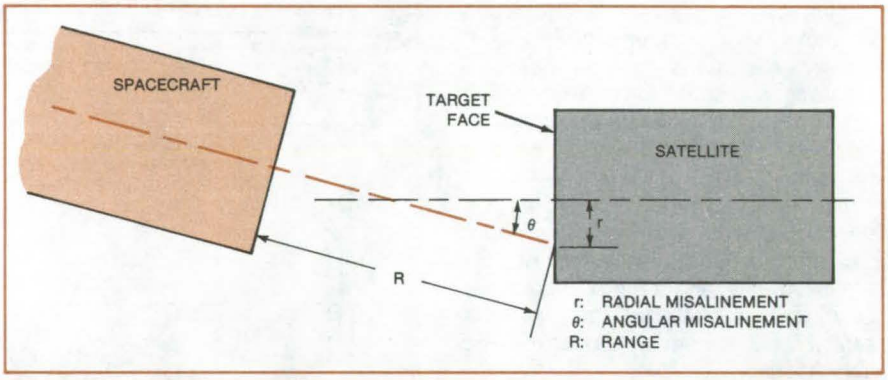

Figure 1. **The Docking Sensor System** determines radial misalinement, angular misalinement, and range.

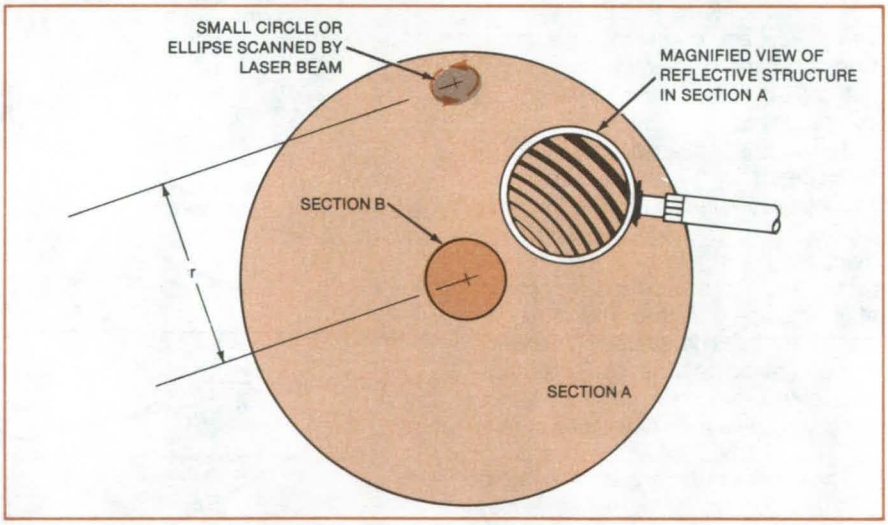

Figure 2. **The Target Pattern** consists of rings of alternating high and low reflectivity and a central section where reflectivity varies with the angle of incidence but not with position.

As the radial misalinement is reduced to a small value, the beam illuminates more and more of the central circular area of the target, section B. The low reflectivity of section B produces increasingly long dips at the output of the light sensor, signaling the approaching end of the radial correction phase. That phase is ended when the entire conical scan falls into section B.

The amount of angular misalinement is indicated by the ratio of maximum to minimum power reflected from section B. As the angular misalinement decreases, the fluctuations in reflected power decrease until reflected power remains at a constant level. The required correction for angular misalinement is rotation of the spacecraft about an axis in the plane of the target perpendicular to the plane defined by the scanning beam at the points of maximum and minimum reflection from section B.

This work was done by Fredrick Weindling of United Aircraft Corp. for **Marshall Space Flight Center.** *For further information, Circle 13 on the TSP Request Card.*
MFS-25713

Holographic Microscopy System

System achieves 2-μm resolution throughout a 100-cm^3 sample volume.

Marshall Space Flight Center, Alabama

A holographic system originally developed for testing theories of two-liquid systems could be used for measurements of aerosols, particles in a transparent medium, or microscopic biological specimens. The holograms are recorded in 3- to 5-millisecond exposures on high-resolution holographic film using the system shown in the figure.

In the playback system, the developed holograms are illuminated with the same type of laser used in the construction system. After passing through the hologram, the beam is incident upon the vidicon tube of a television camera, producing a real image of the test cell and its contents.

A commercial automated feature-analysis system measures the size distribution of the particles in the test cell by analyzing the video signal from the TV camera. The analysis system includes a TV monitor, particle-sizing electronics, and a computer (with video monitor, keyboard, and printer).

The portion of the test cell that can be viewed in sharp focus at one time is about 0.1 mm thick. By moving the hologram nearer or farther from the TV camera, any portion of the cell can be observed. Depending on the relative positions of the spatial filter, hologram, and TV camera, the reconstruction system can achieve magnifications ranging from 1X to 1,200X even though no magnifying lenses are used.

For the experiments on phase separation of immiscible liquids, an isothermal test cell maintains a fixed temperature within ± 0.001 K. A temperature bath surrounding the test cell is monitored with a thermistor connected in an ac Wheatstone-bridge circuit. The bridge is in balance at the preset temperature, and the bridge error signal controls power to a heater wire in the temperature bath.

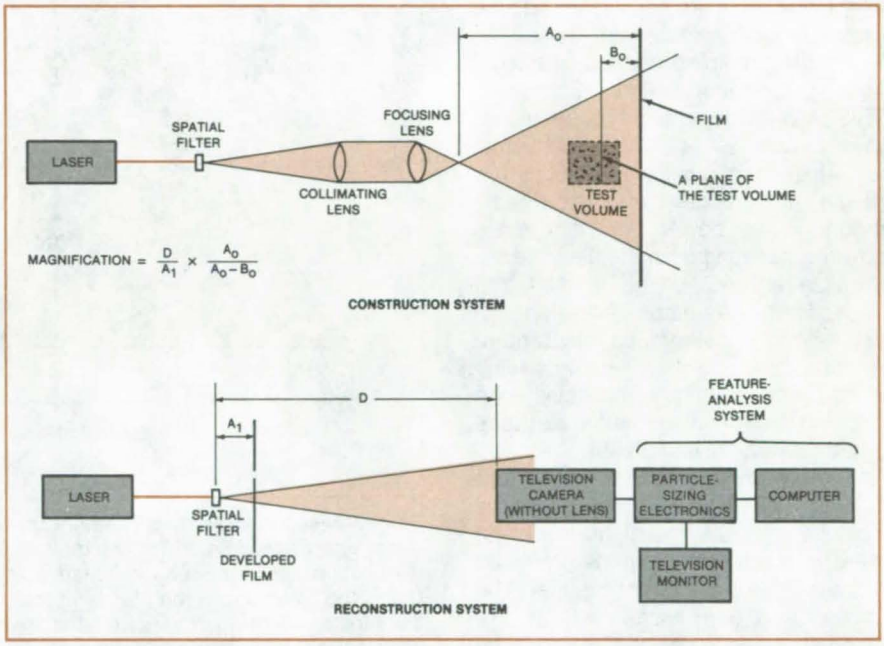

The **In-Line Holographic Microscopy System** includes a construction or recording system and a reconstruction or playback system. Both systems use 1-watt argon-ion lasers operating at a wavelength of 514.5 nm, TEM_{00} mode, with a coherence length of approximately 1 m.

Liquids analyzed thus far with the system include diethylene glycol and ethyl salicylate. A thin test-sample cell (0.1 mm thick along the optical axis) was used because high particle densities (10^5 to 10^7 particles/cm^3) were predicted by theory. Particle size and growth rate were monitored over a 1/2-hour period. By comparing holograms taken at different times, particle motion was also studied.

This work was done by William K. Witherow of **Marshall Space Flight Center.** *Further information may be found in NASA TM-82437 [N81-30212/NSP], "Holographic Microscopy Studies of Emulsions" [$9]. A paper copy may be purchased [prepayment required] from the National Technical Information Service, Springfield, Virginia 22161. The report is also available on microfiche at no charge. To obtain a microfiche copy, Circle 14 on the TSP Request Card.*
MFS-25673

TRISCAN Antenna-Positioning Algorithm

A method developed expressly for digital positioning improves accuracy and sensitivity.

NASA's Jet Propulsion Laboratory, Pasadena, California

TRISCAN is a scanning algorithm that improves the alinement between the boresight of a radar antenna and a target. The algorithm was originally developed for digitally pointed antennas in the deep-space network; however, it could possibly be used in locating radio sources on Earth.

TRISCAN (the acronym stands for triangular scan) estimates the coordinate errors in hour angle and declination between the predicted and the true locations of a radio source. For stars, TRISCAN employs a set of measurements made by a noise-adding radiometer. This device yields a temperature reading proportional to the system background noise power plus any noise power emanating from the star; the latter is attenuated by an amount that depends on the antenna boresight offset. When the background temperature is subtracted from the total reading while the boresight is in the vicinity of a star, the result is the effective star temperature at the given offset.

The algorithm uses the measurement of three effective star temperatures from the same star (see figure). The first measurement is made at the predicted or best-known location of the star. The second and third measurements are made at the base points of a known triangle. The ratios T_0/T_1 and T_0/T_2 are used to calculate offset parameters, using the general relationship between relative temperature reading and boresight offset. The offset parameters are then used in trigonometric calculations to estimate the offset from the predicted point to the star. A typical TRISCAN star scan takes about 5 minutes. For applications where the signal source changes direction rapidly, the process would have to be automated to speed up the analysis.

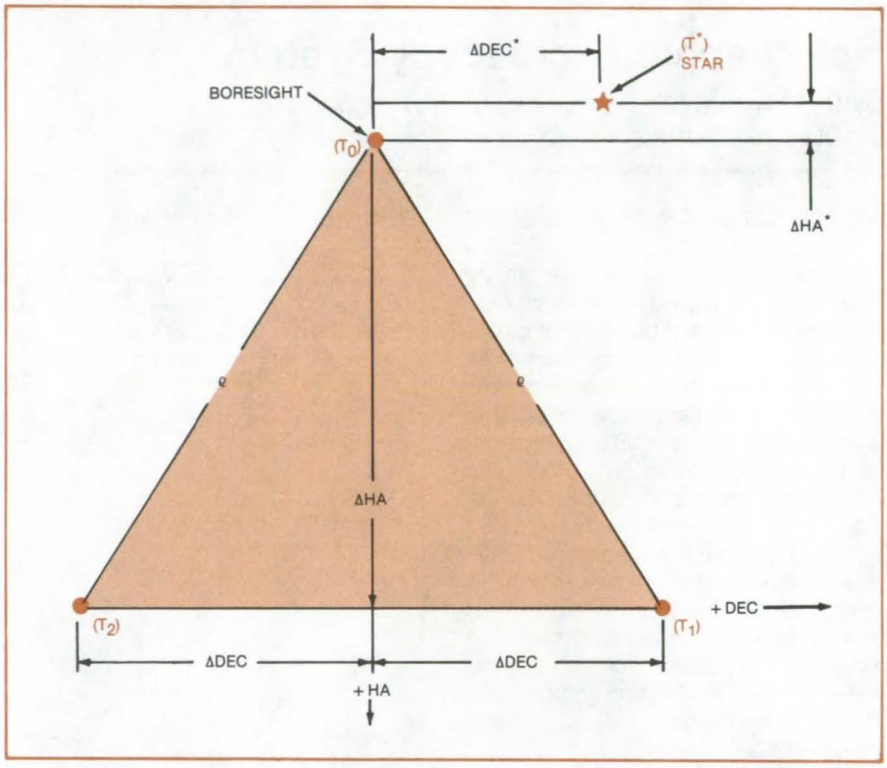

Three Measurements of Star Temperature form a triangle having apexes representing the temperatures T_0, T_1, and T_2. The triangle height is a downward excursion in hour angle (HA), while the triangle base consists of sideways excursion in declination (± DEC). Using the three measured star temperatures and the triangle geometry, an algorithm calculates estimated offsets from the predicted point to the star, indicated as ΔHA* and ΔDEC*, for final antenna positioning.

This work was done by Robert C. Bunce of Bendix Field Engineering Corp. for **NASA's Jet Propulsion Laboratory.** *For further information, Circle 15 on the TSP Request Card.*
NPO-15577

Ion Mass/Velocity/Charge Spectrometer

m/q is resolved to 1 part in 40.

NASA's Jet Propulsion Laboratory, Pasadena, California

An ion spectrometer, originally developed for spacecraft analysis of the solar wind and cometary ions, distributes ions two-dimensionally and measures three characteristics of the incident-ion beam: (1) mass/charge distribution, (2) ion velocity distribution, and (3) the direction of incidence. It could also be useful for diagnosis in experimental plasma physics in the collisionless regime.

Ions that enter from directions within the field of view are reflected by a charged-grid electrostatic mirror into the accelerator grids (see figure). The voltage on the accelerator grids is modulated to scan a wide range of incident-ion speeds, v, and to bring those speeds within the narrower acceptance range of the magnetic analyzer. The azimuth angle, ϕ, of incoming-ion velocities is scanned by spacecraft rotation or by stepping the electrostatic mirror in azimuth.

The magnetic analyzer serves as a momentum/charge (mv/q) filter with an angular acceptance of $\pm(0.5°$ to $0.9°)$ in ϕ and $\pm 30°$ in the elevation angle, θ. The ions selected by the magnetic analyzer are dispersed two-dimensionally by the electrostatic deflector according to mass/charge (m/q) and θ.

The two-dimensional sensors in the electrostatic-deflector section include 2,500-volt accelerating grids followed by microchannel-plate (MCP) electron multipliers. The MCP output at each point is collected by 1 of 40 conductive anode strips that run along the m/q axis, each strip receiving ions with θ values in a $\pm 3.75°$ range. The location of the incident-ion beam, and therefore the m/q value, is deduced by sensing the pulses on the strip. The data are manipulated by a microprocessor before transmission.

In tests, a model of the spectrometer resolved m/q to 1 part in 40 (with m/q measured in atomic mass units per elementary electric charge). Some other performance figures include:

- m/q ranges, 1 to 4, 12 to 24, and 28 to 56;
- Ion-energy range, 0 to 8[1 + 1/(m/q)] keV; and
- Energy resolution (digitization), ± 7.8 eV.

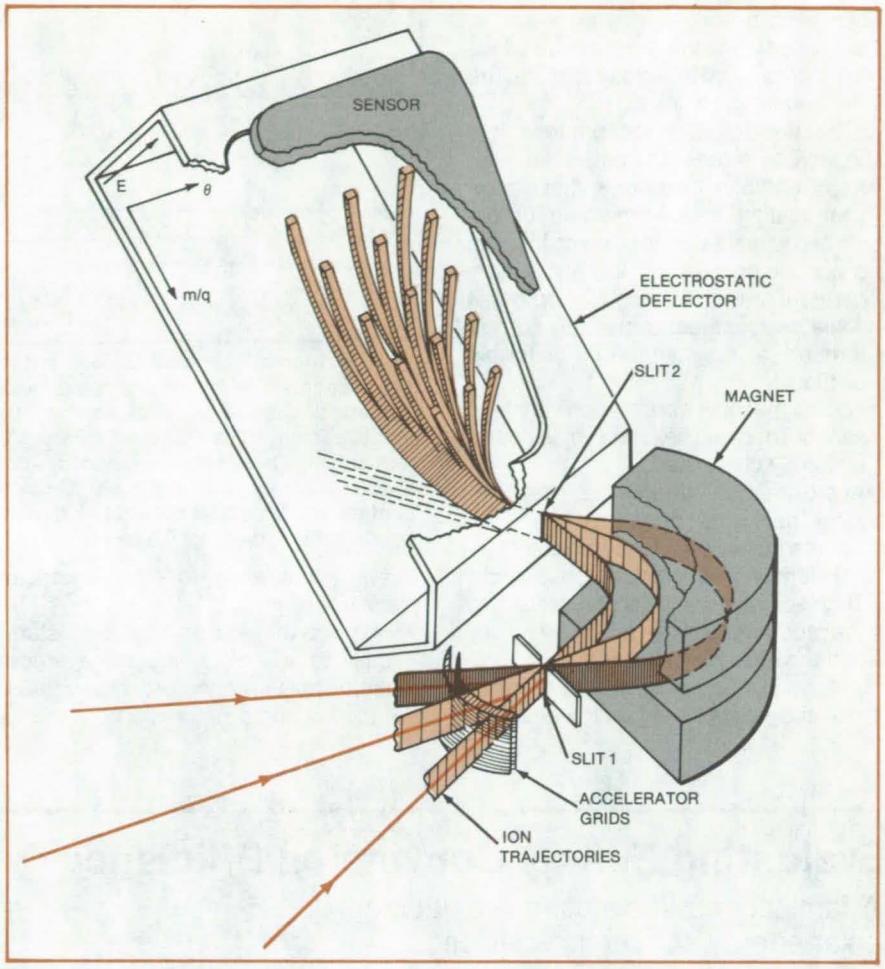

The **Ion Spectrometer** uses a novel combination of standard electrostatic and magnetic deflection techniques to sort incident ions according to speed, the direction of incidence, and mass/charge ratio.

This work was done by Marcia M. Neugebauer, Douglas R. Clay, and Bruce E. Goldstein of Caltech for **NASA's Jet Propulsion Laboratory.** *For further information, Circle 16 on the TSP Request Card.*
NPO-15423

Design Calculations for Thermoelectric Generators

Heat rate, power delivered to load, and thermodynamic efficiency can be calculated with high accuracy.

NASA's Jet Propulsion Laboratory, Pasadena, California

Nine simplified analytic models based on average properties accurately predict heat rates for silicon/germanium thermoelectric generators. Solutions from these simplified models were compared with those obtained using sophisticated numerical analysis. The maximum errors in calculated heat rate range from about 4 percent to about 0.2 percent. The models may also be used to calculate power delivered to a load and thermodynamic efficiency.

Even with modern computers, the differential equations that describe steady power generation in semiconductor thermocouples are difficult to solve. The reason is that such devices experience sizable temperature differences, and the properties of the silicon/germanium vary widely and nonlinearly with temperature.

A silicon/germanium thermoelectric generator (shown schematically in the figure) may be operated between thermocouple hot-junction temperatures as high as 850° C and cold-junction temperatures below 200° C.

(continued on next page)

Over such a large temperature range, the properties of the thermocouple legs vary greatly with position in the temperature gradient.

The new models are grouped into three types in order of complexity:

- Approximation I assumes that Thomson heating (heat generated or absorbed when a current passes through a conductor in which there is a temperature gradient) is negligible and that Joule heating (heat evolved by current through a resistance) is uniformly distributed.
- Approximation II assumes only that the sum of Thomson heat and Joule heat is uniformly distributed.
- Approximation III assumes that the local net heat generated per unit volume is made of two components — a uniformly distributed Joule heat and a Thomson heat, which is proportional to the product of the thermal conductivity and the temperature gradient.

Each type of approximation in turn has three subgroups based on the three different averages $\hat{\varrho}$ for the electrical resistivity ϱ:

- Subgroup (a) regards $\hat{\varrho}$ as a constant equal to a simple integral average taken over the range of temperatures of the hot and cold junctions.
- Subgroup (b) regards $\hat{\varrho}$ as equal to an integral average obtained by using the thermal conductivity as a weighting function over the range of temperatures of the hot and cold junctions.
- Subgroup (c) expresses $\hat{\varrho}$ as a spatial integral average over all positions within the device between cold and hot junctions.

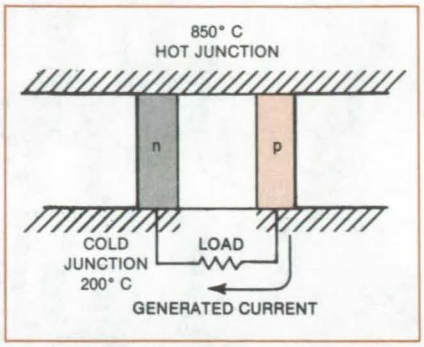

New Mathematical Models apply to thermocouple-type generators composed of n- and p-type semiconductor alloys (78 atomic percent silicon, 22 atomic percent germanium). Calculations were made for an 850° C hot junction and a 200° C cold junction and for a ratio of load to internal resistance ranging from 0.8 to 1.5.

Approximation I, subgroup (b) introduces the greatest error (4.2 percent) in heat rate. Approximation III, subgroup (b), introduces the least error, (less than 0.2 percent.

The models can be selected according to the accuracy needed. Similar average-property models can be used to refine the accuracy of lumped-parameter approximations for electrical transmission lines, flow through chemical reactors, and limit-stressed structural members.

This work was done by Burton Zeldin of Caltech for **NASA's Jet Propulsion Laboratory.** *For further information, Circle 17 on the TSP Request Card.*
NPO-15286

Evaluating Energy Conversion Efficiency

A family of curves aids in evaluatiing solar-energy conversion devices.

Langley Research Center, Hampton, Virginia

Devices that convert solar radiation directly into storable chemical or electrical energy, such as photovoltaic, biological photosynthetic, photochemical, and photoelectrochemical, have a characteristic energy absorption spectrum; specifically, each of these devices has an energy threshold. The conversion efficiency of a generalized system that encompasses all threshold devices has been analyzed, resulting in a family of curves for devices of various threshold energies operating at different temperatures.

The system consists of a blackbody source at 6,000 K and a radiant energy converter having a threshold energy E_0 operating in contact with a reservoir at a fixed temperature T_R. The analysis is based on the first and second laws of thermodynamics and leads to a determination of the limiting or ultimate efficiency for any conversion system having a characterestic threshold energy (such as the band gap of a solar cell) and an operating temperature.

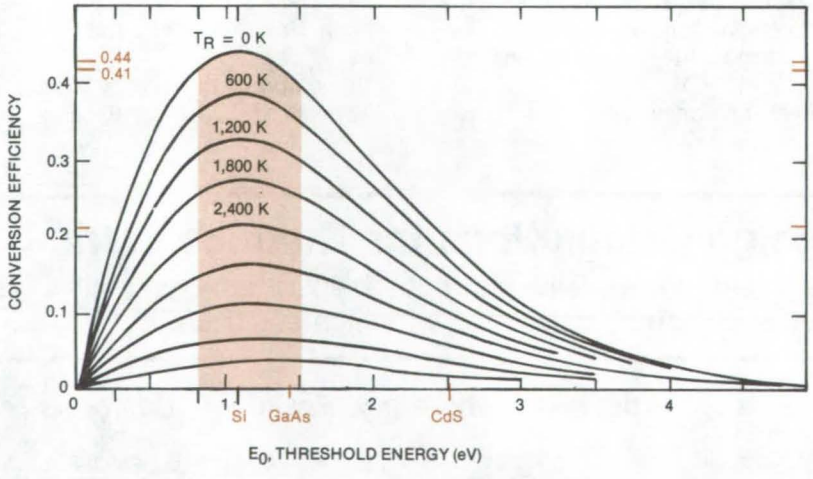

Conversion Efficiency Limits vs. threshold energies of various photosensitive devices can be compared with the aid of a family of characteristic curves. The maximum efficiency is 44 percent for silicon. The highest solar-energy conversion efficiencies correspond to threshold energy levels between 0.75 and 1.5 eV for all operating temperatures.

The curves shown give the maximum possible conversion efficiency for any device having a threshold energy. The maximum efficiency of 44 percent requires an operating temperature of 0 K and a threshold energy of 1.1 eV. This threshold energy coincides with the energy band gap for silicon. For comparison, the limiting efficiency for a gallium arsenide device is 41 percent and

for a cadmium sulfide device is 22 percent at this same temperature.

As the operating temperature of a threshold device increases, its limiting solar conversion efficiency decreases. The curves indicate that the highest solar conversion efficiencies will be for devices with threshold energies between 0.75 and 1.5 eV for all temperatures. Limiting efficiencies decrease rapidly for threshold energies greater than 1.5 eV or less than 0.75 eV for practical operating temperatures.

Although the efficiency curves refer specifically to the conversion of solar radiation, they can also be used to find the limits to the conversion efficiency for threshold devices and radiation from a blackbody at any temperature with a simple modification. In addition, they can be used to find the maximum conversion efficiency for devices that have both a threshold and a cutoff energy (i.e., an absorption band.)

The analysis gives the limits to the conversion efficiency of any threshold device, given only its temperature and threshold energy and the temperature of the blackbody radiator. It does not include any specific device characteristics. The inclusion of specific characteristics will result in conversion efficiencies less than the limits indicated.

This work was done by C. E. Byvik of **Langley Research Center** *and A. M. Buoncristiani and B. T. Smith of Christopher Newport College. Further information, may be found in:*

NASA TM-83230 [N82-18696/NSP], "The Ultimate Efficiency of Photosensitive Systems" [$6.], and

NASA TM-83228 [N82-18697/NSP], "Thermodynamic Limits to the Efficiency of Solar Energy Conversion by Quantum Devices" [$6].

Copies of these reports may be purchased [prepayment required] from the National Technical Information Service, Springfield, Virginia 22161.

LAR-12948

Books and Reports

These reports, studies, and handbooks are available from NASA as Technical Support Packages (TSP's) when a Request Card number is cited; otherwise they are available from the National Technical Information Service.

Large Electrochemical Storage Systems

Batteries are evaluated that can deliver megawatts for hours.

A study released in 1979 assesses the status of electrochemical energy storage for powerplants that utilize the Sun's heat to drive electric generators. Electrochemical energy storage is also applicable to photovoltaic arrays, wind turbines, and similar variable and intermittent sources of electricity.

The study considered the stage of development, cost, and performance of existing storage systems and projected their cost, performance, and availability as advanced systems. It addressed three broad areas:

- The electrochemical, or battery, component of the storage system;
- The remaining parts of the storage system, including inverter or converter; and
- The overall solar-thermal plant.

The study produced a tabulation of the costs of delivered energy from complete plants with 16 different advanced electrochemical systems, ranking the systems in order of economic attractiveness. Manufacturers and developers were consulted during the assessment.

A major conclusion was that the familiar lead/acid battery is the only existing cell that can meet the needs for near-term demonstration programs. Lead/acid batteries are expensive, however, costing from $170 to $220 (1979 dollars) per kilowatt hour. These values apply to batteries that can operate for 2,000 cycles at 80 percent depth of discharge and efficiency of 70 to 85 percent. Between 1985 and 1990, lower cost batteries are expected to become commercially available.

Inverter and converter equipment was found to consitute a sizable part of system cost exclusive of cell cost. Inverter/converter costs are lower for higher bus voltages.

This work was done by Stanley Krauthamer and Harvey A. Frank of Caltech for **NASA's Jet Propulsion Laboratory.** *Further information may be found in JPL Publication 79-95, Revision 1, [N80-29858/NSP], "Electrochemical Energy Storage Systems for Solar Thermal Applications" [$12]. A copy may be purchased [prepayment required] from the National Technical Information Service, Springfield, Virginia 22161.*

NPO-15185

Computer Programs

These programs may be obtained at very reasonable cost from COSMIC, a facility sponsored by NASA to make new programs available to the public. For information on program price, size, and availability, circle the reference letter on the COSMIC Request Card in this issue.

Estimating Insolation Incident on Tilted Surfaces

Solar radiation on several types of solar collectors is calculated from ASHRAE relationships.

In designing or analyzing a solar-energy system, the principal question is how much energy the system can deliver to meet load demands. One of the main parameters determining the amount of energy the system delivers is the amount of solar energy available (energy incident on the surface of the collector array) to the system. The ASHMET computer program estimates the amount of solar insolation incident on the surfaces of several types of solar collectors, including fixed-position flat-plate, monthly-tilt-adjusted flat-plate, beam-tracking, and fixed-azimuth-tracker.

(continued on next page)

The basic methodology employed in ASHMET is to use ASHRAE relationships to obtain the clear-day total daily insolation incident on the collector surface for a representative day of each month of the year. The clear-day total daily insolation is then multiplied by a clearness index to obtain the typical or average daily insolation. Climatological data for determining this clearness index for 248 U.S. cities are included with the ASHMET program. The breakout of direct and diffuse insolation may be selected as either the ASHRAE relationships or the correlation of Liu and Jordan.

ASHMET is an interactive program and prompts the user for all required data. These data include the latitude of the desired location, the collector slope measured from the horizontal, the azimuth of the collector surface, the type of collector, the ground reflectance (if desired), and the city to be used for cloud-cover calculations. Output consists of an echo of the input data, the hourly clear-day incident insolation, the total clear-day insolation, and the typical daily insolation for each month. Also output are the maximum yearly insolation and the probable yearly insolation.

The ASHMET program is written in FORTRAN IV-Plus for interactive execution and has been implemented on a DEC PDP-11/70 computer with a central memory requirement of approximately 48K of 16-bit words. ASHMET was developed in 1980.

This program was written by Robert E. Elkin and Ronald G. Toelle of **Marshall Space Flight Center.** *For further information, Circle A on the COSMIC Request Card.*
MFS-25501

Materials

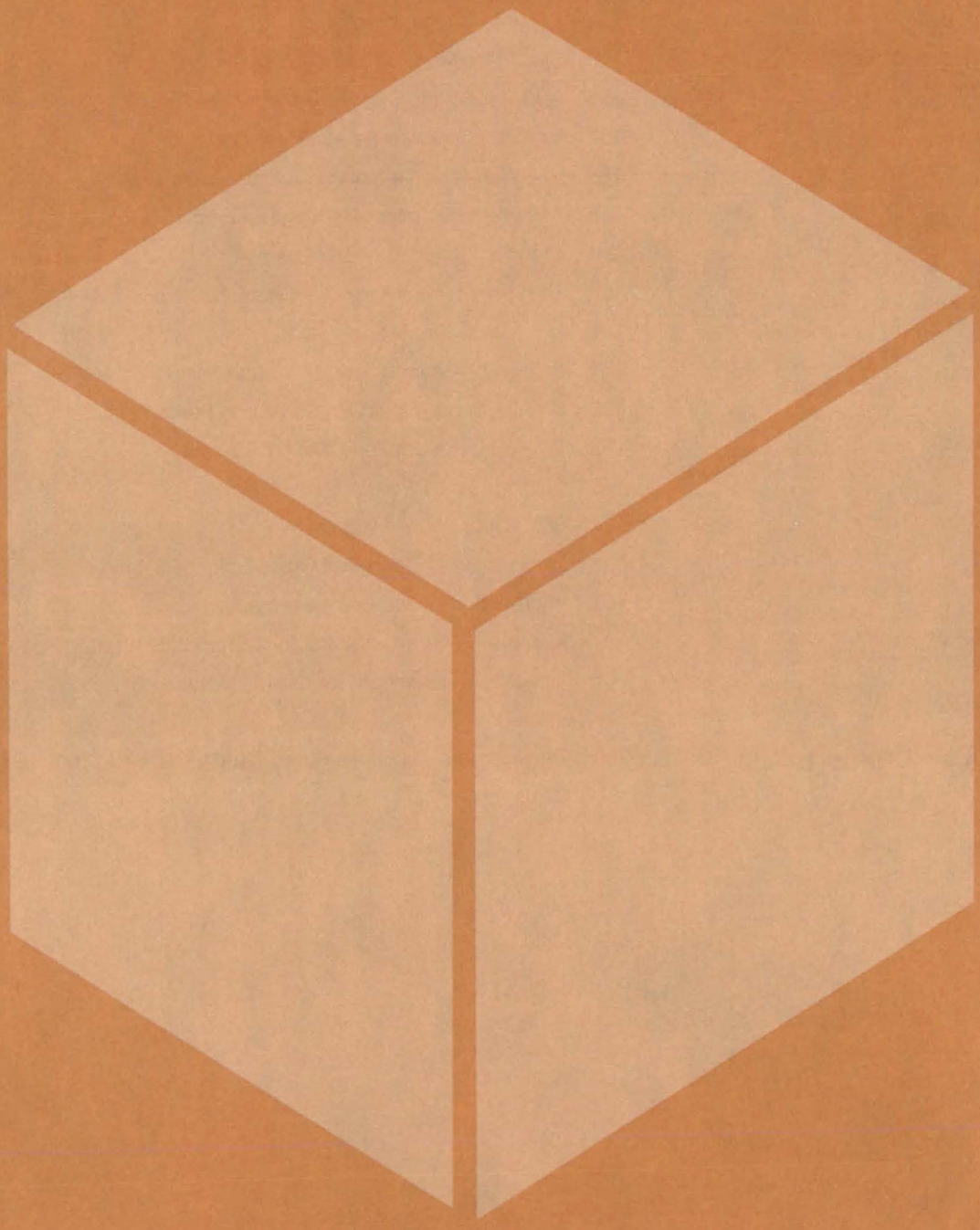

Hardware, Techniques, and Processes

Books and Reports

Efficient Silicon Reactor

Narrow temperature excursions and large surface area minimize heat expenditure and processing time.

NASA's Jet Propulsion Laboratory, Pasadena, California

High-purity silicon can be efficiently produced and transferred by a continuous two-cycle reactor. The new reactor operates in a relatively-narrow temperature range, 1,200° to 1,450° C, and uses a large surface area to minimize heat expenditure and processing time in producing silicon by the hydrogen reduction of trichlorosilane. Conventional methods of silicon production, by the hydrogen reduction of trichlorosilane, produce solid silicon units and require shutdown, setup, and startup between each production run, which requires a much greater heat expenditure.

The new quartz reactor produces silicon and deposits it at 1,200° C, melts and feeds the silicon to a melt crucible or crystal puller, and then seals the feed tube at 1,200° C to begin another cycle of silicon production. The large internal surface area is created by inserting vertical baffles (see figure). The baffles create gas turbulence, which aids in mixing the reactants, and provide heat-transfer area that speeds the reaction. Heat loss from the reactor is minimized by covering the heating elements that surround the reactor with adequate insulation.

The two cycles of the reactor consist of silicon production and removal. Initially, the reactor is brought up to the reaction temperature under an inert-gas flow. A small amount of silicon is then melted in the U-tube below the reactor vessel to form a positive seal, and the U-tube temperature is dropped to about 1,200° C to seal itself; the tube has its own separate heating element and insulation and a vent that prevents complete drainage of its lower section. With the tube sealed, the reactant-gas flow begins and continues until the desired amount of silicon is deposited.

At that point the reactant gases are flushed out of the reactor with argon to begin the silicon-removal cycle. Keeping the U-tube at 1,200° C, the reactor is raised to about 1,450° C to melt the deposited silicon, and the gas pressure between the reactor and delivery tube is equalized. Next, the temperature of the U-tube and delivery tube is raised to about 1,415° C, causing the silicon to drain, under gravity, from the reactor. When drained, the reactor is returned to reaction temperature, and the U-tube and delivery tube are returned to 1,200° C. Finally, the reactant gases are readmitted to the reactor to start another silicon-production cycle.

To prevent the reaction vessel from sagging when the silicon melts from it, a pressure equalizer maintains a slight positive pressure inside the vessel. The same pressure equalizer also prevents any larger pressure buildup that would rupture the vessel.

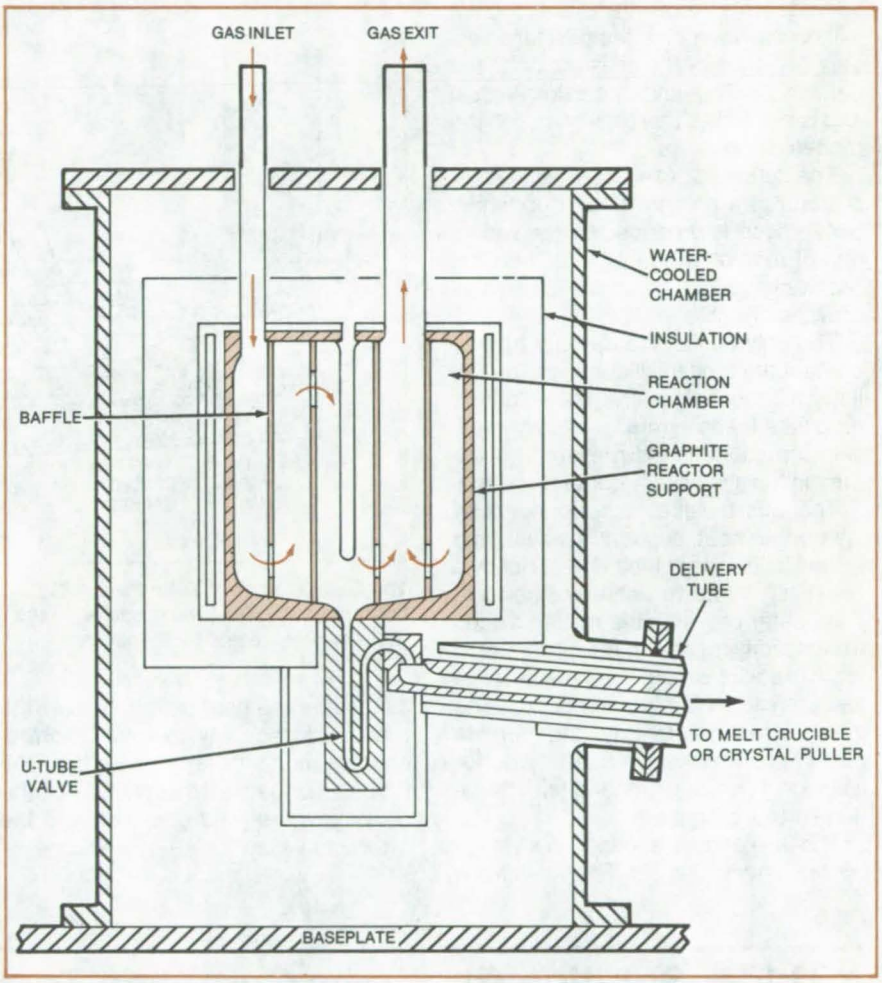

The **Reactor Walls and Baffles** combine to create a large surface area onto which silicon can deposit. In the two cycles of the reactor, silicon is first deposited and then removed. Details of the delivery tube that transfers the silicon from the reactor to a crucible appear in the article that follows this one.

This work was done by Herbert E. Bates, David M. Hill, and David N. Jewett of Energy Materials Corp. for **NASA's Jet Propulsion Laboratory.** *For further information, Circle 18 on the TSP Request Card.*
NPO-15636

Silicon-Delivery Tube

Heated quartz tube transfers molten silicon.

NASA's Jet Propulsion Laboratory, Pasadena, California

A delivery tube transfers molten silicon between high-temperature vessels. The transport tube is sealed to the delivery vessel and receiving vessel and is slanted so that gravity moves the molten silicon.

The delivery vessel could be the output end of a growth reactor, in which pure silicon is produced by the reduction of trichlorosilane at 1,200° C. The receiving vessel could be a crystal-growing crucible.

The only part of the delivery tube to contact the molten silicon is the quartz inner tube (see figure). A heated quartz drop tube feeds it from the delivery vessel. Contamination is prevented since the molten silicon only contacts quartz.

The quartz tube is surrounded by layers that heat, support, insulate, and isolate it. The inner tube is kept hot by a resistively-heated graphite rod below it. The heater prevents the molten silicon from solidifying and interrupting transfer. A graphite casing supports the tube and completes the heating circuit. The graphite rod, quartz tube, and graphite casing are wrapped in quartz tape for isolation from the graphite-felt insulation surrounding them.

The insulation is encased in a water-cooled steel jacket. The insulation distributes the heat uniformly over the tube. Strategically placed thermocouples monitor the temperature. The tube is flanged to the bottom of the delivery vessel and gasketed into the receiving vessel.

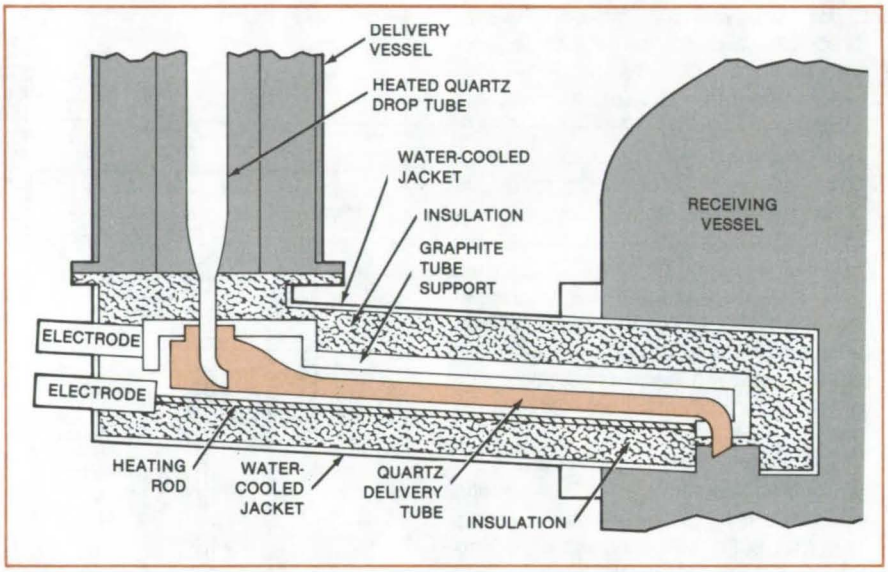

The Quartz Delivery Tube transports the molten silicon and isolates it from potential contaminants. The tube is sealed to the bottom of the delivery vessel by a flange and to the receiving vessel by a gasket.

This work was done by Herbert E. Bates, David M. Hill, and David M. Jewett of Energy Materials Corp. for **NASA's Jet Propulsion Laboratory.** *For further information, Circle 19 on the TSP Request Card.*
NPO-15637

A Milder Solution for Stress-Corrosion Tests

Excessive pitting is eliminated.

Marshall Space Flight Center, Alabama

A solution of 2.86 percent NaCl and 0.52 percent $MgCl_2$ in H_2O is suitable for stress-corrosion testing of aluminum alloys. It gives test results similar to those obtained with synthetic seawater, but is less expensive to prepare.

In a stress-corrosion-cracking (SCC) test, the alloy sample is strained in a coated aluminum stressing jig, then alternately immersed in the corrosive solution until failure or until the end of the test period (typically, 3 months). The test solution should be just corrosive enough to enable discrimination among metals of low, intermediate, and high SCC resistance.

If the solution causes extensive pitting, it is too corrosive for sensitive testing: The tensile stresses at the apexes of the pits are difficult or impossible to calculate, and the net section stress is greater than the original applied stress. As a result, the SCC effects are masked by pitting effects.

In the search for a mild corrosive, 14 different salt solutions were screened in alternate-immersion tests on 3 aluminum alloys. The most-widely-used solution of 3.5 percent NaCl in H_2O was too corrosive when prepared with pure salt and pure water. The best results were obtained with the NaCl/$MgCl_2$ solution and with the synthetic seawater (which contains nearly the same proportions of NaCl and $MgCl_2$ along with precise, minute amounts of eight other salts).

Material		Stress		$NaCl/MgCl_2$		Synthetic Seawater		Saltwater	
Alloy	Raw Form**	MPa	kpsi	Ratio***	Days to Failure	Ratio***	Days to Failure	Ratio***	Days to Failure
2024-T4	Plate	140	20	5/5	2, 2, 5, 5, 6	5/5	2(4), 5		
2024-T6	Plate	310	45	0/4		3/5	36*, 36*, 34*	3/3	47, 48, 61
7075-T651	Plate	205	30	5/5	2(4), 12	5/5	2, 2, 5, 15*, 20*		
7075-T651	Bar	275	40	4/5	12*, 28*, 33*, 43*	4/5	12, 15*, 15*, 40*	5/5	2(4), 15
7075-T7651	Plate	240	35	3/5	2, 5, 6	4/5	5, 7, 15*, 15*	4/5	2, 2, 5, 5

*Failed at edge or under coating

**Machined to round tensile specimens that were exposed by alternate immersion to the indicated solutions until failure or a maximum of 90 days

***(Number of specimens that failed)/(Number of specimens tested)

Stress-Corrosion-Cracking Tests were performed on aluminum alloys to assess the $NaCl/MgCl_2$ and synthetic-seawater solutions. The highly corrosive saltwater was included for comparison.

The table summarizes SCC tests performed with the $NaCl/MgCl_2$, "seawater," and saltwater solutions. The results with the first two solutions are generally consistent with the previously-known corrosion resistances of the alloys. Because the $NaCl/MgCl_2$ solution is less expensive than the artificial seawater, it will probably be preferred for future SCC testing.

This work was done by T. S. Humphries and J. E. Coston of **Marshall Space Flight Center.** *Further information may be found in NASA TM-82452 [N82-13216/NSP], "An Improved Stress Corrosion Test Medium for Aluminum Alloys" [$6]. A paper copy may be purchased [prepayment required] from the National Technical Information Service, Springfield, Virginia 22161. The report is also available on microfiche at no charge. To obtain a microfiche copy, Circle 20 on the TSP Request Card.*
MFS-25792

Heated Aluminum Tanks Resist Corrosion

Keeping a tank warm prevents moisture from condensing on it.

Marshall Space Flight Center, Alabama

The simple expedient of heating foam-insulated aluminum alloy tanks prevents them from being corroded by salt-laden moisture. A relatively-small temperature difference between such a tank and the surrounding air will ensure that the life of the tank is extended by many years.

Aluminum is corrosion-resistant in air containing water vapor alone because of the protective oxide film that forms on its surface. However, the aluminum can corrode near seawater. The salt in the air breaks down the protective film and causes pitting.

Water vapor penetrates the foam insulation from its warm exterior surface to the cool surface of the aluminum tanks. The vapor from seawater, condensing on the cool tank, thus initiates corrosion. However, heating the interior of the tank to a temperature above that of the ambient air reverses the vapor-permeation trend and prevents moisture from condensing on the aluminum.

(continued on next page)

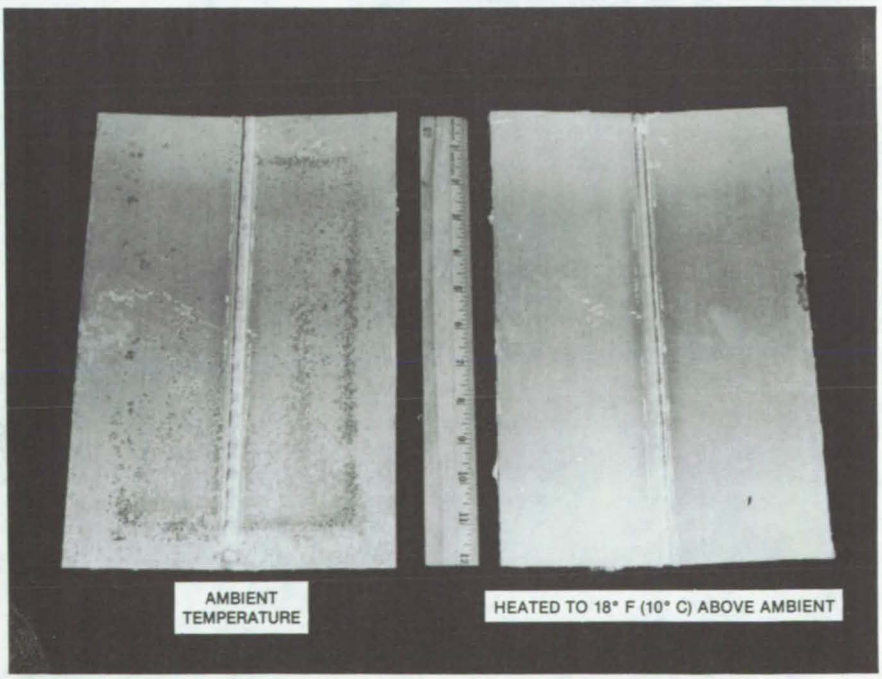

The **Pitted Aluminum Specimen** at the left was not heated above the ambient temperature in the salt-spray chamber. The completely uncorroded specimen at right was heated to 112° F (44° C) by a small light bulb in a box behind the specimen.

Corrosion tests were conducted on foamed aluminum panels in a 5-percent-salt fog. One panel was heated from the back to a temperature 18° F (10° C) above the 94° F (34° C) air temperature in the test chamber. After 11 days exposure, the panels were removed from the test chamber, and the foam was stripped from them. The heated panel showed no corrosion, but the unheated panel was pitted (see figure). Interestingly, the foam was much more easily removed from the unheated panel. Apparently moisture not only corrodes the aluminum but also decreases the adhesion of the foam.

The 18° F temperature difference on the heated panel was selected arbitrarily. The corrosion of aluminum tanks occurs most rapidly when the outside temperature and humidity are both high [on a warm day, the outside of the foam can reach 114° F (46° C) while the aluminum is 8°F (4° C) less]. On cool days or on days when the humidity is low, water-vapor permeation is negligible. Thus, the heating of tank interiors would not be required at all times; it would be needed more in the warm and humid summer months than in the cooler and dryer months.

Further study is needed to determine precisely the minimum temperature difference that will prevent corrosion under various atmospheric conditions. Further study will also determine the types of heaters, heating capacity, and heat circulation necessary to maintain tank interiors at the requisite temperature.

This work was done by Lyle E. Johnson of Martin Marietta Corp. for **Marshall Space Flight Center.** *For further information, Circle 21 on the TSP Request Card.*
MFS-25780

Vacuum Ampoule Isolates Corrosive Materials

A quartz vacuum container assures reliable thermophysical measurements of molten materials.

Langley Research Center, Hampton, Virginia

A quartz vacuum ampoule provides a measurement window and sample containment isolation for determining the thermophysical properties of semiconductor materials in a molten state. The quartz ampoule permits reliable measurement of the melt properties of a material such as lead/tin/telluride (PbSnTe). Confinement of the sample in a vacuum prevents contamination of the measurement system by hot corrosive vapors and any interference by preferential evaporation of the melt.

The sample is contained in a quartz tube between two quartz plugs polished on both ends. One plug is inserted into the quartz tube and sealed with a torch (the bottom plug in the figure). After this seal cools, a PbSnTe wafer with parallel faces and known thickness is placed in the tube. The PbSnTe wafer is sized to allow for thermal expansion and an expansion in volume when the phase change occurs at the melting temperature.

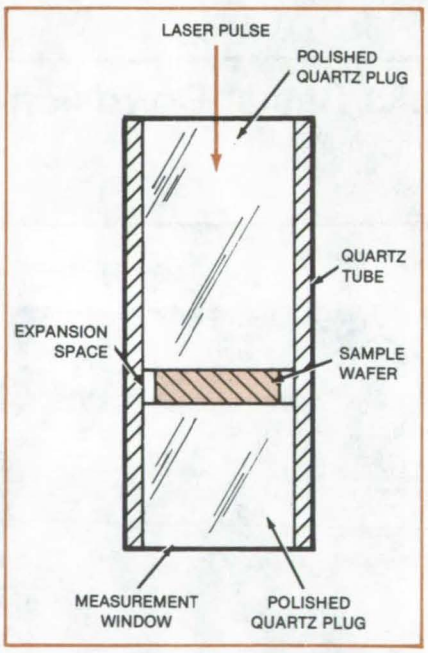

A **Quartz Vacuum Ampoule** confines a corrosive sample wafer between two quartz plugs inserted in a quartz tube. One quartz plug is a window for measuring sample thermodynamic properties while a laser pulse entering the other quartz plug heats the sample to a molten state.

The tube is then mounted on a special attachment to the vacuum system, and the second (top) quartz plug is inserted flush with the top of the PbSnTe wafer. A vacuum seal is made between the top quartz plug and the tube.

Thermal diffusivity measurements are made using the laser flash technique with one of the polished quartz plugs serving as the window to the sample. In addition to its use with PbSnTe, this technique could be applied to other semiconductor materials, such as germanium and mercury/cadmium/telluride.

This work was done by Roger K. Crouch and William J. Debnam of **Langley Research Center** *and Ray Taylor of CINDAS. For further information, Circle 22 on the TSP Request Card.*

This invention is owned by NASA, and a patent application has been filed. Inquiries concerning nonexclusive or exclusive license for its commercial development should be addressed to the Patent Counsel, Langley Research Center *[see page A5].* *Refer to LAR-12898.*

A Solvent-Resistant, Thermoplastic Poly(imidesulfone)

Polymer incorporates the desirable properties of polyimides and polysulfones.

Langley Research Center, Hampton, Virginia

A process for preparing a thermoplastic poly(imidesulfone) results in a material that has the excellent thermoplastic properties generally associated with polysulfones and the excellent solvent resistance generally associated with polyimides. The new thermoplastic, solvent-resistant polymer can be used as a molding resin, as an adhesive, and as a matrix resin for fiber-reinforced composites. The process for thermoplastically forming this resin can be used to produce moldings, adhesive bonds, and fiber-reinforced composites.

Aromatic polysulfones, a class of thermoplastic polymers, are soluble in such solvents as chloroform, methylene chloride, cyclohexanone, cresol, and hydraulic fluids. Since components fabricated from these polysulfones are susceptible to damage by these solvents, this polymer system cannot be used in many applications where the solvents are present. Aromatic polyimides, on the other hand, are a class of polymers that are exceptionally resistant to solvents but that are generally considered not readily processable by thermoplastic techniques. Both polymer systems have good thermal stabilities.

The desired poly(imidesulfone) is obtained through the incorporation of an aromatic sulfone moiety in the backbone of an aromatic linear polyimide to yield an aromatic poly(imidesulfone) prepared in bis(2-methoxyethyl) ether solvent. This polymer system results in a thermoplastic with better processability than the base polyimide. Conversely, the incorporation of an imide segment into the base polysulfone results in a solvent-resistant polymer that was previously soluble in common solvents. The structure of the polymer is shown in the figure. In the structure shown, it is the 3,3′-disubstituted diphenylsulfone segment of the polymer that causes it to be thermoplastic.

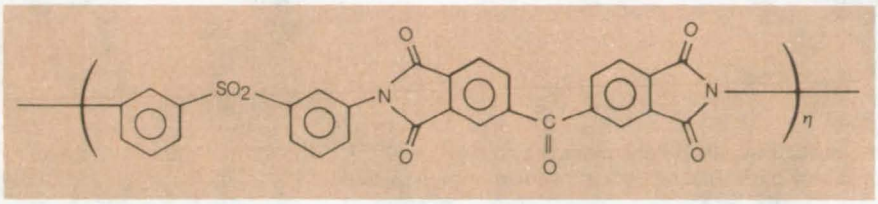

The **Solvent-Resistant Thermoplastic Poly(imidesulfone)** has the structure shown here. The parameter η represents several hundred repeated units.

Thin films of the poly(imidesulfone) placed in various solvents were not affected. After removal from the solvents, the films had the same softening temperatures as before exposure. Even slight solvation of the polymer would cause a considerable lowering of the softening temperature.

Adhesive lap-shear samples prepared with the poly(imidesulfone) had exceptionally high strengths when tested at ambient temperature, at 177° C, and at 232° C, both before and after aging for 1,000 hours at 232° C in a flowing-air oven. Unfilled moldings prepared from the poly(imidesulfone) were clear and had properties that are reasonable for a linear thermoplastic. Graphite-fiber-reinforced moldings (composites) were successfully prepared using unidirectional high-tensile-strength fibers in the resin.

This poly(imidesulfone) can be thermoplastically processed in the 250°-to-350° C range to yield high-quality tough moldings, strong high-temperature-resistant adhesive bonds, and well-formed structural composites. The poly(imidesulfone) should be an excellent candidate for further development as a high-temperature adhesive and molding compound for aerospace applications.

This work was done by Terry L. St. Clair of **Langley Research Center** *and David Yamaki of the Massachusetts Institute of Technology. For further information, Circle 23 on the TSP Request Card.*

This invention is owned by NASA, and a patent application has been filed. Inquiries concerning nonexclusive or exclusive license for its commercial development should be addressed to the Patent Counsel, Langley Research Center [see page A5]. Refer to LAR-12858.

High-Performance Matrix Resins

Modified PMR polyimides have better processability and thermo-oxidative stability.

Lewis Research Center, Cleveland, Ohio

State-of-the-art PMR polyimides (in situ polymerization of monomer reactants) provide good strength and light weight in a wide variety of critical applications. However, improved processability and elevated-temperature thermo-oxidative stability are desired in such polyimide systems. A series of improved polymer resins was developed at Lewis Research Center. These high-performance matrix resins, intended for use in advanced composites, adhesives, and neat resin articles, show improvements in both processability and elevated-temperature stability over the state-of-the-art PMR-15 polymers.

(continued on next page)

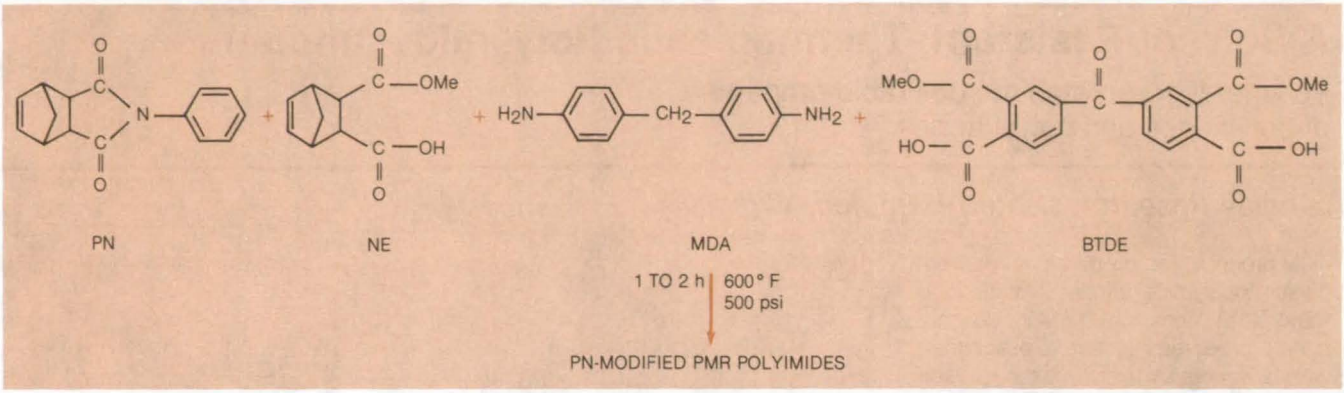

Highly-Cross-Linked Polyimides are formed at 600° F (315° C) from the in situ thermopolymerization of the four monomer reactants. A variety of PMR compositions can be formed by adding 4 to 20 mole percent PN to the standard PMR-15 composition.

The improved modification of the PMR-15 system results from the addition of N-phenylnadimide (PN) to the basic three-monomer reactant system. The basic three monomers are monomethyl ester of 5-norbornene-2, 3-dicarboxylic acid (NE), dimethyl ester of 3,3', 4,4'-benzophenonetetracarboxylic acid (BTDE), and 4,4'-methylenedianiline (MDA) and are present in their standard concentrations. A varity of modified-PMR compositions are formulated by adding 4 to 20 mole percent PN to the standard PMR-15 composition. As shown in the figure, highly-cross-linked polyimides are formed at 600° F (315° C) from in situ thermopolymerization of the four monomer reactants.

A 50 weight percent solid solution is prepared by dissolving the four monomer reactants of known composition in anhydrous methanol at room temperature. The solution is applied to fibers, fabrics, or chopped fibers and then molded into composite articles by curing at 600° F (315° C) and 500 psi (3.45×10^6 N/m^2) pressure for 1 to 2 hours. It can also be applied to surfaces of adherents for bonding composites, metals, or other materials. The solventless powders can be molded into neat resin objects having various shapes and forms.

Of the five modified polymers evaluated, PMR-P1 and PMR-P2, which contain 4 and 9 mole percent PN, respectively, are unique in that they exhibited simultaneously-improved resin-flow properties and thermo-oxidative stability over PMR-15. These materials are low-cost, similar to PMR-15, while having superior processing and elevated-temperature performance compared to PMR-15.

This work was done by Ruth H. Pater of **Lewis Research Center.** *Further information may be found in NASA TM-82733 [N82-11117/NSP], "Novel Improved PMR Polyimides" [$6.00]. A copy may be purchased [prepayment required] from the National Technical Information Service, Springfield, Virginia 22161.*

Inquiries concerning rights for the commercial use of this invention should be addressed to the Patent Counsel, Lewis Research Center [see page A5]. Refer to LEW-13864.

Thermal-Gradient Fining of Glass

Temperature gradients may drive off bubbles in a gravity-free environment.

Marshall Space Flight Center, Alabama

Molten glass could be fined (cleared of bubbles) by heating with a suitable temperature gradient, according to preliminary experiments. Although thermal-gradient fining has been studied by NASA as one of several material-processing methods for use in low-gravity manufacturing, the technique could also be of value in terrestrial glass processing.

A temperature gradient produces a force on gas bubbles trapped in molten glass pushing the bubbles to a higher temperature region where they can be collected. The concept has been demonstrated in experiments on Earth and on a rocket.

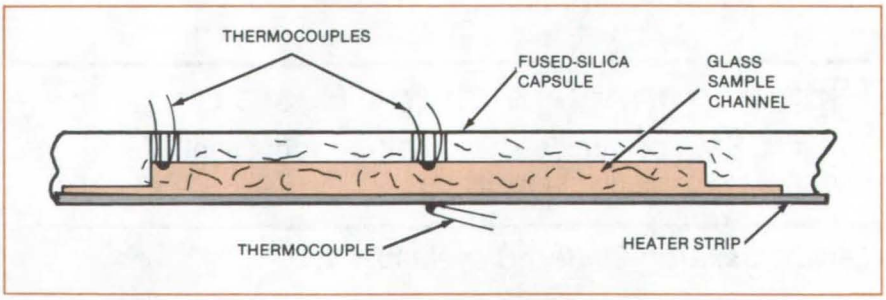

A **Sample of Sodium Borate Glass** is encapsulated by fused silica and a strip heater. The sample channel dimensions are 0.5 by 1 by 10 mm.

In a NASA experiment, a glass sample was packaged in a test cell consisting of a silica glass capsule, a platinum/rhodium strip heater, and thermocouples (see figure). Housed in an automatic test payload, the cell was

launched on a Spar rocket, and the sample was heated during the 4 minutes of zero gravity before the payload returned to Earth. The sample was a sodium borate glass, which has a negative temperature coefficient of surface tension.

During the zero-gravity period, a camera in the payload took 246 photographs of the molten glass sample at 1-second intervals. At the same time, temperature data from the thermocouples embedded in the glass and welded to the heating strip were telemetered back to Earth. A signal proportional to the current drawn by the camera film-advance motor was also telemetered as a time indicator for the film sequence.

The photographic record shows that many of the bubbles in the glass were rapidly swept out by the high temperature gradient as it heated up to about 913° C. Since there was also a strong transverse gradient, bubbles migrated not only longitudinally along the sample-capsule channel but also transversely to the strip heater. Once they contact the strip, bubbles move slowly if at all. As the experiment progressed, bubbles that were in cooler regions were slowly drawn to the center of the channel.

This work was done by W. R. Wilcox of Westinghouse R&D Center for **Marshall Space Flight Center.** *For further information, Circle 24 on the TSP Request Card.*
MFS-25757

Designing Glass Panels for Economy and Reliability

Method considers such factors as glass temper and load duration.

NASA's Jet Propulsion Laboratory, Pasadena, California

An analytical method determines the probability of failure of rectangular glass plates subjected to uniformly distributed loads such as those from wind, Earthquake, snow, and deadweight. Although developed as an aid in the design of protective glass covers for solar-cell arrays and solar collectors, the method should also be useful in estimating the reliability of large windows in buildings exposed to high winds and can be adapted to nonlinear stress analysis of simply supported plates of any elastic material.

For economy, glass plates should have the minimum thickness consistent with a reasonably low risk of failure. In the past, the minimum allowable thickness has been determined from design curves published by glass manufacturers, but such curves have certain shortcomings: They are sometimes derived from tests on only a few samples and therefore do not have a strong statistical base. Usually the curves do not take load history into account, even though the breaking strength of glass depends strongly on load duration. Snow and deadweight ordinarily are not important in vertical windows; but because solar-collector panels are tilted, such loads last longer than windloads and may cause failure at lower stress.

The new method allows the designer to select the glass thickness that will sustain given normal pressure loads at a specified failure rate. There are two key elements of the method: First, design curves were developed that permit the user to estimate the stress in the glass caused by the given applied loads. Second, statistical analysis was used to produce curves that give the breaking strength of the glass as a function of failure rate, glass temper, load duration, and panel area. A satisfactory design is attained when the estimated applied stress is slightly less than the estimated breaking strength corresponding to the accceptable failure rate.

This work was done by Donald M. Moore of Caltech for **NASA's Jet Propulsion Laboratory.** *For further information, Circle 25 on the TSP Request Card.*
NPO-15252

Processor Generates and Extracts Silicon

An impinging jet/funnel system separates the silicon and salt formed in the reduction of silicon tetrachloride by sodium.

NASA's Jet Propulsion Laboratory, Pasadena, California

A processor now under development would continuously generate pure silicon and separate it from reaction byproducts. In a laboratory prototype, the reduction of silicon tetrachloride by sodium is the key reaction and the byproduct is NaCl, although other silicon halides could probably be substituted for the tetrachloride.

In the processor (see figure), vapors or fine liquid sprays of sodium and silicon tetrachloride react to form gaseous NaCl and liquid droplets of silicon. To prevent condensation of the salt vapor or solidification of the silicon, the reactor temperature is held above 1,415° C, 5° C above the melting point of silicon. The reactor pressure is about 0.25 atm (2.5×10^4 N/m^2).

The products exit through an orifice at the bottom of the reactor into a volume

(continued on next page)

kept at less than half the reactor pressure. The pressure difference creates a jet of gaseous NaCl that carries the silicon droplets.

A separator/collector surface, placed across the jet in the low-pressure region, intercepts the impinging jet. The silicon hits the surface, which is held near 1,412° C, and collects on it. The salt flows away to cooler surfaces in regions of even lower pressures. These cooler surfaces rapidly condense the salt vapor, eliminating the need for vacuum pumps.

The separator/collector surface is a pedestal in the center of a crucible. The silicon, separated from the salt, flows down the funnel-shaped walls of the separator/collector into a much larger collector, where it rapidly solidifies. The collector is isolated from the reactor and separator in the process vessel by a vacuum lock. The filled collector is periodically removed and replaced by an empty one.

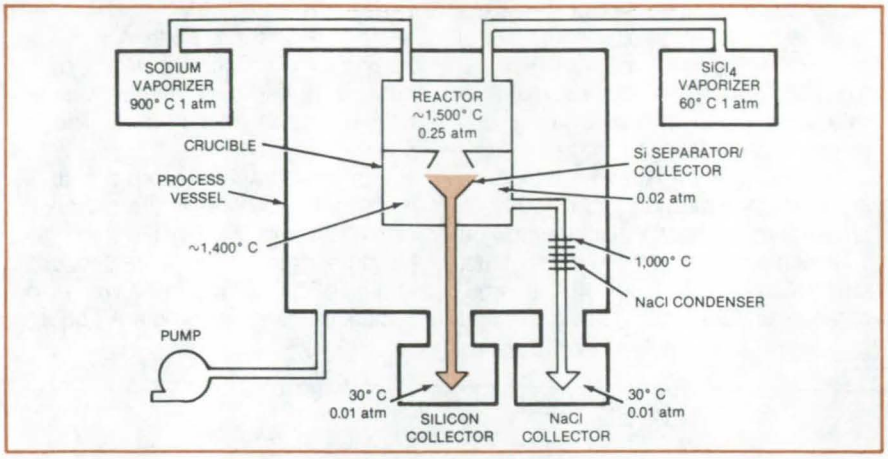

The Silicon Separator/Collector intercepts an impinging jet of reaction products and selectively funnels the silicon into a larger collector. The salt byproduct is removed by a tubular condenser, which is held at 1,000° C, and then flows into a collector, where it solidifies. Vacuum locks permit periodic salt removal without disturbing continuous operation.

This work was done by Robert K. Gould and Charles R. Dickson of Aero-Chem Research Laboratories, Inc., for **NASA's Jet Propulsion Laboratory.**

For further information, Circle 26 on the TSP Request Card.
NPO-15582

Sodium Spray Would Speed Silicon Production

The production rate of solar-grade silicon in a sodium/silicon tetrafluoride reactor would be increased by a spray feed.

NASA's Jet Propulsion Laboratory, Pasadena, California

Liquid sodium would be sprayed into a sodium/silicon tetrafluoride reactor according to a new proposal for increasing the production rate of solar-grade silicon. The large surface-to-volume ratio of the sprayed sodium droplets would make the reaction proceed faster than if the liquid sodium was poured into the reactor.

In the proposal, the liquid sodium at about 100° C is sprayed (see figure) into the silicon tetrafluoride gas and reacts with it only at the bottom of the reactor, where the temperature is 400° to 900° C. The rest of the reactor temperature is low enough to avoid excessively vaporizing the sodium, so that the reaction products form only on the reactor bottom. Also, to insure that the sodium spray does not clog the reactor, by hitting the walls, the angle of the spray cone is sufficiently narrow, and a baffle is installed.

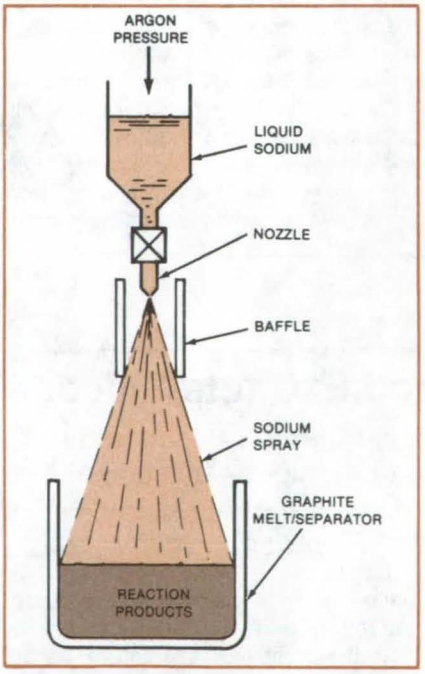

The Liquid-Sodium Droplet Size is controlled by the pressure of argon gas and by the nozzle design. The baffle helps to prevent the reactor opening from becoming clogged by reaction products.

When the reactor is full, the sodium and silicon tetrafluoride flows stop. The silicon and sodium fluoride products in the reactor are then separated.

This method could be applied to similar processes where electropositive metals reduce halides. Halides that can be reduced this way include $TiCl_4$, ZrF_4, and HfF_4; and the metals used include sodium, magnesium, and zirconium.

This work was done by K. M. Sancier of SRI International for **NASA's Jet Propulsion Laboratory.** *For further information, Circle 27 on the TSP Request Card.*
NPO-15246

Two-Temperature-Zone Silicon Reactor

Temperature profile confines SiF_4 reduction by sodium to the reactor bottom.

NASA's Jet Propulsion Laboratory, Pasadena, California

When high purity silicon is synthesized by the reduction of silicon tetrafluoride by sodium, a very-fast highly exothermic reaction takes place. A controlled reaction has been proposed in which a SiF_4-pressurized vertical reactor operates with two temperature zones (see figure). The lower part of the reactor is kept at a temperature higher than 300° C, and the upper part is kept at 110° C. Liquid sodium feeds from a nozzle at the top of the reactor without reacting with the SiF_4. When the sodium reaches the higher temperature region at the bottom, the reaction takes place immediately.

Some of the advantages that this technique has over previous batch techniques are:

- A constant pressure can be used, simplifying the SiF_4 feeding system;
- The temperature of the reaction can be controlled easily by changing the feeding rate of Na and the pressure of SiF_4, resulting in more-homogeneous reaction products;
- The efficiency of material consumption is almost 100 percent;
- The impurity pickup from the reactor walls is minimized; and
- The reaction products only contact the reactor walls at the base, making it easier to remove them from the reactor.

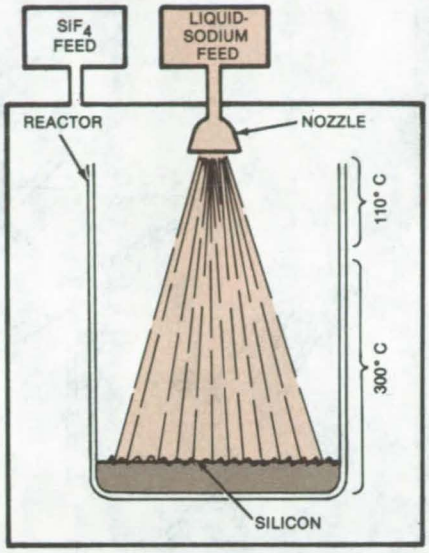

Small Droplets of Sodium sprayed from a nozzle flatten and react when they hit the bottom of a reactor. This technique creates a large reaction area over a narrow depth.

Reaction parameters for a two-temperature-zone reactor have yet to be worked out. These parameters include the size of the sodium droplets, the rate of sodium delivery, and the reactor temperature.

This work was done by Angel Sanjurjo, Leonard Nanis, Vijay K. Kapur, and Robert D. Weaver of SRI International for **NASA's Jet Propulsion Laboratory.** *For further information, Circle 28 on the TSP Request Card.*
NPO-15368

Casting Silicon Pellets From Powder

Fine silicon powder melts in a thin quartz bubble that breaks upon cooling.

NASA's Jet Propulsion Laboratory, Pasadena, California

A new technique converts finely powdered silicon into solid pellets. The pellets are used in spark-source mass-spectroscopic analysis of the silicon and in electrical-resistivity measurements for detecting low-level contaminants.

Powdered silicon is produced when silane is cracked in a free-space reactor. It must be converted to pellet form to perform the impurity testing.

A previous method for casting the powder using silica containers sometimes caused the solid pellets to crack because of the difference in thermal expansion between the melt and the mold. The new technique uses a thin-walled quartz mold. Although the quartz fractures on cooling, the solid silicon remains crack-free.

The pellets are fabricated in a thin-walled bubble blown in the end of a quartz tube. In a test, the tube was 24 mm in diameter, and the bubble wall was about 0.1 mm in thickness. With silicon powder packed into the bubble, the tube is heated in a vacuum furnace. Upon cooling, the bubble shatters, leaving behind a crack-free pellet of silicon.

This work was done by Ernest G. Farrier and Joachim Rexer of Union Carbide Corp. for **NASA's Jet Propulsion Laboratory.** *For further information, Circle 29 on the TSP Request Card.*
NPO-15272

Short Shot Tower for Silicon

Passage through a cold liquid reduces the drop length for shot formation.

NASA's Jet Propulsion Laboratory, Pasadena, California

The drop length necessary to convert molten silicon to shot is expected to be reduced by a proposed new process. In addition to falling through a gas, the droplets of molten silicon fall through a cold liquid. Both the heat-transfer coefficient and the temperature difference between the hot silicon and the cold surrounding liquid are greater than they would be for a gas. Therefore the heat of the silicon droplets is transferred more quickly, and they become hard spheres within a shorter drop distance.

The conversion of silicon from powder or chunks to shot often simplifies processing. Shot is more easily handled in most processing equipment — in furnaces, for example.

The silicon droplets are ejected from a nozzle into gaseous argon, through which they fall into liquid methanol (see figure). In the methanol, the silicon cools and solidifies, falling as shot to the bottom of the tower, where it can be collected. The methanol liquid collected with the shot is recycled.

The argon flowing above the liquid methanol prevents methanol vapor from entering the upper part of the tower and the nozzle. What methanol vapor does arise is carried off through the argon vent pipe and recycled.

This work was done by Herbert E. Bates, David M. Hill, and David N. Jewett of Energy Materials Corp. for **NASA's Jet Propulsion Laboratory.** *For further information, Circle 30 on the TSP Request Card.*
NPO-15607

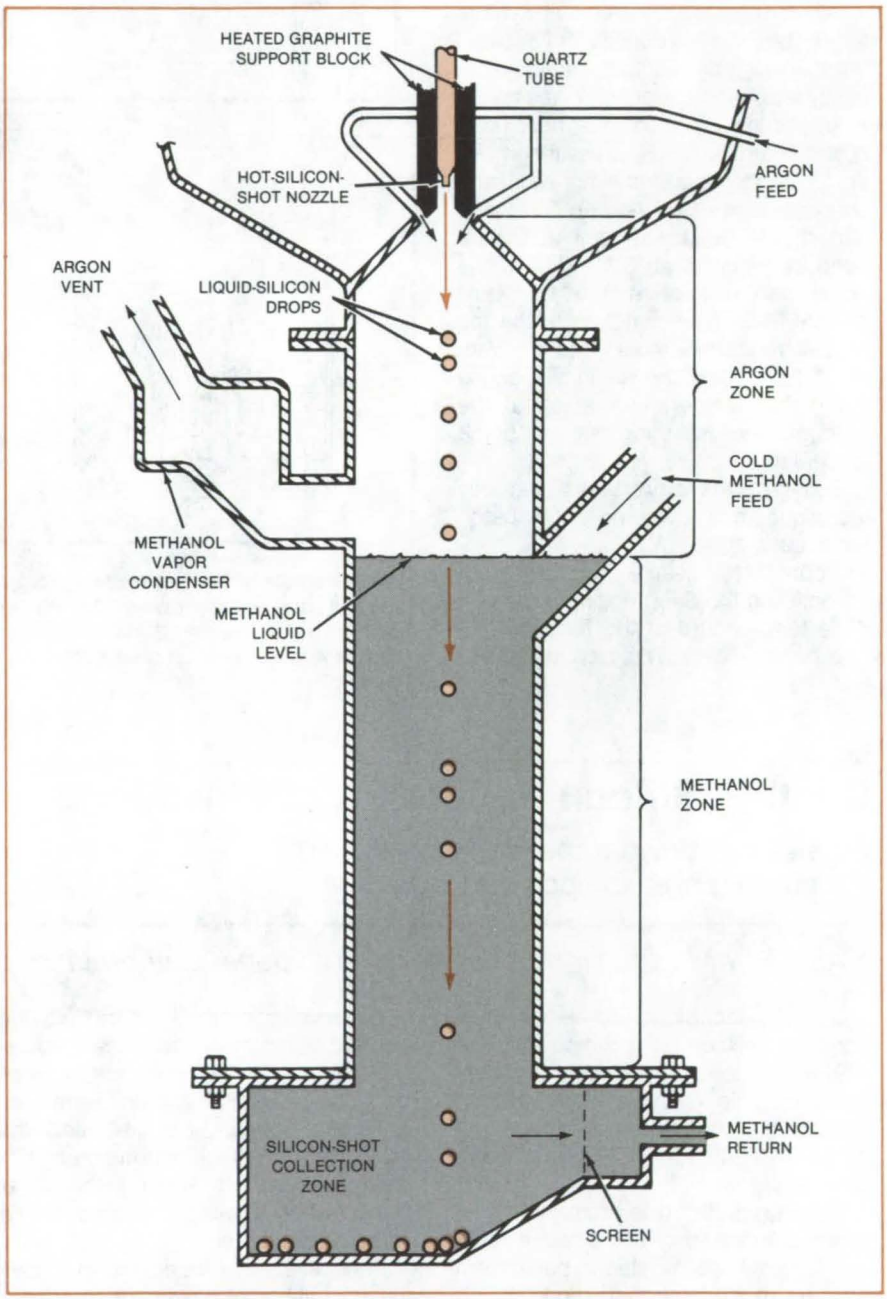

Drops of Liquid Silicon fall through a protective cloud of argon, then through a rapidly cooling bath of methanol, where they quickly turn into solid shot.

Estimating the Degree of Cross-Linking in Rubber

A new analysis of both the extension and retraction may give better estimates.

NASA's Jet Propulsion Laboratory, Pasadena, California

The degree of cross-linking or network chain concentration of rubber is estimated with the aid of a new method. The quantity is needed in studies of the mechanical behavior of rubber. The new method is based on the finding that rubber follows different stress/strain relationships in extension and retraction.

Previously, chain concentration was estimated by measuring the uniaxial stress/strain response in extension and using the measurements in an equation having the chain concentration as one of its terms. One deficiency of this method is that rubber is basically viscoelastic, and therefore equilibrium or time-independent data are difficult to obtain. However, it has recently been found that while the stress/strain response in extension invariably follows equation (1) in the figure, the subsequent stress/strain response in the same specimen in retraction almost invariably obeys equation (2) provided that elongation is not close to the elongation at which stress was reversed and that the maximum elongation is relatively large.

Tests were performed on ring specimens in a standard stress/strain testing machine. When the maximum extension was reached, the test machine was reversed so that retraction occurred at the same constant rate as in extension. The strain for both extension and retraction was calculated on the basis of the original dimensions of the specimen — that is, no account was taken of permanent set, which was quite small.

The network chain concentration in the samples was estimated by this method to be 122×10^{-6} mole/cm^3, which agrees well with the value of 110×10^{-6} mole/cm^3 found by an independent technique. However, if one were to use the data from extension alone, the value would be much lower: 73×10^{-6} mole/cm^3.

It is suggested that a gum vulcanizate is composed of two interdependent networks. One network is composed of those chains attached at each end to chemically cross-linked units and known as permanent network chains. The other network consists of entangled but not cross-linked chains; it is referred to as the transient network.

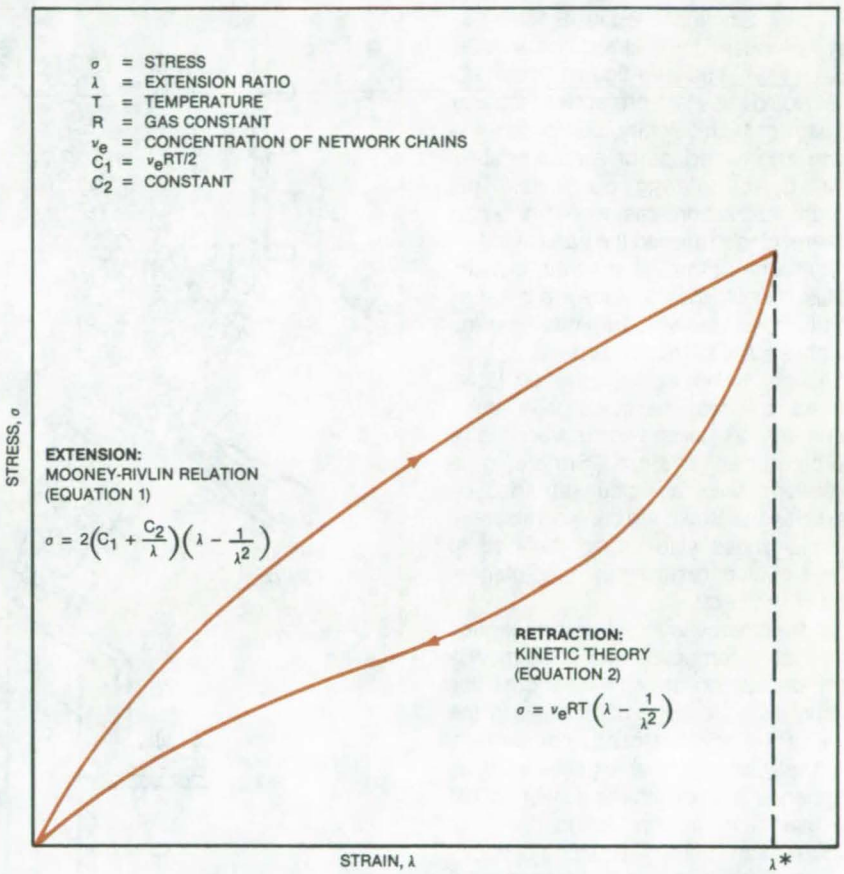

When a Rubber Specimen is stretched to a given extension ratio λ and then released, its stress-vs.-strain curve follows two paths: one for extension and another for retraction.

When the combined networks are subjected to a load, the permanent chains respond almost immediately, but the chains in the transient network move more slowly from their initial position to a final position, which is reached after the entanglements have gone through their maximum travel. The transient-network chains then function as if they formed a permanent network and continue to do so until the load is reduced to near zero; then relatively slow rearrangements occur, and the entanglements move back to a stress-free position.

For rubber containing a filler material, there is the additional effect of dewetting or separation of the rubber from the surface of the filler particles under load. The modulus of filled rubber is given by two contributions: (1) that from the network chain concentration of the rubber itself and (2) that from the presence of filler. This latter contribution is proportional to the fraction of surface area of filler in contact with the rubber. The higher the elongation, the lower will be the modulus because some fraction of the surface area of the filler will have separated from the rubber. As the load is reduced in the retraction portion of the load cycle, rewetting does not occur instantly, and therefore the response is equivalent to that of a sample with a lower filler level. When the load is reduced to zero, the rubber rewets the particles, and eventually the properties of the original unstressed sample are restored.

This work was done by Robert F. Fedors of Caltech for **NASA's Jet Propulsion Laboratory.** *For further information, Circle 31 on the TSP Request Card.*

NPO-15590

Improved Fluidized-Bed Gas Injector

Annular gas flow would cool and protect the injector cone.

NASA's Jet Propulsion Laboratory, Pasadena, California

A new single-cone gas injector has been proposed for fluidized-bed particle-coating systems (see figure). The injector would use a protective annular stream of high-velocity gas to cool the cone and to reduce or eliminate abrasion by circulating particles. This diluent/fluidization gas would enter at several places around the base of the injector cone or through a continuous annulus. It would then flow toward the apex of the cone, carrying particles into the highly-agitated reaction zone.

A very highly agitated region is required to coat particles with such materials as silicon or carbon in a fluidized-bed system. Simple gas-injection cones are often abraded by particles that strike the base of the cone. Simple cones also cause the bed to surge or slug, resulting in some stagnation of the bed.

In the improved injector, the reaction gas that decomposes to provide the silicon or carbon to coat the particles would enter through a tube along the axis of the injector cone. For carbon, thermally decomposable gases, such as methane (CH_4) or ethane (C_2H_6), could be used. For silicon, silane (SiH_4) or trichlorosilane ($SiHCl_3$) could be used.

The reaction gas decomposes as it comes in contact with the hot particles. If necessary to prevent premature decomposition, the reaction gas could be cooled right up to the moment it enters the fluidized bed.

The seed particles would enter through a piston valve at one side of the bed and flow quickly down the side, up the cone, and into the reaction zone. Coated particles would be drawn off through a similar valve on the other side. Depending on purity requirements, injector components could be constructed from such materials as quartz, carbon, or metal.

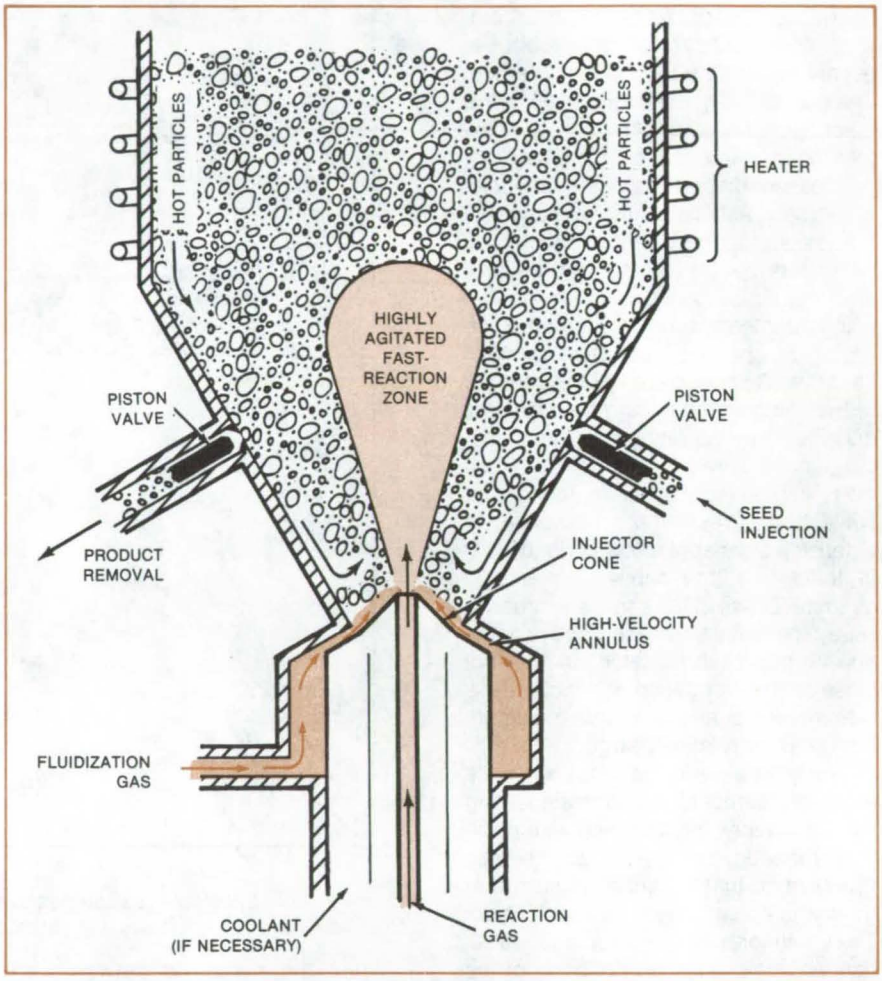

The **Gas-Injection Cone** in a fluidized-bed reactor for coating particles with silicon or carbon could be cooled and protected from abrasion by a stream of gas flowing over the surface of the cone. Hot particles entering the reaction zone would be coated with silicon or carbon supplied by thermal decomposition of a suitable gas injected into the reaction zone.

This work was done by Richard A. Hogle of Caltech for **NASA's Jet Propulsion Laboratory.** *For further information, Circle 32 on the TSP Request Card.*
NPO-15572

Membranes Remove Metal Ions From Industrial Liquids

The low-cost membranes are simply suspended in metal-ion/liquid solutions to remove impurities.

Lewis Research Center, Cleveland, Ohio

Disposing of contaminated liquids is an increasing problem in today's industrial society. Metal cations (positively charged atoms) are present as contaminants or impurities in many industrial liquids. Liquids with these impurities are either enviromental pollutants or possible sources of recoverable materials. In either case it is desirable to remove these metal ions efficiently. Current systems employ cation-exchange resins as powders, beads, or granules for use in metal-removal filtration systems. In terms of energy requirements and capital equipment costs, however, these systems are not optimized since they are expensive and not necessarily cost-effective. These systems require pumping a liquid through a filtration system that is subject to both clogging and resin fouling.

A method has been developed at Lewis Research Center that is a major improvement in metal-ion removal. It eliminates the need for costly pumping and filtration equipment in specific applications. This technique enables the cation-exchange resin to be fabricated into a more efficient form, that of a thin membrane film of various sizes. Membranes of this type may be simply suspended in metal-ion/liquid solutions to remove the impurities. This removal system does not require pumping, filtration equipment, or constant movement of the solution. The unique quality of these membrane films is that they are nonfouling and have outstanding high-absorption capacity.

The use of these membrane films affords a convenient and economical alternative for removing and recovering metal cations present in low concentrations from large quantities of liquid solutions. Possible applications of these membrane films include use in analytical chemistry for the determination of small amounts of toxic metallic impurities in lakes, streams, and municipal effluents. It is also possible that this type of ion-exchange membrane may be suitable for use as an absorber of certain pollutant gases and odors present in confined areas.

These membrane films comprise a cross-linked copolymer of polyacrylic acid (the active ion exchanger) and polyvinyl alcohol (the antifouling agent). An aqueous solution of these constituents is cast (poured) onto a smooth surface and dried. The dried film is removed and formed into any desired shape. It is then exposed to ionizing radiation that causes copolymerization and cross-linking. Treatment with aqueous calcium hydroxide converts the polyacid and has a wide variety of applications.

This work was done by W. Philipp, L. Hsu, and C. May of **Lewis Research Center.** *Further information may be found in:*

NASA TM-81670 [N81-16123/NSP], "New Ion Exchange Membranes" [$6], and

NASA TP-1407 [N79-21120/NSP], "Three Methods for In Situ Crosslinking of Polyvinyl Alcohol Films for Application as Ion Conducting Membranes in Potassium Hydroxide Electrolyte" [$12].

Copies of these reports may be purchased [prepayment required] from the National Technical Information Service, Springfield, Virginia 22161.

Inquiries concerning rights for the commercial use of this invention should be addressed to the Patent Counsel, Lewis Research Center *[see page A5].*
Refer to LEW-13853.

Viscosity Depressants for Coal Liquefaction

Certain unsaturated hydrocarbons would prevent coal from solidifying during liquefaction.

NASA's Jet Propulsion Laboratory, Pasadena, California

A proposed process modification would incorporate viscosity depressants to prevent coal from solidifying during liquefaction. The depressants would reduce the amount of heat needed to liquefy coal.

While the coal is processed, unsaturated hydrocarbons containing eight or more carbon atoms would be put into the liquid medium to act as viscosity depressants. Among possible depressants are metallic soaps, such as lead stearate, and amides, such as stearamide and dimer acid amides. Other possibilities are such epoxylated fatty acids as epoxylated linseed oil, epoxylated olive oil, and epoxylated linolenic acid, and waxes, such as beeswax, carnauba wax, and paraffin wax. Any of these compounds would be satisfactory viscosity depressants for coal, but the epoxylated fatty acids are preferred when used in an amount of less than 0.1 weight percent, based on the amount of coal used.

This work was done by Sarkis H. Kalfayan of Caltech for **NASA's Jet Propulsion Laboratory.** *For further information, Circle 33 on the TSP Request Card.*
NPO-15174

Books and Reports

These reports, studies, and handbooks are available from NASA as Technical Support Packages (TSP's) when a Request Card number is cited; otherwise they are available from the National Technical Information Service.

Development of Silane Hydrolysate Binder for Thermal-Control Coatings

Tough coating requires a cure temperature of only 66° C.

A technical report describes the theoretical and experimental development of a methyltriethoxysilane (MTES) hydrolysate binder for white, titanium dioxide-pigmented thermal-control coatings such as are often needed on satellites. The new coating is tougher and more abrasion-resistant than the conventional coating, S-13G, which comprises zinc oxide in a hydroxyl-terminated dimethylsiloxane binder. For an earlier article on methyl trialkoxysilane hydrolysates, see "Binders for Thermal-Control Coatings," in *NASA Tech Briefs*, Vol. 6, No. 3 (Fall/Winter 1981), page 287 (MFS-25620).

Ultraviolet absorptance on both the old and new coatings held at about 0.2 during a 930-h exposure in a solar-radiation simulator. (Longer tests would be required to assess any difference between the two coatings in ultraviolet resistance.) In an outgassing test of the new coating run at 10^{-6} torr and temperatures up to 212° F (100° C), weight loss was less than 0.2 percent per hour, which is considered acceptable for coating materials in space. In a thermal-cycling test — five cycles, -150° to 150° F (-101° to 66° C), bend tests on cycled samples of the new coating showed no significant increase in tendency to craze or crack.

In the optimum formulation, MTES monomer is polymerized by hydrolysis with water in the mole-equivalent ratio 10/3.25 ($MTES/H_2O$) and mixed with TiO_2 (previously ball-milled in ethanol) in a weight ratio 12/26 (TiO_2/binder). The formulation is then sprayed on an aluminum substrate and cured for 24 h at 75° F (24° C) followed by 3 days at 150° F. Cured thickness is 2 to 2.5 mils (0.05 to 0.06 mm).

In arriving at this formulation, a series of tests was run to determine the parameters of pigment/binder ratio, ethanol content, pigment particle size, coating thickness, and cure conditions. The effect of elevated temperature on the hydrolysis rate was striking and undesirable: At 120° F (50° C), some gelation and precipitation of insoluble polymer occurred.

This work was done by W. J. Patterson of **Marshall Space Flight Center.** *Further information may be found in NASA Technical Paper 1900 [N81-31365/NSP], "Development of a Silane-Hydrolysate Binder for UV-Resistant Thermal Control Coatings" [$6]. A paper copy may be purchased [prepayment required] from the National Technical Information Service, Springfield, Virginia 22161. The report is also available on microfiche at no charge. To obtain a microfiche copy, Circle 34 on the TSP Request Card.*
MFS-25749

Life Sciences

Tissue-Culture Method of Cloning Rubber Plants

By adjusting the culture medium, an excised shoot tip can produce up to 50 identical guayule plants.

NASA's Jet Propulsion Laboratory, Pasadena, California

The guayule plant, a high-yield rubber plant, can be cloned by a tissue-culture method to produce multiple new plants that mature quickly. With this method many clones can be bred from a single parent, and each clone can then be rooted and transplanted to soil where it will grow and mature. The method preserves a desired genetic identity (genotype), so that the clones should produce as prolifically as their parents if planted in the same environment.

The guayule plant, *Parthenium argentatum*, forms many lateral buds, the majority of which can be removed without affecting the growth of the parent plant. The small shoot tips, the most regenerative parts of the plant, are removed by microscalpels and placed on slants of sterilized tissue-culture medium. The culture medium contains water, agar, minerals, sucrose, thiamin hydrochloride, and the cytokinin benzylaminopurine (BAP).

By varying the concentration of the cytokinin, a single excised tip can produce either 1 or several (up to 50) new plants. In a medium with a 0.1-mg/l concentration of BAP, the tips respond quickly and produce new leaves, which does not occur with shoot tips grown in a culture medium that lacks BAP. Higher concentrations of the cytokinin accelerate these developments.

The figure shows plantlets grown in cultures with different concentrations of BAP. After a month of growth, the cultures can be either transferred intact or separated into individual shoots and placed in a rooting medium containing 3 percent B-indolybutyric acid and no cytokinin, which inhibits root growth.

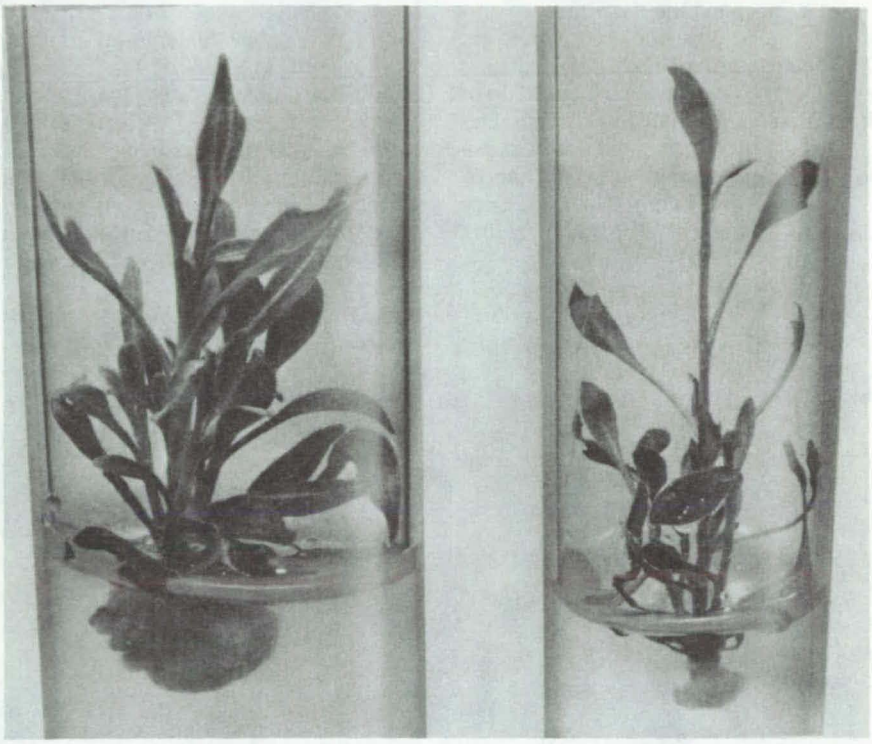

The **Numerous Shoots of the Clone Plantlets** grown in cultures containing 1 mg/l of BAP were short and thick stemmed (left). Plantlets from media containing 0.1 mg/l BAP were slender (right). However, within 30 days after removal from the culture medium, both plantlets produced numerous roots.

To compare the growth of the clones with that of seeded plants, potted clone plantlets were grown in full Sunlight for 13 months along with equal-aged seedlings. During the first 6 months, a few of the plantlets flowered, a sign of a mature plant, but only one seedling did so; most of the seedlings continued vegetative growth without flowering. A check of the chromosome count of the plantlets and seedlings showed they were both the same, 36 — the normal number for sexually-reproducing guayule plants.

This work was done by Ernest A. Ball of The Regents of the University of California for **NASA's Jet Propulsion Laboratory.** *For further information, Circle 35 on the TSP Request Card.*
NPO-15756

Computer Programs

These programs may be obtained at very reasonable cost from COSMIC, a facility sponsored by NASA to make new programs available to the public. For information on program price, size, and availability, circle the reference letter on the COSMIC Request Card in this issue.

Life Sciences MIS

An interactive system utilizing "form-fillout" capability

The Management Information System, MIS, provides the Life Sciences Projects Division at Johnson Space Center with an automated system for project management. MIS development objectives included:

a. A simple system that allows for the rapid and accurate update and review of the status of any active task within the project,
b. The ability to store and update desired

(continued on next page)

management-level data and to manipulate the data for display,

c. The ability to display the information to conduct status meetings with a large number of participants,
d. To provide a network among remote users enabling them to exchange and review information, and
e. To provide an access-limiting security system around the data base.

The Life Sciences commitment to the Shuttle Program will ultimately include a series of multiple payloads consisting of from 5 to 50 experiments and supporting equipment. This committment necessitated the development of MIS to handle the management information necessary to keep abreast of all aspects of the program.

NASA has found that a disciplined "goal-oriented" program is the only effective approach in meeting launch dates with confidence. In building a data base to support a goal-oriented program, the project schedule becomes the focal point around which all other information revolves; i.e., cost, open items, problems, and narrative status. MIS provides the Life Sciences Projects Division with just a schedule-centered information system. MIS utilizes the Tektronix 4027 color graphics display terminal and its form-fillout capability. User interface with the MIS data base is through a series of forms including: a technical assessement form, an event-planning form, a milestone schedule form with 6-month, 1-, 2-, or 4- year schedule displays, a project cost/funding status form, a cost-trend chart form, and a miscellaneous form for maintaining information in the data base that is not covered by one of the other forms.

MIS is written in VAX COBOL and FORTRAN for interactive execution on the DEC VAX-11/780 through the Tektronix 4027 terminal. MIS was developed in 1981.

This program was written by Robert A. Dittman of **Johnson Space Center** *and Victor Marks of MATSCO. For further information, Circle B on the COSMIC Request Card.*
MSC-20238

Mechanics

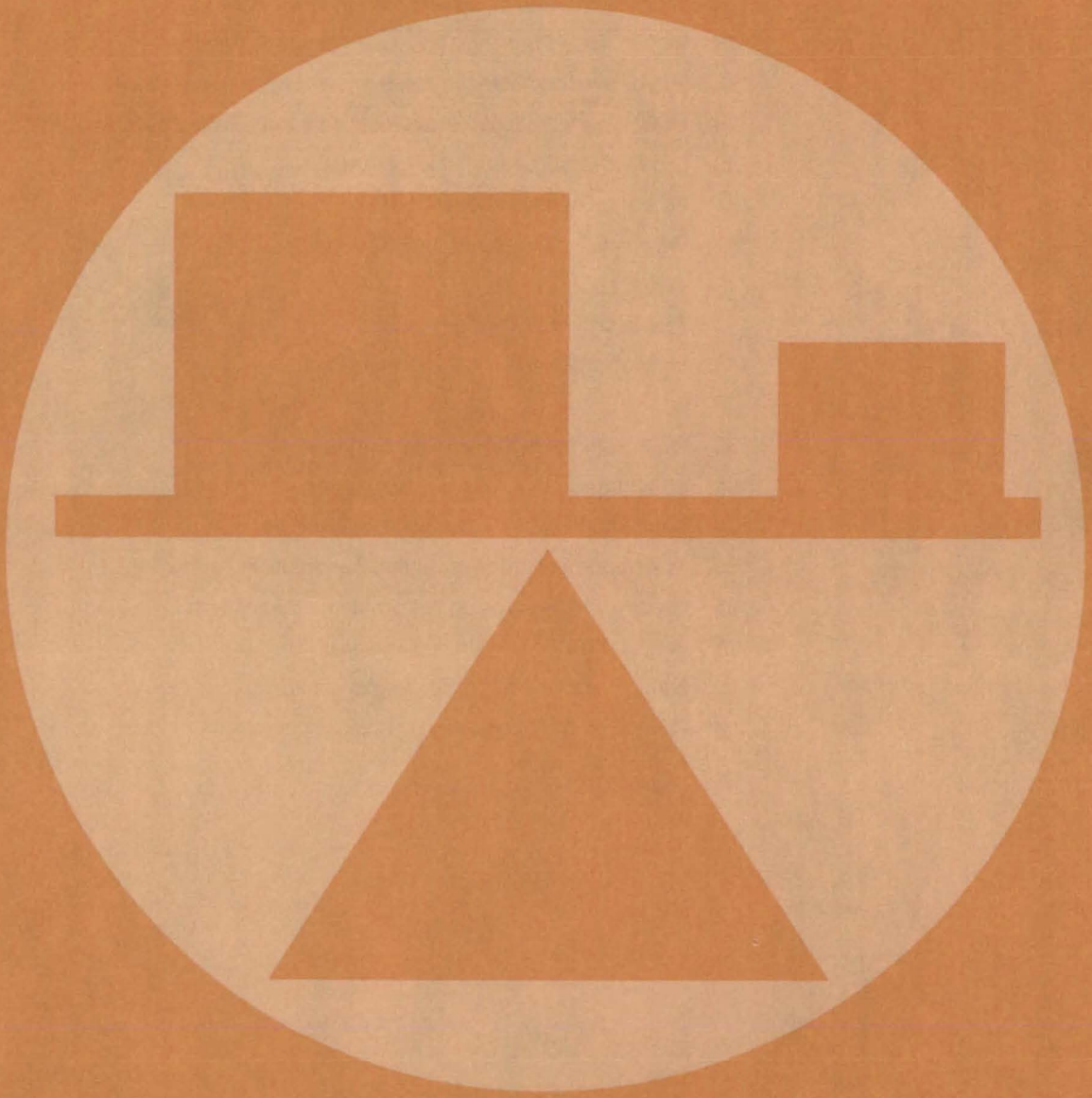

Hardware, Techniques, and Processes

Books and Reports

Computer Programs

Boom Deploys With Controlled Energy Release

A lanyard and a spring-mounted viscous damper regulate rate of stored-energy expenditure.

NASA's Jet Propulsion Laboratory, Pasadena, California

A collapsible boom is deployed in a controlled fashion, yet has no electric or commandable elements. In effect, the structure consists of many fiberglass "springs" that are forcibly coiled during initial stowage in a canister. A considerable amount of energy stored in the structure is released during deployment.

The boom has two sections: an "outboard" mast, containing electronic instrumentation or other hardware that is carried by the boom, and "inboard" mast, which holds the canister in which the collapsed boom is stored before it is deployed. The inboard mast unfolds first during the deployment sequence, followed by the outboard mast.

The deployment rate is controlled by a viscous damper located at the base of the inboard mast (see figure). As the inboard mast deploys, its elastic energy produces a force of 20 pounds (89 newtons) on a lanyard along the center of the mast. The lanyard transmits the force to a rotary damper at its end, which limits the rate at which the lanyard pays out.

Simultaneously, the 20-pound lanyard force is transmitted around an outboard pulley and back to the inboard structure, thereby producing a force of 40 pounds (178 newtons) across the stowed outboard mast. The force holds the outboard mast closed until the inboard mast completes deployment. Then the outboard mast is freed to begin deployment by its own stored energy, producing a 10-pound (45-newton) load on the lanyard.

Springs initiate deployment at the inboard end of the longitudinal members (longerons) of each mast. The springs produce a uniform torque through the first 45° of longeron uncoiling and guarantee that the erection sequence will begin as shown in the figure.

The batten members are 14 percent smaller in diameter in the first and second batten frames on the inboard end of each mast. This provision ensures that the base of the mast will lock up into a fully erect structure before the remaining stowed portions of the mast begin to deploy.

At the completion of deployment, a large transient load is applied to the lanyard from the final release of stored energy as the longerons rapidly rotate into their fully deployed state. The peakload can be as great as 220 pounds (980 newtons) and could break the lanyard. To prevent a break, the viscous damper is attached to the baseplate by springs. When the spring force is exceeded by the peak deployment force, the body of the rotary damper rotates, paying out additional lanyard and greatly reducing the lanyard load.

The controlled deployment sequence allows a boom 27 feet (8.2 meters) long to be uncoiled from a canister only 2 feet (0.61 meter) high. Possible applications include antennas and other lightweight structures that are rapidly erected in the field.

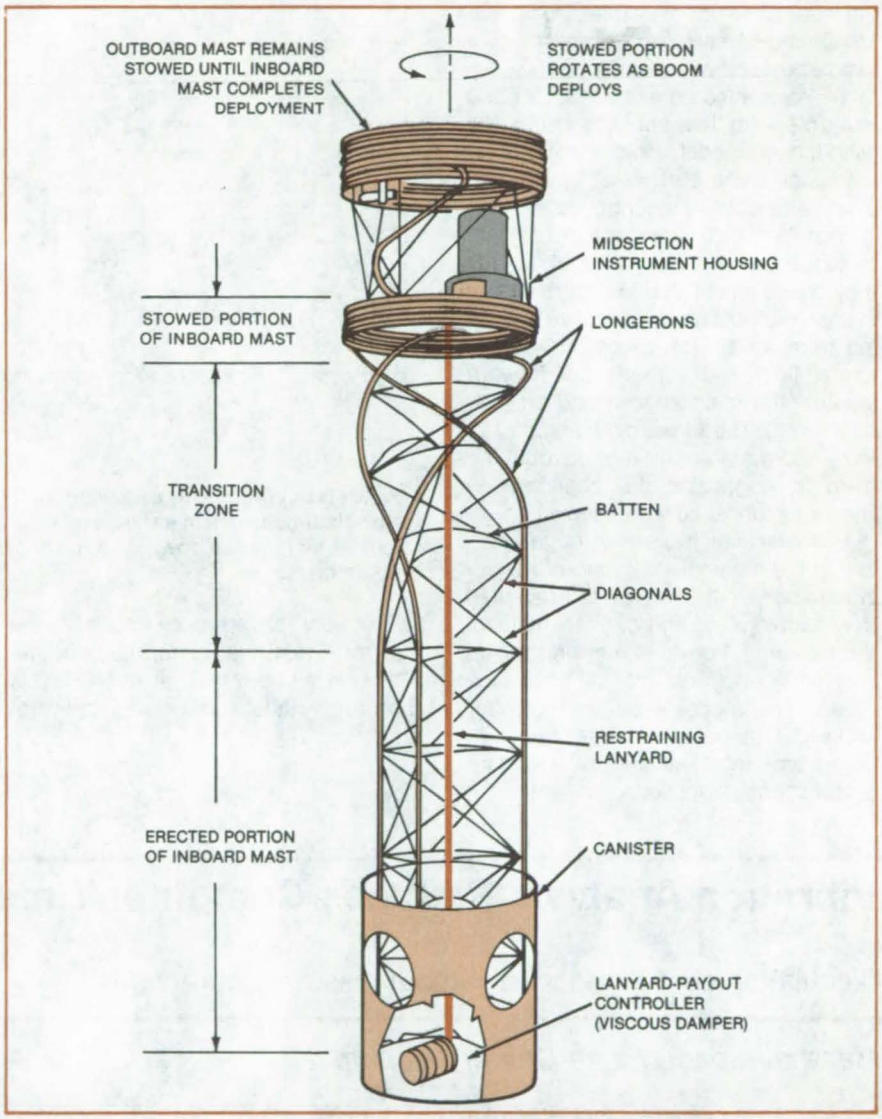

This **Partially Deployed Boom** consists of an erect base, an uncoiling transition zone, and still-coiled zones. The boom members form a lattice structure that is shear-stiffened by diagonal elements when erected.

This work was done by Douglas T. Packard of Caltech and Max D. Benton and Robert F. Crawford of AEC-ABLE Corp. for **NASA's Jet Propulsion Laboratory.** *For further information, Circle 36 on the TSP Request Card.*
NPO-15418

Eliminating Wind-Tunnel Flow Breakdown

Floor nozzle ensures more realistic airflow.

Ames Research Center, Moffett Field, California

Undesirable vortexes near the floor in small wind tunnels are suppressed by a simple device that alters the flow pattern there. Air is injected along the floor and interacts with the backflow from the wind-tunnel model. This results in a smoother, more correct airflow and so to more-reliable wind-tunnel data.

Models of high-lift aircraft are difficult to test in small wind tunnels because they create jets of air that disturb airflow in unpredictable ways. A jet of air emerging from an aircraft model strikes the tunnel floor and spreads out forward (against the main airflow) and aft (see figure, left). The forward-moving part of the jet forms a vortex that disrupts the main flow, causing the phenomenon known as tunnel flow breakdown.

However, if air is blown through a nozzle on the tunnel floor into the forward-spreading jet, the vortex is prevented from forming (see figure, right). Instead, the blowing jet creates a mixing region that hardly interferes with the flow at the model. The model experiences better lift, and test data correlate well with data from large tunnels after standard corrections are applied.

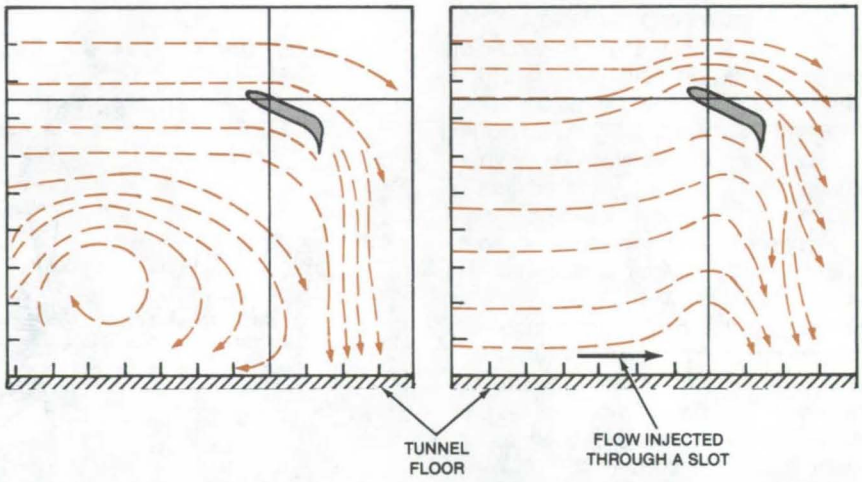

A Vortex Is Suppressed by a Blowing Jet from a floor nozzle. Without the floor jet (left), the vortex disturbs the main airflow around an aerodynamic model. With the floor jet (right), turbulent air is blown downstream. The flow vectors are plotted from laser velocimeter measurements.

The floor jets are easy to use. At the start of a test, the appropriate floor-jet airflow is set up with a valve. The test is then run without further adjustment of airflow.

This work was done by James E. Hackett of Lockheed-Georgia Co. for **Ames Research Center.** *No further documentation is available.*
ARC-11338

Vibration Analysis Reduces Computer Time

Calculation cost is reduced without loss of accuracy.

Marshall Space Flight Center, Alabama

An improved calculation method promises to reduce computer time by a factor of 10 for vibration analysis of complex structures. The method was originally developed to predict the mechanical response of a spacecraft to maneuvers in various cases in which the same booster is used with different payloads (see figure). Many nonaerospace applications are possible whenever major components of a system remain the same while some are varied: These include the design of vehicles and the design or modification of floors, walls, and structural modules.

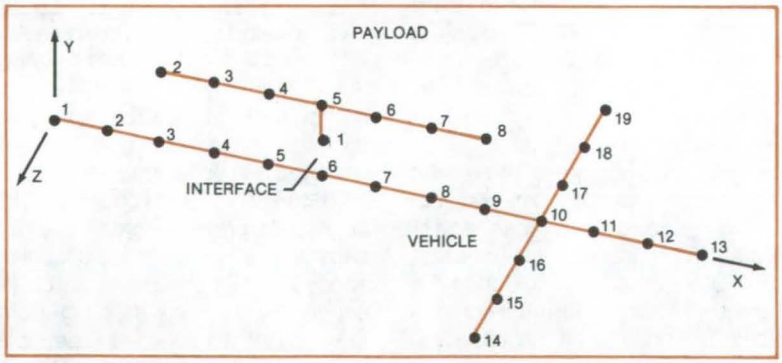

A Representative Analysis separates payload, interface, and vehicle into segmented finite elements. Values of acceleration, velocity, and displacement calculated by the new method and the conventional method differed by as little as a few parts per million.

The method is more exact than conventional normal-mode methods in that it involves no initial approximations or assumptions. An adaptation of the Newmark-Chan-Beta numerical integration technique is directly applied to the coupled system equations, and thus the expensive solution of a system eigenvalue problem is avoided. In the Newmark-Chan-Beta technique, the step size can be based on the cutoff frequency associated with the forcing function regardless of the highest system frequency — a valuable feature since the highest system frequency is usually not known in advance.

Several improvements over conventional techniques and cost-saving features were introduced in the new method. For an indeterminate interface, it is not necessary to express the interface displacements in terms of accelerations and forces. Several simplifications were made in the preliminary calculations that lead to more efficient and convenient calculation of loads.

The method is readily adaptable to short cuts. For example, if a solution of a response and load problem is already available and design changes are made in the payload, it is possible to develop a criterion to determine whether the loads will change significantly.

This work was done by Remi C. Engels of Martin Marietta Aerospace for **Marshall Space Flight Center.** *For further information, Circle 37 on the TSP Request Card.*
MFS-25711

Optical Temperature Sensor Has Digital Output

Device uses a Fabry-Perot multiple-beam fringe sensor.

Lewis Research Center, Cleveland, Ohio

A new instrument* from the world of fiber optics can measure temperatures reliably and accurately. A remote light source feeds light into an optical fiber or cable. The measurement end of the fiber is attached to a Fabry-Perot sensor, which consists of a small spacing that varies with temperature. This spacing is controlled by a temperature-sensitive material. A second output fiber transmits the light passing through this "Fabry-Perot" gap to a photodetection unit and finally to a decoder, before the output is routed to the utilization means.

The gap widens as temperature increases. With this increase in temperature is an increase in the number of spectral bands passing to the receiver. The count of the number of bands passed to the decoder is translated into temperature changes.

A number of advantages accrue to this optical system. Both the temperature sensor and the optical lines are free of all electrical and electromagnetic effects and interference. Variation in the spacer can be made sensitive to other physical quantities, such as pressure. The sensing element itself can be made quite small, enhancing its use in confined areas.

*NOTE: This new instrument is a prototype that is still being further developed; therefore, its accuracy and repeatability have not been determined.

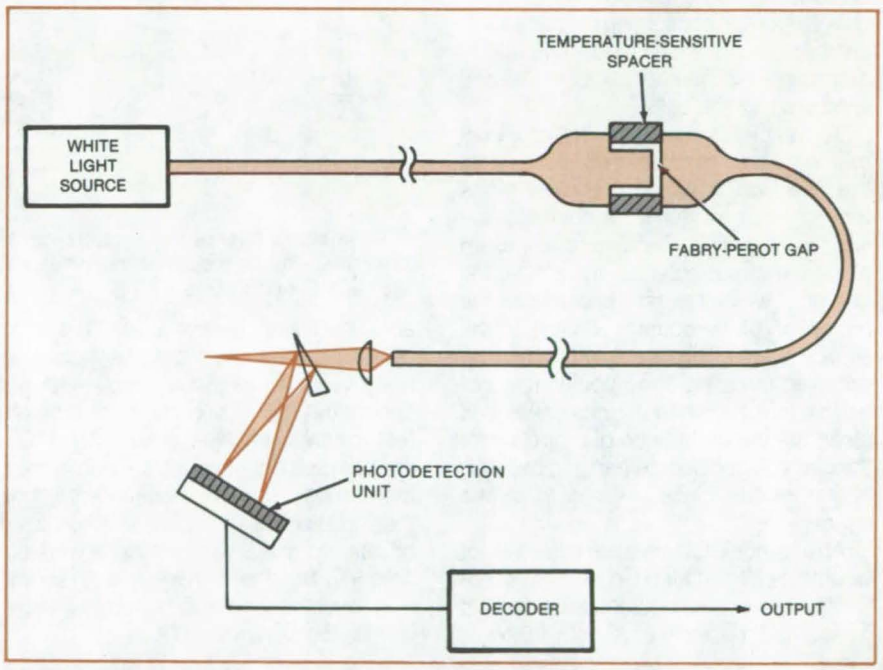

The **Fiber-Optics Temperature Sensor** is free of electromagnetic interference. The sensing element can be made quite small, enhancing its use in confined areas.

This work was done by K. A. James, W. H. Quick, and V. H. Strahan of Rockwell International Corp. for **Lewis Research Center.** *Further information may be found in NASA CR-159519 [N79-27975/NSP], "Analysis and Preliminary Design of Optical Sensors for Propulsion Control" [$10.50]. A copy may be purchased [prepayment required] from the National Technical Information Service, Springfield, Virginia 22161.*

Inquiries concerning rights for the commercial use of this invention should be addressed to the Patent Counsel, Lewis Research Center [see page A5]. *Refer to LEW-13413.*

Radionuclide Counting Technique Measures Wind Velocity

The change in position of a radioactive source translates into wind-velocity measurement.

Langley Research Center, Hampton, Virginia

A proposed technique for measuring wind velocity is based on the inverse-square-law variation of radioactive counting rates. In the proposal, a radioactive source is deposited on the bottom of a light, hollow sphere, such as a plastic table-tennis ball, and suspended by a flexible wire over a radiation counter. The ball can be punctured with symmetrically distributed holes or otherwise roughened for aerodynamic stability.

If the source position is changed because of wind drag on the ball, the solid angle subtended by the counter decreases, and the counting rate is reduced. A graph of counting rate as a function of source position would be used to determine the source position and the wind drag on the ball.

The single-source/single-detector anemometer just described does not yield the direction in which the source has moved, however. Also, the counting rate will not change if the source is moved along the circumference of a circle, the center of which lies on the center of the projection of the counter window on the source plane. This ambiguity would be removed by using three coplanar radiation counters located at equal distances along the circumference of a circle with the undisplaced source hanging over the center of the circle, as shown in the figure.

An anemometer based on this concept would be self-contained, portable, yet not too fragile. It could be used for extended periods of time, even at remote, inhospitable, and inaccessible sites. The proposed anemometer would be accurate and would have good frequency response (≤1 kHz). Calibration would be affected only by changes in humidity. Thus, in fair weather, it would be stable over long periods. The only requirement is that the radiation detectors be checked periodically to make sure they are working properly. The anemometer would require little maintenance and could measure wind velocities up to 100 m/s.

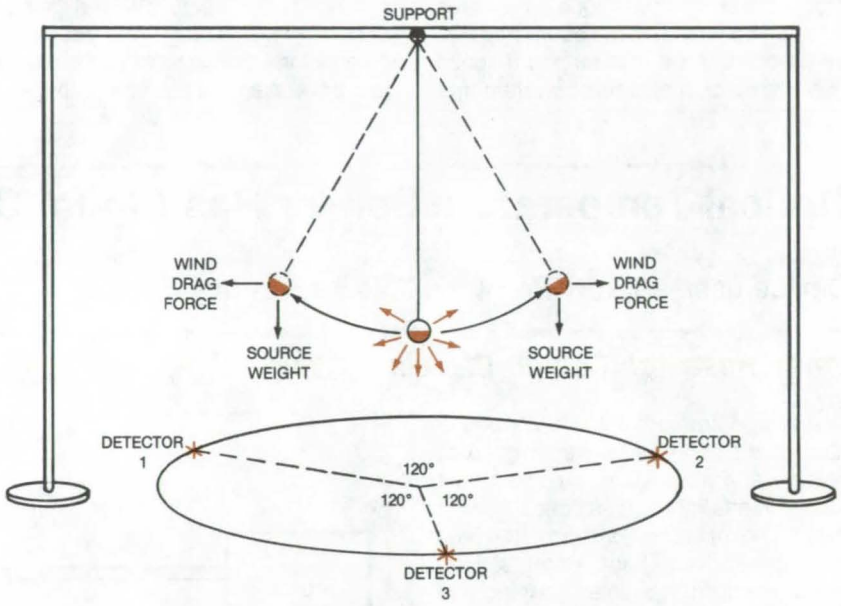

A **Radioactive Source** suspended over three detectors yields both windspeed and wind direction. The concept has been tested using a weak Bismuth 207 source and three Geiger-Müller counters.

This work was done by Jag J. Singh of **Langley Research Center,** *G. S. Khandelwal of Old Dominion University, and Gerald H. Mall of Computer Sciences Corp. Further information may be found in NASA TM-83202 [N82-12419/NSP], "A Radionuclide Counting Technique for Measuring Wind Velocity" [$6]. A copy may be purchased [prepayment required] from the National Technical Information Service, Springfield, Virginia 22161.*
LAR-12971

Microwave Ice-Accretion Measurement Instrument (MIAMI)

Microwaves detect icing on aircraft surfaces.

Lewis Research Center, Cleveland, Ohio

An instrument can be used on operational aircraft to warn the pilot of the onset of dangerous ice buildup or as a research tool for use in studying aircraft icing phenomena and in cloud research. Other ice-detection instruments use probes that project from the surface on which ice will collect, thus creating the problem of having to infer how much ice is really on the surface of interest. This is particularly troublesome when the surface of interest is an aircraft surface since the water-droplet catch efficiencies will be different for the ice-detector probe and the aircraft surface. The MIAMI is embedded in the surface to be monitored and conforms to the surface contour. It automatically measures

the ice forming on the surface of interest. The MIAMI is the only instrument that measures actual ice thickness and accretion rate in addition to giving an icing-onset warning.

The MIAMI detects the onset of icing on a surface (e.g., aircraft wing), continuously monitors ice thickness, and displays ice thickness and accretion rate. A small, 1.4- by 0.4- by 0.2 inch (35.5- by 10.2- by 5.08-mm), microwave waveguide is implanted just below the surface to be monitored. One or more waveguides may be mounted on different components of the aircraft. A microprocessor monitors the resonant frequency of the waveguide(s). As ice forms on the surface of the waveguide, it causes the waveguide resonant frequency to decrease. The frequency shift is measured by the microprocessor and converted to a dc voltage that is proportional to the ice thickness. The microprocessor also computes the change in ice thickness with respect to time to get the ice-accretion rate. The ice thickness and accretion rates are displayed on digital panel meters.

The theoretical basis for the development of the MIAMI is that a resonant surface waveguide is tuned by the application of a substance (such as ice) with approximately the same dielectric constant as the waveguide material. The resonant frequency of the transducer is very sensitive to the thickness of the ice accreting on top of it. Ice layers of approximately 0.005 to 0.100 inch (0.13 to 2.5 mm) are capable of being measured. The transducer and its associated microprocessor convert the ice thickness to a dc voltage that varies in time in a manner proportional to the ice thickness. The time derivative of this voltage is proportionate to the icing severity (accretion rate) and is continuously being computed and displayed by the microprocessor either as a severity level ("TRACE," "LIGHT," "MODERATE," or "HEAVY") or numerically in inches or centimeters per minute.

The effect of ice on the transducer is different from other substances, such as oil, grease, dirt, insects, or other contaminants. The microprocessor is programed to recognize the difference between ice and other substances so that valid icing signals are generated only when ice forms. Water droplets that may form in the boundary layer are neglected by the system. Should a contaminant or foreign body other than ice adhere to the surface of the MIAMI, a continuous tone will be generated providing a fail-safe indication of its operating ability until the foreign object is removed.

Because no probe projects into the airspace, the transducer may be mounted anywhere on the aircraft without interfering with the aerodynamic properties of the aircraft. Also, since no probe exists, there is no opportunity to damage it or break it off or have it ingested by the engine.

If desired, the MIAMI transducer may be equipped with an electrothermal deicer to remove existing ice. With the MIAMI, ice removal is not necessary until the ice thickness exceeds its dynamic range [0.125 inch (3.2 mm)]. Deicing may be programed to occur repetitively in a manner analogous to magnetostrictive transducers or not to occur until the transducer approaches the limit of its dynamic range, thereby saving aircraft energy. The MIAMI will provide a complete history of ice thickness, including the loss of ice by intentional deicing or natural causes.

This work was done by Bertram Magenheim of Ideal Research, Inc., for **Lewis Research Center.** *For further information, Circle 38 on the TSP Request Card.*
LEW-13784

Minimizing Vibrations While Orienting Large Structures

Control algorithm times thrustor pulses to minimize vibrations.

Marshall Space Flight Center, Alabama

Structural vibrations and dynamic loads have been theoretically analyzed for their effects on the pointing and sluing of a large antenna (100 meters in diameter) deployed from the Space Shuttle at the end of a 100-m-long mast. The analysis resulted in a control algorithm that insures pointing accuracy while minimizing vibrations of the long flexible mast. The approach is applicable to terrestrial antennas or other large lightweight structures.

To point the antenna in a particular direction, the Space Shuttle is maneuvered into the appropriate orientation by its pitch, roll, and yaw thrustors. This involves a problem in vibration and attitude control analogous to that of carrying a bowl of soup: One has to move carefully to avoid spills.

(continued on next page)

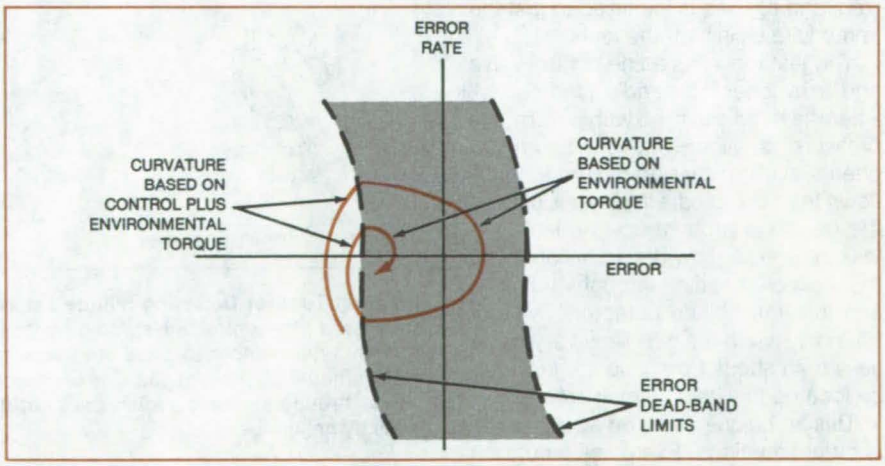

Attitude Error and Error Rate are minimized by a properly-designed control law. The control thrustor returns the attitude to a point within the control dead band whenever the attitude error or error rate strays outside. Within the dead band, the attitude drifts under environmental torque. The leftward thrustor fires when the system phase point is to the right of the error dead band. The opposite is the case for the rightward thrustor.

Similarly, the Space Shuttle or other platform carrying a large antenna on the end of a flexible mast must be moved carefully to avoid setting up oscillations in the mast. Therefore step-by-step plans (more specifically, the turn-on and turn-off times for the thrustor pulses) must be devised for each maneuver, and the mast must be designed to conform to the characteristics of the thrustors.

The analysis resulted in a combined attitude-and-vibration-control law for the attitude-control vernier thrustors. The control law is a function of the calculated vibration modes of the structure, and of the response of the system to environmental torques (gravity gradient, aerodynamic, and solar radiation). The system response to a single control pulse is computed by numerically integrating the equations of motion. The performance of a representative system is illustrated in the figure.

This work was done by Fred Austin of Grumman Aerospace Corp. for **Marshall Space Flight Center.** *For further information, Circle 39 on the TSP Request Card.*
MFS-25439

Locating Small Leaks in Large Structures

"Dead" needle pinpoints small leaks.

Lyndon B. Johnson Space Center, Houston, Texas

A "dead" needle technique pinpoints the exact locations of very small leaks in plumbing and vacuum systems. The new technique confines helium exposure to a small region rather than flooding the entire leak area with helium gas.

In conventional leak detection, helium gas is usually fed to the vicinity of the leak under low pressure, while a mass-spectrometer leak detector monitors the interior of the system for the presence of helium gas. While this method indicates whether or not a leak is present and notes the approximate location of the leak, it usually does not precisely pinpoint the leak. The helium gas floods too wide an area around the leak to enable the operator to determine the leak position with certainty. With the new technique the helium source is not pressurized, and the gas is localized to just the immediate vicinity of the leak.

The test tool uses a fine-control valve and a hypodermic needle (see figure). After the needle is filled with helium, the pressure is allowed to fall to atmospheric level, so that no helium actually flows from the needle if the air is still. As the needle is brought up to a leak, the leak-induced airflow draws helium from the "dead" needle, through the leak, and into the helium detector. This occurs only when the needle is very close (less than about 1 mm), so the leak can be located to within a small area.

This technique could be applied in industrial situations. Examples would be nuclear-powerplant plumbing, valve-and-pump bodies, vacuum systems, or pressure vessels.

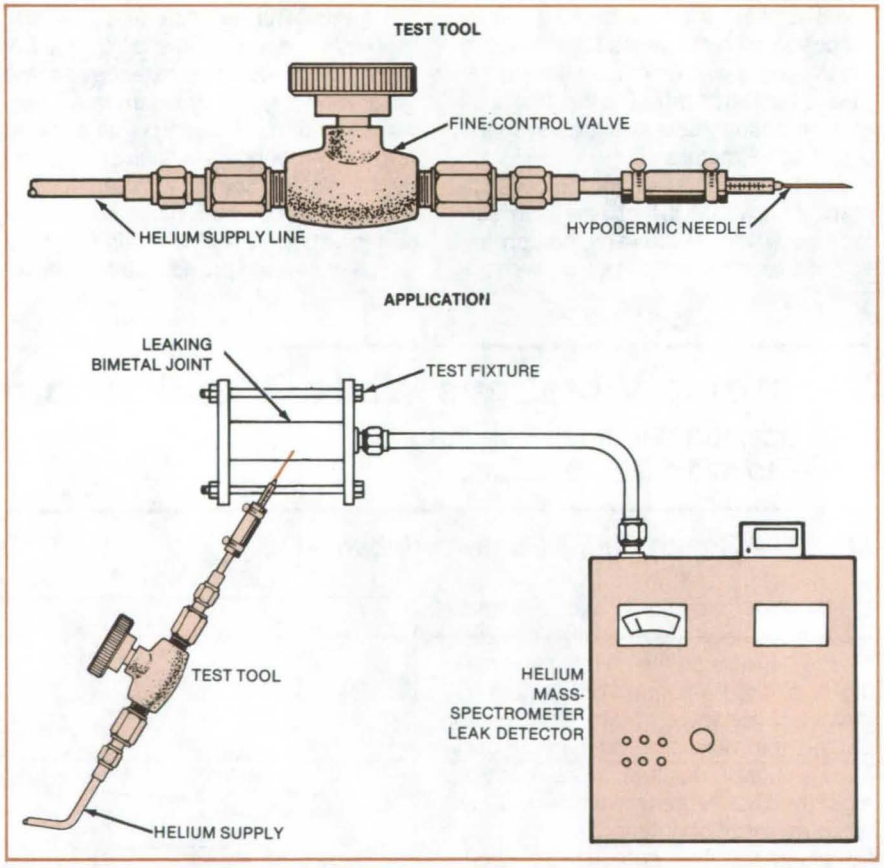

The **Test Tool for Detecting Minute Leaks** in bimetal joints, welds, or other locations employs a fine-control valve and a hypodermic needle. The test item is connected in a conventional manner to a helium mass spectrometer that is tuned to read extremely small amounts of helium gas. The uniqueness of this method is the ability to detect tiny leaks, through surfaces, which were not discoverable by gross coverage of test structures by helium gas.

This work was done by W. F. Lawler, Jr., of Beech Aircraft Corp. for **Johnson Space Center.** *No further documentation is available.*

Inquiries concerning rights for the commercial use of this invention should be addressed to the Patent Counsel, Johnson Space Center [see page A5]. Refer to MSC-20327.

Acoustic Ground-Impedance Meter

Portable device is based on the Helmholtz-resonator principle.

Langley Research Center, Hampton, Virginia

A Helmholtz resonator is used in a compact, portable meter that measures the acoustic impedance of the ground or other surfaces. The Earth's surface is the subject of increasing acoustical investigations because of its importance in aircraft noise prediction and measurement.

Constructed of heavy-walled stainless steel but open at the bottom, the resonator is positioned over a surface having unknown impedance. The sound source, a cam-driven piston of known stroke and thus known volume velocity, is located in the resonator neck. The cam speed is variable up to a maximum of 3,600 rpm.

The sound pressure at the test surface is measured by a microphone flush-mounted with the wall of the chamber. An optical monitor of the piston displacement permits measurement of the phase angle between the volume velocity and the sound pressure, from which the real and imaginary parts of the impedance are evaluated. Measurements using a 5-lobed cam can be made up to 300 Hz; these can be extended to nearly 1,000 Hz by a 15-lobed cam.

Previous methods for measuring the acoustic impedance of the ground, all having various unsatisfactory features, are organized into the three basic categories of impedance tube, free field, and direct sound-pressure/volume-velocity measurements. The acoustic ground-impedance meter utilizes direct pressure/volume-velocity measurement, but avoids the major difficulty in the measurement of volume velocity found with other such methods in that the volume velocity is defined by the known stroke of a cam-driven piston.

The acoustic ground-impedance meter offers several advantages. It is compact and portable and can be set up at any test site, irrespective of landscape features, weather, or other environmental conditions. Its speed of operation makes it well suited for use in conjunction with other acoustic measurements, such as aircraft noise measurements; and its operation is simple: At each frequency the acoustic impedance is evaluated from the measurement of one sound pressure and one phase angle for the test surface and from similar data for a calibration plate.

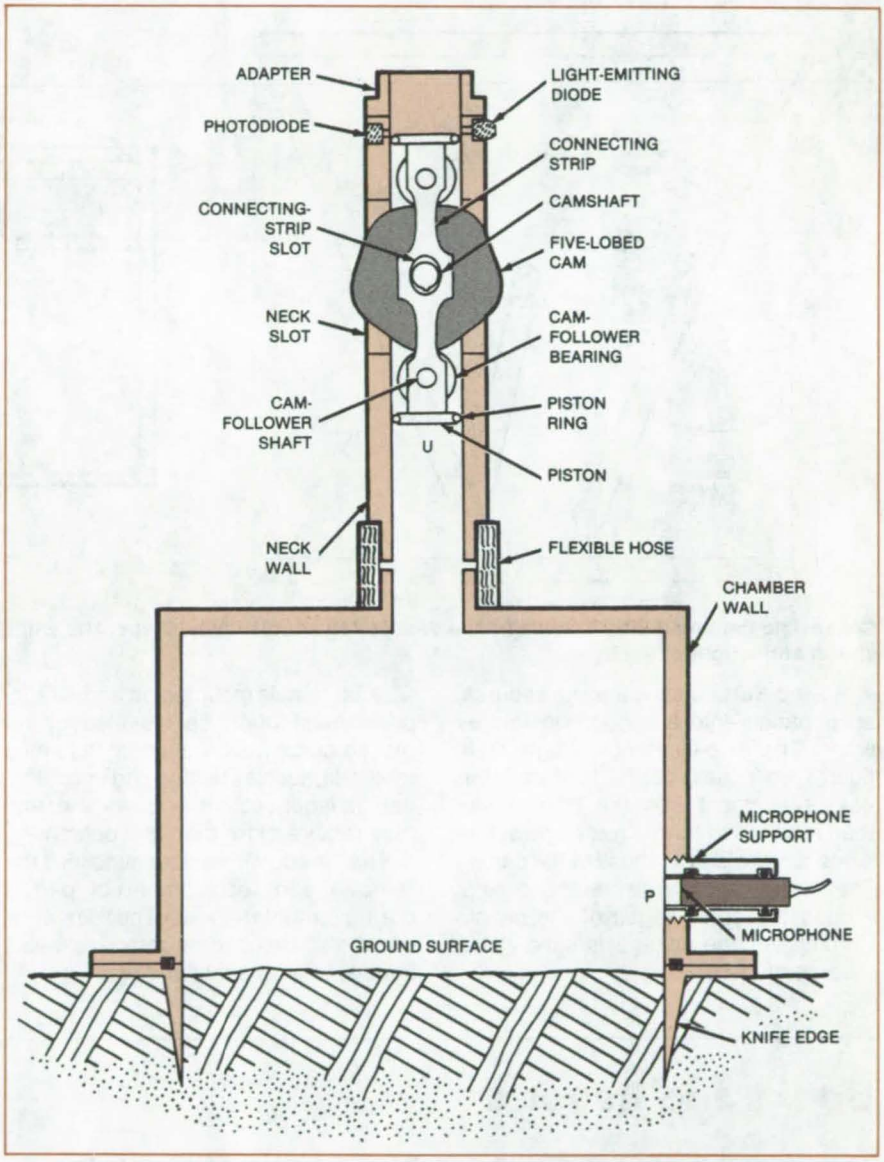

A Helmholtz Chamber is sealed to the test surface by a sharp knife edge. The resonator is 0.220 m in diameter by 0.152 m in height.

This work was done by Allan J. Zuckerwar of **Langley Research Center.** *Further information may be found in NASA TM-83227 [N82-17476/NSP], "Acoustic Ground Impedance Meter" [$6]. A copy may be purchased [prepayment required] from the National Technical Information Service, Springfield, Virginia 22161.*

This invention is owned by NASA, and a patent application has been filed. Inquiries concerning nonexclusive or exclusive license for its commercial development should be addressed to the Patent Counsel, Langley Research Center [see page A5]. Refer to LAR-12995.

Retaining Ring Fastener for Solar Panels

A collapsible linkage enables rapid installation and removal of panels.

NASA's Jet Propulsion Laboratory, Pasadena, California

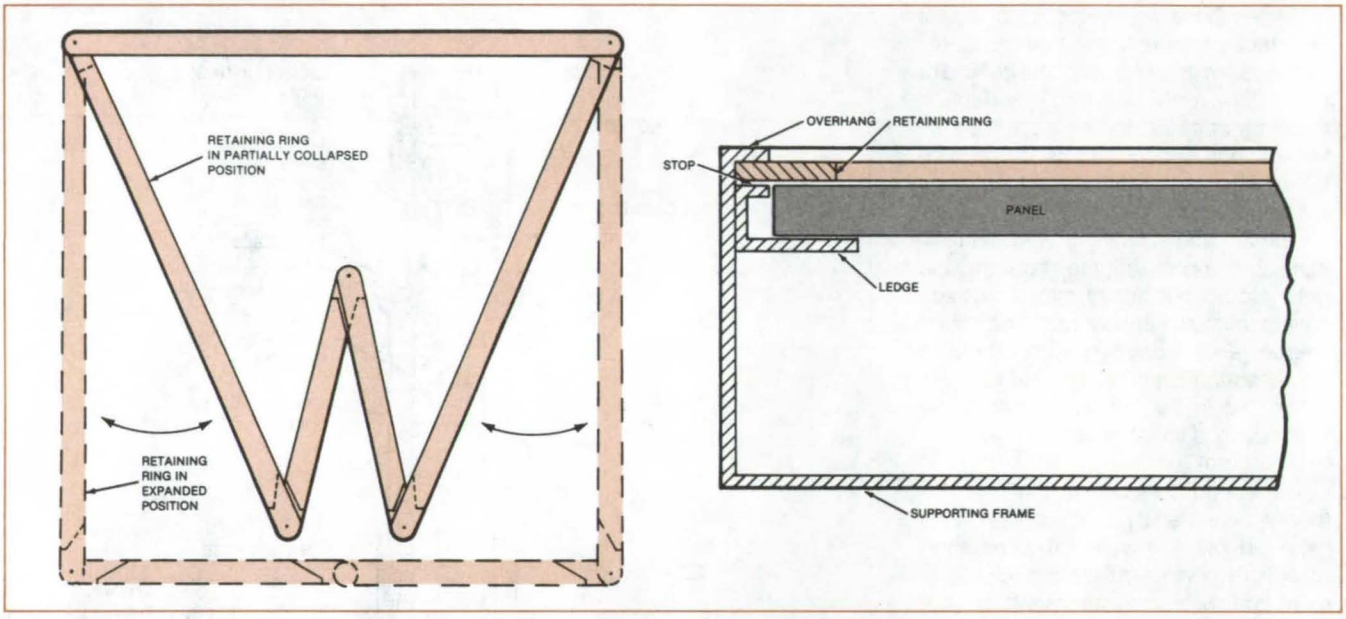

Collapsible Retaining Ring unfolds from a W-shape to a rectangular shape. The unfolded ring holds the solar panel in the frame as shown at the right of the figure.

A simple articulating linkage secures solar panels into a supporting framework. The five-element linkage (see figure) collapses into a W-shape for easy placement into the framework, then expands to form a rectangle of the same dimensions as those of the panel. The result is a large retaining ring around the outer edges of the panel. Removal of the linkage is simply the reverse of installation.

Solar panels mounted on angled supports must often be installed or removed quickly. Conventional fastening methods, such as bolting and unbolting, can be laborious, time consuming, and may require more than one person.

The new quick fastener simplifies the removal and replacement of panels during maintenance. The fastener could also be used on removable wall panels, photographs, and signs.

This work was done by Abraham H. Wilson of Caltech for **NASA's Jet Propulsion Laboratory.** *For further information, Circle 40 on the TSP Request Card.*

Inquiries concerning rights for the commercial use of this invention should be addressed to the Patent Counsel, NASA Resident Office-JPL [see page A5]. Refer to NPO-15369.

Books and Reports

These reports, studies, and handbooks are available from NASA as Technical Support Packages (TSP's) when a Request Card number is cited; otherwise they are available from the National Technical Information Service.

The Design of Lightning Protection

Engineering study could guide the design and monitoring of lightning protection.

Severe environmental conditions, including hurricane-force winds and a corrosive seacoast atmosphere, as well as the need for a 10-year system lifetime were taken into account when refitting and transferring an existing lightning protection system to the Space Shuttle service and access tower. Many components of the system were salvaged from a system used to protect the Apollo-Soyuz mobile launcher.

Engineering design studies for this project have been collected in a 150-page report. It contains a wealth of information both on the design of lightning protection systems and on instrumentation for monitoring the current waveforms of lightning strokes. Also included are the results of examinations

of the components of the earlier system that had successfully sustained a direct lightning strike.

Basically, the lightning protection system consists of a 1/2-inch (12.7-mm) stainless-steel wire-rope catenary cable strung over the launchsite in a broad inverted V. At the apex 390 ft (119 m) above ground, the cable is supported by a 65-ft (20-m) fiberglass insulating mast that is mounted atop a hammerhead crane. The cable is anchored at points 1,000 ft (305 m) on either side of the tower and is stretched to clear all grounded objects by at least 50 ft (15 m). The cable is grounded at each end through current coils, which are part of the lightning current-monitoring system.

The lightning current-monitoring system is designed to monitor the first 100 μs of each ligthning stroke; the current range is 2 to 200 kA. Current is monitored via the voltage across the coils at each end of the cable. The rate of change of current is monitored and integrated to obtain the current. To protect the event recorders that monitor the lightning strokes, the signals from the transient recorder are transmitted optically to the data lines.

Various other structural and safety considerations were studied. Loads from hurricane-force winds impose requirements more severe than those due to launch conditions.

Floodlighting of the mast was selected as the simplest economical way to provide aircraft safety warning. The report also describes the testing of ablative coatings used to protect the mast from repeated exposure to the heating effects of Space Shuttle launches.

This work was done by Planning Research Corp. for **Kennedy Space Center.** *Further information may be found in NASA TR-1530 [N81-31277/NSP], "Lightning Protection System for Space Shuttle" [$15]. A copy may be purchased [prepayment required] from the National Technical Information Service, Springfield, Virginia 22161.*
KSC-11224

Measuring Contours of Coal-Seam Cuts

Microprocessor-based instrument integrates small changes in angle and distance.

A final report describes work on an automated system for measuring the contour of a coal face as it is mined by a longwall shearer. [See "Transducer System Traces Mine-Face Curve," (MFS-25289), p. 424, [*NASA Tech Briefs*, Vol. 6, No. 4 (Spring/Summer 1982).]

Angle transducers measure the angle between track sections as the longwall shearer proceeds along the coal face. A distance transducer functions in conjunction with the angle transducers to obtain relative angles at known positions. When a cut is complete, the accumulated data are stored on cassette tape, and the track profile is computed and displayed. The angle and distance transducers are intrinsically safe in the potentially hazardous environment of a coal mine and therefore need no special packaging . The data storge and reduction electronics are not intrinsically safe but are housed in an explosionproof enclosure.

The angle transducers are brushless resolvers in a support structure called the angle cart. The transducers are directly connected to angle-measuring shoes. The angle between track sections is measured differentially by the two resolvers, which are attached to a common reference surface.

Distance is measured by counting pulses that originate from an optical encoder. The encoder is in a support structure called the distance cart. A five-point star-wheel-type gear in the distance cart makes contact with the track and rotates one-fifth of a revolution for each 126 mm of forward travel. Gears transmit the star-wheel rotation to the encoder. The reference point from which distance is measured is established by the simultaneous activation of limit switches and the encoder zero pulse. Once the zero reference point is established, absolute distance is measured by an up/down counter, which accumulates pulses from the encoder as the shearer moves along the face.

Yet another transducer — for roll measurement — is contained within the explosionproof enclosure. The transducer determines the deviation of the face from vertical. The transducer produces an electrical signal proportional to the angular displacement of a pendulum submerged in a damping fluid.

A microprocessor in the explosionproof enclosure calculates the cut surface contour from the trigonometric relations among track angles, distance, and roll measurements. The data reduction process for a 600-ft. (183-m) track takes about 2 minutes.

This work was done by Benton Corp. for **Marshall Space Flight Center.** *To obtain a copy of the report, Circle 41 on the TSP Request Card.*
MFS-25734

Computer Programs

These programs may be obtained at very reasonable cost from COSMIC, a facility sponsored by NASA to make new programs available to the public. For information on program price, size, and availability, circle the reference letter on the COSMIC Request Card in this issue.

Flow Distribution in Hydraulic Systems

Program solves fixed or variable flow problems for series, parallel, or series/parallel systems.

The General Flow Distribution Program analyzes pressure drops and flow distribution in closed and open hydraulic systems. It analyzes a system on the basis of incompressible flow even though the system may contain either compressible or incompressible fluid. The program has been used to analyze Space Shuttle orbiter hydraulic systems used for environmental control and life support. The General Flow Distribution Program solves fixed or variable flow problems for series, parallel, or series/parallel systems.

A flow system is represented by a nodal network with elements of flow resistance. Either a closed network with

(continued on next page)

pumps and fans or an open network with a known total fixed flow rate may be analyzed. The adjustment of variables is permitted through the use of user-supplied routines.

The analytical method is generally based on the successive-approximation method. Flow across a resistance, which may be either a duct, tube, or a black box with known characteristics, is calculated using the Bernoulli pressure-drop equation. Starting with assumed pressures at active nodes, the program iteratively corrects the pressures and flows until pressure and flow balance tests are satisfied. The balanced pressure drops and flows computed are output as analysis results.

This program is written in FORTRAN V for batch execution and has been implemented on a CDC CYBER 170-series computer. As currently dimensioned to accommodate a network of up to 500 nodes and 1,000 line elements, the program has a central memory requirement of approximately 77K (octal) of 60-bit words. The program was developed in 1980.

This program was written by Son N. Nguyen of Rockwell International Corp. for **Johnson Space Center.** *For further information, Circle C on the COSMIC Request Card.*
MSC-20306

Structural Optimization

An interface between SPAR structural analysis and CONMIN optimization

The Programming Structural Synthesis System (PROSSS) provides structural synthesis capability by combining the SPAR and CONMIN computer programs with a set of interface procedures. SPAR is a large general-purpose finite-element structural-analysis program, and CONMIN is a large general-purpose optimization program. The user supplies two small problem-dependent programs to define the design variables, constraints, and the objective function. Unlike many other structural-optimization programs, the design variables, constraints, and the objective function can be represented in PROSSS by any choice of quantities, or combination of quantities, that form input and output of structural analysis. This allows the user to solve practical optimization problems formulated in many different ways.

Execution of the PROSSS analysis/optimization process results in a set of optimum design variables and a minimized objective function subject to a set of constraints. Examples of the applications are (a) minimum-mass design with cross-sectional areas as variables and stress constraints, or (b) the first natural frequency as the objective function with overall shape design variables and stress and buckling constraints.

PROSSS is intended to be used in the following basic ways:

- As a research tool for developing optimization techniques that will interface with an efficient analysis program,
- As a research tool for testing new analysis techniques that will interface with an efficient optimization program, and
- As an application tool for a wide range of problems.

With PROSSS, the analysis and optimization programs are executed repeatedly in a loop until the process is stopped by a user-defined termination criterion. This part of the system is referred to as the repeatable part of PROSSS. However, some of the analysis, such as model definition, need only be done one time and can be saved for future use; these parts are performed outside of the loop and are referred to as the nonrepeatable part of PROSSS. Five options organize optimization procedures by combining nonlinear or piecewise linear programing methods with analytic or finite-difference gradients.

The analysis is always performed on the mainframe, a CDC 6000-series computer, because of the speed on the mainframe CPU. The end processor is also run on the mainframe to reduce the large amount of data generated by the analysis to the small amount of data required by the optimizer. The optimizer may be run on either the mainframe or the minicomputer, a PRIME 750 computer. The minicomputer offers the advantage of virtual memory; for many applications the optimizer requires a significant memory allocation. The primary difference in implementing PROSSS all on the CDC computer and in "distributing" part of PROSSS to the PRIME computer is the method of controlling the flow of the options.

PROSSS is written in FORTRAN IV for batch execution and has been implemented on a CDC 6000-series computer and a PRIME 750 computer. The implementation of PROSSS all on the CDC computer requires approximately 100K (octal) of 60-bit words. The PROSSS user must have access to the CDC version of SPAR (available from COSMIC). PROSSS was developed in 1981.

This program was written by James L. Rogers, Jr., and Jaroslaw Sobieszczanski-Sobieski of **Langley Research Center,** *Rama B. Bhat of George Washington University, and A. R. Dovi and K. M. Riley of Kentron International, Inc. For further information, Circle D on the COSMIC Request Card.*
LAR-13010

Structural-Vibration-Response Data Analysis

Modal frequencies and dampings are obtained from free-decay records.

One area in dynamic testing that continues to be of interest is the selection of a proper anlaylsis method for determining structural parameters from the measured data. A computer program was developed as a structural-vibration-response data analysis tool for use in the dynamic testing of the Space Shuttle.

The program provides a fast and efficient time-domain least-squares curve-fitting procedure for reducing transient response data to obtain structural modal frequencies and dampings from free-decay records. The procedure simultaneously identifies the frequencies, damping values, and participaton factors for noisy multiple-response records. The computer program and the methodology it is based on can be applied to the analysis of transient response data for a wide range of structures and might also be applied to such other areas as the analysis of seismograms.

This program is written in FORTRAN IV for batch execution and has been implemented on an IBM 370-series computer with a central memory requirement of approximately 970K of 8-bit bytes. The program was developed in 1981.

This program was written by William R. Smith, Richard N. Hechenlaible, and Ramon C. Perez of Rockwell International Corp. for **Johnson Space Center.** *For further information, Circle E on the COSMIC Request Card.*
MSC-20182

Costs and Benefits of Advanced Aeronautical Technology

Programs determine the advantages and disadvantages of advanced technology applied to civil aircraft.

Programs available from COSMIC can be used to evaluate the economic feasibility of applying advanced aeronautical technology to civil aircraft of the future. The programs are composed of three major models:

- The Fleet Accounting Module,
- The Airframe Manufacturer Module,
- The Air Carrier Module.

The Fleet Accounting Module estimates the number of new aircraft required as a function of time to meet demand. This estimate is based primarily upon the expected retirement age of existing aircraft and the expected change in passenger-miles demand. Fuel consumption estimates are also generated by this module.

The Airframe Manufacturer Module analyzes the feasibility of manufacturing the new aircraft. This module includes logic for production scheduling and for estimating manufacturing costs. For a series of aircraft selling prices, cash flow is analyzed, and rates of return on investment are calculated.

The Air Carrier Module is a tool for analyzing the financial feasibility of an airline purchasing and operating the new aircraft. This module includes a methodology for computing direct and indirect operating costs, performing cash-flow analyses, and estimating the internal rates of return on investment for a set of aircraft purchase prices.

Input to the Fleet Accounting Module includes data describing growth rate of revenue passenger miles and flight load factors. Descriptions of currently operating aircraft are entered in terms of the year in which the aircraft became operational, seating capacity, fuel consumption, and normal retirement age. The type, number, and age of aircraft currently in operation are entered to complete the description. Similar data are required for the new aircraft that are potential replacements. The module output includes statistics describing the projected fleet composition and activity.

The input to the Airframe Manufacturer Module includes a detailed description of the manufacturing requirement for the new aircraft and the manufacturing cost data. The output includes data describing the manufacturers, their production capacity, the production scheduling, and selected cost parameters.

The input to the Air Carrier Module includes data on the carrier operations and cost factors. The output includes computed direct and indirect cost, as well as various statistics and parameters computed in the financial analysis.

The models are written in FORTRAN IV and COMPASS for batch execution and have been implemented on a CDC 7600 computer with a central memory requirement of approximately 154K (octal) of 60-bit words in small core memory and 144K (octal) of 60-bit words in large core memory. Plotted output is generated for a ZETA 230 plotting system. The models were developed in 1979.

This program was documented by J. C. Bobick, R. L. Braun, and R. E. Denny of SRI International for **Ames Research Center.** *For further information, Circle F on the COSMIC Request Card.*
ARC-11382

Loads and Pressures on Axisymmetric Bodies with Cruciform Fins

Program computes forces and moments on supersonic configurations experiencing pitch and roll.

The NSWCDM computer program calculates the aerodynamic loading and pressure distributions on supersonic configurations consisting of axisymmetric bodies with cruciform or planar canard and tail fins. This versatile program allows for the configuration to be pitched and rolled, and the fins may be deflected. The tail fins may be interdigitated with respect to the foward fins. Fins may have arbitrary planform and thickness but must be planar. The load calculations provide aerodynamic forces and moments acting on the entire configuration.

NSWCDM treats the body and lifting surfaces and performs vortex tracking along the complete configuration in a single application. The theoretical approach is based on representing the configuration components by three-dimensional singularities associated with supersonic, linear flow theory.

The body is modeled by a distribution of supersonic line sources, sinks, and doublets along the centerline. Constant u-velocity panels are laid out over the fins. Interference-containing constant u-velocity panels are placed around the body over a length at least equal to the fin root chord to account for finbody interference. Forebody vortex shedding is modeled by two potential flow vortexes with strengths and positions obtained from an analytical/empirical approach. Canard fin trailing-edge vorticity is calculated and tracked along the afterbody and tail with or without the body nose vortexes. The effects of the body nose and canard vortexes are included in the pressure distributions, and loads are computed for the body and fins. Afterbody vortexes, as well as leading and side-edge vortexes, are not accounted for.

Input to NSWCDM includes configuration geometry and modeling parameters, free-stream and body orientation parameters, and program control parameters. Output from the program includes intermediate and final results used in obtaining the aerodynamic loads and pressure distributions.

NSWCDM is written in FORTRAN IV for batch execution and has been implemented on a CDC CYBER 170-series computer with a central memory requirement of approximately 175K (octal) of 60-bit words. NSWCDM was developed in 1979.

This program was written by M. F. E. Dillenius and C. A. Smith of Nielsen Engineering & Research, Inc., for **Langley Research Center.** *For further information, Circle G on the COSMIC Request Card.*
LAR-12936

Vertical Profiles for Turbojet-Powered Aircraft

Optimum profile minimizes operating cost.

The OPTIM computer program generates optimum vertical profiles for turbojet-powered aircraft. Specifically, OPTIM generates a profile of altitude, airspeed, and flightpath angle as a function of the range between a given set of

(continued on next page)

origin and destination points for particular models of transport aircraft. The profile may be optimized in the sense of minimizing fuel or time or in minimizing the direct operating cost expressed as a combination of fuel and time.

Inputs to the program include the vertical wind profile, the aircraft takeoff weight, and the aircraft engine and aerodynamic characteristics. The optimum vertical flight profile is generated by calculating the airspeed and thrust required to minimize the Hamiltonian at specific energy increments.

OPTIM is written in FORTRAN IV for batch execution and has been implemented on a CDC 6000-series computer with a central memory requirement of approximately 140K (octal) of 60-bit words. The OPTIM program was released in 1981.

This program was written by John A. Sorensen and Mark H. Waters of Analytical Mechanics Associates, Inc., for **Langley Research Center.** *For further information, Circle H on the COSMIC Request Card.*
LAR-12940

Supersonic-Wing Nonlinear Aerodynamics

Predictions of wing overall force and moment coefficients are improved.

The Supersonic Wing Nonlinear Aerodynamics computer program, LTSTAR, estimates the nonlinear aerodynamics characteristics of a wing at supersonic speeds. This corrected linearized-theory method accounts for nonlinearities in the variation of basic pressure loadings with local surface slopes, predicts the degree of attainment of theoretical leading-edge thrust forces, and estimates detached leading-edge vortex loadings that result when the theoretical thrust forces are not fully realized.

The comparison of LTSTAR computations with experimental results show significant improvements in detailed wing-pressure distributions, particularly for large angles of attack and for regions of the wing where the flow is highly three-dimensional. The program provides generally improved predictions of the wing overall force and moment coefficients. LTSTAR could be useful in design studies aimed at aerodynamic performance optimization and in providing more-realistic tradeoff information for the selection of wing planform geometry and airfoil section parameters.

Input to the LTSTAR program includes wing planform data, free-stream conditions, wing camber, wing thickness, scaling options, and output options. The program output includes pressure coefficients along each chord, section normal and axial force coefficients, and the spanwise distribution of section force coefficients. With the chordwise distributions and section coefficients at each angle of attack, three sets of polars are output. The first set is for linearized theory with and without full leading-edge thrust, the second set includes nonlinear corrections, and the third includes estimates of attainable leading-edge thrust and vortex increments along with the nonlinear corrections.

The LTSTAR program is written in FORTRAN IV for batch execution and has been implemented on a CDC CYBER 170-series computer with a central memory requirement of approximately 150K (octal) of 60-bit words. The LTSTAR program was developed in 1980.

This program was written by Harry W. Carlson and Robert J. Mack of **Langley Research Center.** *For further information, Circle J on the COSMIC Request Card.*
LAR-12788

Flexible Aircraft Takeoff and Landing Analysis

Program includes maneuver logic and autopilots for glide slope, flare, landing, and takeoff.

The Flexible Aircraft Takeoff and Landing Analysis program, FATOLA, simulates aircraft takeoff and landing dynamics. FATOLA represents an airplane either as a rigid body with six degrees of freedom or as a flexible body with multiple degrees of freedom. The airframe flexibility is represented by the superposition of up to 20 free vibration modes on the rigid-body motions. The analysis includes maneuver logic and autopilots programed to control the aircraft during glide slope, flare, landing, and takeoff. The program is modular so that the performance of the aircraft in flight and during landing and ground maneuvers can be studied separately or in combination.

Nine effects are simulated in FATOLA:

1. Flexible aircraft control and performance during glide slope, flare, landing roll, and takeoff roll in the presence of changing winds, engine failures, brake failures, control-system failures, strut failures, and restrictions due to runway length, control variable limits, and timelags;
2. Landing-gear loads and dynamics for up to five gears;
3. Single and multiple engines (maximum of four), including selective engine reversing and failure;
4. Drag chute and spoiler effects;
5. Wheel braking (including skid control) and selective brake failure;
6. Ground effect aerodynamics;
7. Aircraft-carrier operations;
8. Inclined runways and runway perturbations; and
9. Flexible or rigid airframes.

Input to FATOLA includes data that describe runway roughness, vehicle geometry, flexibility and aerodynamic characteristics, landing gear(s), propulsion, and initial conditions, such as attitude, attitude-change rates, and velocities. The program time-integrates the equations of motion and outputs comprehensive information on the airframe, state-of-maneuver logic, autopilots, control response, and aircraft loads from impact, runway rollout, and ground operations. Flexible-body and total (elastic plus rigid-body) displacements, velocities, and accelerations are also output in the flexible-body option for up to 20 points on the aircraft.

The FATOLA program is written in FORTRAN IV for batch execution and has been implemented on a CDC 6000-series computer with an overlaid central memory requirement of approximately 115K (octal) of 60-bit words. FATOLA was developed in 1975 and last updated in 1978.

This program was written by Huey D. Carden and John R. McGehee of **Langley Research Center.** *For further information, Circle K on the COSMIC Request Card.*
LAR-12992

Machinery

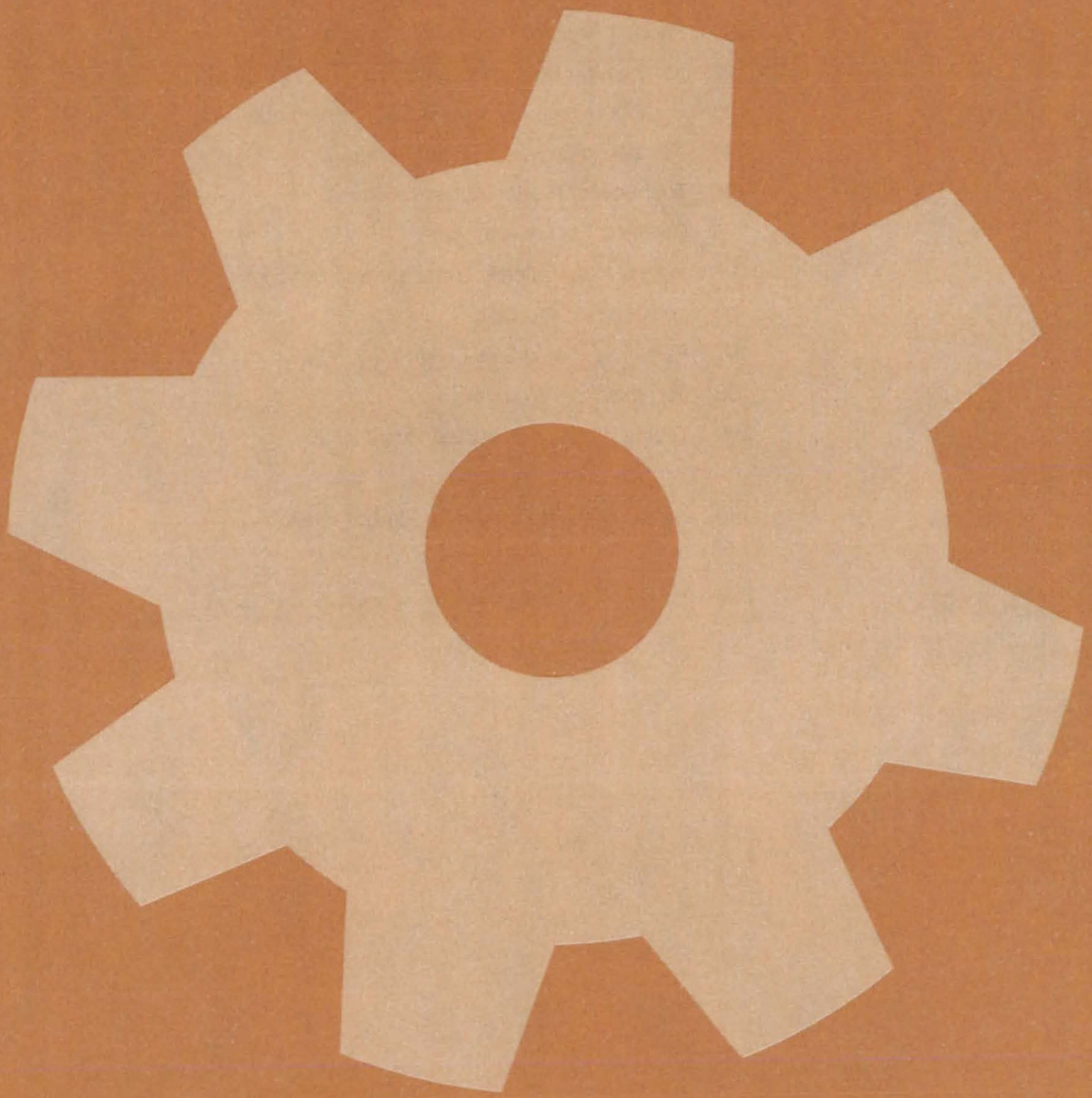

Device Stores and Discharges Metered Fluid

A portable device accepts, stores, and discharges a preset amount of fluid.

Lyndon B. Johnson Space Center, Houston, Texas

A hand-held container accepts a measured amount of liquid from a pressurized supply. The supply pressure drives a spring-loaded piston that stores enough mechanical energy to discharge the measured liquid into another container. An operator triggers the discharge by turning a valve handle.

The container, shown in Figure 1, attaches to a water (or other fluid) supply through a "quick-disconnect" fitting. The desired amount of fluid is selected by turning a collar that controls the length of the piston travel.

A three-way selector valve is set at "fill," "discharge," or "off." When the selector is set to "fill," the piston is forced back to the preset volume. After the selector is turned to "discharge," a spring-loaded toggle valve triggers the delivery of water to its final destination. The device is stored safely in the "off" position when it is full.

The spring is long enough to apply nearly constant force against the piston over its operating range. It compresses under the liquid pressure available from the source [20 psi (140 kN/m^2) in the case of the spacecraft application]. Once the toggle valve is opened, the spring delivers the water at a lower pressure [15 psi (103 kN/m^2) in the spacecraft application]. The device stores mechanical energy from the water supply in the coiled spring and releases the energy by displacing the water.

The liquid comes into contact with a rolling rubber diaphragm (see Figure 2) but not with the piston. If the fluid is water, this feature keeps the water sterile until use and prevents corrosion of the metallic parts.

The original application of the container was to rehydrate sterilized prepackaged food in the zero-gravity environment of space vehicles. Its possible terrestrial applications include the dispensing of toxic fluids or the metering of fluids for household, commercial, or laboratory uses.

This work was done by Sonne L. Hooper and Drel Setzer of Pan American World Airways, Inc., for **Johnson Space Center.** *For further information, Circle 42 on the TSP Request Card.*

This invention is owned by NASA, and a patent application has been filed. Inquiries concerning nonexclusive or exclusive license for its commercial development should be addressed to the Patent Counsel, Johnson Space Center [see page A5]. Refer to MSC-20275.

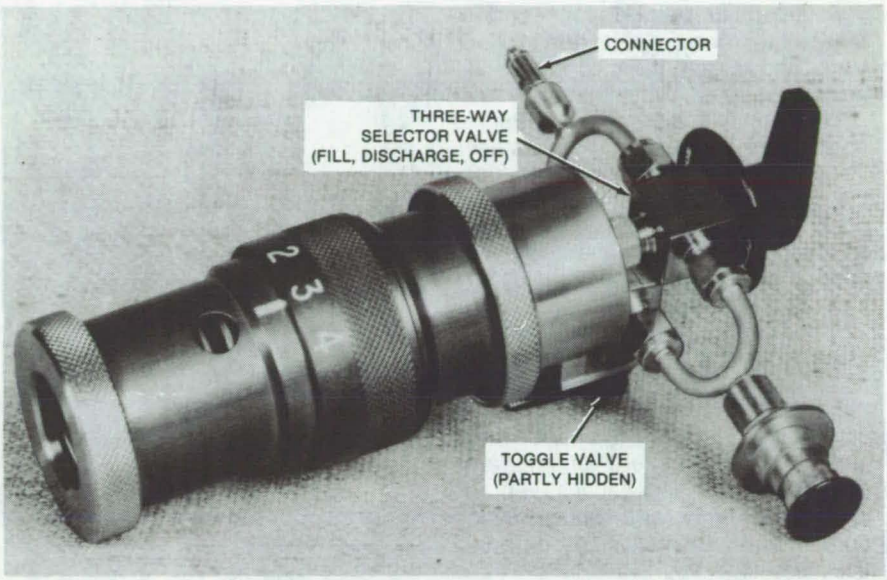

Figure 1. This **Metering Container** stores a preselected amount of fluid from a pressurized source. The amount is selected [in this case, 2 to 4 ounces (60 to 120 ml)] by turning a calibrated collar on the body of the device. The window in the body permits observation of the amount of stored fluid.

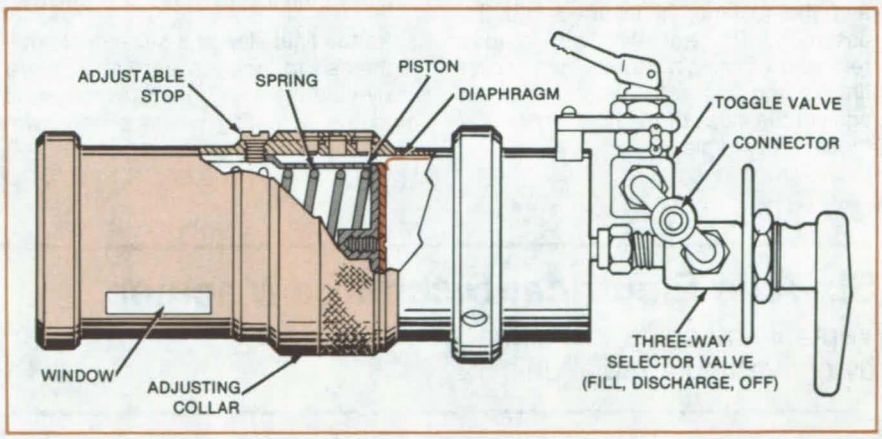

Figure 2. A **Spring and Adjustable Collar** determine the amount of fluid captured in the container. The required spring characteristics depend on the pressure and flow properties of the fluid.

Quick-Disconnect Fastener

A proposed fastener would have good shear- and moment-load-carrying capacity.

Langley Research Center, Hampton, Virginia

A proposed quick-disconnect fastener for two or more parts resists shear loads and torque. It would center the parts to be joined, clamp them, and then tighten them into a single unit. Potential applications for the removable fastener include holding parts for welding, brazing, soldering, riveting, and gluing. Other possible uses would be for attaching removable panels and panels with poor access on one side and for plugging leaks in pressure vessels.

The fastener consists of a spring-loaded hexagonal actuating pin, six springy collet fingers, and a hexagonal-nut locking collar. The collet fingers clamp the fastener in position and should give excellent shear- and moment-load-carrying capacity. An adjustable locking collar compensates for component assemblies of differing thicknesses.

The figure shows the fastener before and after locking. Holes are first drilled in the parts to accept the fastener. With the spring-loaded actuating pin retracted, the six fingers remain together, and the fastener is inserted into the assembly. The actuating pin is then released. The pin enters the collet fingers and forces them to spread out against the sides of the hole, anchoring the fastener in place.

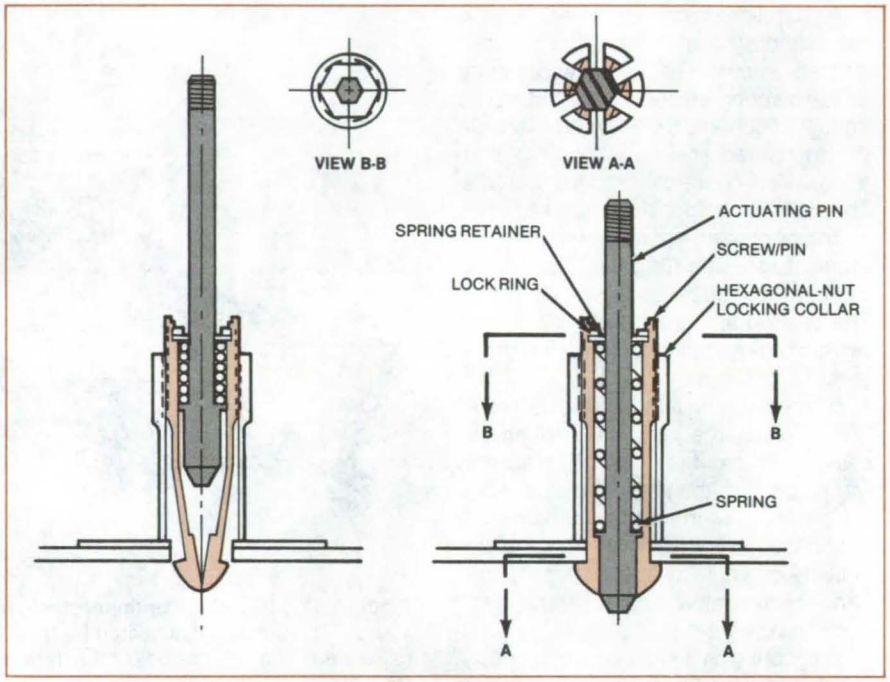

The **Collet Fingers** remain together (left) until forced apart by the hexagonal actuating pin (right). In the proposed fastener, there are six fingers and a hexagonal shank.

In the final step, the hexagonal nut is tightened to lock the assembly. To remove the fastener, the nut is loosened, and the actuating pin is pulled away from the collet fingers.

This work was done by Louis W. Palmer and Jack A. Billyard of Rockwell International Corp. for **Langley Research Center.** *No further documentation is available.*
LAR-12895

Six-Axis Electrical-Discharge Machine

Versatile machine tool is made by converting a radial drill.

Marshall Space Flight Center, Alabama

An electrical-discharge machine (EDM) of unusual versatility has been made by the conversion of a radial drill. The drilling head is replaced by a ram that holds and positions the electrode. A tank and recirculation system for the coolant are added.

A conventional radial drill, used for machining in the tool-and-die industry, has a spindlehead that moves the drill in the z-direction and a worktable that moves the workpiece in the x- and y-directions. The EDM, however, has six independent motions:

1. X-axis motion provided by the radial-drill crossarm and mounting table;
2. Y-axis motion provided by the mounting table;
3. Z-axis motion provided by the ram;
4. Angle motion, as shown in the figure;
5. Arc motion provided by the radial arm; and
6. Rotation of the spindle quill.

Use of the six axes of motion allows full exploitation of the principle of electrical-discharge machining. The mechanical versatility also simplifies the positioning of work fixtures, thus reducing setup time and costs.

Many of the features of the machine may be seen in the figure. The large size of the EDM is apparent: The ram has a traverse of 36 inches (91 cm), and the table working surface is 44 by 44 inches (112 by 112 cm). The dielectric tank is 50 by 50 by '50 inches (127 by 127 by 127 cm). One side of the tank can be removed (as in the photograph) to facilitate installation, inspection, or removal of the workpiece and the electrode.

The capabilities of the machine were demonstrated in performance tests that included an overcut test, a through-hole test, a cavity test, and a small-hole test. All of these required precise machining in steel, using either copper or graphite as the electrode.

This work was done by A. R. Werner of Rockwell International Corp. for **Marshall Space Flight Center.** *For further information, Circle 43 on the TSP Request Card.*
MFS-19695

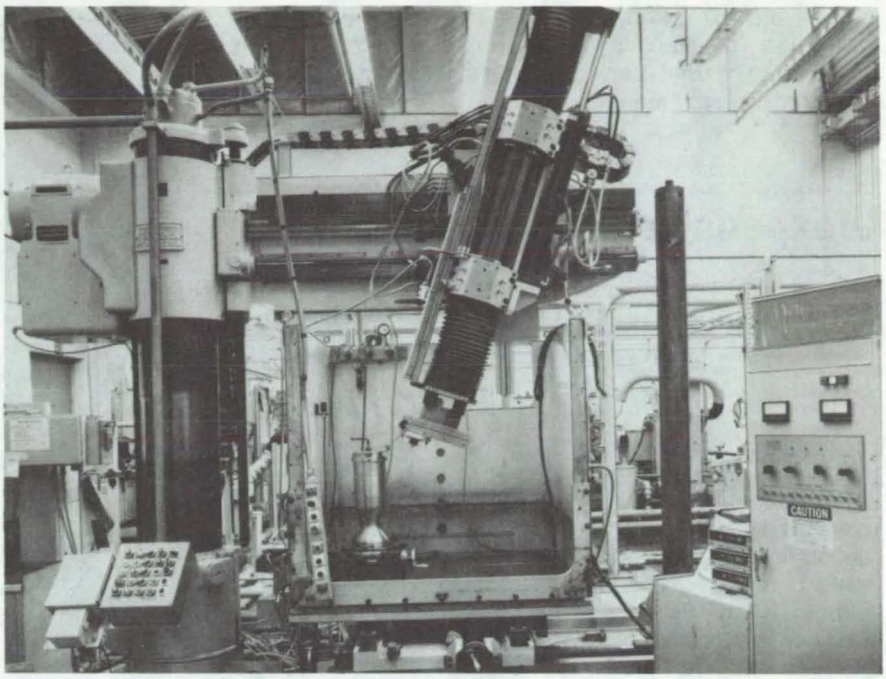

This **Electrical-Discharge Machine** (EDM) has drastically reduced the cost of manufacturing, and new applications for it are constantly being found.

Padded Allen Wrench Grips Fastener

Screws can be inserted in hard-to-reach places.

Marshall Space Flight Center, Alabama

The addition of a PTFE pressure pad increases the utility of a hexagonal socket wrench. The pad presses against opposing inside socket walls, causing a frictional force that retains a socket-head screw against gravitational and handling forces. Developed for spacecraft repairs, the tool is useful wherever there is a possibility of losing the screw due to awkward working conditions or wherever a tight clearance prevents the insertion or removal of the screw by hand.

The modified wrench (see figure) is easy to construct. A hole is drilled through a pair of flats near the end of a basic hexagonal wrench. A tight-fitting PTFE rod is pressed into the hole, then machined until it protrudes by the desired distance.

Unlike magnetic tools, the new device works with socket-head capscrews of both nonferrous and ferrous materials.

(continued on next page)

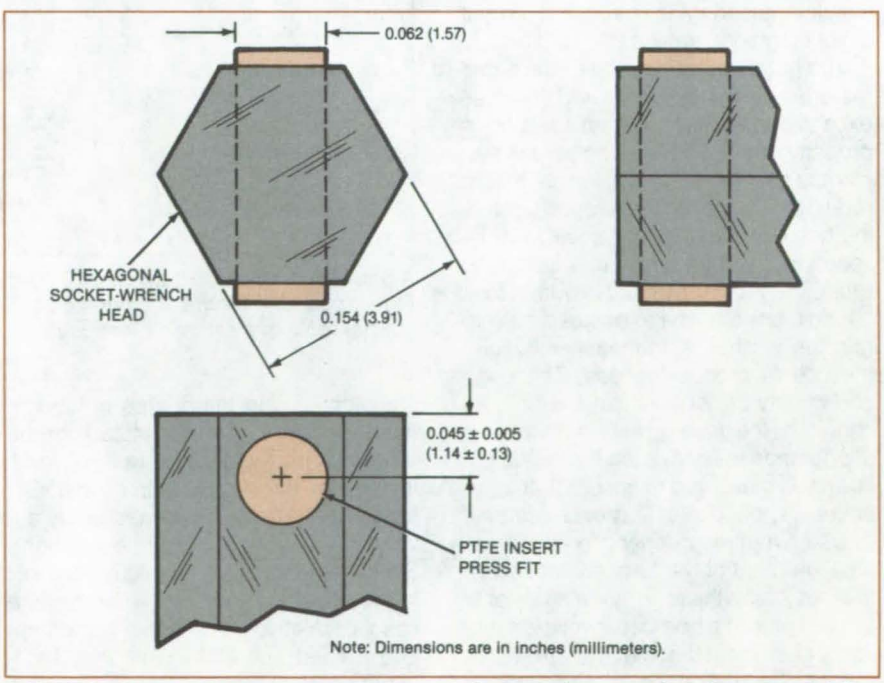

A **PTFE Pad** is inserted in a hole near the end of a basic hexagonal socket wrench (allen wrench). The concept is not limited to one wrench size: Dimensions are shown for example only.

Since PTFE is relatively unaffected by gases, oils, or temperature extremes, the tool can be used in a wide variety of environments and working conditions.

This work was done by Michael K. Salisbury of **Marshall Space Flight Center.** *No further documentation is available.*

Inquiries concerning rights for the commercial use of this invention should be addressed to the Patent Counsel, Marshall Space Flight Center [see page A5]. Refer to MFS-25739.

Inexpensive Bolt-Load Gage

A simple screw-and-washer strain gage indicates the optimum torque on bolts and studs.

Langley Research Center, Hampton, Virginia

A "built-in" gage determines whether a large bolt or stud has been torqued to the desired load and also provides for continuous inspection to ensure that proper load is being maintained. The gage, a simple screw-and-washer combination (see figure), detects the longitudinal stress/strain on the bolt; it requires no electronic or sonic test equipment.

The strain gage is based on setting and maintaining a maximum longitudinal "stretch" that the bolt or stud should have under the desired load or stress. This "stretch" can be either calculated or determined by calibration.

The gage screw is fed through a cruciform washer and installed in a drilled hole through the centerline of the bolt or stud. The precise bolt "stretch" length is set between the washer and screwhead by a feeler gage or other simple measuring device, and a jamnut locks in the gap setting.

The gage screw is made of the same material as the bolt to avoid thermal-expansion problems. When the bolt is properly stressed, the gage screwhead clamps the washer and prevents it from rotating, indicating that proper tightening has been achieved. Subsequent inspections require only an attempt to rotate the washer by hand or with a tool.

The cruciform shape makes it easy to grip the washer. If the washer is tight, the bolt is properly loaded. The gage screw may be longer than the bolt, as shown, or the gage screw length may be shorter than the bolt, such that sufficient stretch is measured to ensure that tolerances do not adversely affect accuracy.

Other methods depend primarily on measurement of the torque imposed on the nut or bolthead. The relation of a torque value to a bolt load involves a frictional coefficient that may vary from bolt to bolt, depending on thread surface smoothness and the degree of lubrication. Therefore, the calculated torque value may not yield the desired bolt load. In addition, the stress/strain condition of a bolt or stud may be measured by advanced sonic/electronic equipment. Sonic measurement techniques are still in the developmental stage and require special, relatively expensive equipment and trained operators. This new technique requires neither.

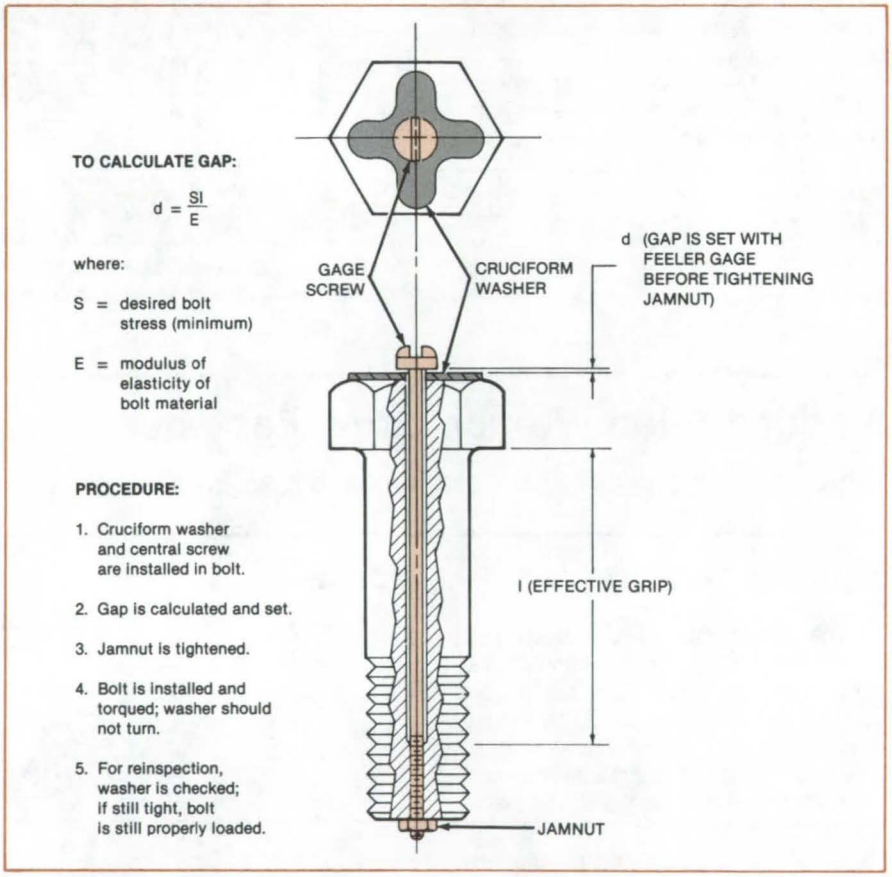

A **Screw-and-Washer Strain Gage** placed through the center of a bolt or stud indicates proper bolt load for initial tightening and for continuous, easy bolt-load inspection. No special tools or electronics test equipment are needed.

This work was done by Moses J. Long of **Langley Research Center.** *No further documentation is available.*

This invention is owned by NASA, and a patent application has been filed. Inquiries concerning nonexclusive or exclusive license for its commercial development should be addressed to the Patent Counsel, Langley Research Center [see page A5]. Refer to LAR-12774.

Parachute Line Hook Includes Integral Loop Expander

Parachute packing is simplified with a modified line hook.

Langley Research Center, Hampton, Virginia

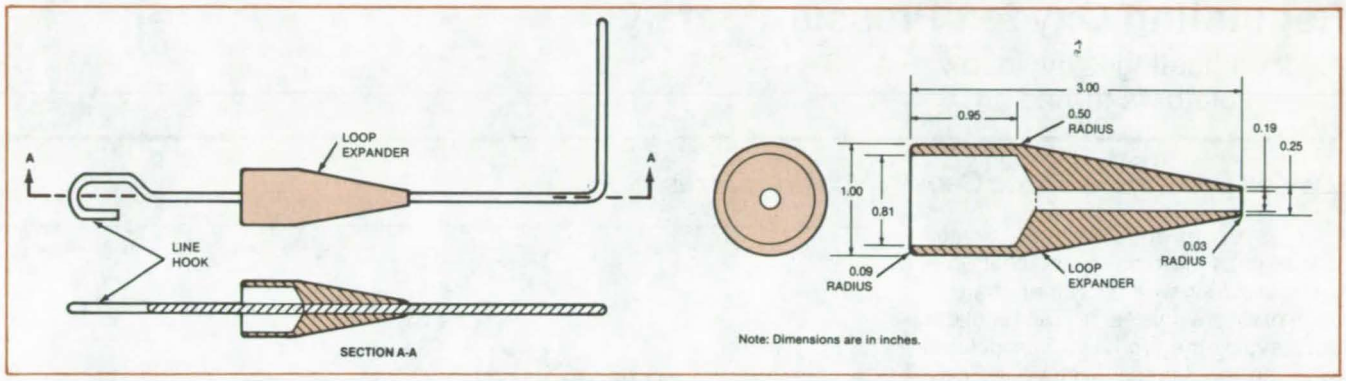

Figure 1. The **Parachute Line Hook** includes a tapered brass fitting that expands locking loops on the parachute bag so that the parachute lines can be pulled through them.

Using a modified line hook developed at Langley Research Center, one person now packs parachutes for test recovery vehicles faster than it previously took a two-person team. The new line hook includes an expander that opens up two locking loops so that the parachute lines can be pulled through them. In the old method, one person operated the line hook while the other person expanded the loops by hand.

The parachutes are packed at high pressure because they have to be compressed into the limited space available in the test vehicles. The pressure creates a large force on the parachute locking flaps.

Two flaps at the mouth of the parachute bag are joined together to lock the parachute in the bag. One flap has two square holes through which two locking loops from the second flap fit. Once the loops from the second flap are pulled through the holes in the first flap, the parachute lines are looped together and pulled through the two loops by using the line hook.

The modified line hook with the loop expander holds the first flap down while expanding the loop and also allows the parachute lines to be pulled through in a one-step operation. The tapered brass piece on the line hook, shown in Figure 1, allows the loop to slide over it, thus expanding the loop. As the line hook is pulled, the loop slides off the expander and over the lines. Once the lines are

(continued on next page)

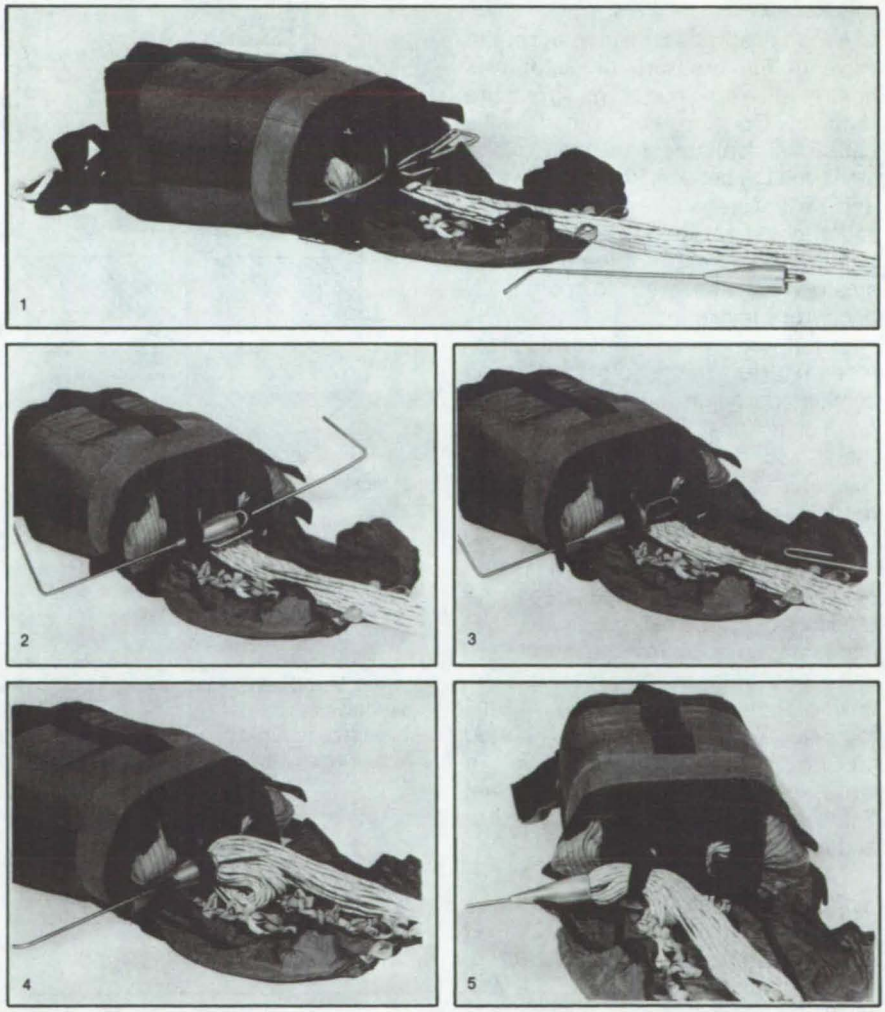

Figure 2. This **Five-Photo Sequence** shows the tapered fitting expanding the loops as the line hook pulls the lines through.

threaded through the loops, the line hook is unlocked, and the packing operation is complete. The photographs in Figure 2 show the parachute lines being pulled through the locking loops.

This work was done by Gary B. Bayless of **Langley Research Center.** *No further documentation is available.*

This invention is owned by NASA, and a patent application has been filed. Inquiries concerning nonexclusive or exclusive license for its commercial development should be addressed to the Patent Counsel, Langley Research Center [see page A5]. Refer to LAR-12875.

Regulating Oxygen Pressure Safely

Sudden heating is avoided when the regulator is turned on.

Lyndon B. Johnson Space Center, Houston, Texas

A pressure regulator for oxygen allows gas flow to be shut off on its low-pressure (outlet) side rather than its high-pressure (inlet) side. The regulator thus avoids the fire hazard associated with the rapid pressurization and consequent adiabatic heating of oxygen on the input side when the regulator is turned on. The new regulator can reduce the danger of fire in aircraft and in medical oxygen supplies.

As originally designed, the shutoff valve of the pressure regulator was upstream of a two-stage pressure reducer. Opening the shutoff valve caused sudden pressurization of the small volume between the shutoff valve and the first stage. The heat of pressurization could not be dissipated rapidly, and the temperature of the gas in the small volume soared to potentially dangerous levels.

In the new version of the regulator (see figure), the shutoff valve is eliminated from the supply side, and its function is transferred to a lift rod. With the lift rod in the up (off) position, the regulator valve stem floats freely, and the inlet pressure holds the valve ball against the regulator valve seat.

However, when the lift rod is pushed down to a position that frees the pressure-sensing bellows plate, the plate can move against the valve stem in response to outlet pressure. The device then functions as a normal regulator. When the regulator is turned on, the oxygen flows suddenly into a large volume instead of a small one: There is no rapid buildup of pressure and temperature.

This work was done by Charles Simons of United Technologies Corp. and Lawrence Gill of Carlton Controls for **Johnson Space Center.** *No further documentation is available.*
MSC-20300

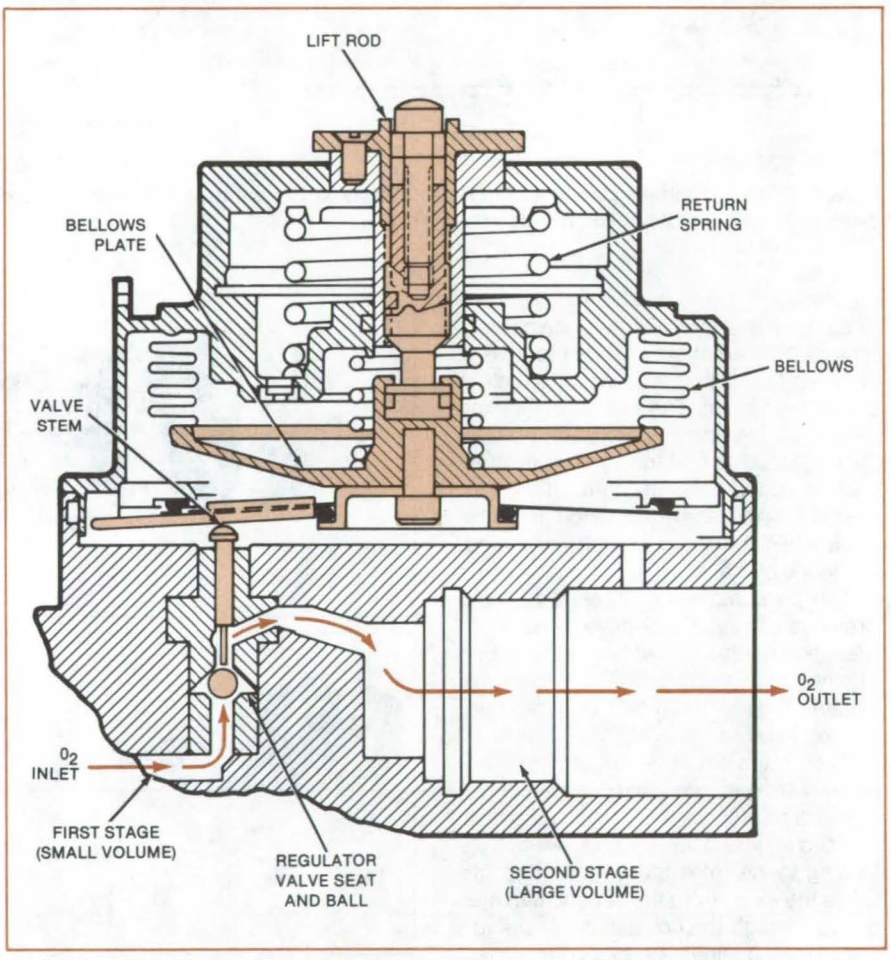

In the **Modified Pressure Regulator** (shown here in simplified form), the initial rush of oxygen occurs in the second stage rather than in the first stage of pressure reduction. The large volume of the second stage prevents excessive heating of the gas. The high-pressure source can remain on, and the first stage can remain pressurized at all times.

Tool Severs Hidden Adhesive Bonds

It reaches deep into narrow crevices without damaging adjacent surfaces.

Lyndon B. Johnson Space Center, Houston, Texas

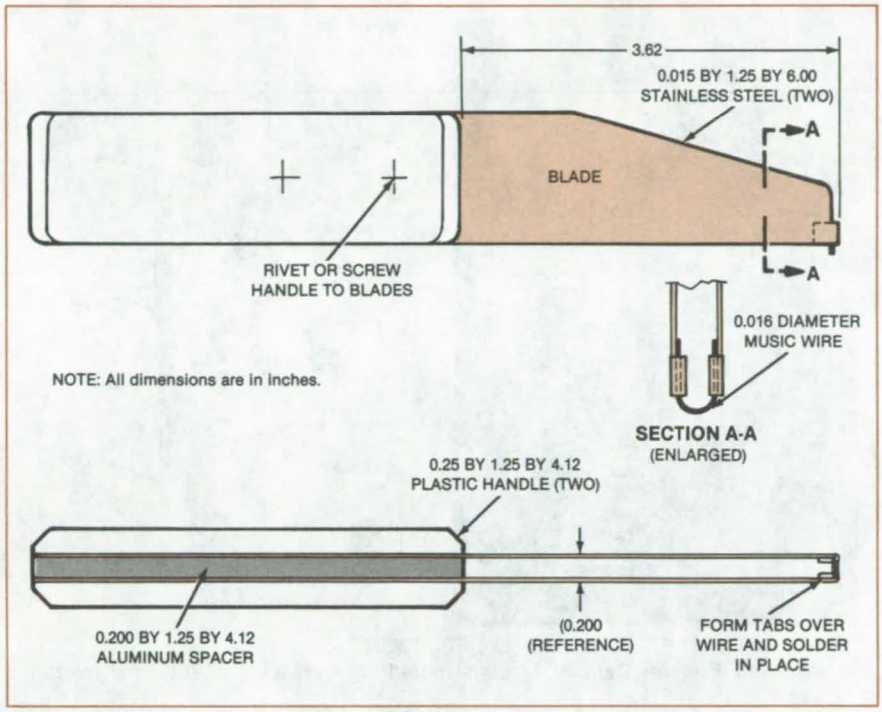

Figure 1. **Two Parallel Blades,** sandwiched between an aluminum spacer and plastic, support the cutting wire. The wire is crimped to the blades, and the handle is held together by either rivets or screws.

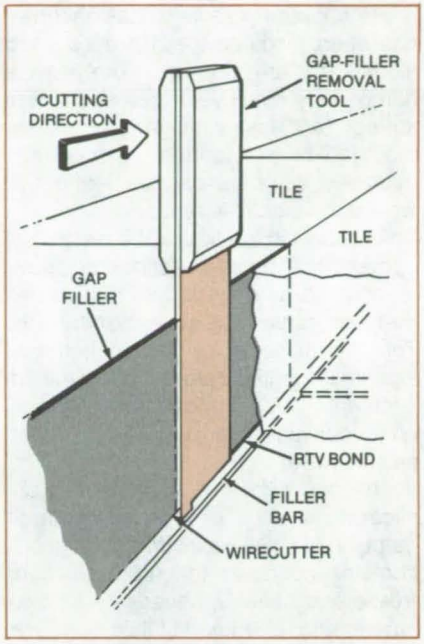

Figure 2. The **Gap Filler Is Removed** by undercutting the adhesive alternately from one end and then from the other end of the filler.

A new tool enters a narrow gap between fragile materials and removes an adhesively bonded filler without damage to the adjacent surfaces. It reaches deep into narrow crevices to reach hidden bond lines. The tool was originally developed to remove ceramic filler from between the Space Shuttle surface-insulation tiles.

The tool (see Figure 1) has two blades that support a short length of music wire, 0.016 in. (0.4 mm) in diameter. A set of tools with blades spaced at different widths would fit a range of gaps. In the Space Shuttle application, only the length of music wire is used to sever the adhesive bonds; the blades do not actually do any cutting.

As shown in Figure 2, the tool is inserted over the filler to be removed with the two blades straddling the filler. Any adhesive bonds between the filler and adjacent walls are broken by a sharpened spatula before the tool is inserted.

The wire is inserted down to the bond line and pulled with a slight downward pressure along the gap filler, stopping about 2 in. (5 cm) from the end. The path of the tool is then reversed, and the tool is removed at the same place it entered. The tool is then reinserted at the opposite end of the gap filler, and the last remaining bond is severed. The gap filler can then be removed.

This work was done by Andrew R. Keir and Xavier A. Dominguez of Rockwell International Corp. for **Johnson Space Center.** *No further documentation is available.*
MSC-20198

High-Production Silicon-Ingot Slicer

A new ingot slicer comprised of stacks of up to 250 rotating, ganged blades promises to increase wafer production, to improve silicon wafer yield, and to cut manufacturing costs. The rotating ingots are fed into the circular cutters.
(See page 216.)

Explosive Joining for Nuclear-Reactor Repair

A remote ribbon explosive yields a joint with double the parent metal strength. For reactor repair, a 30-grain/foot (0.63-gram/cm) ribbon drives a machined adapter flange into a bellows. This joining technique is useful in remote, dangerous, and inaccessible areas.
(See page 211.)

Boom Deploys With Controlled Energy Release

A self-deploying boom stows in a canister and stores its own erecting energy in coiled, fiberglass springs. The erected boom members form a lattice structure stiffened by diagonal members. Applications include lightweight field-erectable structures.
(See page 175.)

Coulomb Friction Damper

A linear friction damper is effective at low velocities.

Lyndon B. Johnson Space Center, Houston, Texas

A standard hydraulic shock absorber has been modified to form a coulomb (linear friction) damper. The device damps very small velocities and is well suited for use with large masses mounted on soft springs. In contrast, hydraulic dampers can be ineffective when the velocity is reduced.

As shown in the figure, the piston of a conventional hydraulic shock absorber is replaced by a cylindrical friction pad that rubs against the inner cylinder wall. The lateral force of the friction pad against the wall is determined by the adjustment of a spring that presses axially on a conical wedge to force the friction pad outward.

The coulomb friction damper is applicable in situations requiring large damping of small oscillating velocities. It contains no liquid that could leak or freeze and heaters, necessary for low-temperature operation of fluid dampers, are not needed. Performance is relatively insensitive to temperature and to cycle frequency. The damping force is easily adjusted for different loads. These dampers are therefore more reliable than fluid dampers and also more economical to build and to maintain.

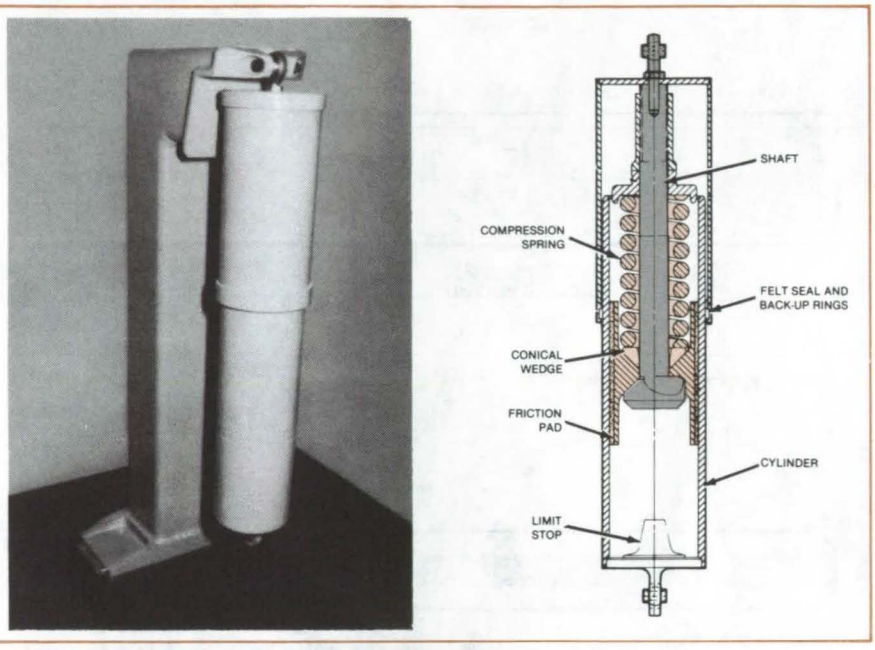

The **Coulomb Friction Damper** is constructed by modifying a standard hydraulic shock absorber.

This work was done by Walter T. Appleberry of Rockwell International Corp. for **Johnson Space Center.** *For further information, Circle 44 on the TSP Request Card.*
MSC-20179

Inserts Automatically Lubricate Ball Bearings

Small inserts in the ball pockets provide a steady supply of lubricant.

Marshall Space Flight Center, Alabama

Inserts on the ball-separator ring of ball bearings will provide a continuous film of lubricant on the ball surfaces. Developed for hard-to-lubricate turbopumps for cryogenic liquids, the yet-to-be-tested technique could be utilized on equipment for which maintenance is often poor and lubrication interval is uncertain — household appliances, automobiles, and marine engines, for example.

The inserts are made from a material high in molybdenum disulfide and poly(tetrafluoroethylene) content — both solid lubricating agents. The ball pockets in a separator are elongated in the circumferential direction by machining. An insert is then snapped into elongations on two adjacent pockets, bearing against the inside surface of the separator (see figure). Lips on the insert hook over the outside surface of the separator, thereby holding the insert in place. When all inserts are in position

Ball Bearings Are Lubricated by small inserts of a material rich in molybdenum disulfide and poly(tetrafluoroethylene). The inserts can be machined or molded.

on the separator, all ball pockets are circular.

In operation, the balls rub against the inserts as they turn. They thus pick up a film of lubricant, which they transfer to the bearing races.

This work was done by J. A. Hager of Rockwell International Corp. for **Marshall Space Flight Center.** *No further documentation is available.*
MFS-19727

Locking Nut and Bolt

Threaded fastener resists strong loosening forces.

Marshall Space Flight Center, Alabama

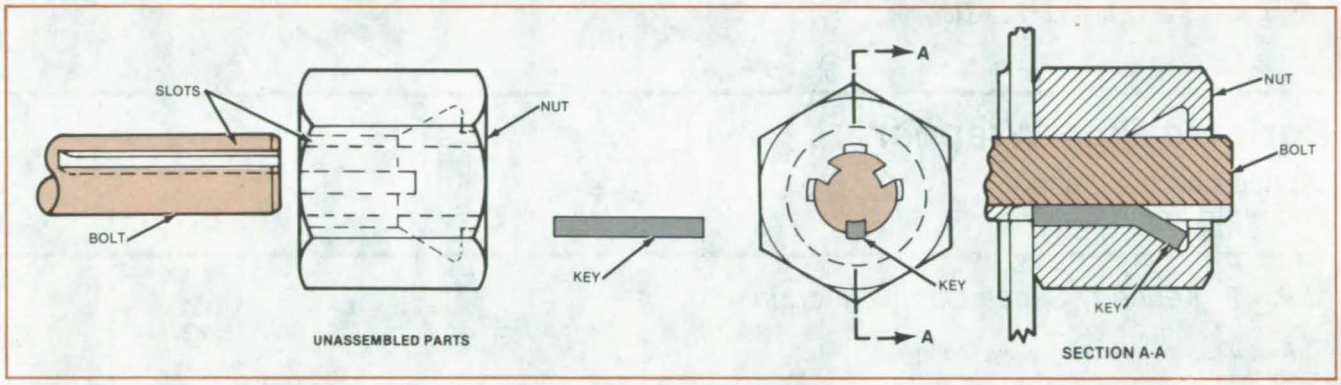

Bolt, Nut, and Key are joined together so that the key occupies alined slots in bolt and nut and prevents the nut from rotating off the bolt.

A new threaded fastener locks parts securely together despite large loosening torques, even under conditions of high temperature and vibration. The positive locking action is suitable for use where conventional fasteners tend to work loose — for example, on high-speed rotating machinery.

The fastener consists of a bolt, a key, and a nut containing an inner annulus (see figure). Longitudinal slots are machined in the external surface of the bolt and in the internal surface of the nut.

In installation, the nut is screwed on the bolt and tightened to the required torque. The nut is rotated farther until one of its slots is alined with the nearest slot in the bolt. Three slots in the bolt and four in the nut allow for easy alinement. The key is inserted in the alined slots and bent into the nut annulus. The bolt and nut are then locked together by the key — one cannot move in relation to the other. The assembly can be separated only by cutting away the nut.

This work was done by Ray Bishop of Rockwell International Corp. for **Marshall Space Flight Center.** *No further documentation is available.*
MFS-19687

Ferrofluid Would Seal Linear-Motion Valve

A magnetic fluid would seal against pressure or vacuum.

Lyndon B. Johnson Space Center, Houston, Texas

A proposed valve would employ a ferrofluid to make a tight seal. The seal would require no precisely machined parts, and hand lapping of valve seats would be unnecessary. [Ferrofluids have low vapor pressure — about 1×10^{-8} torr (10^{-6} N/m^2). They can therefore be used in low and moderate vacuum.]

The valve consists of a hollow shaft with magnetically soft sheaths that can slide through a ring magnet with annular pole pieces (see figure). In its open position, the shaft carries gas, liquid, or vacuum through its hollow core. In its closed position, both ports on the shaft are on the same side of the wall, so that the hole in the wall is sealed.

A ferrofluid — a magnetic liquid — is held in place around the shaft by the ring magnet. The ferrofluid fills the void between the shaft and the pole piece in the chamber wall, providing a tight seal against vacuum or high pressure. The shaft should be made of a nonmagnetic material so that it does not continually wipe away ferrofluid as it is opened and

(continued on next page)

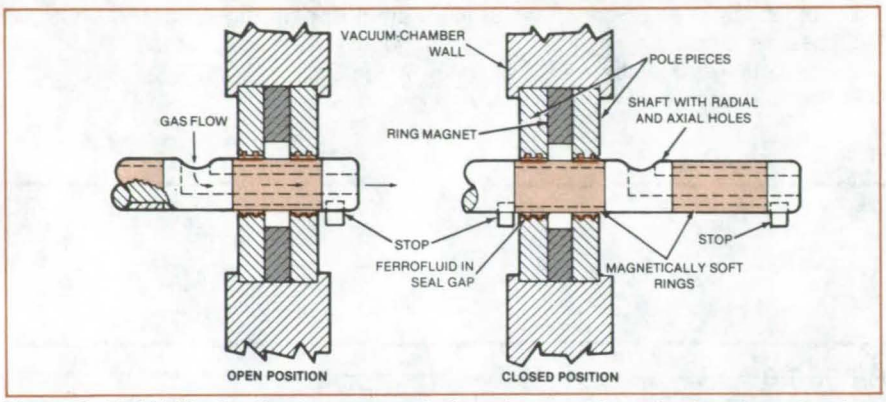

Magnetic Fluid Fills the Gap between a shaft and an annular pole piece in a chamber wall. A precise shaft fit is not necessary.

closed. An inexpensive molded plastic should serve well.

More than one ferrofluid seal can be used on a shaft. It can then be used as a multiple-position switching valve in a plumbing system.

This work was done by Joseph A. Chandler of **Johnson Space Center.** *For further information, Circle 45 on the TSP Request Card.*

Inquiries concerning rights for the commercial use of this invention should be addressed to the Patent Counsel, Johnson Space Center [see page A5]. Refer to MSC-20148.

Portable Pipe Wrapper

Device controls tension and wrap angle.

John F. Kennedy Space Center, Florida

A new tool applies fragile layered insulation to cryogenic tubing. It has been used routinely to apply two layers of fiberglass and one of aluminum foil on pipe used as the inner line in vacuum jacketed cryogenic plumbing. Applying the layers one at a time by hand had proved to be too delicate and time consuming a task: The insulation tended to tear when handled with gloves (required to avoid contamination), and the layers were difficult to apply uniformly.

The new portable pipe wrapper (see figure) has three freely revolving drums that hold the wrapping material. They are mounted on a four-wheeled cart that is pushed along the pipe as wrapping proceeds. The pipe is held in a turntable that turns like a lathe. As the pipe turns, it pulls the wrappings off the rolls and onto the pipe in tight, even layers. An adjustable arm on the wrapper controls the angle of wrap. There is no handling of the wrapping material except at the start and end of the wrap.

The wrapper is easy to use and is made from inexpensive, readily available parts. It can be wheeled to whatever location is convenient for wrapping the pipe. The wrapper should prove useful in applying thermal insulation to hot-water pipes and refrigerant-distribution lines. A similar tool could be used to wrap electrical insulation.

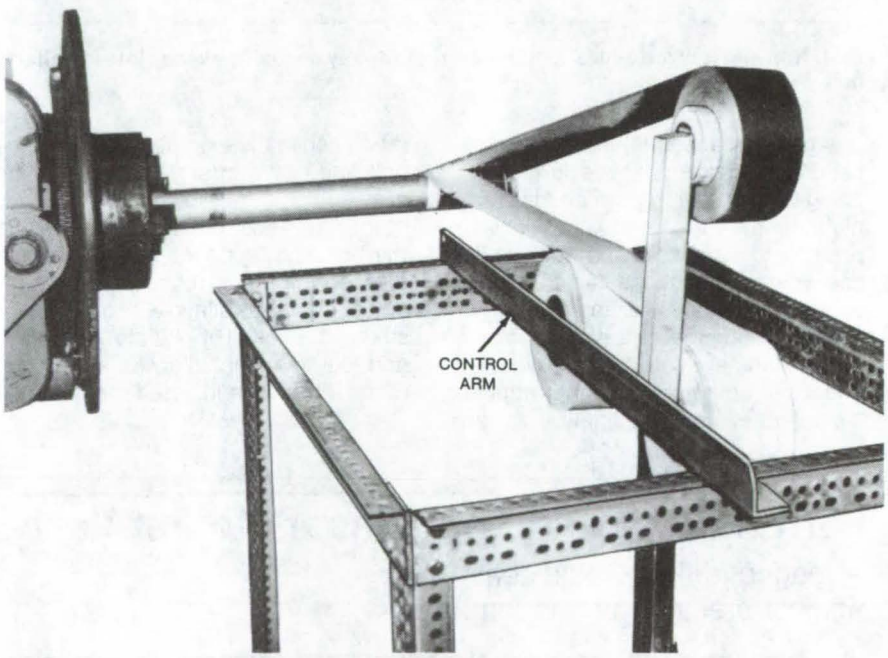

The **Portable Pipe Wrapper** is rolled along parallel to the pipe as the wrappings are applied. The control arm can be adjusted to control the angle of wrap.

This work was done by Gale B. Dennis of Boeing Services International for **Kennedy Space Center.** *No further documentation is available.*
KSC-11244

Tubing Cutter Is Activated Hydraulically

A hydraulic cutter deactivates aircraft ejection seats in rescue operations.

Langley Research Center, Hampton, Virginia

The hydraulically powered tool shown in the figure severs tubing and cable in areas where accessibility is limited. The cutter jaws are attached to one end of a flexible "gooseneck" extension and are closed by a hydraulic piston when the operator squeezes the handle grip. The jaws are released by flipping an on/off lever. The double-jawed cutters cut out a complete section of tubing.

The cutter was originally intended for use by fire/crash crews to deactivate aircraft ejection seats during rescue operations. In that application, the cutter severs the pressure supply lines to the ejector. The cutter has potential as a flight-line tool and can also be useful in automobile and fire rescue work.

A manually-operated cutting tool was utilized prior to use of the hydraulic cutter. The manual tool has long handles, which are necessary to provide sufficient torque to the cutting jaws. The use of both hands is required for operation.

In contrast, the hydraulic tool employs a trigger-grip handle that can be operated easily with one hand. Its gooseneck frame is flexible and can be manipulated so that tubing can be cut in a cramped location.

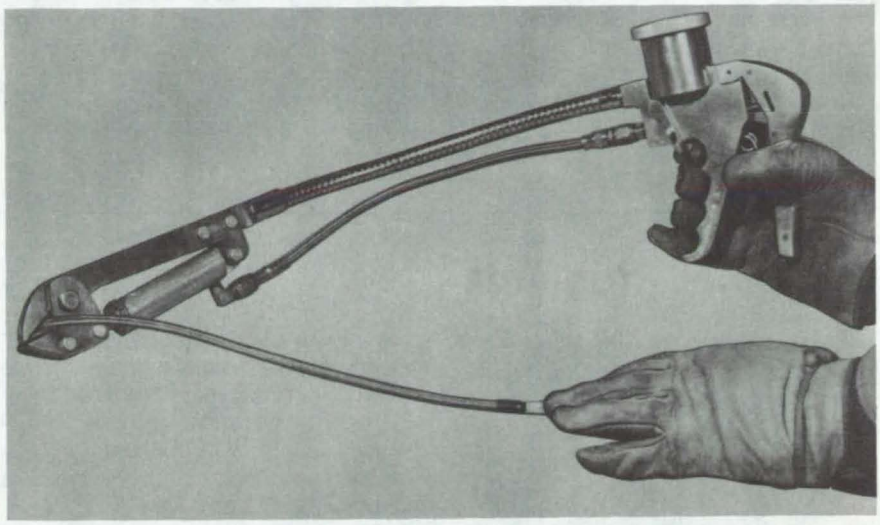

The **Hydraulically-Actuated Tubing Cutter** severs the tubing when the operator squeezes the handle grip. The "gooseneck" extension enables the cutter to be used in areas where accessibility is limited.

This work was done by Dwight G. McSmith and James I. Richardson of **Langley Research Center.** *No further documentation is available.*
LAR-12786

Books and Reports

These reports, studies, and handbooks are available from NASA as Technical Support Packages (TSP's) when a Request Card number is cited; otherwise they are available from the National Technical Information Service.

Light, Compact Pumper for Harbor Fires

Aerospace technology is utilized in a transportable, powerful unit.

A recent report describes the development of a new transportable water-pumping unit for firefighting. The compact, self-contained unit provides fire protection at coastal and inland ports and is lighter than a standard firetruck pumper of the same capacity. [The same report was made available to readers requesting further information on "Mobile Firefighting Module," the technology illustrated on the cover of *NASA Tech Briefs*, Vol. 6, No. 3, Fall/Winter 1981.]

A prototype model has been delivered to the U.S. Coast Guard, and an improved model has been delivered to the U.S. Maritime Administration. Incorporating aerospace technology and materials, the unit is a skid-mounted gas turbine and pump that delivers up to 2,500 gal/min (9,500 liters/min) of water at a discharge pressure of 150 lb/in.^{2} (1 MPa). The water source can be any open stretch of freshwater or saltwater or a high-capacity fire hydrant. The unit primes itself and can draft water to a height up to 20 feet (6.1 meters) above the sea or river surface. It can operate for 4 hours at maximum flow without refueling. It measures 4 by 5.4 by 6.8 feet (1.22 by 1.65 by 2.07 meters) and weighs 1,600 lb (726 kg) dry.

When the unit is delivered at a fire site, an operator drops the suction hose into the water and pushes the start button. The starter/generator spins the engine to 15 percent rated speed, at which point ignition occurs. The engine accelerates to 60 percent speed. The operator pushes the prime button, and the unit automatically primes itself. Atmospheric pressure on the river or sea surface forces water up the suction hose. The unit begins pumping water through the discharge hose and water cannons.

The operator can then set the discharge pressure, and the unit controller will automatically maintain that level. Thus, if a discharge line valve is

(continued on next page)

opened or closed, the controller will change the engine power to maintain the original pressure setting. Alternatively, the operator can manually set the speed.

The primary structural element is the fuel tank, which contains longitudinal stiffeners that also serve as forklift tunnels. Each corner of the tank holds a shock-mounted skid. The engine and pump are integrally mounted on a lightweight frame that is bolted to the fuel tank. A firewall separates the engine combustion chamber from the pump. The engine gearbox, fuel control, starter/generator, exhaust ducts, primer, oil cooler, air eductor, oil pump, pump discharge line, and check valve are in the combustion-chamber section. The engine compressor, inlet filters, pump shock mounts, oil reservoirs, battery, and emergency internal-fire-extinguisher bottle are in the pump section.

The unit can be operated from a riverbank, light truck, trailer, dock, barge, or boat. It can be transported by truck, trailer, boat, forklift, or helicopter. It can be used to fight fires in harbors, cities, forests, refineries, chemical plants, and offshore drilling platforms. Other possible applications include cleaning up oilspills, pumping out ships, and flood-control pumping.

This work was done by Ralph A. Burns of **Marshall Space Flight Center.** *To obtain a copy of the report, Circle 46 on the TSP Request Card.*

Inquiries concerning rights for the commercial use of the invention described in the report should be addressed to the Patent Counsel, Marshall Space Flight Center [see page A5]. *Refer to MFS-25784.*

Computer Programs

These programs may be obtained at very reasonable cost from COSMIC, a facility sponsored by NASA to make new programs available to the public. For information on program price, size, and availability, circle the reference letter on the COSMIC Request Card in this issue.

Rotating-Machinery Critical Speeds

Solutions are obtained assuming motion in one plane.

A computer program available from COSMIC provides quick, efficient, and accurate results in support of preliminary and proposed rotating-machinery designs. Advanced rotating-machinery design is an iterative process in the early stages of development. With the higher-operating-speed requirements of these flexible rotor designs, the rotor dynamic analysis becomes more important. Location of the critical speeds is not only important from a resonant-response standpoint but also for stability considerations.

To support the designer in the iterative, conceptual design phase, the critical speeds and mode shapes must be accurately calculated. With the complexity of modern rotors, an accurate hand calculation is not practical, and a full finite-element model analysis can be expensive and time consuming. This new program provides timely, critical-speed calculations to support preliminary rotating-machinery designs.

The analysis develops a model from data files that represents the stiffness and mass properties of the rotating assembly. The critical-speeds problem is solved by assuming motion in one plane. Each joint has a translational and rotational degree of freedom; no axial motion is assumed. Bearings are modeled as radial linear springs to ground, and a moment spring may also be added. Typically, critical speeds are calculated by a parametric study that includes gyroscopic motion effects for a wide range of bearing stiffnesses. Output includes plots of rotor modes at critical speeds and of critical speed versus bearing stiffness.

This program is written in FORTRAN V for batch execution and has been implemented on a UNIVAC 1100-series computer with a central memory requirement of approximately 40K of 32-bit words. Plotted output is generated for the Tektronix 4014 graphics terminal. This program was developed in 1980.

This program was written by R. F. Beatty, A. L. Mowers, and E. Mogil of Rockwell International Corp. for **Marshall Space Flight Center.** *For further information, Circle L on the COSMIC Request Card.*
MFS-19669

Fabrication Technology

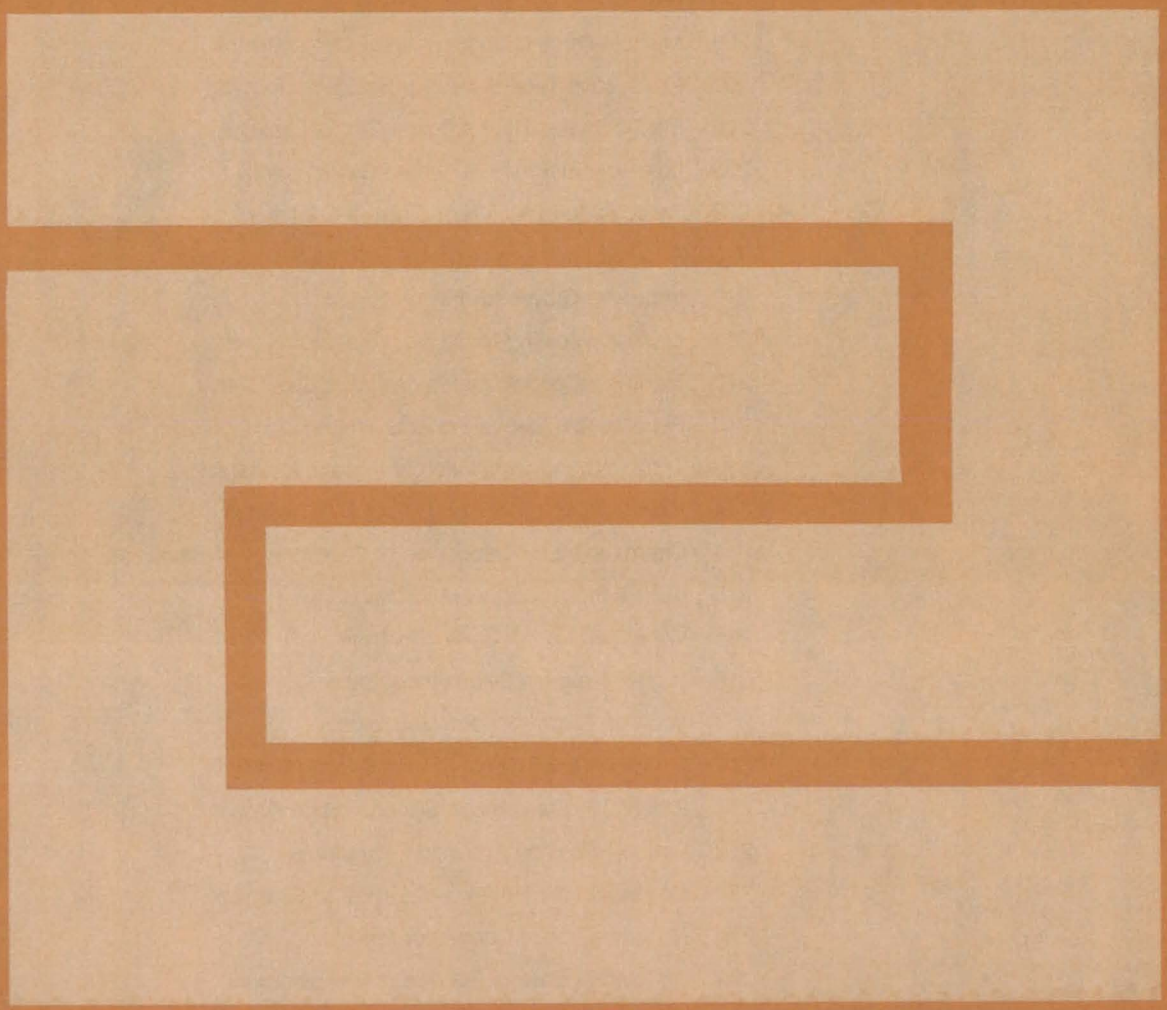

Hardware, Techniques, and Processes

Books and Reports

Computer Programs

Process Yields Strong, Void-Free Laminates

An accurate, reproducible fabrication process produces composites of consistent quality.

Langley Research Center, Hampton, Virginia

The **Laminate Assembly,** with vacuum ports and thermocouples installed, is placed in an autoclave and cured at 332° C (630° F) maximum temperature, 30 inches (76 cm) of Hg vacuum, and 200 ksi (1.4 GPa) pressure.

The need for lightweight materials as structural components for future space transportation systems has stimulated the development of a systematic method for manufacturing a polyimide/graphite composite. Laminates manufactured by this process are void-free, exhibit excellent thermo-oxidative stability up to 315° C (600° F), and are 40 percent lighter than aluminum. The mechanical properties of this material at 23° C (73° F) include ultimate tensile strength of 200 ksi (1.4 GPa), flexural strength of 250 ksi (1.7 GPa), and interlaminar shear strength of 12 to 15 ksi (0.08 to 1.0 GPa).The process is precise and repeatable. It is ideally suited for researchers and small-lot producers of composite materials.

The composite material consists of an LARC-160 polyimide resin matrix reinforced with graphite fibers. The resin system is formulated to a molecular weight of 1,600 with ethyl alcohol as the solvent. Other monomers in the resin are 5-norborene-2, 3-dicarboxylic anhydride (NA), 3,3′,4,4′-benzophenonetetracarboxylic acid dianhydride (BTDA), and polymethylene polyphenylamine. Polymerization occurs in situ in the range of 273° C (525° F) to 329° C (625° F).

Prepreg material of LARC-160/graphite for laminates is produced on a drum winding machine. The prepreg is cut to the desired size and fiber direction and stacked for "B"-stage consolidation after which the "B"-staged laminate is cured and evaluated for material integrity. Tack and drape are controlled by carefully drying to remove volatiles. The ratio of graphite to resin in the final cured laminate can be precisely controlled by resin-formulation and prepregging-parameter adjustments. The optimum parameters are fiber weight percent,51; resin solids weight percent,44; and volatiles weight percent,5. The prepreg material is stored in polyethylene bags at 17.78° C (0° F) — an environment in which it maintains an indefinite shelf life. Prepreg containing LARC-160 with a formulated molecular weight of 1,600 and 60 percent resin solids by weight produces a laminate with an average ply thickness of 7 mils (0.003 cm), a fiber weight percent of 60, and a resin weight percent of 40.

Laminates (see photograph) are made with temperature pressure cycles that include a "B"-staging at 232° C (450° F) and 28 inches (71 cm) of Hg vacuum, a cure cycle at 332° C (630° F) and 30 inches (76 cm) of Hg vacuum, and cooling to 65.6° C (150° F) or less before releasing vacuum.

This work was done by Leland E. Bryant, Edward W. Covington III, Walter J. Dale, E. Thomas Hall, Jr., James E. Justice, Edward C. Taylor, and Maywood L. Wilson of **Langley Research Center.**
For further information, Circle 47 on the TSP Request Card.
LAR-12982

Fabrication of a Precise Microwave Reflector

Machined reflector elements are assembled on graphite/epoxy supports.

NASA's Jet Propulsion Laboratory, Pasadena, California

A new antenna reflector integrates several fabrication techniques of optical and composite constraining materials. One of the most critical components in a new radiometer, the reflector must have a precise spherical configuration and must be thermally stable over a very wide temperature range.

The reflector is composed of machined aluminum reflector tiles attached to a graphite/epoxy structure with aluminum flexures (see figure). To obtain sufficient efficiency at the 200-GHz operating frequency, a surface accuracy of ±0.5 mil (0.0127 mm) from a 6-m-radius best-fit sphere is necessary. The tiles, which are about 5¼-by-5¼-by-¼-inch (13.3-by-13.3-by-0.6-cm) squares, are edge-clamped in aluminum surrounds and fly-cut to the desired spherical configuration. Then they are polished to a specular surface with an optical finish of 4 to 10 interference fringes.

The tiles are held by wax on a large aluminum tooling piece of 6-m spherical radius and maintained in that configuration until bonded to graphite/epoxy composite structure. The assembled structure is covered with an electroless copper and nickel flash coat and then sealed with a eutectic metal.

The fabricated optical figure is evaluated by using the specular reflective surface of the tiles to perform a Ronchi test. Distortion is measured in a vacuum chamber. Heat and cold are applied during the tests.

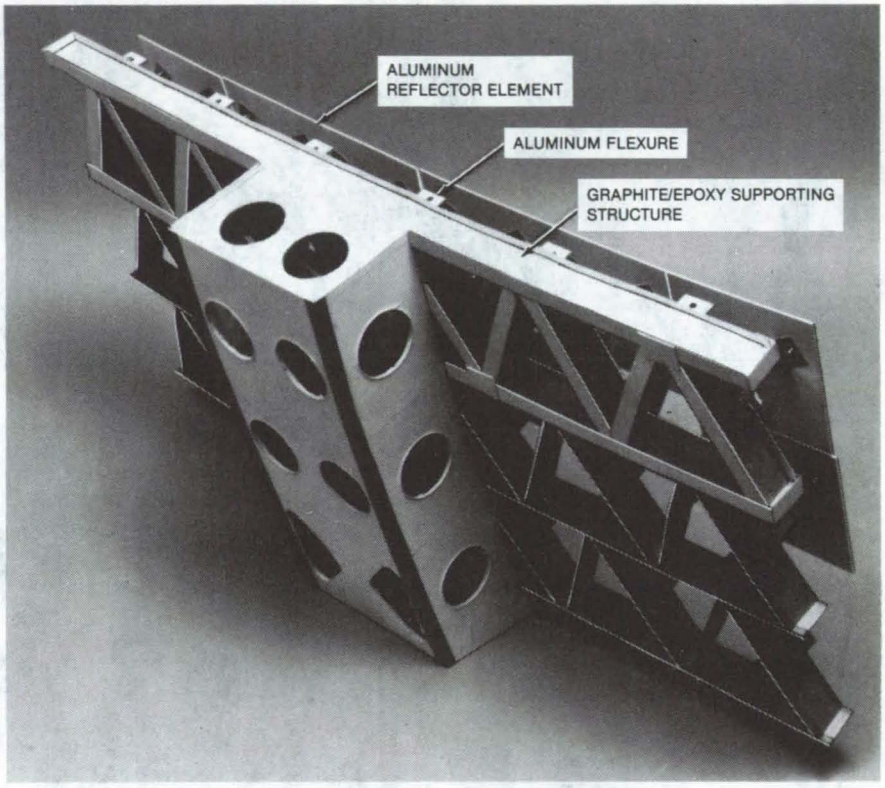

Aluminum Reflector Tiles are supported by a network of beams. Excepting the fasteners, the support structure is composed of lightweight graphite/epoxy composite.

This work was done by Jerome L. Bauer and Eugene W. Noller, of Caltech for **NASA's Jet Propulsion Laboratory.** *For further information, Circle 48 on the TSP Request Card.*
NPO-15377

Curing of Furfuryl Alcohol-Impregnated Parts

A longer cure and improved quality control prevent delaminations.

Lyndon B. Johnson Space Center, Houston, Texas

A delamination problem in reinforced carbon/carbon parts impregnated with oxalic acid-catalyzed furfuryl alcohol is overcome by instituting two additional quality-control tests on the alcohol and by changing the curing conditions. The delamination had occurred following autoclave curing of the catalyzed furfuryl alcohol.

It had been assumed that monitoring alcohol viscosity would suffice as a quality-control check, but from time to time, the impregnating solution developed a froth that interfered with the impregnating process, even though viscosity was proper.

Differential scanning calorimetric (DSC) tests show a rapid, sharp exotherm at 293° F (145° C) as well as a broad exotherm extending beyond 400° F (204° C). It was concluded that

the previous 1-hour cure at 290° F (143° C) was insufficient and that postcuring to 400° F at ambient pressure could also release moisture (as a byproduct of the curing reacton), causing delamination in thick regions of the parts being fabricated.

As a result of the investigation, the added alcohol quality-control tests are as follows:

- Alcohol in production use is tested weekly for water content. Water content must remain below 9.5 percent.
- DSC tests used to check the exothermic reaction characteristics of the impregnating solution. The exotherm must be strong.

The revised curing cycle calls for at least 2 hours at 300° ± 10° F (149° ± 6° C) followed by cooling to 175° F (80° C) under autoclave pressure. The extended cure drives the slower reaction nearer to completion. Since instituting these changes, no part delaminations have occurred.

This work was done by James W. Lawton and Thomas H. Brayden of Vought Corp. for **Johnson Space Center.** *No further documentation is available.*

Inquiries concerning rights for the commercial use of this invention should be addressed to the Patent Counsel, Johnson Space Center [see page A5]. Refer to MSC-20224.

High-Temperature Filler for Tile Gaps

Procedure using ceramic fabric can be used in kilns and furnaces.

Lyndon B. Johnson Space Center, Houston, Texas

Gaps between ceramic tiles can be filled with ceramic-coated fabric that withstands temperatures as high as 2,400° F (1,300° C). The caulking procedure with this material supplements existing gap fillers between surface insulation tiles on the Space Shuttle; it saves time by permitting the repair of fillings already in place, without the need to remove, rework, or replace them. High-temperature liners in kilns, furnaces, and other applications of heat-resistant insulation can also be caulked by this technique.

The ceramic fabric used for the gap-filler shim has a thickness of either 0.012 or 0.040 inch (0.3 or 1.0 mm). It is mounted in a metal frame and sprayed with colloidal silica, then sprayed with ceramic coating, and dried. It is then cut to size for the gap and inserted in place. Finally, it is bonded in place with a room-temperature-vulcanizing (RTV) adhesive, as indicated in the figure.

These gap fillers maintain the required pressure against the sidewalls of the tiles, are flexible, and can withstand airloads and high-temperature exposure for repeated missions.

This work was done by Jack W. Holt and David S. Wang of Rockwell International Corp. for **Johnson Space Center.** *For further information, Circle 49 on the TSP Request Card.*
MSC-20137

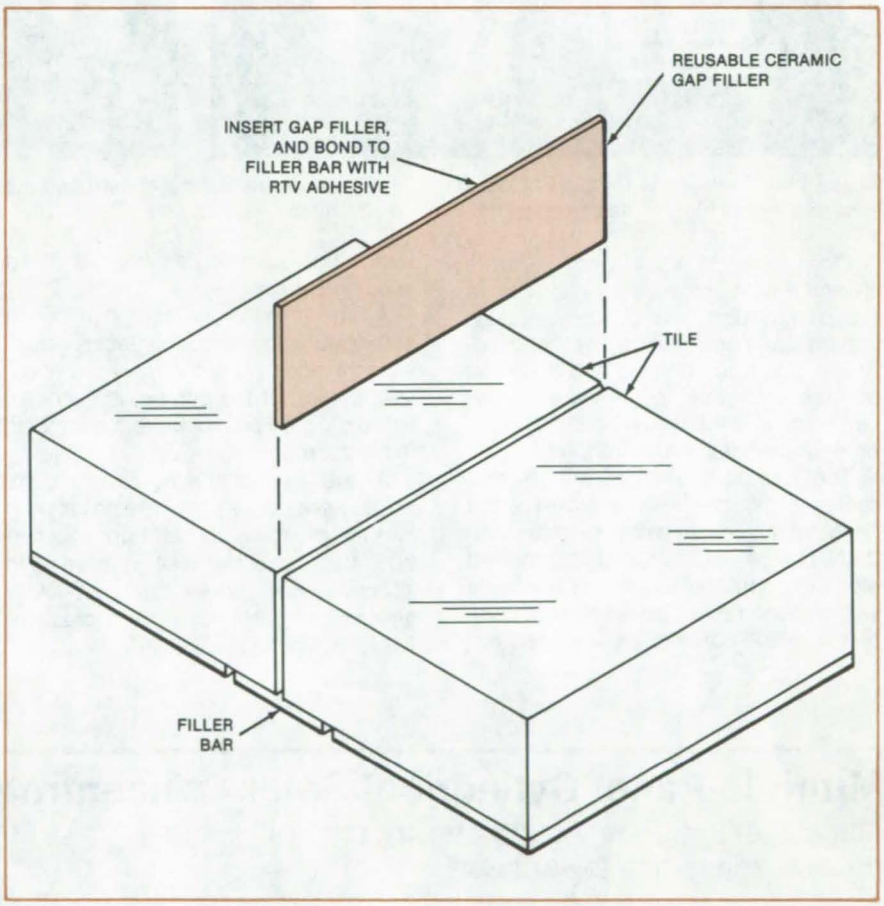

The **High-Temperature Gap Filler** is reusable. It is made of fabric coated with a ceramic slurry and bonded in place with room-temperature-vulcanized adhesive.

Pressure Assist Makes Coating More Reliable

Pressurization forces silicone resin into the pores of an anodized surface.

Lyndon B. Johnson Space Center, Houston, Texas

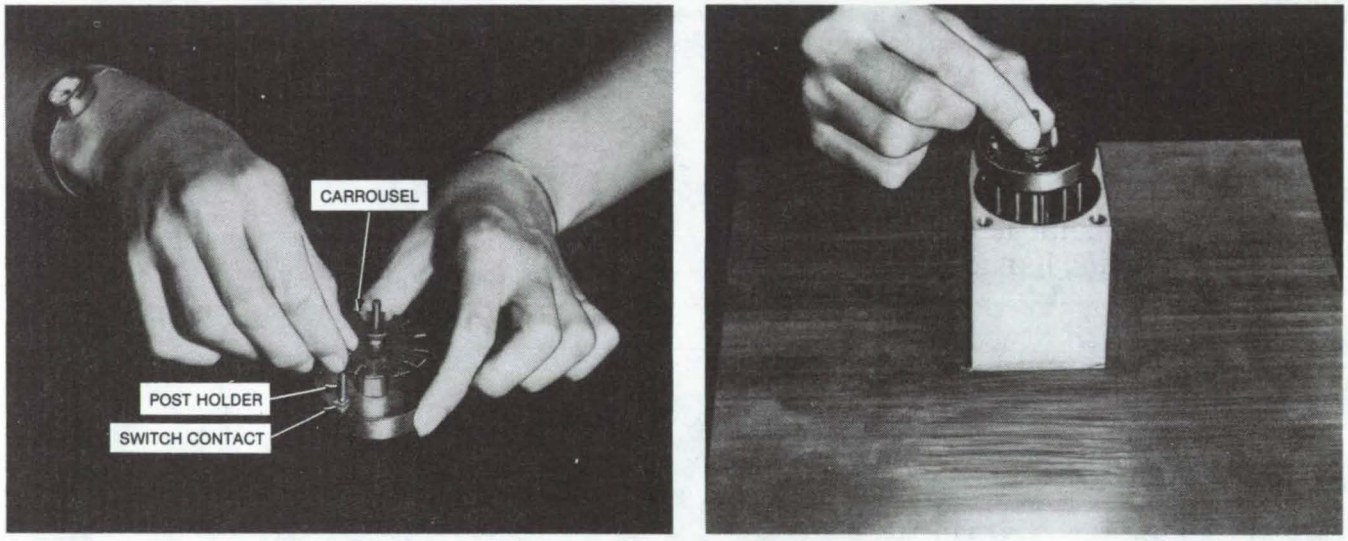

These **Two Views** show the post holder being inserted into the carrousel (left) and the post-holder assembly being inserted into the pressure vessel (right). The carrousel holds up to 12 switch contacts.

Designers of the Space Shuttle S-band communications system have found a new use for an old idea — applying pressure to improve the bond between a viscous coating and a porous surface. In the Shuttle hardware, its new use is to increase the reliability of resin-coated anodized switch contacts.

The contacts used in the S-band switch assembly have a nickel-plated base, which must remain resin-free so that it can be soldered, and an anodized aluminum top contact, which is coated with silicone resin. The resin must completely fill the pores of the anodized surface. If not, the resin can flake off after it is put in service.

As shown in the photograph at the left of the figure, the switch contact is held in a post holder, such that only the anodized portion of the contact is exposed. Up to a dozen post holders can be held in the carrousel.

At the right of the figure, the post-holder assembly is shown being inserted into the pressure vessel. Prior to insertion, the carrousel well is filled with silicone resin. When the post-holder assembly is in place, the pressure vessel is closed and sealed.

The vessel is then evacuated to 25 inches (63.5 cm) of mercury for 3 to 5 minutes. Dry nitrogen gas is applied at 160 psi (1.10×10^6 MPa) for 3 to 5 minutes through a top fitting. After pressure is released, the carrousel is removed. The contacts are removed, and any excess coating is wicked off. The coating is cured, and subsequent coatings are hand-dipped and wiped.

This work was done by A. Warren Berg of Teledyne Microwave for **Johnson Space Center.** *No further documentation is available.*
MSC-20210

Multiple-Panel Cylindrical Solar Concentrator

Multipanel trough reflector does not require precise orientation toward Sun.

NASA's Jet Propulsion Laboratory, Pasadena, California

A solar concentrator composed of many flat-plate mirrors is efficient even when pointing away from the Sun by as much as 5°. Its concentration ratio is 10 or more with a relatively-small reflector area.

The concentrator is designed to backlight an array of photovoltaic cells; that is, to illuminate solar cells pointing toward the concentrator rather than toward the Sun (see figure). Unlike ordinary backlit concentrators, which employ parabolically curved reflectors, the multiple-flat-plate concentrator does not dramatically lose its effectiveness when it is slightly out of alinement with the Sun.

The plates are arranged in a trough, the cross section of which approximates a parabola. The angles between plates, the width of the plates, and the distance from the solar-cell array to the plate are determined from equations that relate these quantities, the solar-array width, the pointing accuracy, and the concentration ratio. For example, for a pointing accuracy of 1° and a concentration ratio of 16, the area ratio (concentrator area to solar-array area) varies from 31 to 28.39 as the H/L ratio (array width to array/concentrator separation) is varied from 9 to 14.

The multiple-flat-plate concentrator was originally developed for use in power sources on spacecraft. For terrestrial applications, the multiple-flat-plate design offers potential cost reduction and ease of fabrication.

This work was done by Edwin M. Brown of Hughes Aircraft Co. for **NASA's Jet Propulsion Laboratory.** *For further information, Circle 50 on the TSP Request Card.*
NPO-15627

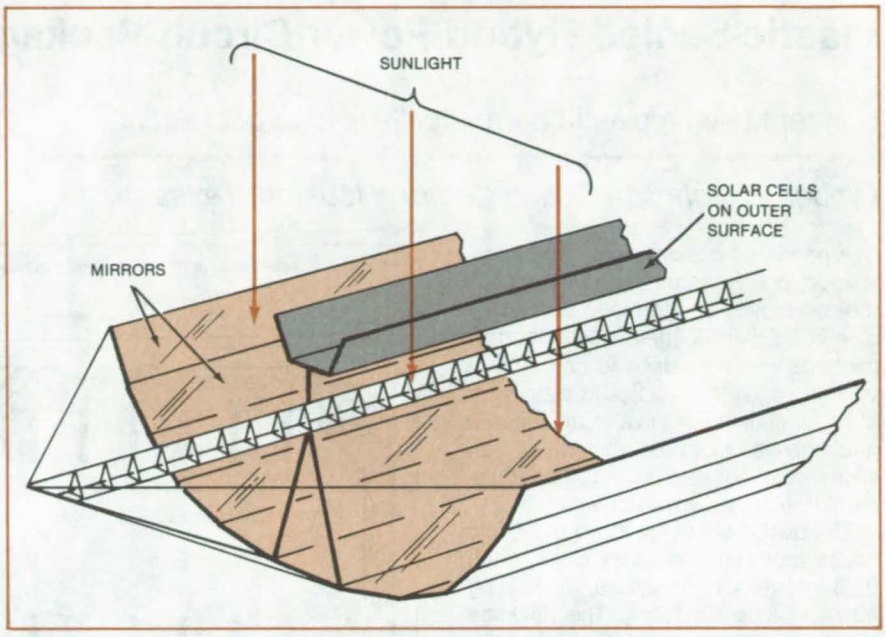

A **Trough Composed of Many Panels** concentrates the Sun's energy on solar cells, even when the trough is not pointed directly at the Sun. It can tolerate a deviation as great as 5° from the direction of the Sun.

Conductive-Tape Substrate for Electroforming

Metal tape has many uses in electroplating.

Marshall Space Flight Center, Alabama

Conductive tape is a versatile substrate for the electroforming of odd-shaped parts. Aluminum-foil tape has been used both as an electrical connection between two metal parts and as a substrate for electroforming a strong mechanical bond between the two parts (see figure). By using a double layer of tape adhesive-to-adhesive, electrical continuity can be established whether or not the tape available has a conductive adhesive.

Copper and aluminum conductive tapes are available commercially. When high dimensional precision is not required, such tape can serve as an electrical conductor, as a fastener, and as a rigid surface on which to electroplate. The tape can be quickly fashioned into the desired shapes with ordinary scissors.

Other uses of such tapes include:

- Taping a wire to a part to be plated, thus avoiding the need for a special clamp or fixture, and
- Using the mechanical strength of the tape to support a part during plating.

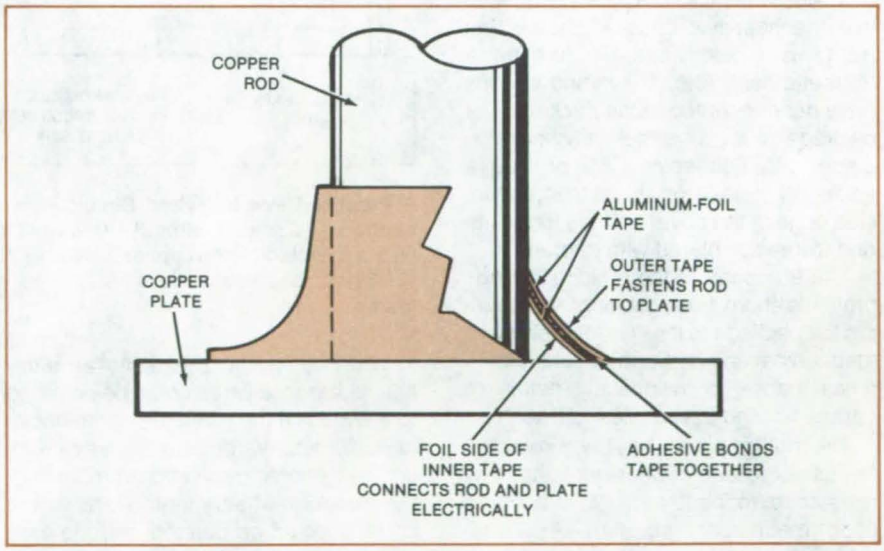

An **Electroformed Joint** was made by electroplating a thick layer of metal on top of a double layer of aluminum-foil adhesive tape. During the plating the tape connected the rod and plate both electrically and mechanically.

This work was done by M. L. Cassidenti of Rockwell International Corp. for **Marshall Space Flight Center.** *No further documentation is available.*
MFS-19715

Plastic-Sealed Hybrid Power-Circuit Package

Concept uses a plastic hermetically sealed package.

Lyndon B. Johnson Space Center, Houston, Texas

A proposed design for a hybrid high-voltage power-circuit package uses a molded plastic for hermetic sealing instead of a glass-to-metal seal. The new package would be used to house high-voltage regulators and solid-state switches for applications in aircraft, electric automobiles, industrial equipment, satellites, solar-cell arrays, and other equipment in extreme environments.

The design shown in the figure could house four semiconductor chips, each 0.25 inch (6.4 mm) square, dissipating 40 watts to a heat sink. The package could operate at up to 1,000 Vdc in air or vacuum at temperatures from that of liquid nitrogen up to 500° F (260° C). By modifying the package size, the design could be adapted for higher or lower power dissipation or to accommodate entire hybrid circuit chip assemblies comprising transistors, diodes, resistors, or thryristors.

The package consists of a copper heat-sink base, a plastic ring frame, and a cover plate. Gold-plated copper wire leads are molded into the sidewalls of the ring frame for stability and hermetic sealing. The ring frame is attached to the heat sink with pins. The pins are molded into the heat-sink base when the ring frame is molded onto it, forming a hermetic seal. After the hybrid circuits have been mounted in the package, the package cover is hermetically sealed in place with soft solder. To provide a soldering surface on the plastic, the inside edge of the cover and the top of the ring frame are plated with copper.

The 90° bend in the molded-in leads prevents them from rotating and causing the package to leak under thermal or mechanical shock. Such shocks sometimes cause conventional metal- or ceramic-cased assemblies to fracture.

The molded plastic has been selected for its excellent dimensional stability, resistance to heat and radiation, and good mechanical strength. At 70° F (21° C) it absorbs or releases no more than 0.22 percent water with no chemical or dimensional changes.

The wire leads point away from the package base to allow direct connection to a printed-wiring board. As an alternative, harness wires could be soldered to the leads if they were bent into hooks as is sometimes done with relay headers. For printed-circuit-board mounting, the threaded attachment inserts in the corners could be deleted and the wire leads pointed in the direction of the package base. For good heat transfer, the package base could be attached to the heat sink with heat-conducting epoxy.

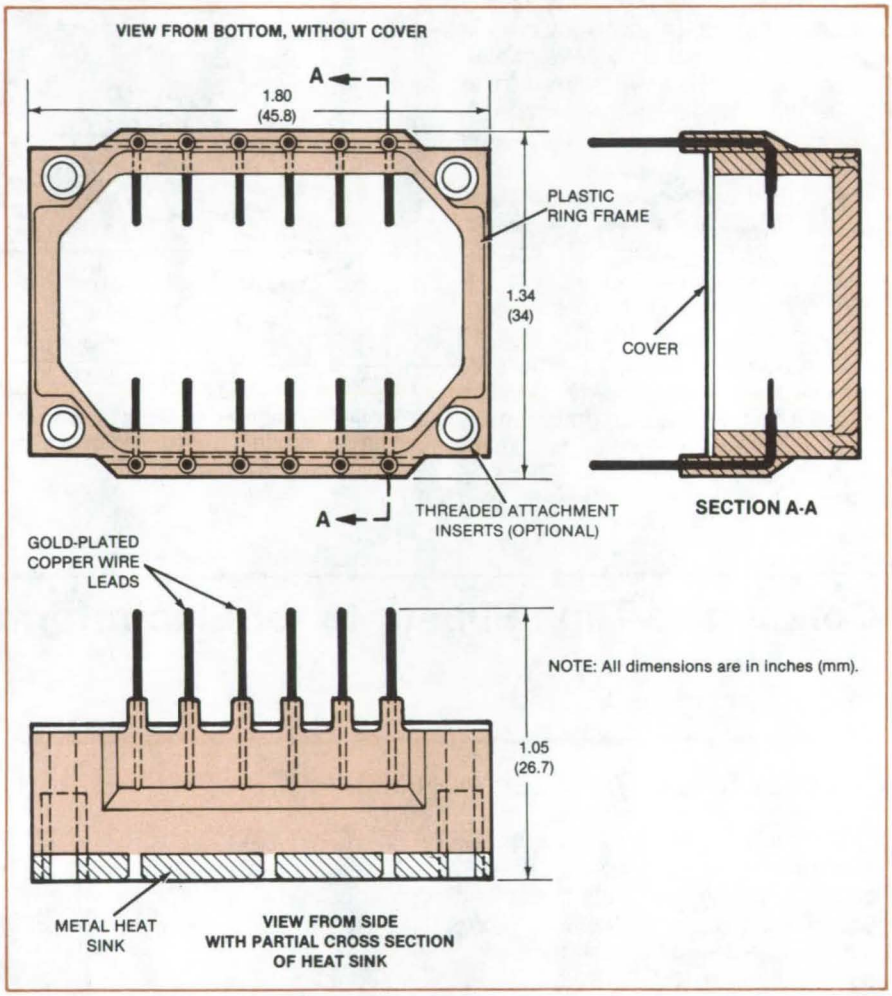

A **Proposed Power Hybrid Circuit Package** constructed mainly of molded plastic is hermetically sealed without the use of costly metal-to-glass seals. The mass of the package including the copper base is 31.75 grams. An equivalent glass-to-metal package in current use has a mass of 78.9 grams, while an all-copper package has a mass of 86.2 grams.

This work was done by Wilson N. Miller and Ormal E. Gray of Rockwell International Corp. for **Johnson Space Center.** *For further information, Circle 51 on the TSP Request Card.*

This invention is owned by NASA, and a patent application has been filed. Inquiries concerning nonexclusive or exclusive license for its commercial development should be addressed to the Patent Counsel, Johnson Space Center [see page A5]. *Refer to MSC-20181.*

Low-Cost Electrically-Heated Glass Panels

Simple process converts reflective glass into electrically heated panels.

NASA's Jet Propulsion Laboratory, Pasadena, California

An inexpensive process converts architectural reflective-coated glass into electrically heated panels. The technique utilizes the reflective layer as a heating element and saves the production costs of applying or embedding heating elements in ordinary glass. The resulting panels have many applications, including automobile windows, home-heating panels, temperature-controlled windows or containers, and food-warming trays. The glass can be maintained indefinitely at temperatures in excess of 100° C.

Architectural reflective glass is usually made by coating clear glass with a metallic film that in turn is covered by a thin protective film. In the conversion process, an electric potential applied between two places on the film surface (see figure) breaks down the high-resistance outer protective layer and brings the reflective film into electrical contact with electrodes on the surface. The reflective film can then be used as a resistance heating element while the protective layer still insulates it from the environment.

Metallic or conductive-paint electrode strips are applied to the reflective side and/or the edge of the glass. After curing, an ac variable voltage source is connected across the electrodes. Breakdown of the protective layer commences with the application of a few volts and is completed at about 40 volts, when sparking between the electrode and the reflective film can be seen from the underside of the glass. After this, the heating panel can be operated stably at any voltage from zero to about 100 volts. The application of higher voltages or immersion in water during operation will cause irreversible breakdown of the resistive film. Therefore, for some applications, the panels must be waterproofed or sandwiched with clear glass.

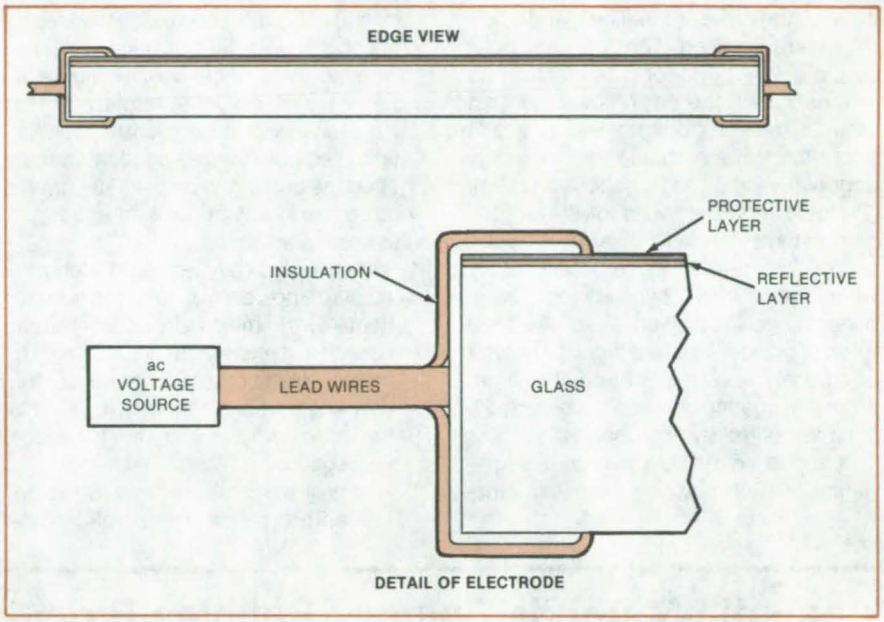

A **Simple Process** converts architectural reflective glass to electrically heated panels. Such glass is usually made by coating clear glass with a metallic film that in turn is covered by a thin protective film. Applying an ac voltage across the protective film causes it to break down, bringing the metallic reflective film in contact with external electrodes.

This work was done by Paul J. Shlichta and Bruce A. Nerad of **NASA's Jet Propulsion Laboratory.** *For further information, Circle 52 on the TSP Request Card.*
NPO-15753

Process Sprays Uniform Plasma Coatings

Multicomponent plasma coatings are applied without the segregation of components.

Lewis Research Center, Cleveland, Ohio

A composite-powder processing procedure has been developed along with plasma-spray parameters to achieve homogeneous, well-bonded, low-porosity, self-lubricating coatings. The purpose was to improve the compositional uniformity of the sprayed coating and to obtain a process that could be used by vendor organizations in preparing and applying these powders and coatings. The coating was NASA-developed lubricant PS 106, which has the nominal composition by weight of 35 silver, 35 Nichrome, and 30 calcium fluoride.

Previous methods for plasma-spray application of multicomponent coatings had been simply to premix powders of the various components and to place them in a hopper from which they were fed to the plasma torch and sprayed onto the surface to be coated. Another ap-

(continued on next page)

proach had been to supply the different powders separately to the torch by means of a multifeed system. Mixing occurred in the torch.

The disadvantages of the prior methods are as follows: (1) Premixed powders of components with different densities tended to segregate when the powders were vibrated, when they flowed through the powder feedlines, and when they were sprayed. The fact that powders manufactured for plasma spraying are designed for easy flow and that often all the component powders are of about the same particle-size range only aggravated the segregation problem. (2) Using separate feeds for the various components tended to seriously complicate the entire system, especially when more than two powder components were involved. Also the feed rates of powders were difficult to control accurately over a period of time; therefore coating compositions were difficult to control by this approach.

It appeared feasible to reduce segregation of such powders by using variations in particle size or by the use of suitable binders. Mixtures of particle sizes promote agglomeration, and small particles may adhere to larger ones, creating a pseudocomposite particle. Such a "particle" might remain essentially intact during the plasma-spraying process. Alternately, binders would be used to improve the between-particle strength of such particle aggregations. The object was to introduce sufficient binder to the particle-connecting necks to achieve maximum strength.

There were two significant steps that minimized powder segregation and permitted the coating to be plasma-sprayed onto a surface without segregation of the components:

1. Very fine (typically 5-micrometer) particle-size powders of selected components were mixed dry with coarser particles (typically 50 to 150 micrometers) of the other components. The very fine particles tended to adhere to the large particles and thus to reduce segregation.
2. A small percentage (2 to 6 weight percent) of monoaluminum phosphate (MAP) aqueous concentrate was added to the powder along with sufficient additional water to form a stirrable slurry. Upon drying, the powder was in the form of a cake in which the particles were loosely held together with the MAP acting as a binder. The powder cake was then broken and passed through a sieve. The sieved powders consisted of multicomponent aggregate particles. The aggregate particles readily flowed through the plasma-spray system and were sprayed with little or no tendency to segregate into the various components.

This work was done by H. E. Sliney and T. P. Jacobson of **Lewis Research Center** *and G. C. Walther and H. H. Nakamura of the IIT Research Institute. Further information may be found in NASA CR-3163 [N79-28315/NSP], "Program for Plasma-Sprayed Self-Lubricating Coatings" [$10.50]. A copy may be purchased [prepayment required] from the National Technical Information Service, Springfield, Virginia 22161.*
LEW-13237

Acoustic Methods Remove Bubbles From Liquids

Sonic oscillation increases the surface area of bubbles and causes them to dissipate.

NASA's Jet Propulsion Laboratory, Pasadena, California

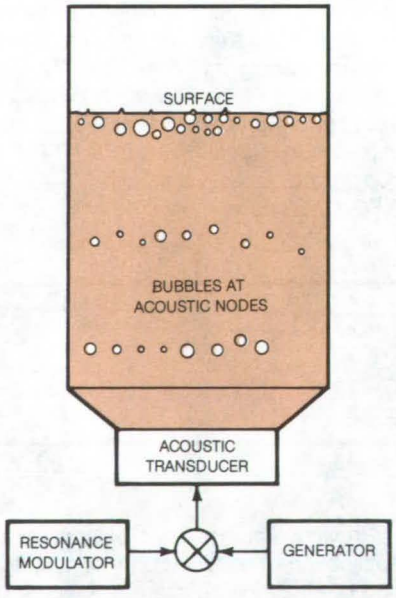

Bubbles Coalesce at the acoustic nodes, which correspond to the succession of resonant frequencies excited in the acoustic resonance chamber, and move to the surface where they break up and dissipate.

Two acoustic methods can be applied to molten glass or other viscous liquids to remove bubbles. Bubbles are either absorbed or brought to the surface by applying a high-intensity sonic field at a resonant frequency. In one method, a swept frequency resonant to bubbles of various sizes is used; and in the second, several resonant modes in an acoustic chamber are applied. The methods could be applied to the production of molds and optical-quality glass.

The first method reshapes the bubbles at their resonant frequency to increase their exposed surfaces to new areas of the liquid and to induce liquid circulation around the bubbles, thus encouraging molecular absorption. The intensity of the acoustic waves, which may be above 160 dB, depends on the density of the fluid.

In the second method (see figure), the liquid is placed in an acoustic resonance chamber. A succession of resonant modes of the chamber is applied, from the higher order modes down to the fundamental. At each frequency, the bubbles migrate to the oscillation nodes; as the frequency is decreased, the number of nodes decreases, and the bubbles tend to coalesce. Eventually they are moved to the liquid/gas interface.

This work was done by Eugene Trinh, Daniel D. Elleman, and Taylor G. Wang of Caltech for **NASA's Jet Propulsion Laboratory.** *For further information, Circle 53 on the TSP Request Card.*
NPO-15334

Improved Gloves for Firefighters

New materials and constructions give better protection.

Lyndon B. Johnson Space Center, Houston, Texas

New firefighter's gloves are more flexible and more comfortable than previous designs. Since some firefighters prefer gloves made of composite materials while others prefer dip-coated gloves, both types were developed (see figure). The new gloves may also find uses in foundries, steelmills, and other plants where they can be substituted for asbestos gloves.

An aramid fabric was selected as the material for the outer shell of the composite glove because it is strong and resistant to flame and heat. It is also flexible, dries rapidly, and retains its flexibility after repeated wetting and drying. The palm side is a durable tightly woven twill. The back of the shell is a knit.

For the liner, aramid felt was selected because it is puncture-resistant and thermally insulating. A neoprene film 4 to 5 mils (0.10 to 0.13 millimeter) thick on the palm side of the liner helps to prevent the rapid conduction of heat; the film is flexible and flame-retardant.

Wristlets 4 inches (10 centimeters) long protect the wearer's wrists. A felt patch increases the protection on the palm side of the wristlet.

For the dip-coated glove, the shell is coated with a yellow, flame-retardant neoprene layer. A friction layer on the palm side improves the wearer's grip. The yellow dip coating shields against radiant heat better than a dark-colored coating.

The wristlet for the dip-coated glove consists of an aramid knit outer layer and a knit cotton underlayer. The underlayer prevents penetration of the dip coating, which extends a short distance up the wristlet from the hand. A patch of aramid felt gives additional protection to the palm side of the wrist.

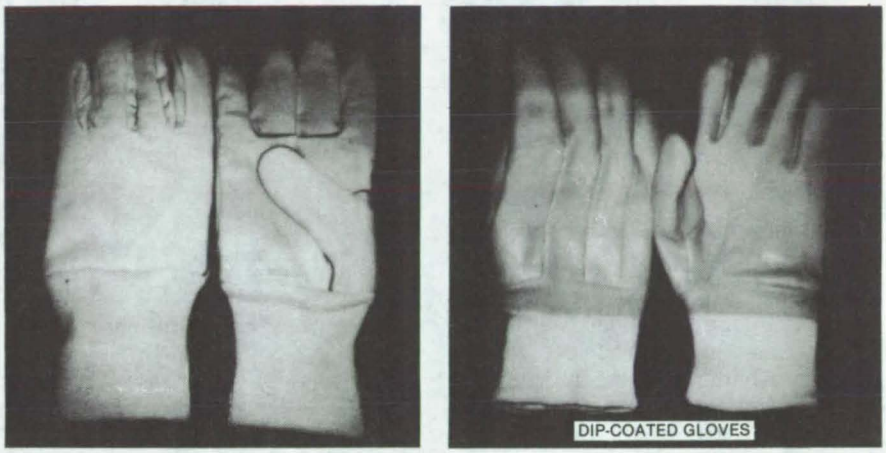

Two Versions of New Firefighter's Gloves accommodate individual preference. The palm of the glove outer shell is a twill, and the back is a knit. A friction layer on the palm side of the dip-coated glove improves the wearer's grip.

Both types of gloves were tested for conformance to standards of the National Institute for Occupational Safety and Health (NIOSH). Both met the cut-resistance criterion — that is, they sustained no cuts with a 16-pound (71-newton) load on a test blade. Puncture tests were conducted on the palm side of the gloves. Both types provided almost double the recommended 13.2-pound (59-newton) puncture resistance.

The standards state that a glove should protect against the injury-threshold temperature for 5 seconds. The composite glove exceeded the threshold after 4.6 seconds. The dipped glove maintained a temperature well below threshold for 5 seconds.

This work was done by Richard P. Tschirch, Kenneth R. Sidman, and Irving J. Arons of Arthur D. Little, Inc., for **Johnson Space Center.** *Further information may be found in NASA CR-167572 [N82-77571/NSP], "Development of Improved Firefighters' Gloves" [$9]. A copy may be purchased [prepayment required] from the National Technical Information Service, Springfield, Virginia 22161.*

This invention is owned by NASA, and a patent application has been filed. Inquiries concerning nonexclusive or exclusive license for its commercial development should be addressed to the Patent Counsel, Johnson Space Center [see page A5]. Refer to MSC-20261.

Explosive Joining for Nuclear-Reactor Repair

A ribbon charge yields a joint with double the parent metal strength.

Langley Research Center, Hampton, Virginia

High radiation levels and crowded workspaces complicate the repair and replacement of fuel channels in nuclear reactors. Using an explosive joining technique demonstrated at Langley Research Center, however, the repairs are made remotely, resulting in a joint that is double the strength of the parent metal.

In the initial assembly of the reactor, each fuel channel (a total of 390) is manually fusion-welded to a bellows assembly (Figure 1) on the reactor face

(continued on next page)

through a thin-walled low-carbon-steel adapter flange. To remove each fuel channel, the fusion weld is severed, the fuel-channel plumbing disconnected, and the fuel channel disconnected from the end-plate fitting on the opposite reactor face. A new fuel-channel assembly with adapter must be inserted into the bellows assembly and reinstalled.

In the explosive joining technique, the adapter flange from the fuel channel is machined to incorporate a V-notch interface, shown in Figure 2. The ribbon explosive, ½ inch (1.3 cm) in width, drives the V-notched wall of the adapter into the bellows assembly, producing an atomic-level metallurgical bond. A 0.030-inch (0.08-cm) wall thickness for the adapter flange, driven by a 30-grain/foot (0.63-gram/cm) explosive ribbon charge, yields a joint with twice the bond area needed to achieve parent metal strength (a 200-percent joint). A machine surface of 64 rms yields 200-percent-strength joints, but a 32-rms finish is needed to achieve a hermetic seal. Degreasing is necessary; wet wiping with standard no-deposit solvents, such as alcohol or Freon, is sufficient.

An acceptable but considerably weaker joint is made without the anvil-ring supporting structure. The anvil ring prevents tube distortion, allowing more of the explosive energy to be utilized. An acceptable but weaker joint was created with a fuel-channel adapter flange undersized in diameter by 0.060 inch (0.15 cm). The joint is unaffected by heat loads from the reactor as demonstrated by 100 thermal shocks from 570° F (300° C) to ambient.

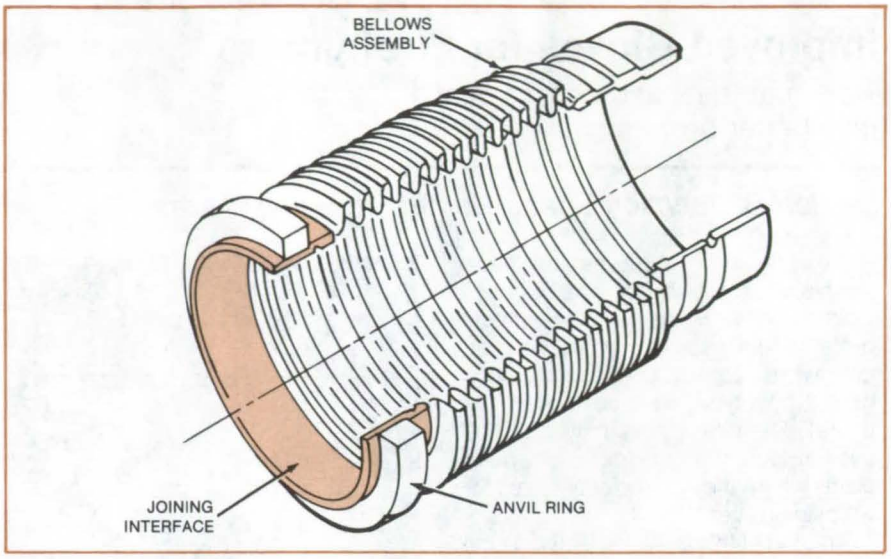

Figure 1. The **Reactor Bellows Assembly,** approximately 8 inches (20.3 cm) inside diameter, includes interface to fuel-channel adapter flange.

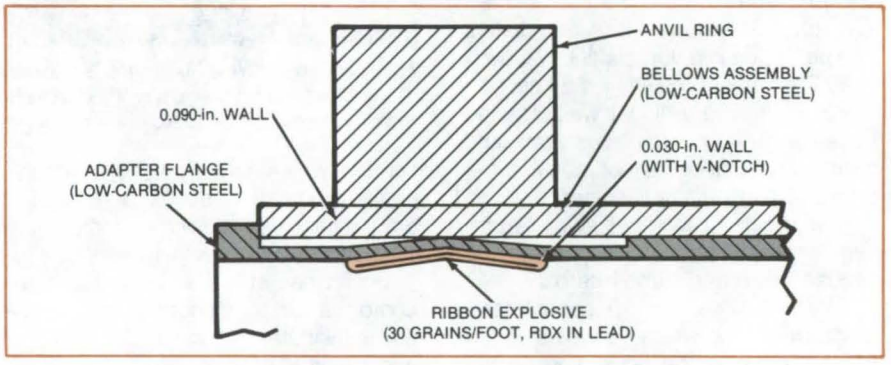

Figure 2. A **Ribbon Explosive** drives V-notched adapter flange into the bellows assembly.

This work was done by Laurence J. Bement of **Langley Research Center** *and James W. Bailey of Kentron International. For further information, Circle 54 on the TSP Request Card.*
LAR-12996

Electrical Conduit Distributes Weld Gas Evenly

Flexible conduit with small holes provides even weld-gas coverage.

Marshall Space Flight Center, Alabama

A purge-gas distributor, made from flexible electrical conduit by drilling small holes along its length, provides even gas flow for welding. The previous method was to drill a rigid tube.

The drilled flexible conduit is inserted into the part being welded and lightly pressurized with the purge gas. The escape holes plus the flexible joints in the conduit distribute the purge gas evenly throughout the interior of the part being welded.

The flexible conduit adjusts to accommodate almost any shape. It can be used for gas coverage in other applications that previously needed formed and drilled solid tubing.

This work was done by D. P. Ambrisco of Rockwell International Corp. for **Marshall Space Flight Center.** *No further documentation is available.*
MFS-19665

Replaceable Sleeve Protects Welder Coil

With a carbon insert, deflection coils last longer and are easier to maintain.

Lyndon B. Johnson Space Center, Houston, Texas

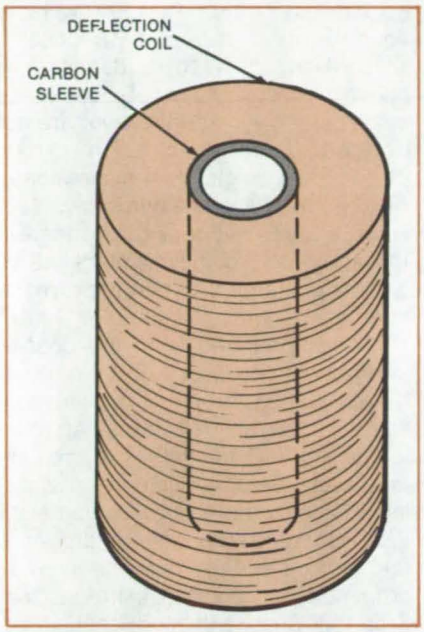

A **Carbon Sleeve** accepts metal-vapor deposits, thereby protecting the electron-beam deflection coil. It is machined from carbon rod 1.500 inches (3.810 cm) in diameter to a length of 1.343 inches (34.11 mm), an inside diameter of 1.000 inch (25.40 mm), and an outside diameter of 1.260 inches (32.00 mm).

A new replaceable carbon insert for the deflection coil in an electron-beam welder promises to decrease maintenance costs. Inserts made from materials other than carbon (not yet tried) may be less expensive, thus reducing costs even further.

During electron-beam welding, metal vapors condense on the inside wall of the deflection coil through which the electron beam passes. A metal film builds up gradually. If the metal is magnetic, it interferes with the operation of the deflection coil, and the beam does not respond to commands as it should.

The usual maintenance practice has been to overhaul the deflection coil regularly, cleaning metal film from the inside wall and recoating it with a protective layer of colloidal graphite. After several such cleanings, the colloidal graphite no longer adheres, and the deflection coil has to be discarded.

The new insert is a cylindrical sleeve machined from carbon rod. The diameter is carefully controlled to assure a snug fit in the deflection coil. Since carbon is nonmagnetic, the sleeve does not interfere with coil operation.

The sleeve is much easier to clean than are conventional protective coatings. Metal deposits are brushed away, and the sleeve is then returned to service.

The carbon sleeve is in regular production use. It reduces welder downtime for coil cleaning and extends the useful life of deflection coils.

This work was done by William L. Baker and Clifton E. Simpson of General Dynamics Corp. for **Johnson Space Center.** *No further documentation is available.*
MSC-20236

Transport and Installation of Fibrous Insulation

Two methods preserve the fiber orientation before and during installation.

Lyndon B. Johnson Space Center, Houston, Texas

Two new techniques simplify the transport and installation of oriented-fiber thermal insulation. Other applications involving oriented fibers or loose fillings might also be able to utilize the methods.

It is necessary to fill spaces around the Space Shuttle reaction-control thrustors with insulation fibers in specific orientations. Each thrustor has to be wrapped with fibers able to withstand 2,500° F (1,370° C) and having the proper density so that the temperatures of thrustor components can be kept within safe limits.

In one installation method, layers of uncured phenolic-impregnated batting in various shapes are wound around a mold and then compressed to the required density by a mandrel. The mold and insulation are then heated to 425° F (218° C) to cure and evaporate part of the binder. The insulation has the minimum practical binder content — 4-1/2 percent, just enough to prevent the parts from breaking up in transit. The rest of the binder is volatilized after installation, when the thrustor is heated to 600° F (316° C) for 48 hours.

The second method uses no resin. Instead, the insulation is compressed in a mold and saturated with water. The wet insulation is then frozen in the shipping container. After the frozen insulation is installed around the thrustor, it is heated until the water is driven off.

This work was done by Sieg Borck, Frederick L. Falconer, and Raymond V. Loustau of The Marquardt Co. for **Johnson Space Center.** *No further documentation is available.*
MSC-20074

InGaAsP CW Lasers on (110) InP Substrates

Threshold current densities are below 1,000 A/cm^2 at room temperature.

Langley Research Center, Hampton, Virginia

Quality InGaAsP/InP CW laser structures have been grown by conventional liquid-phase epitaxy on (110) InP substrates without using special growth procedures. The low broad-area current densities and 1.3-μm CW operation at room temperature indicate that InP/InGaAsP/InP laser structures with characteristics comparable to present state-of-the-art structures can be grown on the (110) InP substrates.

Previous studies of liquid-phase epitaxy of InGaAsP alloy on (110) surfaces of III-V semiconductor substrates had shown layers containing nonwetting defects and terracing. High-quality layers could be grown only after dissolving the substrate surface to a depth of 50 to 100 μm and then growing a buffer layer of approximately 20 μm.

InP wafers having (100) and (110) surfaces with similar doping and similar etch-pit densities were chemimechanically polished, etched, and rinsed. Scanning electron microscopy of the two surfaces showed that the (110) surface had fewer defects.

Double-heterojunction laser structures were grown using liquid-phase epitaxy supercooling with a horizontal sliding boat. Stained cross sections of the samples were examined in an optical microscope. The (110) surfaces were comparable to or slightly better than the (100) surfaces in physical appearance, including layer thickness and interface planarity.

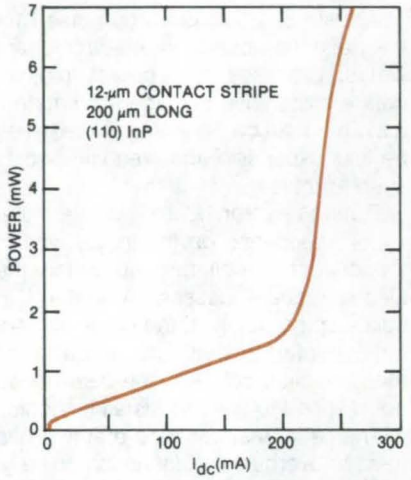

The **Power/Current Characteristic** of an oxide-stripe laser device at room temperature shows a threshold current of about 220 mA for continuous-wave operation.

Improved surface quality and grown-layer morphology are attributable to the nearly-perfect surface stoichiometry of the (110) surface [not available on (100) substrates], which makes available equal numbers of In and P deposition sites. Atoms in (110) surfaces form planar zigzag chains. Since these chains in a given surface layer are not bonded directly to each other, independent single-atom nucleation is required for every chain in a new (110) surface layer, producing an inherent tendency toward the maintenance of surface planarity. This may improve the interface growth.

Diodes prepared from the double-heterojunction laser structures exhibited pulsed threshold current densities as low as 970 A/cm^2 at room temperature. Oxide-defined stripe-contact lasers were fabricated by depositing SiO_2 onto the p-type cap and etching 12-μm-wide stripes perpendicular to the (110) cleavage plane, which is perpendicular to the substrate plane. Stripe devices exhibited continuous-wave thresholds as low as 150 mA at room temperature (see figure).

This work was done by Frank Z. Hawrylo of RCA Corp. for **Langley Research Center.** *For further information, Circle 55 on the TSP Request Card.*

LAR-12840

Chemical Vapor Deposition of Germanium on Silicon

Interface stresses are reduced during both growth and cooling periods.

NASA's Jet Propulsion Laboratory, Pasadena, California

Experimental work has shown that chemical vapor deposition (CVD) by pyrolysis of gaseous germanium tetrahydride provides epitaxial layers of germanium on silicon. The relatively low temperature of the CVD process (500° to 900° C) reduces stresses that occur at the layer/substrate interface during growth and cooling. These stresses are created by the mismatch, between the mechanical, thermal, and crystallographic properties of germanium and silicon. The process is under development; when refined, it could be used for fabricating germainium-on-silicon photovoltaic surfaces of the preferred orientation toward Ge (111).

The chemical-vapor-deposition system consists of a vertical quartz reactor, an RF induction heater, and feedlines. Phosphorus-doped (111) silicon is degreased and chemically etched before being placed in the reactor. In the reactor, gaseous germanium tetrahydride (GeH_4), which is diluted to 5 percent by helium gas, decomposes into germanium and deposits on the silicon.

To explore the effect of temperature on the deposits, a series of several 30-minute depositions was made on different samples using the same carrier-gas flow rate and GeH_4-in-He concentration; the temperatures ranged from 537° to 897° C. From a crystallographic view, the quality of the low-growth-temperature (537° C) deposits is the same as that of the medium (737° C) and high-temperature-growth (897° C deposits.

This work was done by Herzl Aharoni of Caltech for **NASA's Jet Propulsion Laboratory.** *For further information, Circle 56 on the TSP Request Card.*

NPO-15565

CLEFT Process for GaAs Solar Cells

Ultrathin solar cells are repeatedly grown on the same substrate.

Lewis Research Center, Cleveland, Ohio

Basically the CLEFT (cleavage of lateral epitaxial films for transfer) process involves growing an ultrathin gallium arsenide (GaAs solar cell on a much thicker layer of the same material. The growth method is such that the completed solar cell is easily separated by cleaving from the much thicker substrate. The resulting 10-micrometer-thick cell is 90 percent thinner and 77 percent lighter than the thinnest silicon solar cell. Furthermore, the thick substrate is reusable in making additional cells, which reduces cell material cost.

The greatly-reduced material usage in the CLEFT process results in material costs for GaAs cells that are comparable to the costs for silicon cells currently used in space. Since GaAs cells are more efficient (18 percent) than silicon cells (14 percent) and also more radiation-resistant, the process will make GaAs cells more practical for space applications, as well as for uses here on Earth.

The CLEFT process allows a drastic reduction in the usage of GaAs. This is important both as a method of reducing costs of these cells and reducing the usage of comparatively rare material. The reduction in material usage does not result in significant degradation in the high efficiency of GaAs cells, which is the major advantage over Si cells. It is expected that CLEFT cells, when fully developed, will achieve conversion efficiencies as high as 20 percent with GaAs layers only 5 micrometers thick.

The CLEFT process is a peeled-film technique. The basic idea of peeled-film technology is to grow a thin single-crystal epilayer on a single-crystal mold, to separate the epilayer from the mold, and then to use the mold again.

As a demonstration that the CLEFT process can be used to prepare multiple GaAs films, four CLEFT cycles using the same single-crystal GaAs substrate have been carried out. Four successive films of excellent quality were obtained, with thicknesses of 5, 10, 10, and 8 micrometers, respectively. The area of each film is about 4 cm^2. The films prepared and separated in this manner have been shown by Hall measurements to be comparable in quality to conventional single-crystal chemical-vapor-deposition (CVD) layers.

If this goal can be achieved, the cost of GaAs material will no longer be the major obstacle for this material system. Furthermore, there should be enough Ga available for large-scale deployment of GaAs cells.

This work was done by John C. C. Fan, Carl O. Bozler, and Robert W. McClelland of the Massacusetts Institute of Technology for **Lewis Research Center.** *Further information may be found in "Thin-Film GaAs Solar Cells," Proceedings of the 15th IEEE Photovoltaic Specialists Conference, June 1981, pp. 666-672.*

Inquiries concerning rights for the commercial use of this invention should be addressed to the Patent Counsel, Lewis Research Center *[see page A5].* *Refer to LEW-13912.*

Wipe Melt for InP Seed Substrate

A new combination of elements leaves a smooth high-luster surface.

Langley Research Center, Hampton, Virginia

Indium phosphide (InP) semiconductor substrates used as seed wafers for liquid-phase epitaxy growth tend to lose excessive amounts of phosphorus from the surface during the melt-homogenization portion of the growth cycle. The erosion of the surface due to dissociation results in holes, cracks, indium (metal) spheres, and other unwanted artifacts.

Methods previously used to eliminate or lessen the surface erosion include an InP cover wafer (used as a phosphorus source) and wipe melts of various elemental combinations. (A wipe melt is a liquid solution used to etch back or remove an acceptable amount of the surface and substrate material from the seed wafer. The etch is done at a predetermined temperature during the growth cycle before the substrate enters the semiconductor-layer growth solution.) Although somewhat acceptable, these methods have tended to be inconsistent.

A new four-element wipe melt containing indium (In), gallium (Ga), arsenic (As), and phosphorus (P) has consistently produced an acceptable morphology. The approximate proportion of each element is 94.58 percent In, 4.49 percent As, 0.73 percent Ga, and 0.2 percent P. The weights of the components used in the wipe melt are: 4.4657 g In, 13.2 mg InP, 306.5 mg InAs, and 45.1 mg GaAs.

The seed substrate is pulled under the InGaAsP wipe melt at a temperature of 650° C for approximately 15 to 60 seconds. At 650° C the melt is undersaturated with phosphorus, resulting in controlled dissolution of InP from the seed wafer surface. After pullthrough and meltback, the surface has a high smoothness and luster without the meniscus lines, exaggerated erosion, pits, and pearls that are characteristic of other wipe melts. In addition, the layer-to-substrate interface structure is more planar and of better quality.

This work was done by Frank Z. Hawrylo of RCA Corp. for **Langley Research Center.** *No further documentation is available.*
LAR-12912

High-Production Silicon-Ingot Slicer

Spinning ingots would be cut in balanced pairs.

NASA's Jet Propulsion Laboratory, Pasadena, California

A new concept for slicing silicon ingots into wafers promises to increase production rates and to improve yields of good wafers, thereby reducing the cost of manufacturing silicon solar cells. In the proposed wafer slicer, a stack of ganged blades cuts a group of silicon ingots simultaneously. The blades cut horizontally while the ingots rotate about their vertical axes. Rotation of the ingots increases the net cutting speed and reduces by half the depth to which a blade must penetrate an ingot to sever a wafer. As a result, the production of wafers for a given run is higher, even for moderate or low blade-rotation speeds and feed rates. Lower speeds and rates should produce fewer broken wafers.

Either inside-diameter or outside-diameter blades may be used (Figure 1). Pairs of ingots are positioned symmetrically around the cutting edge. The opposing-pair arrangement helps to balance the forces on the blade, thereby reducing vibation, improving wafer quality, and further reducing wafer breakage. Four, six, eight, or more ingots may be cut simultaneously, provided that the number is made up of opposed pairs.

The ingots are fed radially toward the center of rotation of the blade if cutting is done on the outside circumference of the blade and radially away from the center if cutting is done on an inside circumference. The rotation of the ingots about their vertical axes should be in the same sense as that of the cutting blade for outside cutting and in the opposite sense for inside cutting.

The rotation greatly reduces the cutting contact area. Since the contact pressure for effective cutting remains essentially unchanged, the reduced area makes it possible to slice a large number of wafers simultaneously without imposing excessive loads on the machine. Similarly, the thrust applied to each ingot is not unduly large, and bending of the ingots — which are supported only by their upper ends — is reduced.

A further advantage of ingot rotation is that it aids in the removal of debris. Silicon chips and abrasive particles quickly slide off the spinning wafer surface. A potential source of wafer damage and blade wear is thus eliminated, and the flow of coolant over the cut is promoted.

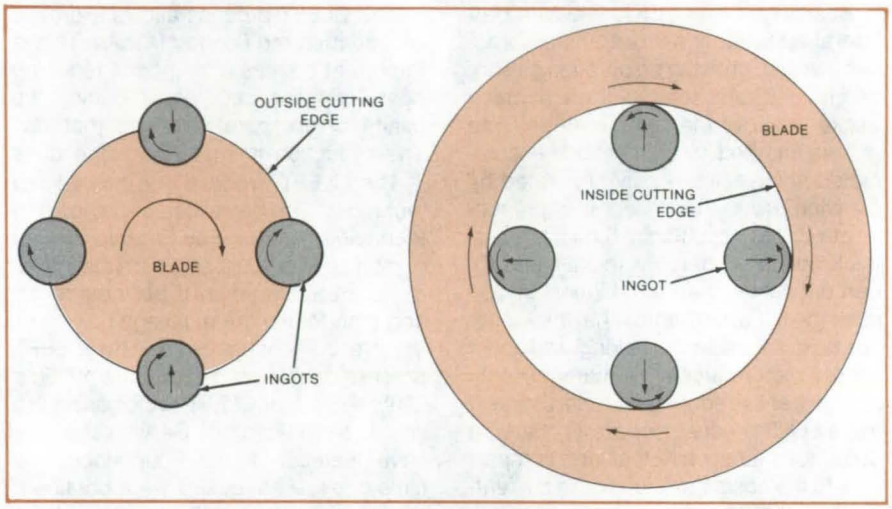

Figure 1. **As They are Rotated,** ingots are fed against the cutting edge of a blade. The cutting edge may be on either the inside or outside circumference of the blade.

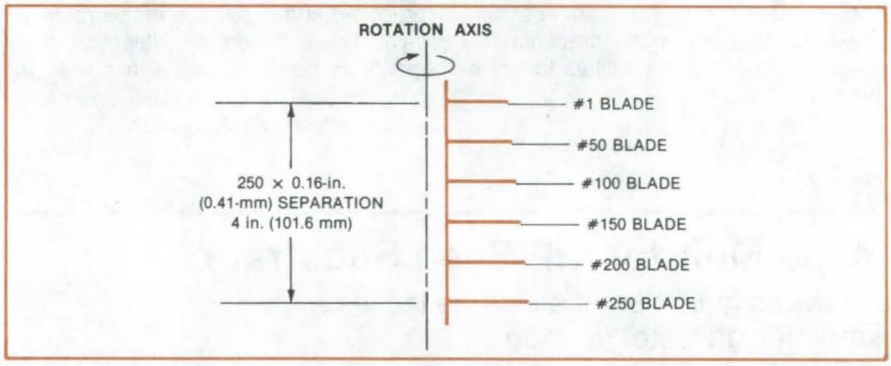

Figure 2. **Blade Edges are Staggered** so that final severance proceeds in rapid succession rather than all at once. Blades shown here are part of a 250-blade stack. Each edge is displaced 0.004 inch (0.1 mm) from the blade below it, for a total displacement of 1 inch (25.4 mm) between the topmost and bottommost edges.

The stacked blades must handle the cut wafers properly to avoid damage. The wafers should leave each ingot from the bottom first in an upward progression. Therefore each blade should have a slightly different diameter from that of its neighbors (Figure 2). If slicing is done by the outside edge of the blade, the diameter of the lowest blade must be slightly larger than that of the blade immediately above it, and so on up the stack. If cutting is done on the inside edge, the cutting hole in the lowest blade must be slightly smaller than the cutting hole in the blade just above it.

The small cutting contact area, the slow feed rate, and the relatively-low rotational speed of the blades may mean that slicing an individual wafer takes a longer time with the new concept. However, the longer time is more than compensated by the large number of ingots that can be cut simultaneously.

This work was done by Yu Shen Kuo of Caltech for **NASA's Jet Propulsion Laboratory.** *For further information, Circle 57 on the TSP Request Card.*
NPO-15483

Growing Silicon Ribbon Horizontally

A faster growth rate is just one advantage over vertical drawing.

NASA's Jet Propulsion Laboratory, Pasadena, California

Horizontal growth of silicon ribbon offers several advantages over vertical growth. It woud be faster — possibly 1 to 2 centimeters per second — and could be done without using drawing dies, a source of contamination in vertical growth. The horizontal process would naturally create a doping profile (decreasing dopant concentration toward the top surface), and it lends itself to continuous removal of impurities from the silicon melt.

In the proposed horizontal-growth process, a seed crystal is introduced into a crucible of molten silicon and withdrawn horizontally, carrying with it a continuous ribbon of newly-solidified single-crystal silicon (see figure). A long-term goal is to pull ribbons 3 1/2 to 7 mils (0.09 to 0.18 millimeter) in thickness at rates of 1 to 2 centimeters per second. Such a high growth rate is possible because the horizontal orientation offers a relatively large area for the rejection of heat by radiation, forced or natural atmospheric convection, and by conduction and convection from the solidifying ribbon to the liquid below it. In contrast, the heat-rejection area available for vertical growth is merely the cross-sectional area of the ribbon.

The meniscus under the moving ribbon at the crucible will leak slightly under certain conditions. If the leakage is carefully controlled, such spillover can be turned to advantage: It removes the impurity-laden top layer of the melt, preventing impurities from building up. The spilled silicon can be purified and recyled.

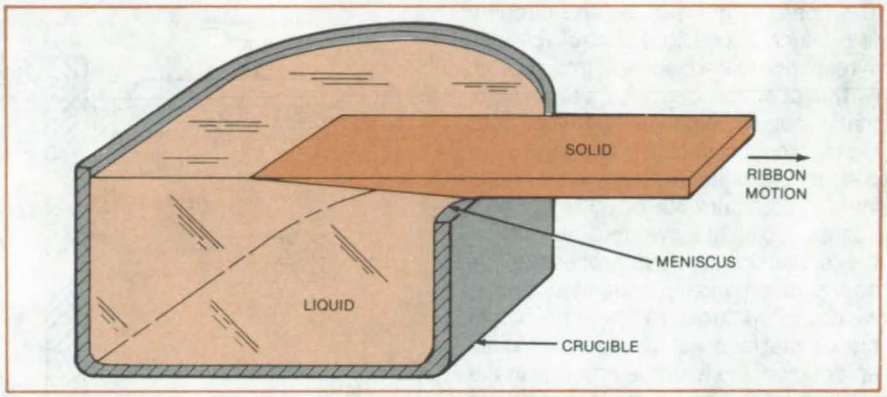

A Solid Ribbon of Silicon is pulled horizontally over the lip of a crucible. As heat leaves the silicon by radiation, conduction, and convection, the surface layer solidifies from the liquid.

The combined effects of thermal diffusion in the solidifying ribbon and the convection induced in the melt by the horizontal ribbon motion result in a dopant-concentration gradient near the surface. As a result, the top (first-to-grow) surface of the ribbon contains a minimum dopant concentration. The dopant density increases with distance below the top surface, reaching a maximum at the bottom (last-to-grow) surface of the ribbon. The low/high-dopant distribution provides a built-in back-surface field — a desirable feature because it makes solar cells more efficient. The top, low-doped ribbon surface is used as the top of a solar cell. The lightly doped region forms a collecting junction that places the material with the highest recombination lifetime in the region of greatest solar-energy absorption. The heavily-doped bottom surface reduces the series resistance of the cell.

To establish the utlimate horizontal-drawing rates for high-quality silicon ribbon, seeded-growth behavior will have to be studied. The rate of surface growth at the leading edge appears to be the factor limiting the drawing rate. A variable-flow jet of helium or argon gas at the leading growth edge may help; the jet will cool the solidifying ribbon more rapidly, thus allowing it to be pulled more quickly.

[For a related article, see "Technique for Crystal-Ribbon Growth" (NPO-15177) on page 93 of *NASA Tech Briefs*, Vol. 7, No. 1.]

This work was done by John A. Zoutendyk of Caltech for **NASA's Jet Propulsion Laboratory.** *For further information, Circle 58 on the TSP Request Card.*
NPO-14977

Meniscus Imaging for Crystal-Growth Control

Anamorphic imaging and adjustable contrast help to monitor growth conditions.

NASA's Jet Propulsion Laboratory, Pasadena, California

Silicon crystal growth is monitored by a new video system that reduces operator stress and improves the conditions for observation and control of the growing process. The system optics produce greater magnification vertically than horizontally, so the entire meniscus and melt is viewed with high resolution in both the width and height dimensions.

The monitoring system can be used for many different crystal-growth processes and in particular for the capillary-die process illustrated in the figure. Here

(continued on next page)

a silicon ribbon crystal is grown for use in solar cells. The size of the ribbon is affected by the pulling speed and growth-interface temperature.

The enhanced anamorphic meniscus image is displayed on a screen along with control data so that the growth process is observed by the operator with a minimum of fatigue and reaction time. The operator manipulates the circuitry to produce the desired control voltages in response to the displayed information.

The operator can also select automatic control: Voltages derived from digital processing of the image are applied to a servocontrol system that regulates heater currents or pulling speed. For example, the average intensity of the enhanced-contrast processed image is automatically computed over a window that includes the crystal/meniscus interface. As the interface moves up or down, the average intensity in the window increases or decreases above or below a reference intensity level that corresponds to the desired position. The difference between the average and reference levels produces an error signal that is used to alter the pulling rate or heater current.

This work was done by Emanual M. Sachs of Mobil Tyco Solar Energy Corp. for **NASA's Jet Propulsion Laboratory.** *For further information, Circle 59 on the TSP Request Card.*
NPO-15349

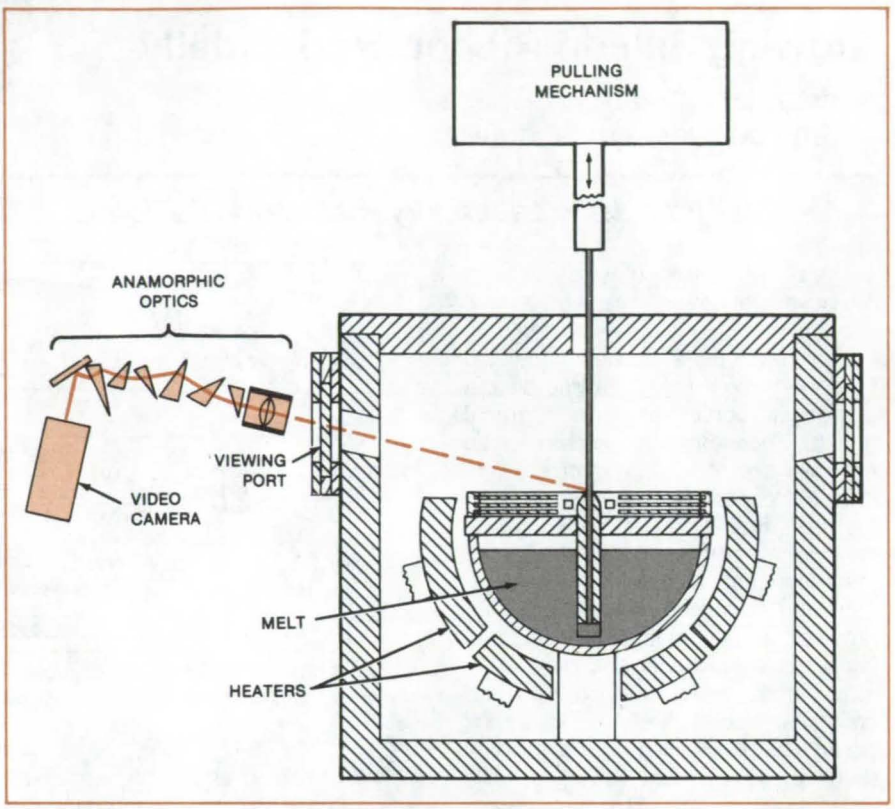

Monitoring Crystal Growth is easier and more effective with this video imaging and control system than with earlier systems employing microscopes and separate control electronics. The camera produces an image on a display screen, and operator-directed circuits for measurement and control adjust crystal-growth parameters.

Preventing Freezeup in Silicon Ribbon Growth

Profiled heat extractor prevents ribbon ends from solidifying prematurely.

NASA's Jet Propulsion Laboratory, Pasadena, California

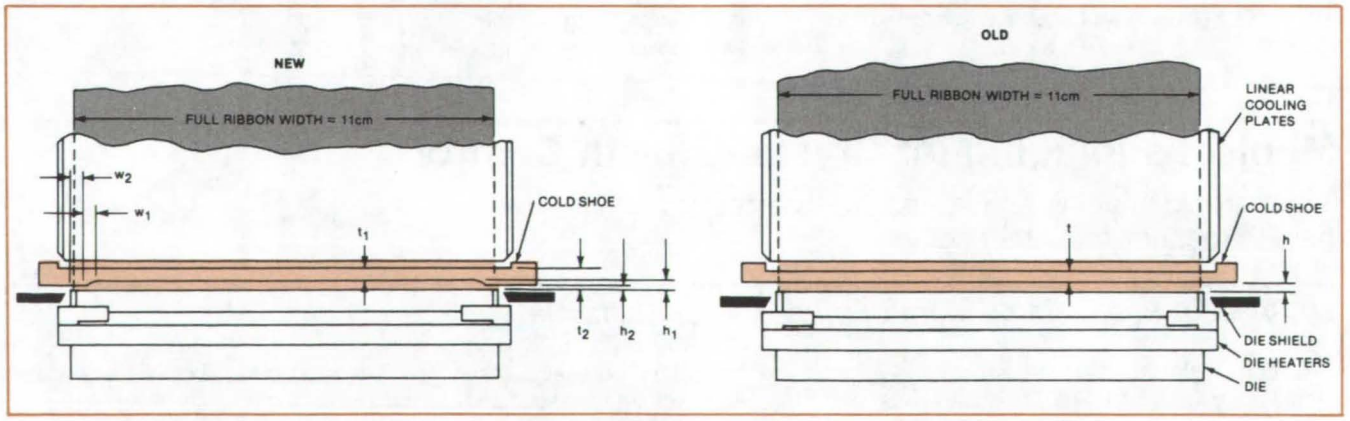

Dimensions of New Cold Shoe are chosen to yield a nearly-zero lateral temperature gradient. New dimensions in centimeters are $h_1 = 0.16$, $h_2 = 0.08$, $t_1 = 0.21$, $t_2 = 0.28$, $w_1 = 0.75$, and $w_2 = 0.39$.

A carefully-shaped heat conductor helps to control the thermal gradients that are crucial to the growth of single-crystal silicon sheets for solar cells. The ends of the die through which the silicon sheet is drawn as a ribbon from molten silicon must be held at a temperature only slightly above the solidification point of silicon. In older systems with poor temperature-gradient control operating near the freezing point, the ribbon often solidifies prematurely, freezing to the die at its ends. The ribbon breaks and must be restarted.

Now, however, a "cold shoe" with contours that are specially shaped promises to solve the freezing problem. The cold shoe, which extracts heat from the ribbon as it emerges from the die (see figure) thus affords a further means of controlling the die-top temperature, in addition to the active control provided by die heaters and the passive control provided by the shape of the die itself. Whereas in previously-designed cold shoes, the distance h between the die top and the cold shoe and the height t of the flat face of the cold shoe are constant, in the new profiled cold shoe, these dimensions are variable.

With the profile dimensions indicated in the figure, the lateral temperature gradient in the ribbon disappeared, and the tendency of the emerging ribbon to freeze prematurely — at its ends before its center — therefore disappeared too. The ribbon grew smoothly at a rate of 3 cm per minute with a uniformly high meniscus across its width and well-developed stable ends.

This work was done by Brian Mackintosh of Mobil Tyco Solar Energy Corp. for **NASA's Jet Propulsion Laboratory.** *For further information, Circle 60 on the TSP Request Card.*
NPO-15294

Variable-Position Acoustic Levitation

Pressure amplitudes and frequencies are varied to change the equilibrium position.

NASA's Jet Propulsion Laboratory, Pasadena, California

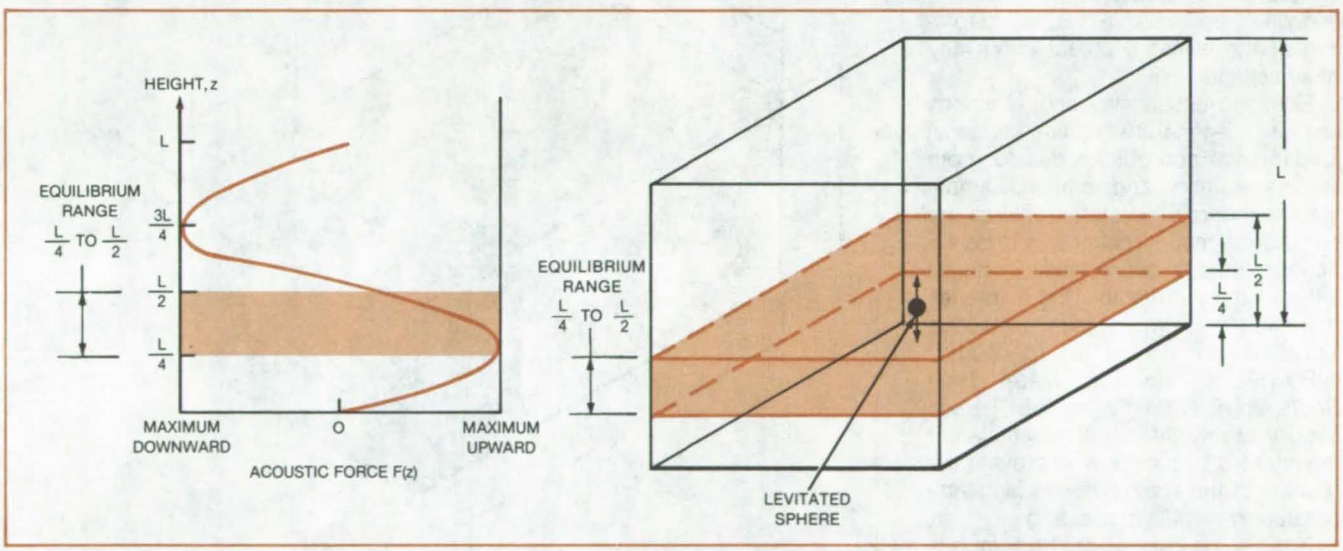

The **Sphere Can Be Raised or Lowered** to any position in the range L/4 to L/2 when the acoustic chamber is excited at its fundamental resonance frequency. When the chamber is excited at harmonics of the fundamental, additional variable-position zones are created.

A method of acoustic levitation supports objects at positions other than the acoustic nodes. Acoustic force is varied so that it balances gravitational (or other) force, thereby maintaining an object at any position within an equilibrium range. When the acoustic frequency is the fundamental resonance of the acoustic chamber, the equilibrium range is one-fourth of the chamber length (see figure).

The levitation method is applicable to containerless processing. In a levitation furnace, for example, it could be used to manipulate specimens without contacting them, perhaps moving them through a temperature gradient.

The acoustic levitation depends upon the sample height, z, and chamber vertical length, L, according to a function that is proportional to $\sin(2\pi Nz/L)$, where N = the order of the harmonic of the fundamental chamber frequency. In the fundamental mode (N = 1), the maximum upward acoustic force occurs at z = L/4. Above this height, the lifting force decreases with increasing height (as with an object supported by a spring). When this maximum force is greater than or equal to the opposing force (gravity), a sample will levitate at or above the L/4 position. Thus, L/4 is the minimum height at which an object can be supported in equilibrium. Above L/2, the force of gravity acts on the specimen in the same direction as the acoustic force, and further levitation is resisted.

A specimen is placed in an acoustic chamber excited at its fundamental mode. The acoustic amplitude (and thus the acoustic force) is increased until it is

(continued on next page)

just sufficient to hold the specimen at a height of L/4. The acoustic amplitude is increased further until the sample rises to the desired position, anywhere between L/4 and L/2. Given the densities of the sample and gas medium, the equilibrium position between these two points can be determined from the acoustic pressure. There are additional regions of equilibrium if the chamber is excited by harmonics of the fundamental frequency.

A variable force such as an electrostatic force can be substituted for gravity and used to vary the position of a levitated specimen. If the variable force can be both positive and negative, the zones of equilibrium will be extended to twice their size in a unidirectional field and will become continuous.

Such objects as table-tennis balls, hollow plastic spheres, and balsa-wood spheres have been levitated in the laboratory by the new method.

This work was done by Martin B. Barmatz, James D. Stoneburner, Nathan Jacobi, and Taylor G. Wang of Caltech for **NASA's Jet Propulsion Laboratory.** *For further information, Circle 61 on the TSP Request Card.*
NPO-15559

Controlling the Rotation of Levitated Samples

Levitation and rotation modes are separated.

NASA's Jet Propulsion Laboratory, Pasadena, California

In a proposed acoustic levitation system, the separate excitation of different acoustic modes would independently levitate and control the rotation of the sample. Three independent axes of rotation would be available, leading to rotation of the levitated object about any other selected axis.

Existing acoustic levitation systems use two degenerate (equal-frequency) fundamental acoustic modes for both sample levitation and rotation. Sample stability (nonrotation state) requires the degenerate mode frequencies to be exactly inphase or out-of-phase. A phase difference gives rise to viscous torques that cause rotation [see "Viscous Torques on a Levitating Body" (NPO-15413), page 56, *NASA Tech Briefs*, Vol. 6, No. 1 (Spring 1981)]. However, these systems are not efficient if the intent is to control or to prevent the rotation of the sample during high-temperature materials processing.

In the proposed system, the sample is levitated by using nondegenerate fundamental frequencies that do not cause rotation. Rotation is introduced either by adjusting the chamber dimensions to produce higher-frequency degenerate normal modes or by exciting degenerate normal modes in a chamber with specific length ratios.

As an example, consider the rectangular chamber of the figure, with sides of length l_x, l_y, and l_z. The frequency of the n_x, n_y, n_z mode is given by

$$f_{n_x n_y n_z} = \frac{c}{2}\left[\left(\frac{n_x}{l_x}\right)^2 + \left(\frac{n_y}{l_y}\right)^2 + \left(\frac{n_z}{l_z}\right)^2\right]^{1/2}$$

where c = the speed of sound.

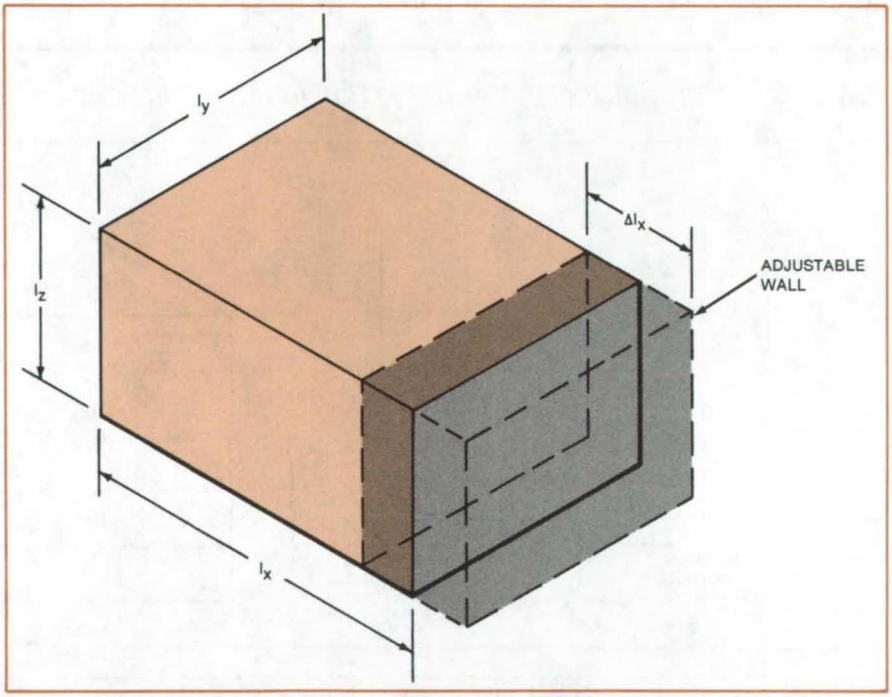

A **Rectangular Chamber With at Least One Movable Wall** exhibits different acoustic normal modes, depending upon the chosen wall position. The manner of selecting modes and frequencies is analogous to that of tunable waveguides or musical instruments.

If $l_y/l_x = 5/3$ and $l_z/l_y = 5/7$, then there are three pairs of degenerate normal modes; namely, $f_{300} = f_{050}$, $f_{700} = f_{005}$, and $f_{070} = f_{003}$. These mode pairs produce torques about the z, y, and x axes, respectively. The torques depend on the amplitudes and relative phases of the two modes in the pairs.

The net acoustic torque on a levitated object equals the vector sum of the acoustic torques applied by the mode pairs. If the three degenerate mode pairs are excited as in the above example, the sample will rotate about an axis alined with the net torque, with a rotational speed dependent on the magnitude of that torque. While the concept is most easily visualized for a chamber of rectangular cross section, it is applicable to any of the common shapes employed for levitation chambers and for which the normal modes are known.

The port through which a mode is excited must be positioned so as to feed energy maximally to that mode while minimizing the coupling to the other mode of the same frequency. The position selected should simultaneously be an excitation node (pressure antinode) for the normal mode desired and an excitation antinode (pressure node) for the corresponding degenerate mode that one is trying not to excite.

This work was done by Martin B. Barmatz of Caltech for **NASA's Jet Propulsion Laboratory.** *For further information, Circle 62 on the TSP Request Card.*
NPO-15522

Repairing Loose Connector Pins

Pins can be glued in place if a spring finger fails.

Lyndon B. Johnson Space Center, Houston, Texas

The electrical serviceability of a damaged connector can sometimes be restored by bonding loose contacts to the connector insert with an adhesive. The procedure eliminates the time-consuming operations of completely removing and replacing the faulty electrical connector and then testing the affected wiring.

A multipin connector (shown in Figure 1) that has removable contacts is widely used in large, integrated electronic systems because it simplifies the assembly of complex harnesses. Each removable contact is held in place by spring fingers that rest behind a shouldered section of the pin. Because the fingers are integral with the plastic insert of the connector, there is no way to replace or repair them if they become damaged.

In the repair procedure, a hypodermic needle is used (see Figure 2) to apply an epoxy adhesive in and behind the cavity containing the damaged locking finger. The damaged connector does not have to be demated or removed from the harness to apply the epoxy.

The epoxy used (Hysol EA956, or equivalent) is relatively thick: It will neither flow past the pin to the front face of the connector to contaminate the contact, nor will it flow from the repair site after the needle is removed. The epoxy fills the space around the base of the contact to anchor it in position, resulting in a permanent repair.

This work was done by William T. Dean III and Eugene J. Stringer of Rockwell International Corp. for **Johnson Space Center.** *No further documentation is available.*
MSC-20374

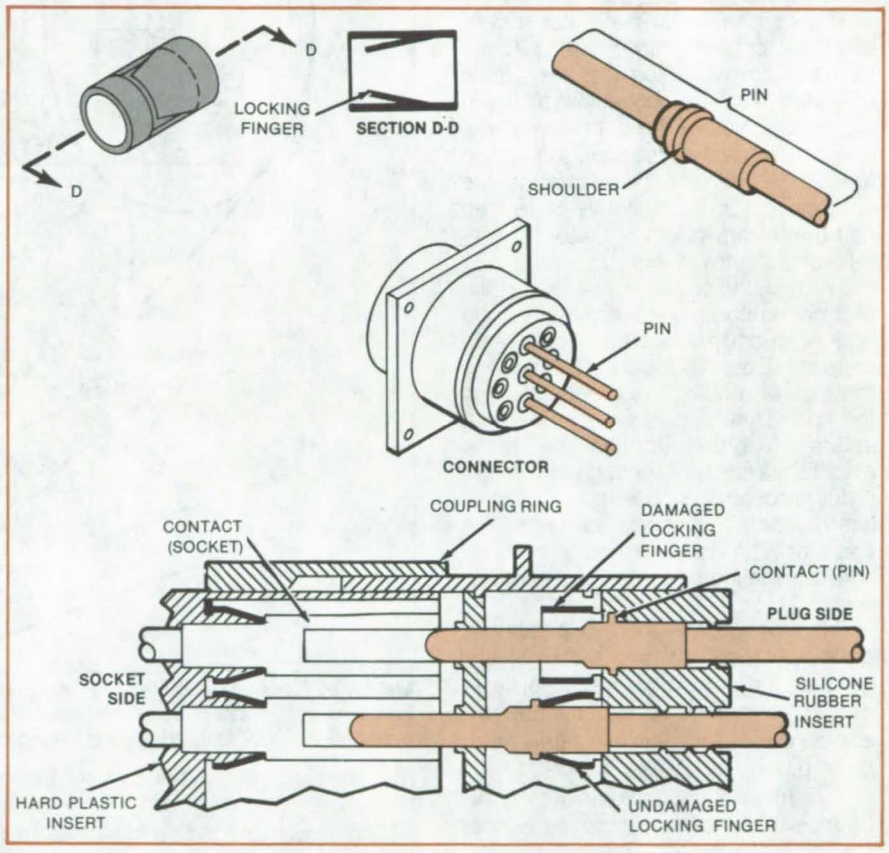

Figure 1. In this **Electrical Connector** (above) a contact pin is inserted and pushed into a spring-locking device to retain it in a secured position. In the two mated connectors (below) both contacts on the socket side are locked in by good locking devices. On the plug side, one pin contact is locked in by a good locking device, while the other pin contact is pushed from its position because of a damaged locking device.

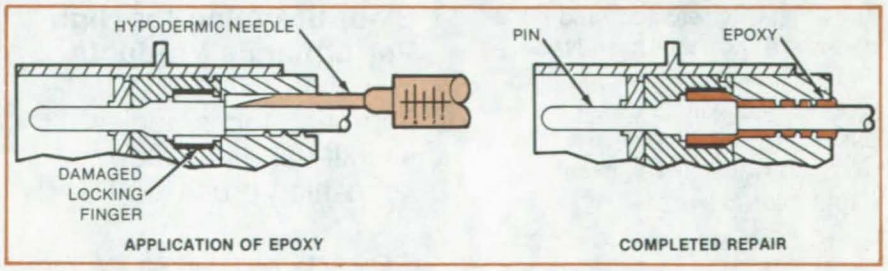

Figure 2. The **Displaced Contact** has been pushed back into its cavity, and a cured epoxy retains it in a secured position. Any number of contacts within the same connector can be repaired the same way.

Jig Quickly Checks Connector-Pin Alinement

Special jig reduces test time from hours to minutes.

Lyndon B. Johnson Space Center, Houston, Texas

A test jig checks whether the pins of a connector are within location tolerance. The jig greatly reduces test time. For a 250-pin connector, for example, a test that takes only 5 minutes with the jig requires 4 hours with a toolmaker's microscope — the conventional way of checking pin location.

The jig is a metal plate that makes electrical contact with out-of-tolerance pins but not with pins that are within tolerance. Parallel longitudinal slots are cut on one side of the aluminum plate, and parallel transverse slots are cut on the other side (see figure). Since the slots are cut through slightly more than half the thickness of the plate, their intersections form rectangular holes.

In a test, the operator inserts the pins of a connector into the holes while the connector body is located by dowels on the plate. If a pin is misalined, it touches the side of a hole. The operator scans the tips of the pins one by one with a stylus. A pin touching the plate establishes electrical continuity from the stylus through the plate to a buzzer or lamp, which provides a signal to the operator. The operator notes the location of misalined pins for later correction.

Jigs can be designed to accommodate a variety of pin patterns and shapes. With chemical milling or laser drilling, extremely-precise hole patterns can be created in stainless-steel sheets only 0.010 to 0.020 inch (0.25 to 0.51 mm) thick. Such templates could be mounted in general-purpose fixtures for checking pin alinement to close tolerances.

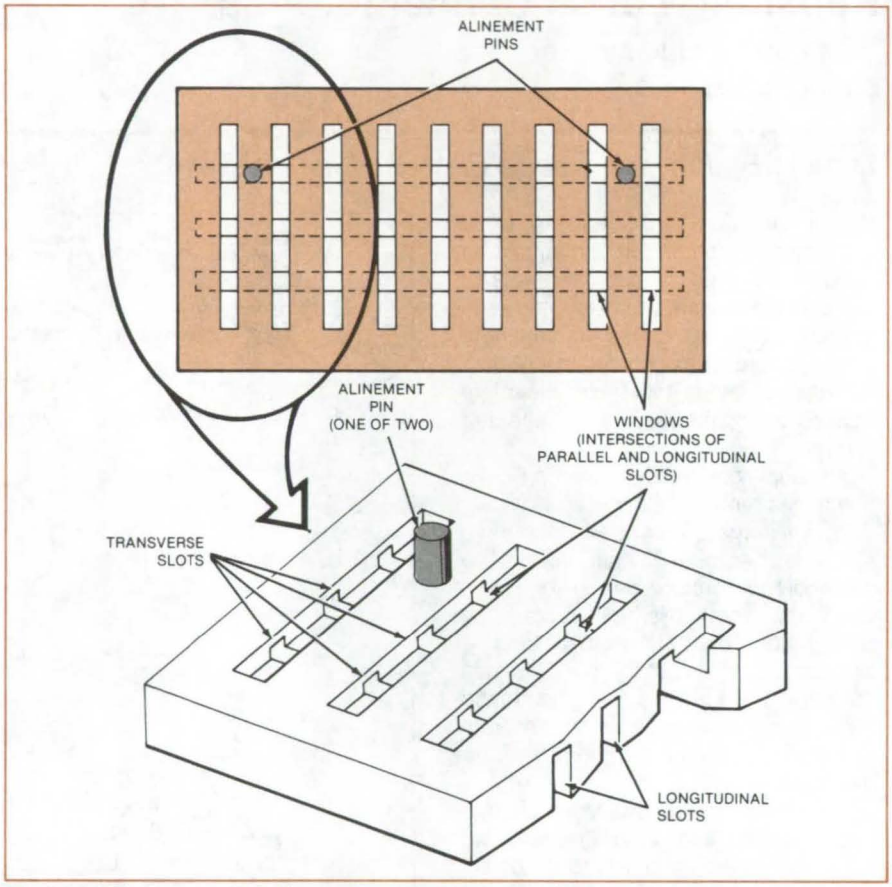

Machined Slots on opposite faces of a plate form a matrix of rectangular windows at their intersections. If a connector pin is out of alinement, it makes electrical contact with the side of a window, thus triggering an indicator.

This work was done by William M. Hall and Thomas P. Papac of Hughes Aircraft Co. for **Johnson Space Center.** *For further information, Circle 63 on the TSP Request Card.*
MSC-20237

Books and Reports

These reports, studies, and handbooks are available from NASA as Technical Support Packages (TSP's) when a Request Card number is cited; otherwise they are available from the National Technical Information Service.

Electroforming for High-Performance Products

Improved technologies simplify and enhance the deposition process.

Electroforming involves the electrolytic deposition of a metal (primarily copper or nickel) on a conductive substrate material. This technique is especially well suited to the forming of certain complex and highly detailed parts. Parts fabricated in this way are used in a variety of applications ranging from rocket engines to phonograph records. Although the basic process is widely used, there is only a limited amount of high-technology experience. This severely limits the potential since high-technology experience is required to utilize electroforming in producing hardware meeting stringent service requirements. The ability to predict and reproduce physical and me-

chanical properties uniformly is of prime importance. Processes and procedures are, for the most part, proprietary information with the producers. As a result, the product of one electroformer will frequently differ from that of another with respect to mechanical properties, deposit quality, bond strengths, and the like.

A NASA-funded contractor report describes the development of processes and procedures for the preparation of specifications for electroforming nickel and copper outer shells on cooled rocket thrust-chamber liners. These specifications represent a merging of technical contributions from many sources into a guide for producers of electroformed, high-performance products. This report provides a basic document with which the electroformer can evaluate his product. Improved technologies are reported that simplify and enhance the deposition process. Raw materials, conducting solutions, and deposition rates are evaluated.

The data generated from this investigation will remove many of the questions and uncertainties associated with the electroforming process. Utilization of these results should expand the potential for electroformed products.

This work was done by Glenn A. Malone of Bell Aerospace Co. for **Lewis Research Center.** *Further information, may be found in NASA CR-134959 [N76-20481/NSP], "Final Report Investigation of Electroforming Techniques" [$13.50]. A copy may be purchased [prepayment required] from the National Technical Information Service, Springfield, Virginia 22161.*
LEW-12719

Heat Flow in Horizontal Ribbon Growth

A theoretical analysis focuses on conditions required for stable growth.

A recent theoretical study reveals some important effects of heat flow in horizontal ribbon growth. Particular attention is paid to the heat flow due to a laminar convection current in the melt induced by the horizontal motion of a ribbon-shaped semiconductor crystal being pulled from the melt.

Horizontal growth allows higher "pull" rates than do vertical growth techniques. This is because of the favorable ratio of the large ribbon area available for heat removal to the small cross-sectional area of the ribbon.

Both the motionally-induced and natural (thermally-induced) convection currents in the melt cause a thermal boundary layer to form adjacent to the liquid/solid interface. This causes a nonuniform heat flow from the melt.

Treatment of the combined effects of both natural and induced convection is complex and would have to be done by numerical computation. However, careful control of melt temperature by judicious design of the melt crucible and its heating can minimize the effects of natural convection. Therefore, in this investigation, only the effects due to the motionally-induced convection current are considered.

A series of different modes of ribbon cooling was analyzed to determine the relationships between ribbon thickness, pull rate, melt temperature, and cooling of the ribbon. For each mode the conditions for which ribbon pull would be stable have been investigated.

Under some conditions ribbon thickness is unstable, tending toward zero thickness: a condition that results in ribbon pullout. This occurs if too little active (forced convective) cooling is provided at the thin tip of the ribbon or where there is too little passive cooling of the rest of the ribbon surface.

With such mixed cooling, the ribbon may increase in thickness in the actively cooled region only to remelt partially in the passively cooled region if heat flow from the melt exceeds passive heat loss. The analysis was done for silicon, but it could be redone for other semiconductors by substituting their physical properties for those of silicon.

This work was done by John A. Zoutendyk of Caltech for **NASA's Jet Propulsion Laboratory.** *To obtain a copy of the study, Circle 64 on the TSP Request Card.*
NPO-14979

Improving Surface Strength of Insulating Tiles

A preglaze densification treatment helps tiles resist impact damage.

A procedure for improving tile resistance to impact damage is described in a new report on tile densification. The tile technology was originally described in "'Densified' Tiles Form Stronger Bonds" (MSC-18741), *NASA Tech Briefs*, Vol. 5, No. 4 (Winter 1980), page 495.

Developed for the Space Shuttle reusable surface insulation, the procedure has potential application when space restrictions necessitate thin layers of insulation with low thermal conductivity. Examples are in advanced heat engines, such as the adiabatic diesel and the automotive gas turbine, as well as in fast-heating high-temperature ovens.

The fused-silica base material for the tiles is formed from high-purity silica fibers (2 to 4 microns in diameter) and a high-purity binder. After firing, the mixture provides a low-strength machinable material having low thermal conductivity, high-temperature resistance, and low thermal expansion. The first step in densifying the machined silica tile surfaces is to mask the tile so that only the surfaces to be treated are exposed. A measured amount of isopropyl alcohol is brushed on to aid in wetting the surfaces. The tile is immediately submerged in a silica slurry for 3 minutes.

The tile is removed from the slurry, and the residue remaining on the tile is brushed into its exposed surfaces. Additional slurry is applied until it starts to build up on the surface. The excess is gently removed by wiping, and further slurry is added, with a total of three brushing and wiping operations. A final brushing operation works the fused-silica aggregate into the surface so that it fills the voids sufficiently to provide a hard surface when the material has dried.

The slurry mix contains approximately 55 percent by weight colloidal silica, 45 percent by weight silica slip (irregularly-shaped particulate silica), and 0.12 percent by weight boron silicide for color. The slurry mix is continuously roll-mixed to keep the silica particles in suspension until they are applied to the tile.

The densification process increases the thermal conductivity of the surface layer but does not seriously affect the effective overall thermal conductivity. For a tile 2 inches (5.1 cm) thick, the overall conductivity is increased by about 4 percent.

This work was done by Jack W. Holt and Laurence W. Smiser of Rockwell International Corp. for **Johnson Space Center.** *To obtain a copy of the report, "Surface Densification of High-Porosity Silica Insulation," Circle 65 on the TSP Request Card.*
MSC-20063

Computer Programs

These programs may be obtained at very reasonable cost from COSMIC, a facility sponsored by NASA to make new programs available to the public. For information on program price, size, and availability, circle the reference letter on the COSMIC Request Card in this issue.

Standard Transistor Arrays

Random-logic integrated MOS digital circuits are generated.

Connections between the transistors in a gate, and connections between gates, occur with such frequency that good physical solutions may be extremely complex. Achieving a good physical solution is especially important in the design of digital large-scale-integration (LSI) circuitry.

The Standard Transistor Array (STAR) design system is a semicustom approach to generating random-logic integrated MOS digital circuits. The primary program in the STAR system is CAPSTAR, the STAR Cell Arrangement Program. CAPSTAR is augmented by an automatic routing program, a display program, and a library of logic cells.

Input to CAPSTAR consists of a description of circuit cells and interconnections. This circuit description is used to form a near-optimum, one-dimensional placement of the cells, which is then "folded" onto STAR to form a two-dimensional layout. By the use of various folding strategies, a number of different layouts are formed. The best of these are selected and are improved by a single interchange technique. The best improved layout is determined, and pads are added to generate the final layout. The placements generated are near-optimum with respect to horizontal and vertical channel usage and the number of nets that can be linearly routed.

STAR includes two programs developed to provide for the simulation of logic circuits and for the generation of test sequences for logic circuits. SIMLOG is a gate-level, logic-simulation program that is based on a three-valued logic model and on a unit-delay timing model. Both combinational and sequential circuits can be handled. Logic elements available for use include NAND gates, NOR gates, unit-delay elements, and edge-triggered D flip-flops. The simulated circuit may also contain single or multiple stuck-type faults. TESTGN is a test-sequence generation program for use with circuits being simulated by SIMLOG. The program can generate tests for unspecified faults or for specified single stuck-type faults.

The programs in STAR are written in BASIC and FORTRAN IV for batch execution and have been implemented on a Xerox Sigma V, with the largest program having a central memory requirement of approximately 128K of 32-bit words. The programs were developed in 1979.

This program was written by G. W. Cox and B. D. Carroll of Auburn University and E. R. Pitts and R. A. Wright of M & S Computing for **Marshall Space Flight Center.** *For further information, Circle P on the COSMIC Request Card.*
MFS-25327

Tile-Failure Analysis

Probability model assesses failure risk of systems with widely-varying loads and material strength.

The Tile Failure Probability Model (TFPM) program was originally developed to quantitatively assess the risk of tile loss of a thermal-protection tile from the Space Shuttle orbiter. TFPM is fairly specific to the orbiter, but the basic technique might be applied in other structural design situations where the anticipated loads and material strength have significantly variable probability distributions.

The model generates probability distributions of the tensile loads acting on a given tile during a mission and combines these with tile material-strength probability distributions to compute the probability of a tile tensile failure during the mission. This probability approach to failure analysis is required because the strength of the system, which consists of the ceramic tile material, strain isolator pad, and room-temperature-vulcanizing bond, exhibits wide variation even for similar sets of material.

The TFPM is written in FORTRAN IV and Assembler for batch execution and has been implemented on an IBM 370-series computer with a central memory requirement of approximately 800K of 8-bit bytes. The program was developed in 1980.

This program was written by Eugene A. O'Hern and Kenneth E. Ryan of Rockwell International Corp. for **Johnson Space Center.** *For further information, Circle Q on the COSMIC Request Card.*
MSC-20139

Mathematics and Information Sciences

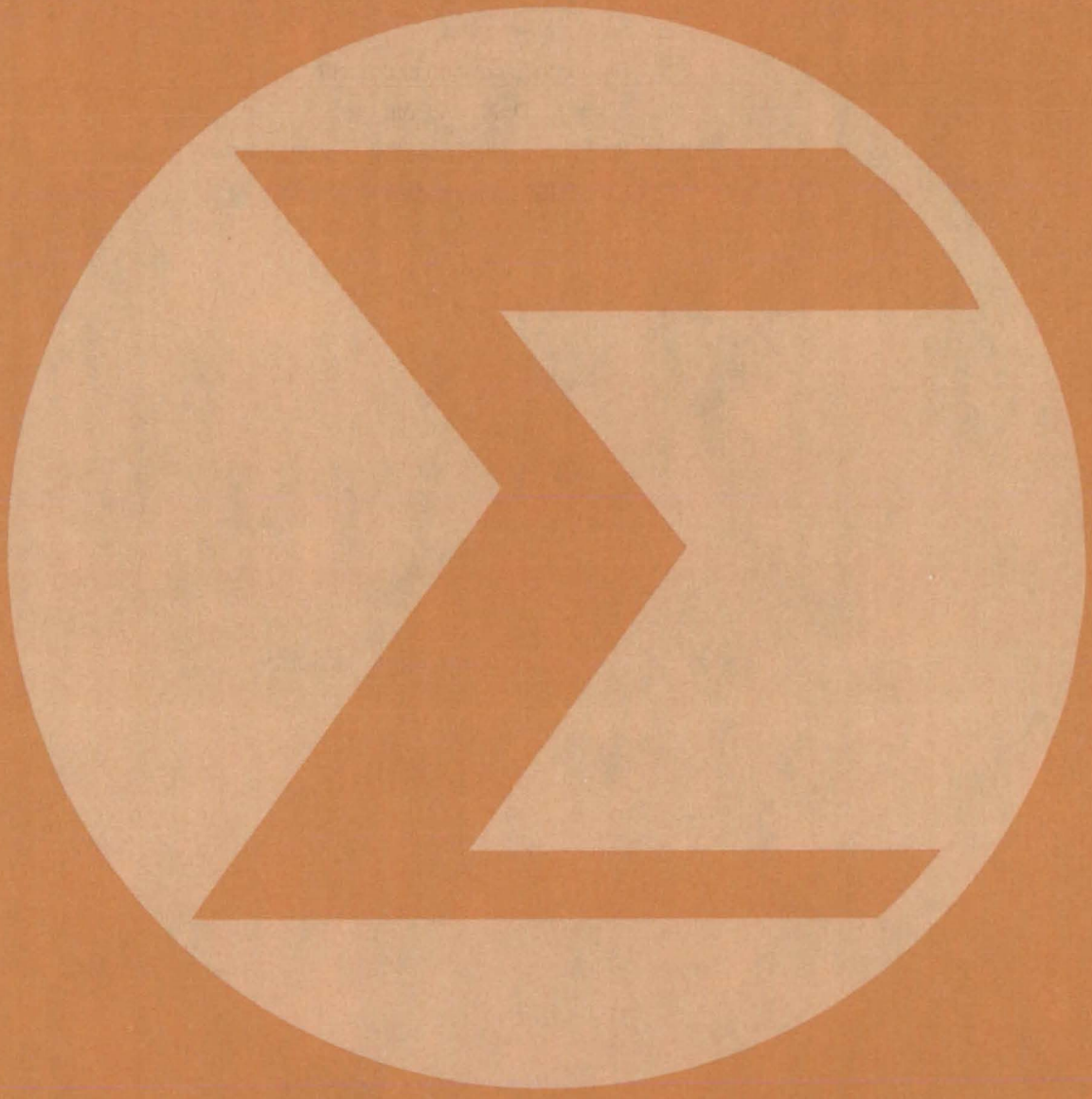

Computer Programs

Computer Programs

These programs may be obtained at very reasonable cost from COSMIC, a facility sponsored by NASA to make new programs available to the public. For information on program price, size, and availability, circle the reference letter on the COSMIC Request Card in this issue.

Document Update and Compare

Documents can be modified and lists of modifications printed out.

Maintaining documentation is an important task that can require a great deal of time and resources if handled manually. The manual maintenance of documentation also increases the probability of documentation error, which can decrease document reliability. The Document Update and Compare programs provide a simple computerized document-maintenance system on the Data General NOVA 840 computer.

The Document Update program allows the user to update a document either by batch or terminal input. It provides for automatic page sequencing, automatic paragraph numbering and renumbering (up to three levels) for insertions and deletions, automatic carry forward of station designator, and selectable headers and formatting. The updated document may be output on a line printer with off-page (outside the standard 8-1/2 by 11 area) printing of line numbers for reference and future editing purposes.

The Compare program compares two versions of a document. It prints a listing, by line number, of all insertions, deletions, and changes.

These programs are written in FORTRAN V for batch or interactive execution and have been implemented on a Data General NOVA 840 computer under RDOS with a central memory requirement of approximately 32K words. The programs were developed in 1981.

This program was written by Charles F. Knoch, Dolores C. Caldwell, and David L. Caldwell of Rockwell International Corp. for **Johnson Space Center.** *For further information, Circle R on the COSMIC Request Card.*
MSC-20349

Text File Comparator

Program compares two files and lists their differences.

The File Comparator program, IFCOMP, is a text file comparator for IBM OS/VS-compatible systems. IFCOMP accepts as input two text files and produces a listing of their differences in pseudo-update form. All differences are reported as lines that should be deleted, replaced, inserted, or moved in the first input file to transform it into the second input file. A summary, listing the number of lines involved in each type of change, is also produced.

IFCOMP has provisions to ignore line numbers and trailing blanks when comparing files with records of different lengths. IFCOMP should be very useful in monitoring changes made to software at the source code level. When used in this manner, IFCOMP allows for the direct comparison of source code to identify changes in a consistent manner.

IFCOMP is written in XPL (an extended PLI language for which the compiler executables are supplied) for batch execution and has been implemented on an IBM 370-series computer with a central memory requirement of approximately 46K of 8-bit bytes. IFCOMP was developed in 1979.

This program was written by Reed S. Kotler of Intermetrics, Inc. for **Johnson Space Center.** *For further information, Circle S on the COSMIC Request Card.*
MSC-20276

Configuration Analysis Tool

An interactive program for storing information and generating reports on project configuration management

The Configuration Analysis Tool (CAT), developed for the NASA Goddard Space Flight Center Mission Support Computing and Analysis Division, is an information storage and report generation system for the aid of configuration management activities. Configuration management is a discipline composed of many techniques selected to track and direct the evolution of complex systems. CAT is an interactive program that accepts, organizes, and stores information pertinent to specific phases of a project. In particular, CAT works with information concerning the design, development, testing, and maintenance of project software. During a CAT interactive data input session, the user is prompted for information and is provided with informative and diagnostic messages to ensure rapid and complete data entry. Various project history reports are generated by CAT in response to user queries.

All data needed by CAT reside in a single project file. This is a direct-access file in which a doubly-linked list structure is used for data organization.

CAT operates in an EDIT mode and a REPORT mode. In the EDIT mode, authorized users can add, change, or delete data. In the REPORT mode the user can request CAT to generate project history reports from the data currently in the data base. Seven types of reports may be generated:

1. The discrepancy history report, which contains all reported errors and associated information for a project;
2. The change history report, which contains all reported modifications and enhancements to correct or to improve the project programs;
3. The documentation history report, which contains all the information concerning the disposition and status of documents generated within a project;
4. The test history report, which contains information concerning what has been tested and the test results;
5. The resource history report, which contains task member assignments;
6. The milestone history report, which includes current milestone information; and
7. The data set status history report, which contains the status and location of the project data sets and associated information.

With these reports the configuration analyst should be better able to track and direct the ongoing progress of complex software projects.

CAT is written in FORTRAN IV Plus and Assembler for interactive execution and has been implemented on a DEC PDP-11/70 computer under RSX-11M

(continued on next page)

with a central memory requirement of approximately 26K of 16-bit words. It was developed in 1980.

This program was written by Phillip D. Merwarth of **Goddard Space Flight Center.** *For further information, Circle T on the COSMIC Request Card.*
GSC-12710

Software Repository

Interactive library system aids in locating available software.

In many large organizations, software development is duplicated from one group to another due to the lack of a formalized system for storing and making available information on internally available software. The Common Software Module Repository (CSMR) system provides such a formalized system.

CSMR is basically a computerized library system with high product and service visibility to potential users. The online capabilities of the system allow both the librarian and the user to interact with the library. The librarian is responsible for maintaining the information in the CSMR library. The user may search the library to locate software modules that might meet his or her current needs.

Associated with each library entry are four files of data. The first three files contain the program abstract, the program prolog, and the program software characteristics. The fourth file contains the program source code. The abstract is intended for use as a quick-look query into the primary function of the library entry. In addition, the abstract contains an assigned library catalog number, the title of the software product, category information, the author, references, the date the software was entered into the library, the date of the last software update, the software support person, the target computer, and the source code language.

The prolog is a more specific description of the module in such terms as module function, the method in which the module accomplished its function, module usage, and module interface requirements. The software characteristics include information concerning the operational efficiency of the software, such as storage and memory requirements, run-time estimates, and software metrics. The CSMR system is designed so that all of this information and the software source code may be readly entered and maintained in the CSMR library.

The CSMR system gives the user an easy method of searching the library for software. The user interactively narrows the number of library entries to be examined by responding to CSMR-generated prompts. Once the selection of entries has been reduced to those that satisfy specific requests, the user may examine the abstract, prolog, characteristics, and source code of each. The users may then select one or more entries for use in their software project.

The CSMR system is written in FORTRAN IV-Plus and Assembler for interactive execution and has been implemented on a DEC PDP-11/70 computer under RSX-11M with an overlaid central memory requirement of approximately 28K of 16-bit words. The CSMR system was developed in 1979.

This program was written by Phillip Merwarth of **Goddard Space Flight Center.** *For further information, Circle U on the COSMIC Request Card.*
GSC-12735

Resource Escalation and Cost Analysis

Cost for projects with hierarchical elements is calculated and spread over time.

The Resource Escalation and Cost Analysis Program (RECAP) is a cost compilation program for any project organized in a work breakdown structure (WBS) format. In a WBS format, activities are broken down and organized by level, so that each activity at a high level includes those activities at a lower level. This permits the organization of activities into classes and subclasses.

RECAP can handle up to 1,000 WBS activities and 4 levels with up to 99 classes of activities within a level. RECAP computes the cost of each activity directly, based on one of six cost equations, or indirectly as a function of the cost of some other activity or activities.

RECAP computes the costs of WBS items and distributes those costs over a span of up to 60 user-defined intervals. Costs for each activity may be spread over time according to a standard function with any one of six spread algorithms. The distributed cost for each activity may be summed into a more general activity to yield distributed cost for each activity class.

In addition to escalating cost due to anticipated inflation, RECAP allows the user to assign a fiscal base period to the input costs. Costs may then be escalated for any inflation known or anticipated to have occurred between the time that the project cost was initially calculated and the period in which escalation is to begin.

Input to RECAP consists of program directive records and task records. The program directive records provide information required by the program and specify the processing option to be exercised in a given run. The task records provide information relevant to each task, including information required for cost computation and distribution. Reports generated by RECAP include a summary report, a summary report with escalated output, and line item reports. RECAP can also generate x-y plots of selected costs versus time.

RECAP is written in FORTRAN IV for batch execution and has been implemented on a CDC CYBER 170-series computer with an overlaid central memory requirement of approximately 78K (octal) of 60-bit words. The program was developed in 1981.

This program was written by Darrell A. Wood of **Langley Research Center.** *For further information, Circle V on the COSMIC Request Card.*
LAR-13018

Driver for DISSPLA Plotter

A driver for plotter, microfilm, microfiche, and terminal graphics

DISPLOT is a generalized outside driver for the commercially-available DISSPLA (Display Integrated Software System and Plotting Language) plotting system. The DISPLOT program provides the user with a simple-to-use graphics capability with a great deal of application flexibility. DISPLOT is independent of whatever program generates the data to be plotted.

DISPLOT may be used for the generation of plotter, microfilm, microfiche, and

terminal plots. The user has complete control of plot titling, axis labeling, and general annotation. Plots using Cartesian, logarithmic, polar, and map projection scales are readily generated. DISPLOT also allows for the manipulation of the data to be plotted prior to plot generation.

DISPLOT offers flexibility while utilizing simple input because of its design as a DISSPLA driver with a data buffer. With the data buffer, multiple variables can be loaded at one time, which increases the speed of the program. The program also allows the user to manipulate the input data before plotting them. The user controls the flow of the DISPLOT program through economical NAMELIST inputs.

DISPLOT is written in FORTRAN V and Assembler for batch execution and has been implemented on a UNIVAC 1100-series computer with a central memory requirement of approximately 93K of 36-bit words. DISPLOT was developed in 1981.

This program was written by Mark L. Baldwin of McDonnell Douglas Corp. for **Johnson Space Center.** *For further information, Circle W on the COSMIC Request Card.*
MSC-20290

Interactive Data-Collection and Display Program with Debugging

It aids designers when time and hardware constraints make scaled-integer arithmetic necessary.

To be cost-effective and to improve reliability, the number of parts in digital systems designed for ruggedized applications is usually cut to a minimum. Such reductions, along with requirements for increased computing speed, demand assembly or machine language techniques that use scaled-integer arithmetic calculations. Implementing such techniques is difficult, and locating errors within such assembly language programs is extremely difficult, increasing the time and effort required to get the programs up and running.

The INFORM program is designed to aid the assembly language programers of SEL 810B computers in working with scaled-integer applications. INFORM was developed to meet the needs of engineers designing real-time digital controls using the SEL 810B where time and hardware constraints make the use of integer arithmetic and scaled integers necessary. In addition to producing displays of quasi-steady-state values, INFORM provides an interactive mode for debugging programs, for making program patches, and for modifying the displays. The package includes auxiliary routines that add dynamic data acquisition and high-speed dynamic display to the INFORM capabilities.

The INFORM package is written in Assembler for interactive execution and has been implemented on an SEL 810B computer with a central memory requirement of approximately 5K of 16-bit words. The INFORM program was developed in 1980.

This program was written by David S. Cwynar of **Lewis Research Center.** *For further information, Circle X on the COSMIC Request Card.*
LEW-13530

NAMELIST Preprocessor

FORTRAN code is modified for use with the F4P compiler.

The NAMELIST Preprocessor Program, NPP, provides the DEC PDP-11/70 with capabilities identical to the IBM FORTRAN IV NAMELIST feature. The preprocessor modifies the FORTRAN code that contains NAMELIST statements acceptable to the IBM FORTRAN IV compiler to generate an equivalent code that is acceptable to the PDP-11 FORTRAN IV-Plus (F4P) compiler.

NAMELIST provides the FORTRAN programer with additional, flexible input and output capabilities. This feature is particularly useful in the area of data input because NAMELIST data are input in the form of the variable symbolic name being set equal to a constant value, similar to a standard FORTRAN statement. This allows the user to review input data readily and relieves the user from having to place data in certain columns and formats as required in formatted READ statements.

NPP software consists of two parts: the NAMELIST preprocessor and the NAMELIST library routines. The preprocessor modifies the FORTRAN code containing NAMELIST statements into a FORTRAN code acceptable to the PDP-11 F4P compiler. The NAMELIST library routines, which must be included in tasks containing the NAMELIST preprocessor code, are the run-time routines called by the inserted preprocessor code. The FORTRAN programer should find it easy and efficient to incorporate the NAMELIST feature into many applications.

The NPP software system is written in FORTRAN IV-Plus and Assembler code for batch exectuion and has been implemented on a DEC PDP-11/70 under RSX-11M with a central memory requirement of approximately 32K of 16-bit words. The NPP software system was developed in 1978.

This program was written by Phillip D. Merwarth of **Goddard Space Flight Center.** *For further information, Circle Y on the COSMIC Request Card.*
GSC-12704

SUBJECT INDEX

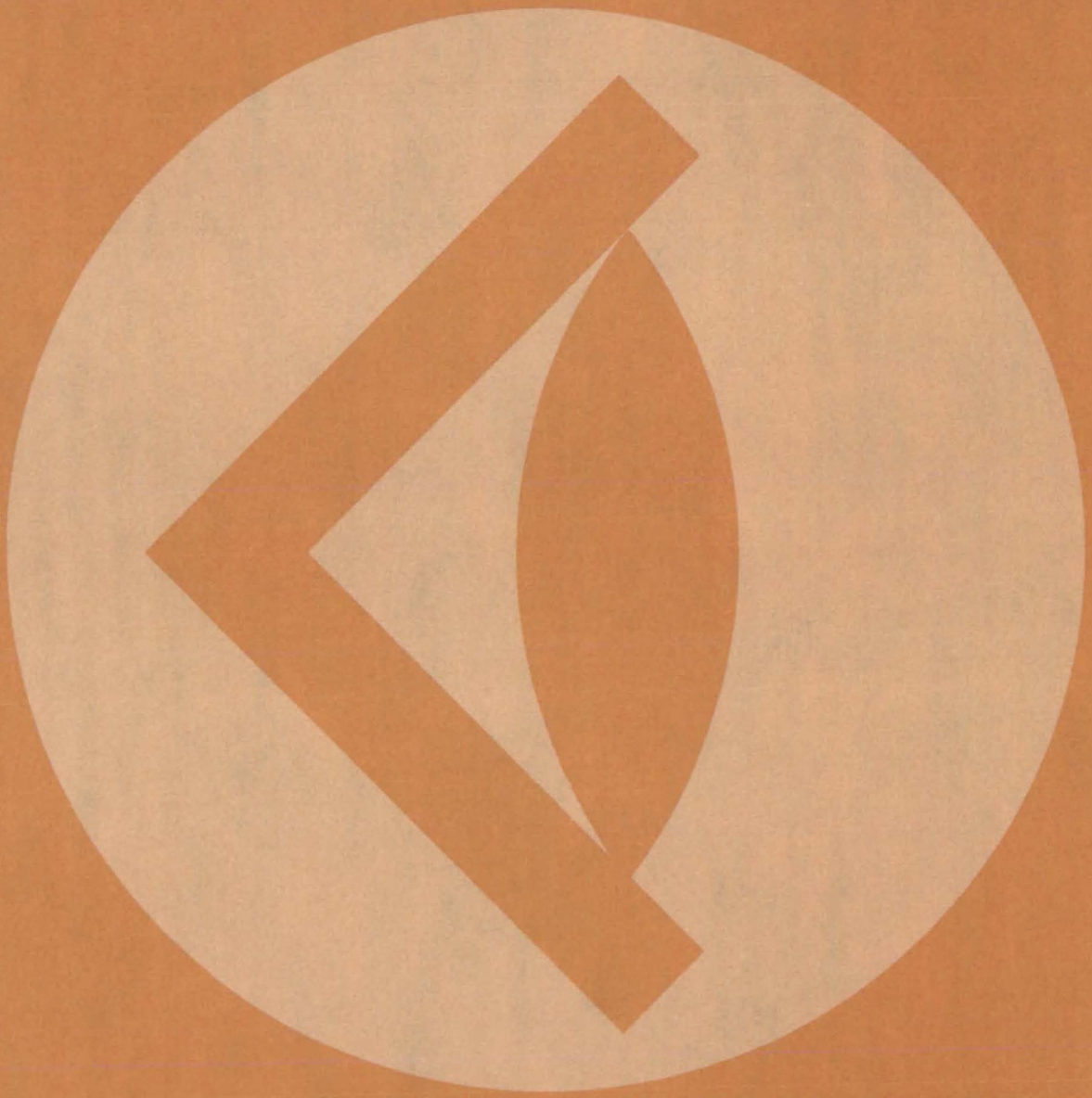

National Aeronautics and
Space Administration

Washington, D.C.
20546

THIRD-CLASS BULK

25th Anniversary
1958-1983

NASA

Xenon lamps used for nighttime illumination of launchsites at Kennedy Space Center have found many commercial spinoffs. Among them are 12,000-watt movie-projector lamps used in theaters worldwide. [*See the bottom of page A1.*]